15
Topics in Heterocyclic Chemistry

Series Editor: R. R. Gupta

Topics in Heterocyclic Chemistry

Series Editor: R. R. Gupta

Recently Published and Forthcoming Volumes

Bioactive Heterocycles VI
Flavonoids and Anthocyanins in Plants,
and Latest Bioactive Heterocycles I
Volume Editor: N. Motohashi
Volume 15, 2008

Heterocyclic Polymethine Dyes
Synthesis, Properties and Applications
Volume Editor: L. Strekowski
Volume 14, 2008

Synthesis of Heterocycles via Cycloadditions II
Volume Editor: A. Hassner
Volume 13, 2008

Synthesis of Heterocycles via Cycloadditions I
Volume Editor: A. Hassner
Volume 12, 2008

Bioactive Heterocycles V
Volume Editor: M. T. H. Khan
Volume 11, 2007

Bioactive Heterocycles IV
Volume Editor: M. T. H. Khan
Volume 10, 2007

Bioactive Heterocycles III
Volume Editor: M. T. H. Khan
Volume 9, 2007

Bioactive Heterocycles II
Volume Editor: S. Eguchi
Volume 8, 2007

Heterocycles from Carbohydrate Precursors
Volume Editor: E. S. H. El Ashry
Volume 7, 2007

Bioactive Heterocycles I
Volume Editor: S. Eguchi
Volume 6, 2006

Marine Natural Products
Volume Editor: H. Kiyota
Volume 5, 2006

QSAR and Molecular Modeling Studies
in Heterocyclic Drugs II
Volume Editor: S. P. Gupta
Volume 4, 2006

QSAR and Molecular Modeling Studies
in Heterocyclic Drugs I
Volume Editor: S. P. Gupta
Volume 3, 2006

Heterocyclic Antitumor Antibiotics
Volume Editor: M. Lee
Volume 2, 2006

Microwave-Assisted Synthesis of Heterocycles
Volume Editors: E. Van der Eycken, C. O. Kappe
Volume 1, 2006

Bioactive Heterocycles VI

Flavonoids and Anthocyanins in Plants, and Latest Bioactive Heterocycles I

Volume Editor: Noboru Motohashi

With contributions by

J. Bariwal · A. Dasgupta · S. G. Dastidar · J. Deli · R. Didiziapetris
H. Engi · M. P. Gangeenahalli · N. Gyémánt · J. Hohmann · M. Inabe
M. Ishihara · S. Jaldappagari · M. Kawase · H. Kikuchi · M. Kobayashi
L. Krenn · T. Kurihara · J. Molnár · N. Motohashi · J. H. Naismith
Y. Nakamura · I. Ocsovski · H. Sakagami · Z. Schelz · A. Shah
K. Shinohara · Y. Shirataki · G. Spengler · M. Szabo · M. Szücs
L. Tanács · H. Wakabayashi

Springer

The series *Topics in Heterocyclic Chemistry* presents critical reviews on "Heterocyclic Compounds" within topic-related volumes dealing with all aspects such as synthesis, reaction mechanisms, structure complexity, properties, reactivity, stability, fundamental and theoretical studies, biology, biomedical studies, pharmacological aspects, applications in material sciences, etc. Metabolism will be also included which will provide information useful in designing pharmacologically active agents. Pathways involving destruction of heterocyclic rings will also be dealt with so that synthesis of specifically functionalized non-heterocyclic molecules can be designed.
The overall scope is to cover topics dealing with most of the areas of current trends in heterocyclic chemistry which will suit to a larger heterocyclic community.
As a rule contributions are specially commissioned. The editors and publishers will, however, always be pleased to receive suggestions and supplementary information. Papers are accepted for *Topics in Heterocyclic Chemistry* in English.
In references *Topics in Heterocyclic Chemistry* is abbreviated *Top Heterocycl Chem* and is cited as a journal.

Springer WWW home page: springer.com
Visit the THC content at springerlink.com

ISBN 978-3-540-79217-8 e-ISBN 978-3-540-79218-5
DOI 10.1007/978-3-540-79218-5

Topics in Heterocyclic Chemistry ISSN 1861-9282

Library of Congress Control Number: 2008924618

Cover design: WMXDesign GmbH, Heidelberg
Typesetting and Production: le-tex publishing services oHG, Leipzig

Printed on acid-free paper

9 8 7 6 5 4 3 2 1 0

springer.com

Series Editor

Prof. R. R. Gupta†

10A, Vasundhara Colony
Lane No. 1, Tonk Road
Jaipur-302 018, India
rrg_vg@yahoo.co.in

Volume Editor

Director and Former Prof. Noboru Motohashi

Meiji Pharmaceutical University
4-31-23 Shimosyakujii
Nerima-ku, Tokyo
177-0042 Japan
noborumotohashi@jcom.home.ne.jp

Editorial Board

Topics in Heterocyclic Chemistry Also Available Electronically

For all customers who have a standing order to Topics in Heterocyclic Chemistry, we offer the electronic version via SpringerLink free of charge. Please contact your librarian who can receive a password or free access to the full articles by registering at:

springerlink.com

If you do not have a subscription, you can still view the tables of contents of the volumes and the abstract of each article by going to the SpringerLink Homepage, clicking on "Browse by Online Libraries", then "Chemical Sciences", and finally choose Topics in Heterocyclic Chemistry.

You will find information about the

- Editorial Board
- Aims and Scope
- Instructions for Authors
- Sample Contribution

at springer.com using the search function.

Color figures are published in full color within the electronic version on SpringerLink.

Preface

As part of the series *Topics in Heterocyclic Chemistry*, this volume titled *Bioactive Heterocycles II* presents comprehensive and up-to-date reviews on selected topics concerning flavonoids and anthocyanins in plants, and heterocycles such as bioactive phenothiazines, phenoxazines, and related compounds. The volume is separated into two sections mainly concentrating on these two topics.

There are abundant and diverse flavonoids with carbohydrates and lipids, alkaloids (betalain alkaloids and other alkaloids), phenols (chromones, coumarins, lignans, quinines, and other phenolics), terpenoids (monoterpenoids, sesquiterpene lactones, triperpenoid saponins, carotenoids, and other terpenoids), and minerals as micronutritional phytochemicals in fruits and vegetables of our daily diets. Among these phytochemicals, the flavonoids have specific functionality in relation to age-related diseases such as hypertension, diabetes, cardiac infarction, cataracts, and cancer. The authors of each chapter in the first section have presented their evidence in relation to the mechanism of the preventative and therapeutic ability of the compounds.

The first chapter, "Functionality of Anthocyanins as Alternative Medicine" by Noboru Motohashi and Hiroshi Sakagami, presents their antioxidant mechanism for anthocyanidins, which are present in common foods. It is possible that anthocyanins may have been used both preventatively and clinically as part of many "folklore medicines" worldwide and may have provided healthcare benefits since the appearance of mankind some 7.5 million years ago. The review will inform the reader as to their functionality and mechanism.

The second chapter, "Bioactive Mechanism of Interaction between Anthocyanins and Macromolecules Like DNA and Proteins" by Seetharamappa Jaldappagari, Noboru Motohashi, Mamatha P. Gangeenahalli, and James H. Naismith, presents the biological activities of anthocyanins, and the interactions of anthocyanins with DNA and protein. Anthocyanins might protect against damage to health by some types of harmful oxidants through various mechanisms such as their antioxidative activity, protein active site binding, and chelating complex formation. The review presents the interesting interactive mechanism of anthocyanin–DNA complex formation.

The third chapter, "Antibacterial Activity of Artificial Phenothiazines and Isoflavones from Plants" by Asish Dasgupta, Sujata Ghosh Dastidar, Yoshiaki Shirataki, and Noboru Motohashi, presents that synthetic phenothiazines and

isoflavonones are not only powerful antibacterial agents as revealed by their activity in tests with hundreds of bacteria, but often also act as antiviral and anticancer agents. Many such compounds can eliminate drug-resistant plasmids and actively participate in inhibition of efflux pumps in pathogens. This study has opened up a new domain in the field of antimicrobial chemotherapy since these compounds can be administered in humans straight away or may be further improved by structural modifications.

The fourth chapter, "Inhibition of Multidrug Resistance of Cancer Cells by Selected Carotenoids, Flavonoids and Anthocyanins" by Joseph Molnár, Helga Engi, Nóra Gyémánt, Zsuzsanna Schelz, Gabriella Spengler, Imre Ocsovszki, Miklós Szücs, Judith Hohmann, Margaret Szabó, Lajos Tanács, Péter Molnár, Joseph Deli, Liselotte Krenn, Masami Kawase, Hidetsugu Wakabayashi, Teruo Kurihara, Yoshiaki Shirataki, Hiroshi Sakagami, Noboru Motohashi, and Remigijus Didiziapetris, tried to indirectly define receptor-structure in the presence of the diverse structurally unrelated carotenoids, flavonoids, isoflavonoids, and terpenoids. This review may contribute to studies of multidrug-resistant (MDR) proteins that belong to the ATP-binding cassette superfamily which are present in a majority of human tumors and are an important final cause of therapeutic failure.

The fifth chapter, "Changes in Polyamine Levels during Cell Death Induced by Heterocycles" by Masaki Kobayashi, Hiroshi Sakagami, Masami Kawase, and Noboru Motohashi, presents changes in polyamine levels during cell death induced by selective properties of diverse heterocycles such as phenoxazines, flavonoids, and other heterocycles. Natural polyamines (putrescine, spermidine, spermine) are aliphatic amines containing two or more amino groups, which play important roles in regulating cell growth and differentiation. Depletion of polyamine in cells has been known to inhibit cell proliferation or induce cell death. This review might help the study of changes in polyamine levels on cell death when induced by heterocycles.

In the second section of the volume, *N*-heterocycles such as phenothiazines, phenoxazines, dihydropyridines, and related compounds are shown also to have interesting biological activity including antitumor activity, vermicide, antibacterial activity, and antischizophrenic activity (i.e. chlorpromazine of the phenothiazine family and its analogs). The activity of phenothiazine and compounds such as phenoxazines and related heterocycles, and also recent bioactive mesoionic heterocycles will be discussed.

The sixth chapter, "Tumor-Specificity and Type of Cell Death Induced by Heterocycles" by Hiroshi Sakagami, Masaki Kobayashi, Mariko Ishihara, Hirotaka Kikuchi, Yukio Nakamura, Masami Kawase, and Noboru Motohashi, presents the tumor specificities of trifluoromethylimidazoles, phenoxazines, 3-formylchromone derivatives, coumarin and its derivatives, and vitamin K_2 derivatives and the type of cell death induced by these heterocycles. This review might beneficially establish a definitive strategy for the exploration of new highly tumor-selective compounds. Also, the screening process of highly

tumor-specific compounds should be introduced before the identification of the type of cell death (either apoptosis, autophagy, or necrosis) and the cell-death induction mechanism.

The seventh chapter, "Advanced Dihydropyridines as Novel Multidrug Resistance Modifiers and Reversing Agents" by Anamik Shah, Jitender Bariwal, Joseph Molnár, Masami Kawase, and Noboru Motohashi, presents a comprehensive review of their synthetic methodology for the preparation of the most-active P-glycoprotein (Pgp) inhibitor dihydropyridine. These "privilege structured" families of compounds are potent inhibitors of P-glycoprotein, which are the main cause of efflux of toxins from the cells. This review might be useful for exploratory future drug development due to the Pgp inhibitory property of the dihydropyridines.

The last chapter, "Theoretical Studies on Phenothiazines, Benzo[*a*]phenothiazines and Benz[*c*]acridines" by Teruo Kurihara, Kazumi Shinohara, Hidetsugu Wakabayashi, Noboru Motohashi, Hiroshi Sakagami, and Joseph Molnár, presents their quantitative structure–activity relationship (QSAR) analysis for minimum inhibitory concentration (MIC) of phenothiazines and benzo[*a*]phenothiazines. The MIC values of phenothiazines were well correlated to $\Delta\Delta$Hf, HOMO energy, and μG. QSAR may be applicable to predict the MIC of phenothiazines. This review could contribute to prediction of the relationship of structure to biological activity.

It is hoped that this volume will serve as a stimulus for researchers with an interest in the field of biological activity of flavonoids and heterocycles, and also stimulate further development for novel therapeutics.

Tokyo, March 2008 Noboru Motohashi

Contents

Top Heterocycl Chem (2008) 15: 1–48
DOI 10.1007/7081_2008_121

Published online: 7 May 2008

Functionality of Anthocyanins as Alternative Medicine

Noboru Motohashi[1] (✉) · Hiroshi Sakagami[2]

[1]Meiji Pharmaceutical University, 2-522-1 Noshio, Kiyose-shi, 204-8588 Tokyo, Japan
noborumotohashi@jcom.home.ne.jp

[2]Division of Pharmacology, Department of Diagnostic and Therapeutic Sciences, Meikai University School of Dentistry, 1-1 Keyakidai, Sakado, 350-0283 Saitama, Japan

Abstract Anthocyanins of the proanthocyanidin-type glucosides in flavonoids are contained as functional constituents of fruits such as cranberry, blueberry, orange and apple and vegetables such as tomato, sweet pepper, spinach and radishes, and have been eaten as part of daily diets from the primitive era of human history. When anthocyanins are coupled with some water-soluble sugar molecules, they produce red, yellow, violet or blue colors. This explains why anthocyanins give a colorful variety of pigments for pansies, petunias, plums and other flowers. Interestingly, chlorophyll in various fruits and vegetables is the main green component, while anthocyanins are probably the most important visible plant pigments having specific colors. Anthocyanins have been clinically used in

many folklore medicines worldwide that provide health benefits. Anthocyanins display antioxidant capacity against superoxide radicals, hydrogen peroxide, and other oxidants, and thus are expected to protect us from oxidative injury. In this review, the antioxidant mechanism of anthocyanidins present in common foods is discussed.

Keywords Anthocyanins · Free radicals · Functionality · Proanthocyanidins

1 Introduction

The red, blue and other coloring of some fruits and vegetables such as blackberries and red cabbage are mainly due to anthocyanins. These anthocyanins are sensitive to changes in pH, when the solutions are acidic, neutral, or basic, the color of the pigments could change from red to purple, blue and other colors, respectively. These plant pigments are highly water-soluble (Figs. 1 and 2).

Recently, anthocyanins have received less attention compared to other flavonoids despite their far-reaching health effects. Because berries might have occupied such a large part of early diets, our ancestors probably ate more anthocyanins when compared to our food intake. In fact, according to some researchers, we might be deficient in anthocyanins. When people understand the antioxidant potential of the phytochemicals, perhaps we could improve the deficiencies by taking them. In due-course, our daily common foods may give even more enjoyment to us.

Anthocyanins such as flavonoid glucosides of apigenidin, capensinidin, delphinidin, cyanidin, malvidin, pelargonidin, puchellidin, peonidin, petunidin, rosinidin and tricetinidin are secondary plant metabolites. Anthocyanins could protect the plants themselves against damage from photodynamic radical reactions by quenching the excited state of the harmful and active oxygen species [1].

Chlorogenic acid (a polyphenol) with a phenylpropanoid structure is highly rich in many food plant extracts and also the most active antioxidant. Surprisingly, a 1.2×10^{-5} M solution of chlorogenic acid could inhibit the peroxide formation of a linoleic acid by more than 80% [1]. On the other hand, chlorogenic acid inhibited the $OH^{\cdot}$ free radical activity only by 13%. Chlorogenic acid scavenged $O_2^{\cdot -}$ or H_2O_2 by 2.43 and 8.14%, respectively. Moreover, ascorbic acid scavenged single oxygen ($^1O_2$) only by 0.44% [2].

Anthocyanins could play probably such diverse roles as the phenolic phytochemicals eaten as part of the human diet. Anthocyanins have been used for several therapeutic treatments for diabetes, retinopathy, fibrocystic disease and other age-related diseases [3], and vision disorders [4].

Anthocyanins also have functional potential to serve as radiation-protective agents, vasotonic agents, and chemoprotective agents [5].

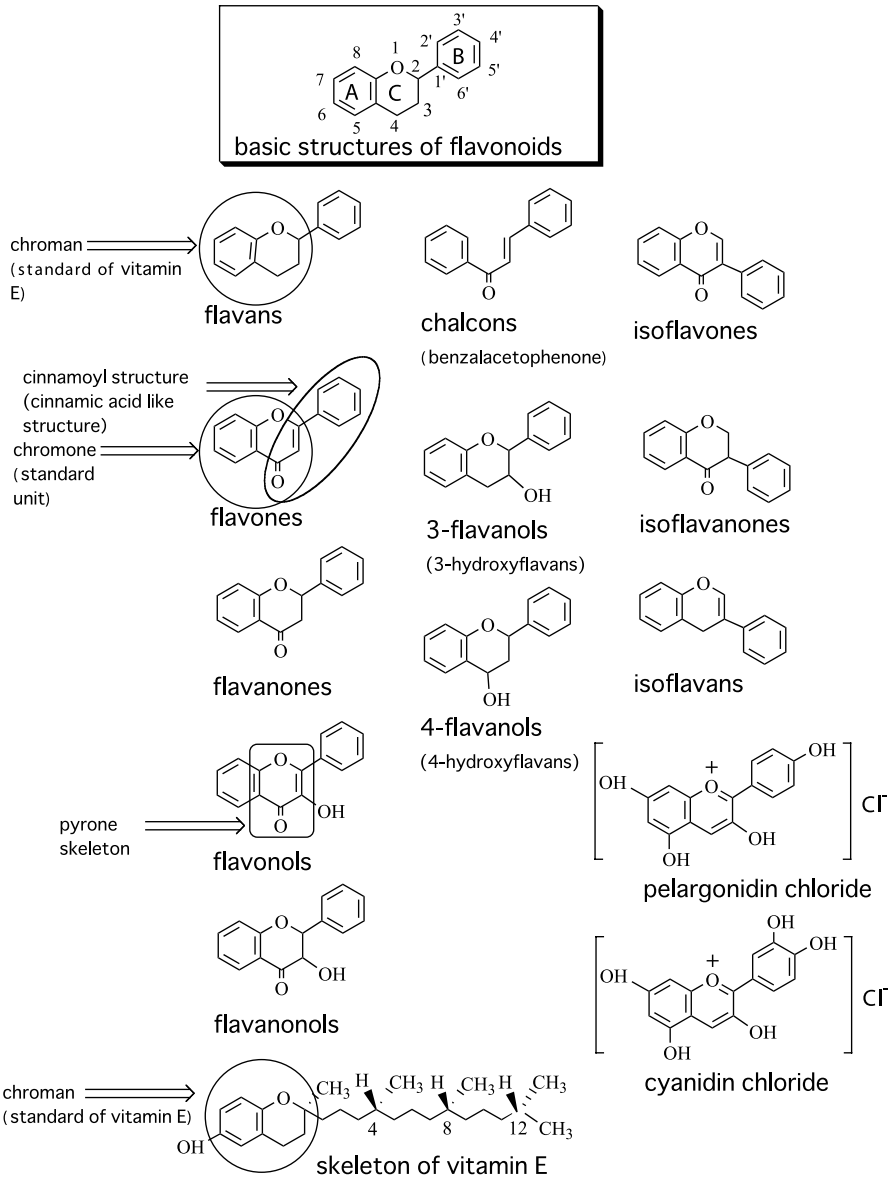

Fig. 1 Skeletal structures of flavonoids and related complexes

Anthocyanins could act against carbon tetrachloride-induced lipoperoxidation. Anthocyanins could also reduce the incidences of fragility of capillaries, inhibit blood platelet aggregation, and strengthen the collagen matrix which is a component of the connective tissues [6].

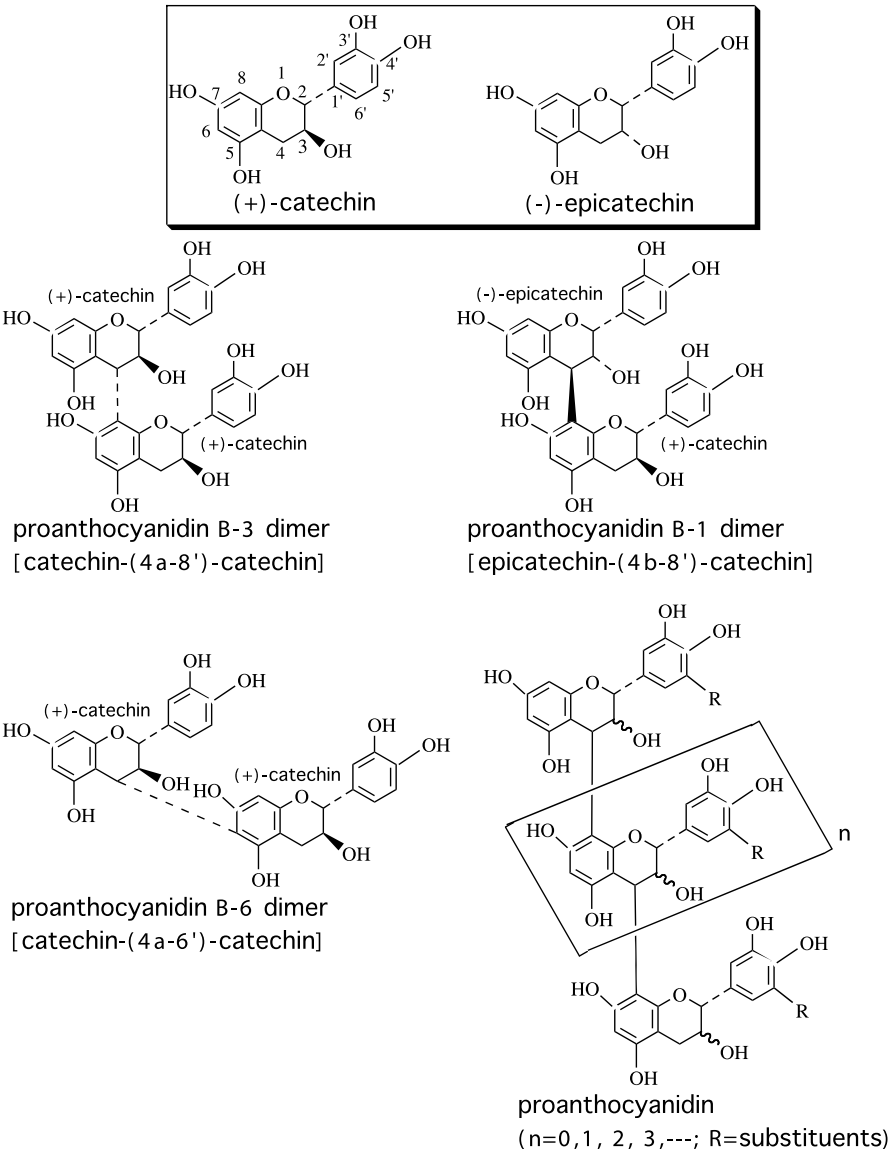

Fig. 2 Structures of catechins and pycnogenols

Anthocyanins may have been eaten for around 7.5 million years since the beginning of mankind. Anthocyanins such as flavones and flavanones are the derivatives of 3,5,7-trihydroxy-flavylium chloride that could provide red, blue, yellow, purple and other colors of vegetables and fruits.

Anthocyanins are a class of flavonoids separated from proanthocyanidins. Anthocyanins have been known to be highly protective and therapeutic against especially age-related diseases such as hypertension, cardiac infraction and cerebral infarction. Additionally, because the colors of anthocyanins could help to ease psychic and physical troubles or tiredness, the anthocyanins could not only relax us, but also the colors themselves could prevent and remedy many diseases, especially, age-related diseases such as hypertension, heart failure, stroke and diabetes. Generally, anthocyanins have antioxidant properties, which could protect and enhance our body systems with bioactive abilities such as the immuno-, anticancer-, antimicrobial potencies and others.

Anthocyanins have been used as part of therapeutic herbal folklore medicines with the phytochemicals, because actually, bilberry (*Vaccinium myrtillus*) in Europe has been used to improve menstruation. During World War II, bilberry was also used to enhance the night vision of UK pilots.

Anthocyanins are composed of anthocyanidines and their sugar molecules. Anthocyanins are one of the most typical phytochemicals in the pigments of the plant kingdom with various colors such as carotenoids. Surprisingly, the anthocyanins of over 150 flavonoids are highly antioxidative. To date, it is thought that more than 4000 flavonoids have been identified [7].

Very recently, we reviewed the role of membrane action of flavonoids. The structure of flavonoids enables specific interactions with different membrane proteins (multidrug transporters, voltage-gated and chemically activated ion channels) and also nonspecific interactions with the lipid phase of membranes [8].

2
Functionality of Anthocyanins

2.1
Diverse Health Effects of Anthocyanins

Anthocyanins could dispense effective benefits to diverse diseases including both physical and mental conditions, because the anti-inflammatory properties of anthocyanins could affect collagen formation, the nervous system and have other healthy effects in the human body. For example, anthocyanins could protect the blood vessel system by maintaining the softness of the artery and vein, or protect against capillary damage from high blood sugar levels, which might cause complications for diabetics through oxidative stresses. Moreover, it is thought that diabetes might also cause a dangerous diabetic retinopathy via damaged eye capillaries.

2.1.1 Free Radical Quenching Ability of Anthocyanins

For the investigations of the protective activity of berry varieties against oxidative damage, the antioxidant activities of the fruit juices from different cultivars of thornless blackberries (*Rubus* sp.), blueberries (*Vaccinium* spp.), cranberries (*Vaccinium macrocarpon* Aiton), raspberries (*Rubus idaeus* L. and *Rubus occidentalis* L.), and strawberries (*Fragaria chiloensis* Duch. var. *ananassa* Bailey) against superoxide radicals (O_2^-), hydrogen peroxide (H_2O_2), hydroxyl radicals ($OH^\cdot$), and singlet oxygen ($^1O_2$) were evaluated. Among the different cultivars, the juice of "Hull Thornless" blackberry, "Earliglow" strawberry, "Early Black" cranberry, "Jewel" raspberry, and "Elliot" blueberry were highly antioxidative against these reactive oxygen species (ROS). Generally, blackberries had the highest antioxidant activity against O_2, H_2O_2 and OH, followed by strawberry. Strawberry had the highest $^1O_2$ scavenging activity, followed by blackberry. Cranberries showed the lowest scavenging activity against H_2O_2. Meanwhile, blueberries had the lowest antioxidant capacity against $OH^\cdot$ and $^1O_2$. Interestingly, significant differences were observed among these three berries in their scavenging abilities against ROS.

β-Carotene had by far the highest scavenging activity against $^1O_2$ but had absolutely no effect on H_2O_2. Ascorbic acid was the most efficient scavenger for H_2O_2.

However, α-tocopherol and ascorbic acid scavenged the $OH^\cdot$ only by 15.3 and 0.88%, respectively. These scavenging abilities represented a wide range of scavenging capacities of each compound, depending on the type of free radical species. Glutathione (GSH) had a higher superoxide radical ($O_2^{\cdot -}$) scavenging activity when compared to the other three antioxidants of α-tocopherol, β-carotene and ascorbic acid [2].

The prevention of toxin paraquat-induced oxidative stress in rats was studied by the administration of acylated anthocyanins from red cabbage. The control rats decreased the food intake and body weight gain, and increased the lung weight and atherogenic index by feeding the rats with paraquat diet. On the other hand, the oxidative stresses of the rats were apparently inhibited by supplementing the paraquat diet with the acylated anthocyanins. Paraquat feeding increased the concentration of thiobarbituric acid-reactive substances (TBARS) in liver lipids, and decreased the liver triacylglycerol level. The toxic effects of the paraquat diet might be suppressed by supplementation of the acylated anthocyanins, thus improving or preventing the side effects. Additionally, the catalase activity in the liver mitochondrial fraction was markedly decreased by feeding the paraquat diet, however, this decrease and suppression could be partially improved by the oral simultaneous administration of acylated anthocyanins. An increase in the NADPH-cytochrome-P450-reductase activity in the liver microsome frac-

tion by a paraquat diet was suppressed by oral administration of acylated anthocyanin supplement. The acylated anthocyanins in the red cabbage might prevent the paraquat-induced oxidative stress in the rats [9].

An oral administration of cyanidin 3-*O*-β-D-glucoside (C3G) of anthocyanins to the rats potently scavenged the active oxygen species in the experimental rats. The loading of the hepatic ischemia-reperfusion (I/R) as an oxidative stress model to rats elevated the liver TBARS concentration and the serum marker enzyme activities for the liver injury, and lowered the liver GSH concentration. Whereas, the oral administration of C3G to the rats significantly suppressed the hepatic I/R-induced changes. These results might suggest that C3G might act as a potent antioxidant in vivo under oxidative stress. Moreover, for clarification of the mechanism of action of C3G, both the absorption and metabolism of C3G in the rats were measured. The C3G of anthocyanin appeared in the plasma immediately after its oral administration. Protocatechuic acid of a phenolic acid, a possible degradation product of cyanidin C3G, existed also in the plasma. In the liver and kidneys, the C3G could be easily metabolized to the methylated C3G derivative. This suggests that cyanidins of anthocyanins might be a potent antioxidant in the rat in vivo model [10]. Similarly, cyanidin 3-*O*-β-D-glucoside protected the cell membrane lipids from the TBARS-induced oxidative stress [11].

The plant-derived polyphenolic flavonoids including fruit, vegetables, tea and wine have been compared for their antioxidant activities against the radicals generated in the aqueous phase. The flavonoids such as quercetin and cyanidin with 3′,4′-dihydroxy substituents in the B ring and conjugation between the A and B rings had antioxidant potentials four-times higher than that of Trolox, a vitamin E analog. On the other hand, when the *ortho*-dihydroxy substitution such as in kaempferol was removed, or the electron delocalization potential by reducing the 2,3-double bond in the C ring such as in catechin and epicatechin was reduced, the antioxidant activity was reduced by more than 50% and their antioxidative effects were significantly weakened, but the antioxidant activities were still higher than the activity of α-tocopherol (vitamin E) or ascorbic acid. The importance of the positions and extents of the hydroxylation on both the A and B rings for the antioxidant activity of these plant flavonoids has been shown [12].

Pelargonidin (Pel) with a mono-hydroxyl group on the B-ring of anthocyanin as a potent inhibitor of tyrosine nitrosylation in vitro scavenged a peroxynitrite ($ONOO^-$). When Pel was reacted with $ONOO^-$, two products were generated and identified as *p*-hydroxybenzoic acid and 4-hydroxy-3-nitrobenzoic acid by a high-performance liquid chromatography (HPLC). Pel could apparently inhibit the tyrosine nitrosylation by peroxynitrite, a harmful radical species formed via *p*-hydroxybenzoic acid and 4-hydroxy-3-nitrobenzoic acid [13].

Nasunin of an anthocyanidin delphinidin glycoside derivative in eggplant peels inhibited the lipid peroxidation of the brain homogenates, suggesting

that nasunin is a potent O_2^- scavenger and protective against lipid peroxidation [14].

2.1.2 Inflammation and Collagen

Ischaemia reperfusion injury in hamster cheek pouch microcirculation was improved by the oral administration of *Vaccinium myrtillus* anthocyanosides. The ischaemia reperfusion induced damage such as an increase in the number of leukocytes sticking to the venular wall and their permeability. The anthocyanosides protected arteriolar tone and induced rhythmic diameter changes in the arterioles. Anthocyanosides could reduce the ischaemia reperfusion-induced microvascular impairments, by protecting the functionality of the vein endothelium, and by attenuating the leukocyte adhesion and improving the capillary perfusion. Especially, the anthocyanins might protect the venular vessel wall and the connective tissue surrounding veins from damage induced by the release of proteases such as elastase and collagenase. The excess release of these proteases could enhance the permeability with concomitant oedema formation. This means that these proteases might damage the connective tissues in the capillaries, because the vein damage might cause the blood to leak into the connective tissues surrounding the veins. Anthocyanins might be released and carried to further damage the blood vessel walls. Anthocyanins could show protective effects as follows: First, anthocyanins might neutralize the enzymes that destroy the connective tissues of veins; second, the antioxidant capacity might prevent the harmful oxidants such as several free radical oxygens which damage the connective tissues. Finally, anthocyanins might repair the damaged proteins in the blood vessel walls [15].

The anti-inflammatory abilities of anthocyanine flavonoids in *Aronia melanocarpa* and rutin-magnesium complex of a water-soluble derivative of rutin were compared with rutin, using histamine- or serotonin-induced inflammation models. Anthocyanine flavonoids were found to be more effective, when compared to rutin in both models. However, the rutin-magnesium complex did not exhibit any anti-inflammatory activity against histamine-induced inflammation. While the potency of anthocyanine flavonoids against the serotonin-induced inflammation was comparable to the potency of rutin, the anti-inflammatory ability of anthocyanins might help to inhibit allergic reactions triggered by the histamine or serotonin [16].

2.1.3 The Nervous System

Generally, it has been thought that age-related neuronal-behavioral decrements might be caused by oxidative stress, and that the brain damage could

be improved by antioxidants. In fact, the oral administration to rats of supplements originating from plants such as strawberry, spinach, or blueberry was effective in reversing age-related deficits in several neuronal and behavioral parameters including the oxotremorine (an agonist to muscarine-like acetylcholine receptor), the enhancement of the K^+-evoked release of dopamine from the striatal slices, the carbachol-stimulated GTPase activity, the striatal Ca^{45} buffering in the striatal synaptosomes, the motor behavioral performance on the rod walking and accelerod tasks, and in the Morris water maze performance. Therefore, in addition to their known beneficial effects on cancer and heart disease, phytonutrients such as anthocyanins and flavonoids which are contained in antioxidant-rich fruits and vegetables might be effective in reversing or postponing the brain's neuronal and behavioral aging process [17].

The Ca^{2+} hypothesis of brain aging and dementia is based on the accumulation of the implicated Ca^{2+} dysregulation. The hippocampal or cortical neurons of rodents and rabbits have revealed the age-related increase in the slow afterhyperpolarization, Ca^{2+} spikes and currents, Ca^{2+} transients, and L-type voltage-gated Ca^{2+} channel (L-VGCC) activity. These changes have been associated with age-related deficits in learning or memory. It is suggested that the Ca^{2+} hypothesis might increase the L-VGCC activity which drives many other Ca^{2+}-related biomarkers for hippocampal aging. Additionally, aging- or Alzheimer's disease-related alterations in the Ca^{2+} release from ryanodine receptors (RyR) on the intracellular stores have been reported. The Ca^{2+}-sensitive RyR channels might amplify the plasmalemmal Ca^{2+} influx by the mechanism of Ca^{2+}-induced Ca^{2+} release (CICR), because a preferred functional link exists between L-VGCCs and RyRs which operate in series in heart and some brain cells. Thus, it is thought that the increased CICR plays a necessary role in the emergence of Ca^{2+}-related biomarkers of aging, because, according to an expanded L-VGCC/Ca^{2+} hypothesis, aging and pathological changes might occur in both L-type Ca^{2+} channels and RyRs, and interact with the abnormally amplified Ca^{2+} transients. After these processes, the increased transients might be responsive for the dysregulation of multiple Ca^{2+}-dependent processes and, through somewhat different pathways, in the accelerated functional declines during aging and Alzheimer's disease [18].

Blueberry has more beneficial effects on the motor and cognitive behavior when compared to the effects on antioxidative or anti-inflammatory activities. The high activity for the nervous syndrons might include alterations of their signaling [19]. Especially, it is thought that flavonoids including anthocyanins could have potent effects on the cell signaling as follows: (1) Delphinidin inhibited the serum- and vascular endothelium growth factor-induced bovine aortic endothelial cell (BAECs) proliferation. This antiproliferative effect of delphinidin is induced by the extracellular signal-regulated kinase (ERK)-1/2 activation which depends on the nitric oxide (NO) pathway. The

effect could be correlated with the suppression of the cell progression by blocking the cell cycle in the G(0)/G(1) phase. Additionally, suppression of the cell cycle progression is also associated with modulation of the mitogenic signaling transduction cascade [20]. (2) The effect on the antideath signaling cascade by proanthocyanidins in grape seed proanthocyanidin extract (GSPE) using rats was examined. The results indicated the significant induction of the JNK-1 and c-fos proteins in the ischemic/reperfused myocardium was inhibited by the proanthocyanidin extract. At the same time, GSPE significantly reduced the apoptotic cardiomyocytes in the ischemic/reperfused hearts. GSPE also could significantly reduce the appearance of reactive oxygen species (ROS) in the hearts. Improved postischemic contractile recovery was achieved with GSPE suggesting its cardioprotective action. It has been suggested that the GSPE might play an effective role as an antioxidant against some harmful radical species. The cardioprotective properties could be at least partially attributed to its ability to block antiapoptotic signals through the inhibition of the proapoptotic transcription factor and gene, and two proteins such as JNK-1 kinase (JNK-1) and c-Jun *N*-terminal kinase (c-Jun) [21].

Phytochemicals such as flavonoids might competitively bind to and regulate two human estrogen receptors (ERα and ERβ), mimicking the antiestrogen actions of the endogenous estrogen (17β-estradiol). Interestingly, some of these estrogenic phytochemicals have also been shown to affect other signal transduction pathways such as the receptor tyrosine kinases and the mitogen-activated protein kinases (MAPK). However, the phytochemicals of flavonoids such as flavone, apigenin, kaempferide and chalcone especially have potent antiestrogenic activity. The antiestrogenicity of these flavonoids is not related to their ER binding capacity, suggesting the alternative signaling as a mechanism for their antagonistic effects which possibly act on the transcription factor activator protein-1 (AP-1). Among these flavonoids, chalcone was the only phytochemical that could activate all three transcription factors in this study, but inhibited phorbol myristoyl acetate-induced c-Jun activity. These results suggest that these flavonoids could affect the multiple signaling pathways which converge at the level of the transcriptional regulations, and selectively regulate the MAPK-responsive pathways which influence human health and disease [22].

The blueberry could reverse the deleterious effects of aging on the motor behavior and neuronal signaling in senescent rodents. In addition here, it has been represented that the protective mechanisms are derived from the blueberry-induced enhancement of memory-associated neuronal signaling such as the extracellular signal-regulated kinase (ERK-1/-2) and alterations in the neutral sphingomyelin-specific phospholipase C activity. This suggests it could overcome the genetic predisposition to Alzheimer's disease through diet choices [23].

Peroxynitrite ($ONOO^-$), an anion of peroxynitrous acid, is produced by interaction between NO and superoxide anion. Peroxynitrite could be formed

in a fast reaction between these radicals, and the cytotoxic peroxynitrite could react with all classes of biomolecules such as DNA or membranes. Then, the cytotoxic peroxynitrite might cause many pathological phenomena such as arteriosclerosis, hypertension and diabetes. Tyrosine and tyrosyl residues in proteins could be nitrated as an important mechanism of the derangement of the biochemical signal transduction by peroxynitrite [24].

This means that peroxynitrite-mediated nitration of tyrosine residues in enzymes and the enzyme proteins could be believed to be a major cause of brain damage in neurodegenerative diseases and in brain trauma. It could be thought that the nitrated tyrosine might block nerve growth-factor receptor sites, thus anthocyanins might prevent new neural growth and inhibit repair processes. By preventing the tyrosine nitration, for example, anthocyanin pelargonidin could help to protect against neurological diseases [24]. Additionally, the blueberry has even been found to reverse age-related neurological deficits in rats [25].

The nutritional improvement achieved by increasing the dietary intake of many diverse kinds of fruits and vegetables could retard or even reverse age-related decline in brain function, and cognitive and motor performances in aging Fischer 344 rats loaded with oxidative stress in their brains. The fruit or vegetable extracts containing the high antioxidative phytochemicals such as blueberry, spinach and other plant-derived foods could decrease the damage from oxidative stress on neuronal signaling and behavioral deficits. The blueberries were effective in inhibiting other age-related changes in brain and behavior. Additionally, the blueberry also could decrease inflammation, and oxidative stress in the gastrocnemius and quadriceps muscles. The blueberry most effectively could protect the cell membranes from oxidative stress-induced damage, due to the antioxidant action of anthocyanins that easily penetrate the cell membranes. The increasing of dietary intake of high antioxidative fruits and vegetables such as blueberry or spinach might be necessary to maintain maximized neuronal and cognitive functioning [25].

In order to stay healthy whilst aging it is important to think of the foods that could retard or reverse the deleterious effects of aging. Inflammation and oxidative stress might play important roles in brain aging, because harmful inflammatory markers such as cellular and molecular oxidative damage might increase daily even during normal brain aging. The increase in oxidative stresses to our bodies might be accompanied by concomitant decrease in cognitive and motor performance, surprisingly even in the absence of neurodegenerative diseases in elderly people. Daily intake of a diet rich in anti-inflammatory antioxidants such as anthocyanins and other polyphenols in fruits and vegetables could decrease the incidence of developing age-related neurodegenerative diseases such as Parkinson's disease and Alzheimer's disease. Additionally, anthocyanins might exert beneficial effects through signal transductions and neuronal communication. This nutritional supplementa-

tion might provide therapeutic protection against age-related deficits and neurodegenerative diseases [26].

Generally, the age-related neurodegenerative diseases superimposed on a declining nervous system might exacerbate the motor and cognitive behavioral deficits of aging. The main symptoms of age-related neuronal diseases are severe deficits in memory or motor function.

The consumption of diets rich in antioxidants and anti-inflammatory phytochemicals in fruits and vegetables could epidemiologically lower the risk of developing age-related neurodegenerative diseases such as Alzheimer's or Parkinson's disease. The anthocyanins and flavonoids in fruits such as blueberries might alter oxidative stress signaling and neuronal communication, strongly suggesting that the therapeutic usage of antioxidative phytochemicals including anthocyanins and flavonoids could protect against age-related deficits in cognitive and motor function [27].

2.1.4 Large Blood Vessels

When the arteriolar vasomotions of bilberry (*Vaccinium Myrtillus*) anthocyanosides (Myrtocyan) were examined in the cheek pouch microcirculation of anesthetized hamsters and in the skeletal muscle microvasculature of the unanesthetized hamster skin, the intravenously injected bilberry anthocyanosides could induce vasomotion in the cheek pouch arterioles and terminal arterioles with higher frequency in the smaller vessels. In the skeletal muscle arteriolar networks, the bilberry anthocyanosides increased vasomotion frequency and amplitude in all vessel orders. Consequently, the bilberry anthocyanosides might be effective in both promoting and enhancing arteriolar rhythmic diameter changes, which play an important role in the redistribution of microvascular blood flow and interstitial fluid formation [28].

In 1992, a French paradox was shown by French researchers. Generally, the daily high intake of saturated fats might be positively related to the high mortality due to coronary heart disease (CHD). However, the situation in France is paradoxical in the sense that there is high intake of saturated fats but low mortality from CHD. The French paradox might be related to the high wine consumption in France. Epidemiologically, it is known that the consumption of alcohol at the level of intake in France (20–30 g/day) could reduce the risk of CHD by at least 40%. It is believed that alcohol could reduce CHD by preventing atherosclerosis via the action of high density lipoprotein cholesterol (HDL), but the serum concentrations of HDL in French citizens are not as high in France as in other countries. Re-examination of previous results suggests that, on the whole, moderate alcohol intake could not prevent CHD through an effect on atherosclerosis, but rather through a haemostatic mechanism. Data from Caerphilly of Wales showed that the platelet aggregation

which is related to CHD could be inhibited significantly by alcohol at the levels of the intake associated with a reduced risk of CHD. The inhibition of the platelet reactivity by the wine (alcohol) might be one explanation for the protective effect against CHD in France, because the platelet reactivity in the pilot studies was lower in France than in Scotland [29]. Additionally, a similar relationship also was represented [30].

In fact, the "French paradox" which represents the apparent compatibility of a high fat diet with a low incidence of coronary atherosclerosis has daily been attributed to the regular drinking of the red wines. However, the alcohol content in the wines might not be the sole explanation for the protection. The red wines also contain an abundance of phenolic components, and the antioxidant properties of these phytochemicals might play an important role. Considering the in vitro relationship of phenolics in the red wines with normal human low-density lipoprotein (LDL), the red wine may inhibit the copper-catalyzed oxidation of LDL. The 1000-fold diluted red wines containing 10 mμmol/L total phenolics could inhibit LDL oxidation significantly more than α-tocopherol, suggesting that the non-alcoholic components such as anthocyanins of the red wines fulfil important functions such as antioxidant action against the oxidation of human LDL such as French LDL [31].

These polyphenolics such as anthocyanins and flavonoids might also act as the beneficial in vivo inhibitors of LDL oxidation [32].

The red wines have an abundance of anthocyanins such as delphinidin 3-*O*-β-D-glucoside, petunidin 3-*O*-β-D-glucoside, malvidin 3-*O*-β-D-glucoside, and cyanidin 3-*O*-β-D-glucoside from grape skins [33, 34]. These anthocyanins also might have antioxidant activity against the oxidation of LDL [11].

Anthocyanins of the plant pigments such as elphinidin 3-*O*-β-D-glucoside and cyanidin 3-*O*-β-D-glucoside could be apparently supplied from the fruits, vegetables and other plants including the red wines [35, 36].

Two anthocyanins from the blue flowers of *Evolvulus pilosus* cv. Blue Daze and the blue-purple flowers of *Eichhornia crassipes* exhibited remarkable color stabilities in aqueous solution under mildly acidic conditions. All the plant pigments possess the same chromophore (delphinidin), but the anthocyanin pigments are susceptible to different patterns of glycosylation and acylation. Moreover, one of the pigments has an apigenin 7-glucoside molecule (a flavone) attached to the glycosidic chain by two ester bonds with malonic acid, instead of an aromatic acid and is the only known anthocyanin with such a structure. All the anthocyanin molecules, except one molecule which has only a 3-gentiobioside (a disaccharide) as substituent, could be responsible for the reduction in the hydration constant, when compared with the parent delphinidin 3-glucoside or 3,5-diglucoside molecules. This supports the existence of the intramolecular hydrophobic interactions between the chromophoric skeleton and the acyl or flavonoid groups. The sugar units on the hydrophobicity/hydrophilicity of the pigments might play a role in the

color changes of anthocyanins, depending on the pH (either acidic, neutral or basic). This means that anthocyanin plant pigments are generally stable under acidic conditions, but unstable, rapidly degraded under neutral conditions [37].

The phenolic antioxidant activity in the corn oil emulsions of 17 selected Spanish wines and two Californian wines was examined for their preventive capability for lipid oxidation as dietary antioxidants. The inhibition of hydroperoxide formation [measured as percent of control for 10 μM gallic acid equivalents (GAE)] was increased from 8.4 to 40.2% in the presence of the red wines, from 20.9 to 45.8% with the rosé wines, and from 6.5 to 47.0% with the white wines. The inhibition of hydroperoxide formation at 20 μM GAE was increased from 11.9 to 34.1% in the presence of red wines, from 0.1 to 34.5% with the rosé wines, and from 3.3 to 37.2% with the white wines. The inhibition of the hexanal formation at 10 μM GAE was increased from 23.6 to 64.4% in the presence of red wines, from 42.7 to 68.5% with the rosé wines, and from 28.4 to 68.8% with the white wines. Moreover, the inhibition of the hexanal formation at 20 μM GAE was increased from 33.0 to 46.3% in the presence of red wines, from 11.3 to 66.5% with the rosé wines, and from – 16.7 to + 21.0% with the white wines. The antioxidant effect declined apparently with increasing concentration. The antioxidant activity might be ascribed to the five main groups of phenolics identified in the wines: benzoic acids, anthocyanins, flavan-3-ols, flavonols, and hexanal [38].

The influence of anthocyanins from the chokeberry on the generation of autoantibodies raised against the oxidized serum LDL during pregnancies complicated by intrauterine growth retardation (which manifests as a decreased rate of fetal growth) has been investigated, with 105 pregnant women (55 women for placebo, 60 healthy pregnant women for control). After 1 and 2 months, the anthocyanin group showed a significantly decreased LDL level (from 1104 to 727 μg/mL), whereas the control group showed an increased level of LDL in 2 months. Therefore, chokeberries with natural antioxidants (anthocyanins) might be useful in controlling oxidative stress during pregnancies complicated by intrauterine growth retardation [39].

Cyanidin 3-*O*-*β*-D-glucoside inhibited the generation of thiobarbituric acid reactive substances (TBARS) and lipid peroxidation in the rat serum. No significant differences were observed in the serum concentrations of phospholipid, triglyceride, esterified cholesterol and free fatty acid, when compared with the anthocyanin-fed control groups. This suggests that the anthocyanin intake might increase the resistancy of the serum against ex vivo oxidation without affecting serum endogenous antioxidant levels, and reduce the TBARS generated during serum formation without affecting serum lipid levels [11].

A red wine and other plant-derived polyphenolics induced endothelial NO-dependent relaxation in thoracic aorta from male Wistar rats.

The relaxation was recorded isometrically on the vessels precontracted by the action of norepinephrine, which constricts the blood vessels. The wine fractions enriched in anthocyanins or oligomeric condensed tannins exhibited the endothelium-dependent vasorelaxant activity (maximal relaxation in the range of 59–77%) when compared to the original red wine polyphenolic compounds (RWPC). However, the polymeric condensed tannins elicited a weaker vasorelaxant activity than the original RWPC (maximal relaxation ranged between 20–47%). Moreover, the representatives of other phenolic acid derivatives (benzoic acid, vanillic acid, gallic acid), hydroxycinnamic acid (*p*-coumaric acid, caffeic acid) or the flavanol [(+)-epicatechin] classes were inactive. Among anthocyanins, delphinidin (maximal relaxation being 89%), but not malvidin or cyanidin, showed the endothelium-dependent vasorelaxation. These results suggest that delphinidin of anthocyanins and oligomeric-condensed tannins could reduce cardiovascular mortality, to the extent comparable to that attained by the original RWPCs, and these polyphenols in the wines, fruits and vegetables might be greatly involved in the reduction of cardiovascular mortality [40].

Delphinidin inhibited the serum- and vascular endothelium growth factor-induced proliferation of bovine aortic endothelial cells (BAECs). Interestingly, the antiproliferative effects of delphinidin were triggered by extracellular signal-regulated kinase-1/-2 (ERK-1/2) activation which is distinct from the NO pathway, but is correlated with the G(0)/G(1) arrest of cell cycle progression. Additionally, the suppression of the cell cycle progression might be associated with the modulation of the mitogenic signaling transduction cascade, which includes the over-expression of caveolin-1 and p21 (WAF1/Cip1) and down-expression of Ras and cyclin D1. From these results, the antiproliferative effect of delphinidin might be of importance in preventing both plaque development and stability in atherosclerosis and tumor dissemination in cancers [20].

Similar epidemiologic studies have shown that a diet rich in fruits and vegetables has a beneficial preventive effect on cancer and cardiovascular diseases. The effects of delphinidin of a vasoactive anthocyanin on endothelial cell proliferation and migration as well as on in vivo angiogenesis were measured. The vascular endothelial growth factor (VEGF)-stimulated human umbilical endothelial cell migration and proliferation are potently inhibited by delphinidin. A flow cytometric analysis showed that delphinidin inhibition of the proliferation might strongly be correlated with the G(0)/G(1) arrest of the cell cycle. A Western blot analysis showed that the delphinidin could reverse the VEGF-induced decrease in the expression of cyclin-dependent kinase inhibitor p27 (kip1) and the VEGF-induced increase of cyclin D1 and cyclin A, both of which are necessary to achieve the G1/S transition. In addition, delphinidin could inhibit the neovascularization in vivo in a chorioallantoic membrane model. Then, delphinidin could overcome in vitro and in vivo

angiogenesis and thus appears promising for the development of an anti-angiogenic therapy [41].

Many edible berries with potential sources of natural anthocyanin antioxidants have been examined for the broad spectra of biomedical functionalities in their phytochemicals. The main age-related diseases are cardiovascular disorders, age-induced oxidative stress, inflammatory responses, and diverse degenerative diseases. These berry anthocyanins could improve the neuronal and cognitive brain functions, ocular health and protect genomic DNA integrity. The common berries such as wild blueberry, bilberry, cranberry, elderberry, raspberry seeds, and strawberry are beneficial in both human health and disease prevention. OptiBerry is a new combination of some selected berry extracts such as wild blueberry, wild bilberry, cranberry, elderberry, raspberry seeds, and strawberry and may be pharmacologically effective for health. The OptiBerry exhibited higher antioxidant efficacy by the high oxygen radical absorbance capacity (ORAC) values, new antiangiogenic and antiatherosclerotic activities, and also potential cytotoxicity towards *Helicobacter pylori*, a noxious pathogen responsible for various gastrointestinal disorders including the duodenal ulcer and gastric cancer, when compared to the individual berry extracts. OptiBerry also inhibited the expression of basal monocyte chemoattractant protein-1 (MCP-1), the nuclear factor-kappa-B (NF-κB) and interleukin 8 (IL-8), an inflammatory biomarker, and markedly reduced the incidence of hemangioma and EOMA hemangioendothelioma cell-induced tumor growth. On the basis of these facts, the berry anthocyanins could trigger the genetic signaling to promote human health and disease prevention [42].

The consumption of isoflavone-containing foods such as soybean and soybean foods was examined for their possible beneficial effects on the cardiovascular system in postmenopausal women, using a model system of apolipoprotein E (apoE)-deficient mice subjected to ovarian resection. When compared to the control mice, the ovariectomized mice had a larger arterial lesion area in the aortic root. Feeding the ovariectomized mice with an isoflavone-containing diet (0.055 mg/kJ of total isoflavones/cal of diet) reduced the size of the arterial damage. Neither ovariectomy nor diet had a significant effect on the serum cholesterol level and the urinary isoprostane level, biomarkers for oxidative stress in vivo. The ovariectomized mice showed a greater increase in mRNA abundance for the monocyte chemoattractant protein (MCP)-I in the aorta and in the level of NO secreted by the cultured peritoneal macrophages than did the sham-operated mice. The isoflavone-containing diet could significantly lower both the MCP-I expression and the NO secretion, when compared to the isoflavone-free diet group. These results suggest that the dietary isoflavones might give an antiatherogenic effect by preventing the ovariectomy-induced activation of macrophages [43].

2.1.5 Small Blood Vessels

Anthocyanins help maintain microcapillary integrity by stabilizing the capillary walls. Blocked or reduced oxygen followed by the reestablishment of normal supplies is called "ischemia-reperfusion". Ischemia-reperfusion could create the oxidants which result in white blood cell adhesion to the microcapillary walls, increase the capillary wall permeability, reduce the blood flow, and often cause permanent capillary damage.

One of the classic experiments on anthocyanins was conducted on hamsters in Italy. Ischemia-reperfusion was created in the cheeks by a brief clamping, causing the white cells to clump onto the capillary wall and damage it. The administration of the bilberry supplementation for several weeks after the reperfusion could restore the normal blood supply through the capillaries, reducing the sticking of white blood cells to the vessel walls, and the permeability [15].

Flavonoids are widely distributed in foods and drinks and could act as antioxidants and iron chelators. It was examined whether pycnogenol (a flavonoid extracted from the bark of *Pinus pinaster*) and catechin could minimize the ischemia/reperfusion-induced myocardial mitochondrial damage. The use of pycnogenol in the perfusate did not show any significant effect on the resultant damage, whereas the catechin could suppress the observed elevation of the low molecular weight iron during the ischemia/reperfusion, which might explain the significant reduction in mitochondrial injury. This suggests that some flavonoids might effectively minimize ischaemic/reperfusion injury [44].

2.1.6 Diabetes

The microvessel damage from high blood sugar levels (glycogen level) might also cause in diabetes the complications. The abnormal accumulation of the polymeric blood vessel collagen might be related to the high blood sugars. For example, diabetic retinopathy could lead to blindness. The damage might be caused by an abnormally increased synthesis of the connective tissues, but the leaking capillaries will be first repaired, and then followed by the formation of new capillaries. However, the treatment of 12 adult diabetics with 600 mg anthocyanosides/day for two months significantly reduced the abnormal biosynthesis of the connective tissues, especially the polymeric collagen and structure-glycoproteins. These results suggest that anthocyanosides could help prevent eye damage in diabetics which have been caused by the dysfunction of the synthesis-activities [45].

Diabetes might make the capillaries become more permeable to large molecules. For example, the alterations in capillary filtration of macro-

molecules could be well explained in diabetic patients and experimental diabetes. Various flavonoids including anthocyanosides and *Ginkgo biloba* extracts could effectively cure the experimentally induced capillary hyperfiltration, and elevated the glomerular filtration rate which was often used as a sign of early insulin-dependent diabetes mellitus. The effects of anthocyanosides on the capillary filtration in diabetic rats were examined by the use of an in vivo method for measurement of the capillary filtration of albumin (CFA) in rats. Anthocyanosides might effectively prevent the increase in CFA and the failure of the lymphatic uptake of interstitial albumin in the diabetic animals [46].

One of the most serious diabetic complications is retinopathy, which could cause blindness. Retinopathy occurs when the body attempts to repair the leaking and damaged capillaries, which are caused by overproduction of abnormal proteins. Anthocyanins could prevent the capillaries from leaking in the first place, at the same time anthocyanins also could prevent the abnormal protein production. Thirty out of 40 people with retinopathy showed significant improvement after taking 120 mg anthocyanin daily for several weeks. However, the control subjects showed no apparent improvement [47].

Sambucus nigra (elder) has been used as a traditional folklore treatment of diabetes. In this experiment, first, an aqueous extract of elder (AEE) significantly increased 2-deoxy-glucose transport, glucose oxidation and glycogenesis of mouse abdominal muscle even in the absence of added insulin. Second, in acute 20-min tests, AEE evoked a stepwise stimulation of the insulin secretion from the clonal pancreatic β-cells. The insulin releasing effect of AEE was significantly potentiated by glucose and significantly reduced by diazoxide. AEE did not further enhance the insulin secretion in the cells stimulated by L-alanine, 3-isobutyl-1-methylxanthine or a depolarizing concentration of KCl. The prior exposure of the clonal pancreatic β-cells to the AEE did not alter the subsequent stimulation of insulin secretion induced by L-alanine. Therefore, harmful effects on the cell viability could be reduced. The insulinotropic action of the AEE might be partially dependent on the use of heat during the extract preparation. However, the known constituents in elderberry (*Sambucus nigra* L.) such as lectin, rutin and the lipophilic triterpenoid (lupeol) and sterol (β-sitosterol) could not stimulate the insulin secretion. This suggests that *Sambucus nigra* of the traditional antidiabetic plant might include any other phytochemicals such as anthocyanins or flavonoids with insulin-releasing and insulin-like activity [48].

Similarly, *Coriandrum sativum* (coriander) has also been used as a traditional treatment of diabetes. The coriander incorporated into the diet and drinking water could reduce the hyperglycaemia of the streptozotocin-diabetic mice. Administration of the aqueous extract of coriander increased the 2-deoxyglucose transport (1.6-fold), glucose oxidation (1.4-fold) and incorporation of glucose into glycogen (1.7-fold) of the isolated murine abdominal muscle, more efficiently than insulin. In acute 20 min tests, the aqueous

extract of coriander evoked a stepwise 1.3–5.7-fold stimulation of insulin secretion from a clonal B-cell line. This effect was abolished by diazoxide, and the prior exposure to the extract did not alter the subsequent stimulation of insulin secretion by L-alanine, therefore negating an effect due to the detrimental cell damage. The effect of the extract could be greatly potentiated by glucose and L-alanine, but not by 3-isobutyl-1-methylxanthine. The insulin secretion by the hyperpolarized B-cells in the presence of glucose and KCl was further enhanced by the presence of the extract. These results suggest that *Coriandrum sativummight* might contain phytochemicals such as anthocyanins, flavonoids and other antidiabetic components that possess antihyperglycemic, insulin-releasing and insulin-like activity [49].

A recent Austrian pilot study in collaboration with the US Air Force has shown that oral administration of elderberry extracts reduced stress-induced blood gases, ionized electrolytes, lactate and blood glucose levels [50].

2.1.7 Eyesight

Anthocyanins might also improve eyesight. Thirty-six people were examined for their ability to adapt to the light and dark both before and after the oral administration of bilberry anthocyanins. For several hours after the administration of the anthocyanins, their eyesight was improved significantly, although the effect declined within 24 h [51].

Anthocyanoside extracts of *Vaccinium Myrtillus* improved night vision [52]. Healthy human subjects were tested for dark adaptation, video display terminal (VDT) work-induced transient refractive alteration, and subjective asthenopia symptoms (visual fatigue) after intaking the black currant anthocyanosides (BCAs). The effect of BCAs on the dark adaptation appeared dose-dependently, lowering the dark adaptation threshold. 50 mg BCA intake resulted in no decrease in the average refraction value for the dominant eye after the visual task. On the assessment of the subjective asthenopia symptoms by questionnaire, a significant improvement was recognized on the basis of the statements regarding the eye and lower back after the BCA intake [53].

To investigate whether anthocyanosides improve night vision in normal individuals, three night vision tests such as the full-field absolute scotopic retinal threshold (SRT), dark adaptation rate (DAR) and mesopic contrast sensitivity (MCS) were performed. Eighteen young normal volunteers were randomly assigned to one of three different regimens after multiple oral administrations of 12 and 24 mg anthocyanosides, and a placebo, given twice daily for 4 days. Unexpectedly, supplementation with 12 and 24 mg anthocyanins daily did not improve SRT, DAR and MCS [54].

The effect of bilberry on night visual acuity (VA) and night contrast sensitivity (CS) was examined by using a double-blind, placebo-controlled, and

crossover design for young males with good vision, where eight received placebo and seven received active capsules for three weeks. Active capsules contained 160 mg of bilberry extract (25-percent anthocyanosides), and the placebo capsules contained only the inactive ingredients. The subjects ingested one active or placebo capsule three times a day for 21 days. There was no difference in night VA between the active and placebo treatments during any of the measurement periods. Additionally, there was no significant difference in night CS between the active and placebo treatments during any of the measurement periods. It is, thus, thought that there is no effect of a high dose of the bilberry treatment on night VA or night CS [55].

Thirty-one patients with various types of retinopathy were tested for the effect of anthocyanosides on the retinal vessels. Among these patients with the retinopathy types, especially the patients with diabetic retinopathy improved with a positive influence on the permeability and the tendency for hemorrhage. The internal treatment of the primary retinopathy seems to be very effective [56].

2.1.8 Antitumor Activity

Micromolar concentration of two anthocyanins such as cyanidin and delphinidin in food were found to inhibit the growth of human tumor cells in vitro, whereas malvidin in grapes was less active. The anthocyanins preferentially inhibited the growth of the human vulva carcinoma cell line A431 which overexpressed the epidermal growth-factor receptor (EGFR). Surprisingly, however, the glycosides such as cyanidin-3-β-D-galactoside (idaein) and malvidin-3-β-D-glucoside (oenin) were inactive up to 100 μM. The tyrosine kinase activity of the isolated EGFR from A431 cells was potently inhibited by cyanidin and delphinidin. Malvidin and the glycosides cyanidin-3-galactoside and malvidin-3-glucoside were inactive up to 100 μM. In the intact cells, the influence of anthocyanin treatment on the downstream signaling cascades was investigated by measuring the phosphorylation of the transcription factor Elk-1. The A431 cells were transiently transfected with a luciferase reporter gene construct, where expression is controlled by microtubule-associated protein (MAP) kinase pathway dependent phosphorylation of a GAL4-Elk-1 fusion protein. These results suggest that two anthocyanidins such as cyanidin and delphinidin in the foods might inhibit some human cancer cells by the inhibition of the EGFR in cancer cells, whereas malvidin is less effective. Because cyanidin and delphinidin inhibited the activation of the GAL4-Elk-1 fusion protein in the concentration range of the growth inhibition. Two anthocyanidins also could be the potent inhibitors of EGFR, shutting off the downstream signaling cascades, contributing to the inhibitory properties towards tumor growth [57].

The edible berry anthocyanins possess a broad spectrum of therapeutic and anticarcinogenic properties. The berries contain an abundance of anthocyanins as the plant antioxidants which could provide the pigmentation to the diverse fruits and vegetables. Anthocyanins could repair and protect genomic DNA integrity. It is known that the berry anthocyanins are beneficial in reducing age-associated oxidative stress, as well as in improving the neuronal and cognitive brain function. These six berry extracts such as wild blueberry, bilberry, cranberry, elderberry, raspberry seeds, and strawberry were examined for their antioxidant, cytotoxic, cellular uptake, and anti-angiogenesis activities. And the berry extracts also reduced the unwanted growth of the blood vessels, which could lead to varicose veins and the tumorgenic properties. OptiBerry of a synergistic formula with a combination of the edible berry extracts exhibited a higher ORAC value, lower cytotoxicity, and superior anti-angiogenic properties, than other combinations tested. The anti-angiogenic approaches to treating cancer are necessary in vascular tumor biology. OptiBerry significantly inhibited both H_2O_2- and TNF-α-induced VEGF expression in human keratinocytes. Therefore, VEGF is a key regulator of tumor angiogenesis. OptiBerry could impair tumor angiogenesis. OptiBerry significantly inhibited the basal MCP-1 and inducible NF-κB transcriptions. The endothelioma cells pretreated with OptiBerry showed a diminished ability to form the hemangioma and markedly decreased the tumor growth by more than 50%. These results suggest that a novel anthocyanin-rich berry extract formula of OptiBerry could have novel anti-angiogenic, antioxidant, and anti-carcinogenic potential [58].

The ability of isoflavone extracts from whole soy bread and two soy bread fractions, crumb and crust was examined for their modulating effect on the proliferation of human prostate cancer PC-3 cells. The total isoflavone content in the two fractions of soy bread were similar (3.17 μmol/g dry weight). Both fractions of soy bread contained a similar level of isoflavone aglycones (approximately 24%). The low concentrations of the soy bread extracts stimulated the PC-3 cell proliferation by 47%, when compared to control. However, the proliferation-stimulation effect was reduced at higher concentrations. The soy bread crust extract (10 mg/mL) also could reduce the PC-3 cell proliferation by 15%. On the other hand, wheat bread extracts stimulated cell proliferation at all concentrations tested. Although these extracts from both breads possessed biological activity, only soy bread crust extract reduced PC-3 cell proliferation. This might be related to the presence of soy in this bread [59].

2.1.9 Antiulcer Activity

The bilberry (*Vaccinium myrtillus*) has traditionally been used to treat ulcers, because bilberry might stimulate the production of the stomach mucus and

protect the stomach from injury. The antiulcer effects of 3,5,7-trihydroxy-2-(3,4-dihydroxyphenyl)-1-benzopyrylium chloride (IdB 1027) in bilberry were estimated in various experimental models. The oral administration of this anthocyanidin could antagonize the gastric ulcerations induced by pylorus ligation, stress, nonsteroidal anti-inflammatory drugs, ethanol, reserpine, histamine and duodenal ulceration induced by mercaptamine (cysteamine). In addition, the anthocyanidin antagonized the chronic gastric ulcers induced by acetic acid. An intraperitoneal (*i.p.*) administration of the anthocyanidin was more potent than the oral administration. The anthocyanidin did not affect the gastric secretion in the pylorus-ligated rats and increased the gastric mucus in normal animals regardless of the indomethacin treatment. These results suggest that the anthocyanidin could have a promising antiulcer activity, possibly by producing a higher potentiation on the defensive barriers of the gastrointestinal mucosa. This means that the anthocyanidin could help to increase gastric juice secretion and mucus, whereas, the stomach acid production remains unchanged [60].

Moreover, the effects of the anthocyanidin on the rat gastric mucosa were evaluated. The administration of the anthocyanidin intragastrically at doses ranging from 100 to 400 mg/kg could inhibit the fall in the transmucosal potential difference and the increase in the H^+ back-diffusion induced by acetylsalicylic acid. Moreover, the intragastric administration of the anthocyanidin at doses of 50 and 200 mg/kg increased the gastric bicarbonate secretion. These results suggest that the gastroprotective activity of the anthocyanidin might be mediated by an increase in the efficiency of the gastric mucosal barrier [61].

Silybin flavanolignan of flavonoids has been mixed at an equimolar concentration to phosphatidylcholine to increase its bioavailability. The antioxidant and free radical scavenger action of this new form of silybin has been examined. At one hour after the intragastric administration of silybin (1.5 g/kg body weight) to the rats, the concentration of silybin in the liver microsomes was around 2.5 μg/mg protein, corresponding to a final concentration (around 10 μM) in the microsomal suspension used. Under these conditions, silybin caused about a 40% decrease in the lipid peroxidation induced in microsomes by nicotinamide adenine dinucleotide phosphate (NADPH), CCl_4 and cumene hydroperoxide, probably by scavenging the lipid-derived radicals. The spin-trapping experiments showed that the complexed form of silybin could scavenge the lipid dienyl radicals generated in the microsomal membranes.

In addition, silybin might interact with the free radical intermediates produced during the metabolic activation of CCl_4 and methylhydrazine. These effects suggest that silybin is potentially protective against harmful free radical-mediated toxic damage [62].

The comparative pharmacokinetics of silipide (IdB 1016, a silybin-phosphatidylcholine complex) and silybin flavanolignan of flavonoids were

investigated by measuring the unconjugated and total plasma silybin levels as well as total biliary and the urinary silybin excretion in rats after oral single administration of 200 mg/kg silybin. The cumulative biliary (0–24 h) and urinary (0–72 h) excretion values after administration of silipide accounted for 3.73 and 3.26% of the administered dose, respectively. After a silybin administration, the biliary and urinary excretion accounted for only 0.001 and 0.032% of the dose, respectively. These results indicate that the superior bioavailability of silybin administered orally as silipide, which is a metabolite of silybin, is derived from the apparent increase in the gastrointestinal absorption [63].

The activity of silipide of a silybin-phosphatidylcholine complex was tested in different models of liver damage in rodents. After the oral administration, silipide exhibited a significant and dose-related protective effect against the hepatotoxicity induced by CCl_4, praseodymium, ethanol and galactosamine. The ED_{50} values of silipide for the inhibition of the rise in the aspartate aminotransferase (ASAT) and alanine aminotransferase (ALAT) levels caused by CCl_4 and praseodymium, and for the antagonism of the increase in the liver triglycerides caused by ethanol have ranged from 93 to 156 mg/kg (as silybin). At a dose of 400 mg/kg (as silybin), silipide was also active in protecting against paracetamol-induced hepatotoxicity. Silybin and phosphatidylcholine at doses equivalent to the active doses of silipide had no significant protective effects in these models. This suggests that the liver protective effect of silipide might be related to its antioxidant activities and to a stimulation of hepatic synthesis of RNA and proteins [64].

2.1.10
Treatment of Fibrocystic Disease of the Breast

The treatment with anthocyanosides for at least three months had therapeutic effects on fibrocystic mastopathy. There was a marked improvement in 75 patients, equivalent to 33.78%, their symptoms were reduced in 61 women (27.47%) and disappeared in 14 (6.30%), whereas the treatment had no effect in 72 cases (32.43%). An echopalpation (clinical examination + echography) was extremely valuable in the treatment of these patients, especially with ages below 40. Moreover, three months' therapy for the patients with mastodynia, consequent to fibrous mastopathy, was efficacious in reducing the symptoms and mammary tension. At the same time, it is important to emphasize the virtual absence of any collateral effects [3].

2.1.11
Skin Care

Many plant species can acclimate to changes in ultraviolet-B radiation (UVB, 290–320 nm) exposure. Because of the wide range of UVB targets the plants have evolved diverse repair and protection mechanisms. This evolution might

include increased biosynthesis for UVB exposed compounds, elevated antioxidant activity and increased rates of DNA repair. *Brassica napus* L. c.v. Topas plants could also acclimate quite effectively to environmental increase of UVB because of the accumulation of specific flavonoids in the leaf epidermis.

However, *B. napus* was found to lose other flavonoids when the plant was exposed to ultraviolet-A radiation (UVA) (320–400 nm) and/or UVB [65].

Interestingly, the levels of all the extractable flavonoids in the leaves of *B. napus* plants are decreased in a dose-dependent manner in response to UVA exposure. Additionally, the accumulation of the extractable flavonoids was examined by a shift from the photosynthetically active radiation (PAR) + UVA to PAR + UVB to assess whether the preexposure of the UVA affects the UVB-induced flavonoid accumulation. The UVA preexposures inhibited the UVB-induced accumulation of some flavonoids. This down regulation was particularly evident for quercetin-3-*O*-sophoroside and quercetin-3-*O*-sophoroside-7-*O*-glucoside of two anthocyanins. This is very interesting because the induction of quercetin by UVB is correlated with the UVB tolerance in some plant species. The photobiological nature of these UVA-mediated effects on flavonoid accumulation might suggest complex interactions between the UVA and UVB responses [66].

It is known that one of the most significant risk factors associated with the development of skin disease might be exposure to UVB radiation from the sun. Especially, UVB (ultraviolet B; 290–320 nm; one of three ultraviolets A, B, C) light could activate the inflammatory and apoptotic pathways, leading to the skin damage. Anthocyanins, a group of flavonoids present in many common vegetable or fruit foods, are known for their chemopreventive activity. The efficacy of cyanidin-3-*O*-glucoside (C3G) on the modulation of their cellular responses following the exposure to UVB doses was examined in human keratinocytes (HaCaT). The UVB-exposed cells stimulated the translocation of the transcription factors such as NF-κB and AP-1, overexpression of the proinflammatory cytokine IL-8, cleavage of procaspase-3 (a key step in apoptotic pathway), and DNA fragmentation. However, all these effects elicited by UVB exposure were clearly inhibited by pretreating the HaCaT cells with C3G. Therefore, it was concluded that C3G could protect skin cells against the adverse effects of UVB radiation and be beneficial as a skin photoprotective agent [67].

3
Functionality of Proanthocyanidin

3.1
Diverse Health Effects of Proanthocyanidins

The flavan-3-ols (catechins), flavan-4-ols/flavan-3,4-diols (leucoanthocyanidins), A-type proanthocyanidins, B-type proanthocyanidins including the

procyanidins, prodelphinidins, propelargonidins, proteracacinidins, promelacacinidins, procassinidins, probutinidins, and non-proanthocyanidins with flavan-3-ol constituent units were mainly reviewed in regard to their structures based on references from 2002 [68].

The pine bark and grape seeds contain the flavonoids oligomeric proanthocyanidins (OPCs), which offer antioxidant protection against heart diseases and cancers.

Numerous health benefits have been epidemiologically associated with these proanthocyanins. Significant benefits of proanthocyanins might be their antioxidant protection especially against age-related diseases such as heart diseases and cancers.

Proanthocyanidins is a class of flavonoids. Proanthocyanidins are derived from the flavonoids oligomeric proanthocyanidins (OPCs) and therefore proanthocyanidins have been formerly called condensed tannins. Moreover, all proanthocyanidins have similar structures and the only differences are slight changes in the shape and attachments of the polyphenol rings. The diverse proanthocyanidins could always be found together, ranging from a proanthocyanidin unit to complex molecules with many linked units as the oligomers in nature.

The oligomeric proanthocyanidins are generally found in many kinds of woody plants. The typically most common sources of two proanthocyanidins are grape seeds (*Vitis vinifera*) and the white pine (*Pinus maritima*, *P. pinaster*) of southern Europe, e.g. in France. The grape seeds could contain 7 to 15% more flavonoid oligomeric proanthocyanidins (OPCs) than pine bark and could be more potent as well as more economical [69, 70]. The flavonoids oligomeric proanthocyanidins (OPCs) are also abundant in the blackjack oak (*Quercus marilandica*), horse chestnut (*Aesculus hippocastanum*), witch hazel (*Hamamelis virginiana*) and hawthorn (*Crataegus oxyacantha*), as well as in apples, berries, barley (and beer made from the barley), bean hulls, chocolate, rhubarb, rose hips and sorghum.

3.1.1 Antitumor Activity

Pycnogenols are a heterogeneous group of flavonoids from French maritime pine bark. The name pycnogenols is a term which was given for the designation of flavan-3-ol derivatives by Masquelier et al. [70]

It is thought that talc and poor diet might increase the risk of developing ovarian cancer, however, that a diet rich in fruits and vegetables might generally reduce the incidence of diseases such as cancers, hypertension and heart failure. The safety of talc foods has been generally doubted on especially their role as a possible carcinogen and their known ability to cause irritation and inflammation.

Recently, pycnogenol in a proprietary mixture (Pyc) of water-soluble bioflavonoids extracted from French maritime pine bark has shown selective cytotoxic property against established malignant ovarian germ cells in talc-induced carcinogenesis and Pyc-induced chemoprevention. Normal human epithelial and granulosa ovarian cell lines and polymorphonuclear neutrophils (PMN) were treated with talc, or pretreated with Pyc and talc. The cell viability against ROS by generation and neoplastic transformation by soft agar assay was measured. The talc increased the proliferation, induced the neoplastic transformation and increased the ROS generation time-dependently in the ovarian cells and dose-dependently in the PMN. The pretreatment with Pyc inhibited the talc-induced increase in the proliferation, decreased the number of transformed colonies and decreased the ROS generation in the ovarian cells. These results suggest that talc might contribute to ovarian neoplastic transformation and Pyc may have reduced the talc-induced transformation. Taken together, Pyc might be a potent chemopreventative agent against ovarian carcinogenesis [71].

Proanthocyanidins have recently been focused upon as chemopreventive agents. The potential of the pre-, post- and co-exposure of proanthocyanidin-rich grape seed extract (GSPE) in preventing, reducing and/or delaying dimethylnitrosamine (*N*-nitrosodimethylamine, DMN)-induced liver carcinogenesis and mortality in male B6C3F1 mice was examined. The DMN-induced liver tumor formation (85%) and animal lethality (38%) could be powerfully antagonized by co-administration of GSPE + DMN (tumor positive: 45%; death: 11%). More than 75% of the DMN-treated animals had numerous tumors (five or more), which could be significantly reduced in the GSPE + DMN group (35%). GSPE also negatively influenced other protocols specifically designed to test the initiation and progression phases. Thus, GSPE could be instrumental for the modulation of metabolic cascades and also regulate the orchestration of the cell death processes which are involved during the multistage tumorigenic process. These results suggest that the long-term exposure to proanthocyanidin-rich grape seed extract might serve as a potent barrier to all three stages of the DMN-induced liver carcinogenesis by selectively altering oxidative stress, genomic integrity and cell death patterns in vivo [72].

3.1.2 Large Blood Vessels

The bilberry and other plant-derived bioflavonoids have been used for vein problems for many years in Europe. Bilberry and their flavonoids might represent a similar mechanism in their action, or their active constituents might include the OPCs.

Active ROS induced in the body and the free radical mediated oxidations of biological molecules, membranes and tissues have been suggested

to be a major cause of age-related diseases such as cancer, atherosclerosis and aging. The damage of endothelial cells might lead to cardiovascular and cerebrovascular diseases. The antioxidant effect of pycnogenol (procyanidins extracted from *Pinus maritima*) was examined in vitro using vascular endothelial cells. The confluent monolayers of the bovine pulmonary artery endothelial cells (PAEC) were preincubated with different concentrations of pycnogenol, washed, and then exposed to an organic oxidant *t*-butyl hydroperoxide (*t*BHP) for 3 or 4 h. The cellular injury was assessed by measuring the cell viability with methylthiazol tetrazolium (MTT) assay and by determining the release of the intracellular lactate dehydrogenase (LDH). The lipid peroxidation products of PAEC were monitored as malondialdehyde (MDA) with a thiobarbituric acid fluorometric assay. These tests showed that (1) *t*BHP reduced the cell viability, increased the LDH release, and elevated the MDH production in PAEC, and (2) preincubation with pycnogenol before *t*BHP exposure significantly increased the cell viability, decreased the LDH release, and reduced the MDA production in PAEC. These results suggest that pycnogenol could protect vascular endothelial cells from free radical oxidant injuries and also that pycnogenol might be useful for the prevention of disorders such as age-related diseases associated with diverse active oxidative damage [73].

A co-culture system was used to study the effect of reactive nitrogen species (RNS) generated by mouse RAW264.7 macrophage like-cells grown on the filters and activated by lipopolysaccharide and interferon-γ. On the α-tocopherol levels in ECV 302 endothelial cells of the blood vessel linings, the RNS generated by activated macrophages or by the direct administration of peroxynitrite led to a significant loss of α-tocopherol in endothelial cells. The pre-incubation with proanthocyanidin extracted from pine bark (pycnogenol) enhanced by about 15% basal endogenous levels of α-tocopherol, and protected the endothelial cells. These results suggest that pycnogenol might play an important role in the protection of the endothelium from oxidative stress induced by RNSs, and participate in the cellular antioxidant network [74].

Pycnogenol is a standardized extract composed of a mixture of flavonoids, mainly composed of proanthocyanidins and phenolic acids. These components are highly bioavailable. Pycnogenol has anticardiovascular activities such as vasorelaxation, angiotensin-converting enzyme (ACE) inhibition, and enhancement of microcirculation by increasing capillary permeability. The main mechanism of the induction of these biological effects by pycnogenol might depend on strong free radical-scavenging activity against both ROSs and RNSs. The radical production and scavenging activity of anthocyanidins in pycnogenol could be quantified by electron-spin resonance (ESR). Pycnogenol also could participate in the cellular antioxidant network such as in the ability to regenerate the ascorbyl radical and to protect the endogenous vitamin E and glutathione from oxidative stress. Pycnogenol could modu-

late the NO metabolism in the activated macrophages by quenching the NO radical and inhibiting both inducible nitric oxide synthase (iNOS) mRNA expression and the iNOS activity. The spectrum of different effects of NO on the circulation and the nervous system might predict strongly the use of pycnogenol as an anti-free radical therapy for improvements of immune and circulatory disorders as well as neurodegenerative diseases in the near future. Pycnogenol could bind to proteins, altering their structure and thereby modulating the activity of their key enzymes and proteins involved in their metabolic pathways. Pycnogenol might enhance the redox-sensitive signal transduction pathways and alter their gene expression [75].

The sparing/recycling effect of catechin oligomers (procyanidins) from *Vitis vinifera* seeds (grape seeds) on α-tocopherol was examined in both homogeneous solution and in the heterogeneous phase (phosphatidylcholine liposomes and red blood cells). The HPLC and ESR spectroscopy showed that the tocopheroxyl radical, generated by the reaction of α-tocopherol with the stable radical DPPH (2,2-diphenyl-1-picrylhydrazyl), could be recycled by their procyanidins. Additionally, procyanidins dose-dependently spared the vitamin E from consumption during the autooxidation phase of the hydroxy radical (HO)-induced peroxidation of phosphatidylcholine, by 23% at 0.5 μM and by 65.5% at 3 μM. In this membrane model, the combination of 0.5 μM procyanidins and 2 μM α-tocopherol synergistically delayed the appearance of the conjugated dienes, whereas catechin was active only at 5 μM catechin. In the red blood cells oxidatively stressed upon UVB exposure, procyanidins at 0.1–1.0 μM significantly prevented the loss of vitamin E in the membranes, decreased the membrane lipid peroxidation, and delayed the onset of hemolysis. In contrast, the protective effect of catechin was observed only at much higher concentrations (5–10 μM) [76].

A coronary artery disease (CAD) remains the major cause of mortality and morbidity worldwide. The oxidation of LDLs by the diverse free radicals is associated with the initiation of atherosclerosis and therefore, the CAD will be developed. The LDLs could be protected from the oxidation by antioxidants, but will more likely be oxidized in the deficiency of the diverse antioxidants. Because, the hypercholesterolaemic patients are at a higher cardiovascular risk, the patients must be protected by antioxidants against CAD damage. An increased consumption of red wine with abundant antioxidants has been thought to be a reason for the lower incidence of CAD in France and neighboring areas of Europe. It has been thought that in spite of the abundance of antioxidative activities, the red wine might not be suitable for routine therapy or prevention of CAD. Then, the effects of an antioxidant polyphenolic grape extract were examined on the serum total antioxidant activity and vitamins C and E levels, using 20 single-blinded randomized and placebo-controlled crossover volunteers. The antioxidants were administered two capsules containing 300 mg of grape procyanidin extracts or placebo daily for 5 days. Their blood samples were taken at the start and end of the

study, and assayed for antioxidant activity and vitamins C and E levels. After a washout period of at least 2 weeks, the study was repeated with the second treatment. The extract had no effect on serum vitamin C and E levels, but the extract surprisingly increased the serum total antioxidant activity (TAC), suggesting that the antioxidative proanthocyanins abundantly contained in the grapes might contribute to the higher TAC value [77].

The pharmacological treatment of non-complicated chronic venous insufficiency is a current and well-debated topic. Twenty-four patients with this disease were treated with oral administration of oligomeric proanthocyanidins (Pycnogenols-OPC) at 100 mg/day. The therapeutic efficacy of the treatment on swelling, itching, heaviness and pain was evaluated. Positive clinical responses such as improved or absent symptoms were observed in over 80% of patients, including significant improvement of symptoms after the first 10 days of treatment. The oligomeric proanthocyanidins might be responsible for the rapid reduction of the swelling of the lower limbs and also correlated with the other evaluative symptoms such as heaviness and itching. The most striking responses were observed for itching and pain, however, which completely disappeared during the course of therapy in 80% (for itching) and 53% (for pain) of the patients, respectively. This suggests that a once-a-day oral administration of the oligomeric proanthocyanidins without side-effects might be effective in the treatment of non-complicated chronic venous insufficiency with significant improvement during the first weeks of treatment [78].

3.1.3 Antihepatotoxicity

Oxidative damage is implicated in the pathogenesis of various liver injuries. The ability of pycnogenol as an antioxidant for protection against the CCl_4-induced oxidative stress and hepatotoxicity in rats was examined. The single oral dose of CCl_4 significantly elevated the serum levels of aminotransferase (AST) and alanine aminotransferase (ALT) activities. The histopathological examinations showed the extensive liver injuries, characterized by extensive hepatocellular degeneration/necrosis, fatty changes, inflammatory cell infiltration, congestion, and sinusoidal dilatation. Additionally, an increased concentration of malondialdehyde (MDA) and decreased level of GSH, catalase, superoxide dismutase (SOD), and glutathione-*S*-transferase (GST) were observed in the hepatic tissues. On the contrary, an oral pycnogenol treatment before the administration of CCl_4 significantly prevented the CCl_4-induced hepatotoxicity (elevation of serum AST and ALT activities and histopathological hepatic lesions), in a dose-dependent manner. Moreover, the MDA and GSH levels and catalase, SOD, and GST activities in the hepatic tissues were not affected by the administration of CCl_4, indicating that the pretreatment of pycnogenol efficiently could protect against the CCl_4-induced oxidative damage in these rats. These results suggest that pycnogenol has a protective effect

against the acute hepatotoxicity induced by the administration of CCl_4 in the rats, and that the hepatoprotective effects of pycnogenol might be due to both the inhibition of the lipid peroxidation and the increase of antioxidant activity [79].

The comparative protective abilities of a grape seed proanthocyanidin extract (GSPE) (25–100 mg/kg), vitamin C (100 mg/kg), vitamin E succinate (VES) (100 mg/kg) and β-carotene (50 mg/kg) on 12-*O*-tetradecanoylphorbol-13-acetate (TPA)-induced lipid peroxidation and DNA fragmentation in the hepatic and brain tissues, as well as production of the ROSs by peritoneal macrophages, were examined. The oral administration to the mice of GSPE (100 mg/kg), vitamin C, VES and β-carotene decreased the TPA-induced ROSs production, as evidenced by the decrease in the chemiluminescence response in the peritoneal macrophages, and cytochrome c reduction. The GSPE, vitamin C, vitamin E and β-carotene decreased the TPA-induced DNA fragmentation in the hepatic and brain tissues. Similar results were observed with respect to the lipid peroxidation in the hepatic mitochondria and microsomes and in the brain homogenates. GSPE exhibited a dose-dependent inhibition against the TPA-induced lipid peroxidation and DNA fragmentation in liver and brain, as well as a dose-dependent inhibition of the TPA-induced ROSs in the peritoneal macrophages. These results suggest that GSPE and other antioxidants might provide significant protection against TPA-induced oxidative damage, and that GSPE showed higher antioxidant activity compared to other antioxidants [80].

The genotoxic and antigenotoxic activities of catechin, hamamelitannin and two proanthocyanidin fractions from the bark of *Hamamelis virginiana* L., were examined against a metabolically competent human hepatoma cell line (HepG2). The DNA-migration was calculated as Olive tail moment (OTM). Catechin and a low-molecular weight proanthocyandin fraction only slightly increased the OTM up to 166 μg/mL, whereas hamamelitannin and the proanthocyanidin fraction with higher molecular weight led to a twofold enhancement of OTM at the same concentrations. These effects were dose-independent. The treatment of the cells with the test catechin and two proanthocyanidin (2–166 μg/mL) prior to the exposure to benzo[*a*]pyrene (10 μM, 2.5 μg/mL) led to a significant reduction in the induced DNA damage. The inhibitory effects of proanthocyanidins were stronger than those of catechin and hamamelitannin; the lowest effective concentrations were about 2 μg/mL. While the benzo[*a*]pyrene toxification towards cytochrome P450 was not inhibited by the catechin, hamamelitannin and two proanthocyanidins, their detoxification by GST was induced by catechin and the higher molecular weight proanthocyandin fraction. The combination with the ultimate metabolite of benzo[*a*]pyrene, (±)-anti-benzo[*a*]pyrene-7,8-dihydrodiol-9,10-epoxide (BPDE; 5 μM, 1.5 μg/mL), was strongly inhibitory, suggesting that the observed protective effects might be caused by their scavenging of the ultimate mutagen by catechin, hamamelitannin or the two

proanthocyanidins. The exposure of the HepG2 cells to the compounds (catechin, hamamelitannin and two proanthocyanidins) after benzo[*a*]pyrene treatment could not influence the benzo[*a*]pyrene-induced DNA damage, suggesting that the repair mechanisms might not be affected [81].

For an understanding of the bioavailability and mechanistic pathways of the cytoprotection by IH636 grape seed proanthocyanidin extract (GSPE, commercially known as ActiVin), a series of in vitro and in vivo studies were carried out. On the comparative protective abilities of GSPE, and vitamins C and E, their single and combination administrations were assessed against a smokeless tobacco extract (STE)-induced oxidative stress, DNA fragmentation and apoptotic cell death in a primary culture of normal human oral keratinocytes. The GSPE protected against the STE-induced oxidative stress, DNA damage and apoptotic cell death, more efficiently than vitamins C and E, in the single or combination administrations. The bioavailability and protective ability of GSPE were examined against the acetaminophen (AP)-induced hepato- and nephrotoxicity, amiodarone (AM)-induced lung toxicity, doxorubicin (DX)-induced cardiotoxicity and dimethylnitrosamine (DM)-induced spleenotoxicity in the mice. GSPE exposure prior to the administration of drugs/chemicals such as AP, AM, DX or DM treatments near-completely protected and inhibited both apoptosis and necrosis. The DNA damage in various tissues triggered by these agents was significantly reduced in the GSPE-fed mice. Furthermore, the histopathological examination of the multiple target organs had similarly positive results. The results suggest that GSPE exposure could be bioavailable and provide significant multiorgan protection against these structurally diverse drug- and chemical-induced toxic compounds such as AP, AM, DX or DM. Additionally, the GSPE also exhibited free radical scavenging ability, anti-endonucleolytic activity, cytochrome P450 2E1 inhibitory activity, antinecrotic, antiapoptotic and anticarcinogenic activities, modulatory effects on the antioxidative and apoptotic regulatory genes such as Bcl2, c-myc and p53, which might be responsible for the novel chemoprotective properties exhibited by this GSPE [82].

Several molecular events in the apoptotic or necrotic death of acetaminophen (AAP) induced-hepatocytes appear to be well defined. Recently, some studies also indicate that the select expression of the *bcl*-Xl gene is possibly modified during AAP-induced liver injury. A 7-day grape seed proanthocyanidin extract (GSPE) preexposure induced a dramatic protection and could markedly decrease liver injury and animal lethality caused by AAP, when compared to a short-term 3-day exposure. The abrogation of their toxicity also appeared in the DNA fragmentation pattern. The histopathological evaluation of the liver sections showed a remarkable antagonism of the AAP-toxicity with the novel GSPE, demonstrating therefore the substantial inhibition of both apoptotic and necrotic liver cell death. By an agarose gel electrophoresis, 7-day GSPE preexposure prior to AAP administration

completely blocked the $Ca^{2+}/Mg^{2+} - Ca^{2+}/Mg^{2+}$-dependent-endonuclease-mediated ladder-like fragmentation of the genomic DNA and significantly altered the bcl-Xl expression. Seven-day GSPE exposure alone substantially stimulated the expression of the *bcl*-Xl gene in the liver. AAP alone significantly modified the bcl-Xl expression. The GSPE dramatically inhibited the AAP-induced modification of *bcl*-Xl gene expression. These results suggest that the GSPE preexposure might significantly attenuate the AAP-induced hepatic DNA damage, the apoptotic and necrotic cell death of liver cells, and, most remarkably, antagonize the influence of the AAP-induced changes in *bcl*-Xl gene expression in vivo [83].

The mechanism of the protective effects of procyanidins was examined by alcohol-induced mice liver injury. Both the low and high doses of procyanidins reduced the ALT, MDA and ROS content, and increased the SOD level, up-regulated the expression of Cu- and Zn – SOD mRNA and also down-regulated the expression of TLR4 mRNA. It is suggested that the liver protective effects against alcohol-induced liver injuries might be greatly associated with promoting the expression of Cu, Zn – SOD and suppressing the expression of TLR4 mRNA [84].

3.1.4 Antioxidation

Free radicals might be involved in the incidences of various diseases such as arthritis, hemorrhagic shock, atherosclerosis, advancing age, ischemia and reperfusion injury of many organs, Alzheimer and Parkinson's disease, gastrointestinal dysfunctions, tumor promotion and carcinogenesis, AIDS, and other human health problems [85]. The oxidative proanthocyanidins as antioxidants could quench the free radicals and might help to enhance the action of other antioxidants such as vitamin C.

The effect of various flavonoids on the ascorbate radical lifetime was examined by ESR spectroscopy. The ascorbate radical was generated via the reaction between ascorbic acid and ascorbate oxidase. The inclusion of the flavonoids in the ascorbic acid-ascorbate oxidase reaction mixture could greatly affect both the initial intensity of the ascorbate radical and its lifetime. Pycnogenol from natural sources (200 μg/mL) prolonged the ascorbate radical lifetime to 80 min, four times that of the control (20 min). The flavonoids could either be regenerating ascorbic acid from dehydroascorbic acid (oxidized form), or interacting with ascorbate oxidase, thus preventing a binding of ascorbic acid with ascorbate oxidase. When *p*-cresol, a known ascorbate oxidase inhibitor, was added to the ascorbic acid-ascorbate oxidase reaction mixture, the ascorbate radical signal intensity was dramatically reduced and did not display the time-dependent decay observed with the flavonoids. This suggests the direct interaction between the flavonoids and ascorbate radical.

Similarly, myricetin also could compete with ascorbic acid for ascorbate oxidase [86].

Antioxidants are potent scavengers of free radicals and serve as inhibitors of neoplastic processes. A large number of synthetic and natural antioxidants have been demonstrated to induce beneficial effects on human health and prevent many diseases. However, the structure–activity relationships, bioavailability and therapeutic efficacy of the antioxidants might differ extensively. The diverse oligomeric proanthocyanidins, naturally occurring antioxidants widely available in fruits, vegetables, nuts, seeds, flowers and bark, are known to possess a broad spectrum of biological, pharmacological and therapeutic activities against the damage induced by free radicals and oxidative stress. The concentration- or dose-dependent free radical scavenging ability of the grape seed proanthocyanidin extract (GSPE) both in in vitro and in vivo models was examined and compared to the free radical scavenging ability of GSPE with vitamins C, E and β-carotene. The GSPE was highly bioavailable and protected against the free radicals and free radical-induced lipid peroxidation and DNA damage more efficiently than vitamins C, E and β-carotene. GSPE showed cytotoxicity towards human breast, lung and gastric adenocarcinoma cells, whereas the GSPE also enhanced the growth and viability of normal human gastric mucosal cells. GSPE could protect against tobacco-induced oxidative stress and apoptotic cell death in human oral keratinocytes, more efficiently than vitamins C and E, singly and in combination. GSPE showed an excellent protection against acetaminophen-induced liver and kidney damage by regulating the *bcl*-X(L) gene, DNA damage and presumably by reducing oxidative stress. GSPE represented excellent protection against myocardial ischemia-reperfusion injury and myocardial infarction in rats. GSPE upregulated the *bcl*(2) gene and downregulated the oncogene *c-myc*. The topical application of GSPE enhanced the sun protection factor in human volunteers, as well as improving chronic pancreatitis in humans. These results suggest that the GSPE might provide excellent protection against oxidative stress and free radical-mediated tissue damage [85].

The effects of a smokeless tobacco extract (STE) on the lipid peroxidation, cytochrome c reduction, DNA fragmentation and apoptotic cell death in normal human oral keratinocyte cells were examined and the protective abilities of three selected antioxidative vitamins C and E, and a novel grape seed proanthocyanidin (IH636) extract (GSPE) were assessed. The treatment of the cells with 300 μg STE/mL induced 1.5–7.6-fold increases in the lipid peroxidation, cytochrome c reduction and DNA fragmentation. The addition of three antioxidants to the cells treated with STE reduced the lipid peroxidation, cytochrome c reduction and DNA fragmentation by 10–54%. Approximately 9, 29, and 35% increases in the apoptotic cell death were observed following treatment with 100, 200, and 300 μg STE/mL, respectively, and 51–85% decreases in apoptotic cell death were observed with the three antioxidants. The results demonstrate that STE produces the oxidative tissue damage and

apoptosis, which could be attenuated by antioxidants including vitamin C, vitamin E, a combination of vitamins C plus E and GSPE. GSPE could exhibit better protection against STE than vitamins C and E, singly and in a combination of vitamins C plus E [87].

3.1.5 Anti-Atherosclerosis

The oxidized LDL might damage cells which connect the blood vessel walls by stimulating numerous responses including inflammation, smooth muscle cell proliferation and clotting mechanisms, all of which might lead to atherosclerosis.

The wine polyphenols were examined for their capacity to protect the lipid and protein moieties of their porcine LDL during oxidation. The efficiency of resveratrol (3,4′,5-trihydroxystilbene), and their defined flavonoids was compared to that of a wine extract (WE) containing proanthocyanidols. The efficiency of resveratrol for protecting the polyunsaturated fatty acids (PUFA) was higher than the efficiency of flavonoids in copper-induced oxidation and lower in 2,2′-azobis-(2-amidinopropane) hydrochloride (AAPH, a radical initiator)-induced oxidation. The LDL receptor activity of resveratrol was evaluated by flow cytometry. The incubation of Chinese hamster ovary cells (CHO-K1) with fluorescein isothiocyanate (FITC)-labeled LDL oxidized for 16 h reduced significantly the proportion of the fluorescent cells from 97% to 4%. Resveratrol and flavonoids (40 μM) or WE (20 mg/L) completely recovered the uptake of the copper-oxidized LDL and the AAPH-oxidized LDL, respectively. This might suggest that resveratrol is more effective than flavonoids as a chelator of the copper and less effective as a free-radical scavenger. Moreover, the flavonoids showed that WE, which contained monomeric and oligomeric forms of flavonoids and phenolic acids, could protect the oxidations of the LDL by two mechanisms [88].

Pycnogenol exhibited protective effects which could be beneficial for the prevention of chronic age-related diseases such as atherosclerosis. These main effects might come from its antioxidant and free radical-scavenging activity. The possibility that pycnogenol exerts anti-NO vascular effects against the stimulation of NO production by vascular endothelial cells was examined. In the in vitro experiments, pycnogenol (1–10 μg/mL) could relax their epinephrine (E)-, norepinephrine (NE)-, and the phenylephrine (PE)-contracted intact rat aortic ring preparations in a concentration-dependent manner. However, when the endothelial lining of the aortic ring was removed, pycnogenol had no effect, indicating the involvement of the endothelium-dependent relaxing (EDR) effect. This EDR response was caused by the enhanced NO levels, because *N*-methyl-L-arginine (NMA) of a NOS inhibitor could reverse or prevent the relaxation, and this response, in turn, could be reversed by the addition of L-arginine of an endogenous substrate for

NOS. The pycnogenol-induced EDR maintained the high levels of SOD by the exposure to the intact rings. In addition to the relaxation, the preincubation of aortic rings with pycnogenol (1–10 μg/mL) inhibited the subsequent epinephrine (E)- and norepinephrine (NE)-induced contractions in a concentration-dependent manner. Among three fractions of pycnogenol, fraction 3 (oligomeric procyanidins) significantly enhanced the potent EDR activity. These results suggest that pycnogenol with the antioxidant activity could stimulate the constitutive endothelial NOS (eNOS) activity to increase the NO levels, which could inhibit and modulate vasoconstrictor effects by epinephrine (E) and norepinephrine (NE). Furthermore, pycnogenol decreased the platelet aggregation and adhesion, as well as inhibited the LDL cholesterol oxidation, all of which could protect against atherogenesis and thrombus formation [89].

The NO has diverse physiological roles and also contributes to immune surveillance against viruses, bacteria, and other parasites. However, the excess production of NO might cause various diseases such as arthritis, diabetes, stroke, septic shock, autoimmune conditions, chronic inflammatory diseases, and atherosclerosis. The cells might respond to their activating or depressing stimuli by enhancing or inhibiting the expression of the enzymatic machinery which produce NO. Thus, the maintenance of a tight regulation of NO production is important for human health. Phytochemicals have been traditionally utilized in ways to treat their pathologies which generally disregulate the NO production. Then, the scavenging activity of pycnogenol against the reactive oxygen and nitrogen species, and its effects on the NO metabolism in the mouse macrophage-like cells RAW264.7 were examined. RAW264.7 cells were activated by LPS of bacterial wall components and interferon (IFN-γ), which induced the expression of large amounts of iNOS. The preincubation of the cells with the physiological concentrations of pycnogenol significantly reduced the NO generation. This effect of pycnogenol might be caused by the ROS and NO scavenging activity, inhibition of iNOS activity, and inhibition of the iNOS-mRNA expression, or a combination of these activities. These biological activities of pycnogenol and other polyphenols might be beneficial for the therapy of age-related diseases [90].

The effects of a bioflavonoid mixture of pycnogenol were assessed on the platelet function in humans. Cigarette smoking increased the heart rate and blood pressure. These increases were not influenced by the oral consumption of pycnogenol or aspirin just before smoking. However, the increased platelet reactivity yielding to the aggregation 2 h after smoking could be prevented by 500 mg aspirin or 100 mg pycnogenol in 22 German heavy smokers. In a group of 16 American smokers, the blood pressure increased after smoking. It was unchanged after intake of 500 mg aspirin or 125 mg pycnogenol. In another group of 19 American smokers, the increased platelet aggregation was more significantly reduced by 200 mg pycnogenol than either 150 or 100 mg pycnogenol. Moreover, a single administration of the 200 mg pyc-

nogenol could still remain effective for over 6 days against smoking-induced platelet aggregation. However, the smoking-induced platelet aggregation was inhibited by 500 mg aspirin as well as by a lower range of 100–125 mg pycnogenol. Aspirin increased significantly the bleeding time from 167 to 236 s while pycnogenol did not. These results suggest that pycnogenol is effective for the prevention of platelet aggregation [91].

The antiatherosclerotic effect of proanthocyanidin-rich grape seed extracts was examined in cholesterol-fed rabbits. The proanthocyanidin-rich extracts [0.1% and 1% in diets (w/w)] did not change the serum lipid profile, but reduced the level of the cholesteryl ester hydroperoxides (ChE-OOH) induced by 2,2′-azo-bis(2-amidinopropane-dihydrochloride (AAPH), the aortic malonaldehyde (MDA) content and severe atherosclerosis. The immunohistochemical analysis revealed a decrease in the number of the oxidized LDL-positive macrophage-derived foam cells on the atherosclerotic lesions of the aorta in the rabbits fed the proanthocyanidin-rich extract. When the proanthocyanidin-rich extract was administered orally to the rats, proanthocyanidin was detected in the plasma. In an in vitro experiment using human plasma, the addition of the proanthocyanidin-rich extract to the plasma inhibited the oxidation of cholesteryl linoleate in the LDL, but not in the LDL isolated after the plasma and the extract were incubated in advance. From these results, proanthocyanidins of the major polyphenols in red wine might trap ROSs in the plasma and interstitial fluid of the arterial wall, and consequently display antiatherosclerotic activity by inhibiting the oxidation of the LDL [92].

One of the key elements of a Mediterranean diet is the use of wine, usually taken with foods in Italy, France, Greece and neighboring countries. Besides the evidence from human experience and ancient medicine, the modern experimental data could support the notion that the most significant protective effect of wine on cardiovascular disease might be produced by lowering the oxidative damage to the plasma lipoproteins. It could be proposed that this oxidative damage might be mediated by eating various foods containing oxidized lipids. In fact, eating a daily meal containing diverse lipids could elevate the plasma level of the lipid hydroperoxides and also the susceptibility to the oxidized LDL. The postprandial increase in the plasma level of an oxidized form of the LDL, with the unfolded and sinking apolipoprotein (apoB) in the core, might be a valuable biomarker for the food-derived oxidative stress. The intake of wine together with daily foods could minimize the postprandial rise in the lipid hydroperoxides and LDL-hydroperoxides, and decrease the LDL oxidizability. The main antioxidant principles are procyanidins. These procyanidins are considered to be better antioxidants than the corresponding monomers with catechol groups. The hydrogen transfer mechanism for the radical-scavenging reaction might possibly make the reaction more specific for peroxyl radicals, independent of the pH. Additionally, the fast intramolecular disproportion among the aroyl radicals could stimulate the antioxidant

reaction by decreasing the oxidation potential and increasing the reaction rate. Apparently, the wine procyanidins could prevent the lipid oxidation of the foods in the digestive tract, and the elevation of oxidants in the postprandial plasma. Therefore, the limited bioavailability of anthocyanidins will not likely affect their relevance as key elements for optimizing nutrition and reducing the risk of atherogenesis. The oral administration of grape seed procyanidins protected rabbits from a high cholesterol diet, not only by decreasing the plasma lipid peroxides, but inhibiting the lipid-laden foam-cell deposition. The wine drinking during meals could be beneficial in preventing the development of atheromatous lesions even under hypercholesterolemic conditions [93].

Postprandial hyperlipemia could be one of the risk factors for atherosclerosis because the mechanism might be related to postprandial increases of plasma lipid hydroperoxides (LPOs), which affect the normal balance between the oxidant and antioxidant, and enhance the susceptibility of the transformation of LDL into its oxidized form. Wine intake in humans could constantly prevent their transformation. The effect of supplementation to a meal with the grape seed proanthocyanidins on plasma postprandial oxidative stress was examined. The LPO content in chylomicrons of the control meal was 1.5-fold higher than the proanthocyanidin-rich grape seed extract (GSE)(300 mg)-supplemented meal. The plasma antioxidant capacity was elevated by the postprandial administration of the GSE. These results suggest that the supplementation of a meal with GSE might minimize postprandial oxidative stress by decreasing the oxidants and increasing the antioxidant levels in the plasma and then enhancing the resistance to oxidative modification of the LDL [94].

The polyphenols such as anthocyanidins might have a protective effect on atherosclerosis. This concept suggests that the "Recommended Optimal Intake" (ROI) is a more important factor for the antioxidation than the "Recommended Dietary Allowance" (RDA). Now, considering the absence of the appropriate methodology to identify anthocyanidins in the plasma, the analysis of the plasma antioxidant capacity might be a suitable index to define the optimal nutritional intake [95].

On the basis of the results of a diet of several potent flavonoids including proanthocyanidins from grape seeds and the increase of the plasma lipid peroxides in the postprandial state, there might be a close relationship between the postprandial hyperlipidemia and an increased risk of cardiovascular disease. Because, the lipid hydroperoxide levels might be elevated within 2–4 h after the meal and then return to base level, corresponding to daily postprandial hyperlipidemia. The postprandial hydroperoxides could be significantly decreased by the wines, suggesting that the lipid hydroperoxides could be formed and then absorbed during the digestive process [96].

Now, there are many evidences, which support the cardioprotective effects of red wine. These cardioprotective properties of wine might have

been attributed to certain polyphenolic constituents of the grapes such as proanthocyanidins. The proanthocyanidin-fed rats were resistant to myocardial ischemia reperfusion injury as evidenced by their improved recovery of post-ischemic contractile functions. The proanthocyanidin-fed rats revealed a lower incidence of myocardial infarction than the control group, and possessed a cardioprotective effect against ischemia reperfusion injury. These results could suggest that the cardioprotective property might directly scavenge both the peroxyl radicals [which were generated by 2,2′-azo-*bis*(2-amidinopropane) dihydrochloride] and the hydroxyl radicals (which were measured as 7-OH-coumarin-3-carboxylic acid), and finally reduce the oxidative stress caused by ischemia and reperfusion [97].

Epidemiologically, the consumption of wines, particularly of red wine, might reduce the incidence of mortality and morbidity from coronary heart diseases. This has given rise to what is now popularly termed the "French paradox". The cardioprotective effect might be attributed to the antioxidants present in the polyphenol fractions of the red wines. The grapes are rich in diverse antioxidants such as resveratrol, catechin, epicatechin and proanthocyanidins. Interestingly, among these antioxidative phytochemicals, resveratrol is present mainly in the grape skin, whereas proanthocyanidin is present in the seeds. It has been shown that the red wine extract as well as resveratrol and proanthocyanidins are equally effective in reducing myocardial ischemic reperfusion injury, suggesting that these polyphenolic antioxidants might play an important role in the cardioprotection [98].

3.1.6
Cancer Protection

The fruit extracts of four *Vaccinium* species such as lowbush blueberry, bilberry, cranberry and lingonberry were fractionated and screened for the presence of anticarcinogenic compounds. The extracts were investigated in vitro for their ability to induce the Phase II xenobiotic detoxification enzyme quinone reductase (QR) and to inhibit the induction of ornithine decarboxylase (ODC), and the rate-limiting enzyme in the polyamine synthesis, primed by the tumor promoter phorbol 12-myristate 13-acetate (TPA). The four crude extracts, anthocyanin and proanthocyanidin fractions, were not highly active in QR induction, whereas the ethyl acetate extracts were active QR inducers. The concentrations required to double the QR activity (designated CDqr) for the ethyl acetate extracts of lowbush blueberry, cranberry, lingonberry, and bilberry were 4.2, 3.7, 1.3, and 1.0 μg tannic acid equivalents (TAE), respectively. Further fractionation of the bilberry ethyl acetate extract revealed that the majority of the inducing potency was concentrated in the hexane/chloroform subfraction (CDqr = 0.07 μg TAE). In contrast to the effects on the QR, the crude extracts of lowbush blueberry, cranberry, and lingonberry actively inhibited the ODC activity. The concentrations of these

three fruit crude extracts needed to inhibit the ODC activity by 50% (designated IC_{50}) were 8.0, 7.0, and 9.0 μg TAE, respectively. The greatest activity was concentrated in the polymeric proanthocyanidin fractions of the lowbush blueberry, cranberry, and lingonberry fruits (IC_{50} = 3.0, 6.0, and 5.0 μg TAE, respectively). The anthocyanidin and ethyl acetate extracts of the four *Vaccinium* species were either inactive or relatively weak inhibitors for the ODC activity. Thus, the components of the hexane/chloroform fraction of bilberry and of the proanthocyanidin fraction of lowbush blueberry, cranberry, and lingonberry exhibited the potential anticarcinogenic activity in in vitro tests [99].

The antitumor promoting activity of a polyphenolic fraction in grape seeds (GSP) was examined, using the CD-1 mouse skin epidermis. The ability of this fraction to inhibit TPA-induced tumor promotion and two markers of promotion in mouse skin, ODC and myeloperoxidase (MPO) activities, was examined. The pretreatment of the mouse skin with GSP dose-dependently reduced the TPA-induced epidermal ODC activity. Additionally, the pretreatment of the mouse skin with GSP resulted in a significant inhibition of MPO activity. The biweekly treatments of the mouse skin with the GSP before the TPA application resulted in the inhibition of 7,12-dimethylbenz[*a*]anthracene (DMBA)-initiated skin tumor incidence. Additionally, GSP treatment significantly reduced the proportion of the mice with tumors. These results suggest that GSP displays the antitumor promoting activity in the mice, possibly by inhibiting the TPA-induced epidermal ODC and MPO activities. Thus, GSP might provide a new cancer neutraceutical therapy as a skin cancer chemopreventative agent [100].

The polyphenol extract from the barley bran (BPE) induced the differentiation of human promyelocytic leukemia HL-60 cells, based on the expression of the differentiation markers such as nitro blue tetrazolium (NBT) reducing activity and α-naphthyl butyrate esterase activity. Prodelphinidin B-3, T1, T2, and T3 induced 26–40% NBT-positive cells and 22–32% α-naphthyl butyrate esterase-positive cells. Proanthocyanidins might potentiate the retinoic acid (all-*trans*-retinoic acid)-induced granulocytic differentiation and sodium butyrate-induced monocytic differentiation in the HL-60 cells [101].

It is known widely that the grape seed proanthocyanidins are natural antioxidants, which possess the broad spectra of chemoprotective properties against free radicals and oxidative stress. The cytotoxicity of a novel IH636 grape seed proanthocyanidin extract (GSPE) was tested against the MCF-7 human breast cancer cells, A-427 human lung cancer cells, CRL-1739 human gastric adenocarcinoma cells and K562 chronic myelogenous leukemic cells and also against the normal human gastric mucosal cells and J774A.1 murine macrophage cells. The concentration- and time-dependent cytotoxic effects of GSPE were observed on the MCF-7 breast cancer, A-427 lung cancer and gastric adenocarcinoma cells. GSPE exhibited no cytotoxicity toward

the K562 myelogenous leukemic cells. However, GSPE enhanced the growth and viability of the normal human gastric mucosal cells and J774A.1 cells. These results suggest that GSPE might exhibit cytotoxicity against some cancer cells, whereas GSPE enhanced the growth and viability of the normal cells [102].

The antimutagenic activity of the *Hamamelis virginiana* bark, a commercial tincture and its methanolic extract against 2-nitrofluorene was examined by Ames assay. The tannin-free samples showed no inhibitory activity. The bioassay-guided fractionation yielded two active fractions, the oligomeric proanthocyanidins and proanthocyanidins. The proanthocyanidins inhibited the mutagenicity by 2-nitrofluorene, the selected *N*-heterocycle. The proanthocyanidins acted as direct-acting desmutagens, but they did not act as bioantimutagens. The antimutagenic activity was increased with the extent of polymerization in proanthocyanidins. Interestingly, the components in the most active fraction consisted of catechin and gallocatechin oligomers with an average polymerization degree of 9.2 [103].

Polymeric proanthocyanidins were isolated from the bark of *Hamamelis virginiana* L. at an approximate yield of 5%. The fractionation yielded the fractions with similar structures, but different molecular weights with a degree of polymerization (DP) between 17–29 (thiolysis) and 11–20 (GPC). The polymers were mainly composed of epicatechin and epigallocatechin as the chain extension units with an approximate ratio of 1.3 : 1.0. The terminal chain units were catechin (approximately 95%) and gallocatechin (approximately 5%). All chain extension units were completely galloylated at position *O*-3, whereas the chain terminating units were not galloylated. The main interflavan linkages were 4 → 8-bonds [104].

The capacity of betel nut extracts (*Areca catechu*), stimulants chewed by millions of Asians, to inhibit the formation of carcinogenic nitrosamines was investigated by measuring the amount of the urinary *N*-nitroso-L-proline of a nitrosoamin following the intake of sodium nitrate and L-proline. A water extract of the dried nuts, an ether extract containing mainly (+)-catechin and (–)-epicatechin, and a caffeine-precipitated *n*-butyl alcohol extract containing primarily proanthocyanidins (tannins) strongly reduced the formation of *N*-nitroso-L-proline. The water extract and the proanthocyanidin (tannin)-containing extract reduced the excreted *N*-nitroso-L-proline to the background level. These results suggest that people who have ingested daily the relatively large quantities of naturally occurring phenolics could prevent the formation of carcinogenic nitrosamines [105].

It is thought that daily intake of green-yellow-orange vegetables and fruits could prevent cancers from the view of the epidemiology. The biological implication of teas as a protective factor in carcinogenesis has not yet drawn full attention. The inhibitory effects of the infusions of Chinese, Japanese, and Ceylonese teas were examined by adding the teas to a nitrosation mixture consisting of 0.8 mg sodium nitrite and 340 mg equivalent of a widely

consumed salt-preserved fish and estimating the frequency of the mutants in the population of TA 1535 strain of *Salmonella typhimurium*. These tea samples exhibited a strong inhibitory effect. Comparable inhibitions might be obtained by several tea phenolics. The formation of carcinogenic nitrosoproline could be strongly inhibited in vitro by the tea infusions and tea phenolics. The effects of tea infusions and caffeic acid on the formation of nitrosoproline have been examined by studying volunteers who have ingested 300 mg sodium nitrate and 30 min later 300 mg proline, and then estimating the excreted nitrosoproline in the collected urine samples over a 24-h period. The tested teas, at doses regularly consumed, again strongly inhibited the endogeneous nitrosoproline formation in humans. The inhibitory effects could be obtained by ingesting caffeic acid, chlorogenic acid, or ferulic acid with the nitrosation mixture. These results suggest that the simultaneous intake of teas with our daily food products could prevent the endogenous formation of nitrosation within the human's stomach [106].

3.1.7 Skin Care and Beauty

The effect of highly purified, high molecular weight procyanidins from *Vitis vinifera* seeds on the sparing and recycling of α-tocopherol was examined in solution, phosphatidylcholine liposomes or in red blood cells. The tocopheroxyl radicals which were induced by the reaction of α-tocopherol with the stable 1.1-diphenyl-2-picrylhydrazyl (DPPH) radicals could be confirmed to be recycled by their procyanidins, using both high-performance liquid chromatography (HPLC) and ESR spectroscopy. Additionally, the procyanidins significantly and dose-dependently spared the consumption of vitamin E during the autooxidation phase of the $HO^{\bullet}$-induced peroxidation of phosphatidylcholine. In this membrane model, the combination of 0.5 μM procyanidins and 2 μM α-tocopherol synergistically delayed the appearance of the conjugated dienes, whereas catechin was active only at 5 μM. Procyanidins (0.1–1.0 μM) prevented vitamin E loss in the membranes, decreased the membrane lipid peroxidation, and delayed the onset of hemolysis in red blood cells that had been stressed oxidatively by UVB exposure [107].

Proanthocyanidins have another more important role in addition to disease prevention, because proanthocyanidins might allow the human body to remain in a more youthful state. Generally, the damage caused by oxidative stress produces the most visible signs of aging in the human skin. Protection from these oxidative damages might make our skin younger and give us a more youthful appearance. Reduction of the damage from UV light might thus be one way to prevent oxidative damage. The photosynthesis of plants could produce diverse antioxidants. The sunscreen products for human skins contain a variety of antioxidants with expectations that the

antioxidants might prevent sun injury to the skin. The grape seed oligoprocyanidins (OPCs) exerted a comparable antioxidant effect with vitamin E that might protect various polyunsaturated fatty acids from UV light-induced lipid peroxidation. Procyanins, polyunsaturated fatty acids (such as linoleic acid, linolenic acid and arachidonic acid) and vitamin E might synergistically elevate the resistance to photo-oxidation, by sparing the consumption of vitamin E. This suggests the quenching of the α-tocopheroxyl radical by the procyanidins [108].

The extracts from *Hamamelis bark* have long been used in the therapy of skin diseases and in cosmetic formulas as traditional folklore medicines. However, the active principles in *Hamamelis* bark have not been well characterized. So far, two major constituents such as the polymeric proanthocyanidins and polysaccharides have been isolated from the *Hamamelis* bark and tested for their effects on the proliferation and the differentiation of cultured human keratinocytes. The proanthocyanidins significantly increased the proliferation of keratinocytes without affecting the differentiation, whereas the polysaccharide fractions mainly consisting of arabans and arabinogalactans were inactive. These results suggest that proanthocyanidins reduce transepidermal water loss and erythema formation in the static light scattering (SLS)-irritated skin, with a possible clinical application in the irritative processes [109].

The chloasma (melasma) of an acquired hypermelanosis is often recalcitrant to various treatments and an amenable, and proper and safe pigment-reducing modality is necessary. The protective effect of proanthocyanidin against the chloasma has been examined in a one-year open design study. A proanthocyanidin-rich grape seed extract (GSE) was orally administered to 12 Japanese women candidates with the chloasma within 6 months. A significant decrease of melanin was observed 6 months after GSE intake, indicating that GSE effectively reduced the hyperpigmentation of women with chloasma. Interestingly, the beneficial effects of GSE were maximally observed after 6 months, but without further improvement after the following 6 months. The GSE is safe and useful for improving chloasma [110].

Higher and lower molecular weight fractions from a crude hydroalcoholic extract from a *Hamamelis virginiana* bark exhibited significant antiviral activity against *Herpes simplex* virus type 1 (HSV-1). Additionally, the extract displayed radical scavenging properties, and inhibited the α-glucosidase as well as human leukocyte elastase (HLE), and exhibited strong antiphlogistic effects on the croton oil-induced ear edema of mouse. The lower molecular fraction possessed weaker activities and might contain mainly hamamelitannin, catechin, and other unidentified constituents [111].

Interestingly, plant species generally acclimate to UVB exposure. These acclimations include the increased biosynthesis of UVB screening phytochemicals such as vitamin E and flavonoids with antioxidant properties. *Brassica napus* L. plants acclimate to environmentally relevant increases in

UVB through the accumulation of specific flavonoids in the leaf epidermis. However, *B. napus* was found to lose other flavonoids upon exposure to UVA and UVB. The levels of all the extractable flavonoids in the leaves of *B. napus* plants are decreased in a dose-dependent manner upon exposure to UVA. UVA preexposures were found to reduce the accumulation of some flavonoids induced by UVB. This down regulation was particularly confirmed for quercetin-3-*O*-sophoroside and quercetin-3-*O*-sophoroside-7-*O*-glucoside. This is interesting, because these two quercetins might be induced by the UVB and correlated with the UVB tolerance in some plant species. From the photobiological nature of the UVA-mediated accumulation of flavonoid, complex interactions between the UVA and UVB responses are suggested [66].

Cupressus sempervirens L. proanthocyanidolic oligomers (PCO) inhibited the esterolytic activity of pancreatic elastase with 50% inhibitory concentration (Cl_{50}) of 0.0075 mg/mL when a sap substrate suc(Al)3NA was used. The inhibition was slightly lower when the ionic strength of the buffer was increased. The elastolytic activity was inhibited using an elastinorcein substrate with a Cl_{50} of 0.05 mg/mL. The oligomers might bind with the elastase to form a precipitant complex. The oligomer-elastin complex seems to be more stable than the complex of oligomer-elastase which could regain part of its esterase activity. The elastic fibers seem to be protected by PCO. This means that a part of the aging process might be the degradation of skin by the enzyme elastase, which might be released during inflammation. PCOs specifically could block the elastase, thus maintaining the integrity of elastin [112].

It is known that proanthocyanidins extracted from grape seeds possess growth-promoting activity toward murine hair epithelial cells in vitro and stimulate anagen induction during the hair cycle progression in vivo. On the basis of this fact, the growth-promoting activity of procyanidin oligomers and the target cells of procyanidins in the skin have been examined. Interestingly, the procyanidin dimer and trimer exhibited higher growth-promoting activity than the monomer. Procyanidin B-2 (30 μM) of an epicatechin dimer might stimulate the growth of hair epithelial cells to 300% of control level during 5 days culture. The optimum concentration of procyanidin C-1 of an epicatechin trimer was lower than that of procyanidin B-2. The maximum growth-promoting activity of procyanidin C-1 (3 μM) was about 220%. No other flavonoids examined exhibited higher proliferative activities than procyanidins. Interestingly, among skin constituent cells, only epithelial cells such as hair keratinocytes or epidermal keratinocytes could respond to procyanidin oligomers. Topical application of 1% procyanidin oligomers on shaven C3H mice at the telogen phase led to significant hair regeneration in the shaven area [procyanidin B-2, 69.6% ± 21.8%; procyanidin B-3, 80.9%±13.0%; procyanidin C-1, 78.3% ± 7.6%], whereas the application of a vehicle only led to the regeneration of 41.7%. The hair-growing activity of

procyanidin oligomers both in vitro and in vivo suggests their possible use as agents to induce hair growth [113].

3.1.8 Antibacterial and Antiviral Activity

A series of nine dimeric procyanidins and six related polyphenols were chosen for their structure–activity relationships. Generally, the epicatechin-containing dimmers showed higher anti-herpes simplex virus (HSV), anti-human immunodeficiency virus (HIV), and radical-scavenging activities. The presence of *ortho*-trihydroxyl groups in the B-ring might play an important role for the anti-HSV and radical-scavenging activities and the inhibition of complement classical pathway. Interestingly, the double interflavan linkages could generate the anti-HSV and anit-HIV activities, and the complement inhibition. The influence of the degree of polymerization or the type of the interflavan linkage ($4 \rightarrow 6$ or $4 \rightarrow 8$) in different biological systems was evaluated. Only minor or moderate antibacterial activities were observed [114].

3.1.9 Sweetener

Selligueain A, a novel sweet trimeric proanthocyanidin with a doubly linked A unit, has been isolated from the rhizomes of *Selliguea feei* collected in Indonesia. Selligueain A was identified as epiafzelechin-$(4\beta \rightarrow 8, 2\beta \rightarrow O \rightarrow 7)$-epiafzelechin-$(4\beta \rightarrow 8)$-afzelechin. Selligueain A was not acutely toxic for the mice and not mutagenic in a premutation assay by *Salmonella typhimurium* strain TM677. Selligueain A was rated by a taste panel as exhibiting about 35 times higher the sweetness intensity than a 2% w/v aqueous sucrose solution, and at a concentration of 0.5% w/v Selligueain A in H_2O was perceived as pleasant-tasting rather than an astringent [115].

An assessment of the possible carcinogenicity of selligueain A was measured by the structure–activity relation analysis with CASE/MULTICASE. On the basis of authoritative databases, it was predicted that selligueain A might have some marginal potential for being a "non-genotoxic" rodent carcinogen. Although the relevance of this potential to possible human health risks of selligueain A might be problematic, selligueain A might be widely consumed as a successful sweetener. However, selligueain A should be investigated for its carcinogenicity and other toxicities also [116].

The flavonoids as naturally occurring compounds of plant-derived foodstuffs could reveal some biological effects such as antioxidative, antimutagenic, anticarcinogenic, which makes flavonoids interesting substances in the prevention of atherosclerosis and cancer in humans. Data concerning flavonoid content in food and human intake of flavonols are scarce or missing in the food composition tables. Consequently, after installing a flavonoid

data base by means of literature data, the 7-day dietary protocols of 119 adults (63 women and 56 men, age 19–49 years) representing a Bavarian subgroup of the German National Food Consumption Survey (NVS) was evaluated. In all subjects, the average intake of all flavonoids (calculated as aglycons) might amount to 54.0 mg/day (median) with a great range of variability. The most important flavonoid groups are flavonols (12.0 mg/day), catechins (8.3 mg/day), and flavanons (13.2 mg/day), followed by anthocyanidins (2.7 mg/day), proanthocyanins (3.7 mg/day) and phloretin (dihydrochalcone) (0.7 mg/day). Differences due to sex did not reach statistical significance. The fruits, fruit products and fruit juices were the most important flavonoid sources. The vegetables and related products provide about half of the flavonol intake. Therefore, statistically significant correlations might exist between the total flavonoid intake and the intake of vitamin C or dietary fiber. When compared to other countries, the flavonol intake in the investigated group of persons is rather low. By building up the data base, it was possible for the first time to calculate the intake of further flavonoids besides flavonols. When compared to the intake of other antioxidants such as vitamins C and E, the amount of the flavonoids in the diet is high and therefore should be further investigated for its role in the human diet in relation to certain diseases [117].

References

1. Larson RA (1988) Phytochemistry 27:969
2. Wang SY, Jiao H (2000) J Agric Food Chem 48:5677
3. Leonardi M, Leonardi M (1993) Minerva Ginecol 45:617
4. Scharrer A, Ober M (1981) Klin Monatsbl Augenheilkd 178:386
5. Wang H, Cao G, Prior RL (1997) J Agric Food Chem 45:304
6. Morazzoni P, Bombardelli E (1996) Fitoterapia 67:3
7. Elliott AJ, Scheiber SA, Thomas C, Pardini RS (1992) Biochem Pharmacol 44:1603
8. Michalak K, Wesołowska O, Motohashi N, Hendrich AB (2007) In: Eguchi S (ed) Bioactive Heterocycles II. Springer, Berlin Heidelberg New York, p 223
9. Igarashi K, Kimura Y, Takenaka A (2000) Biosci Biotechnol Biochem 64:1600
10. Tsuda T, Horio F, Osawa T (2000) Biofactors 13:133
11. Tsuda T, Horio F, Osawa T (1998) Lipids 33:583
12. Rice-Evans CA, Miller NJ, Bolwell PG, Bramley PM, Pridham JB (1995) Free Radic Res 22:375
13. Tsuda T, Kato Y, Osawa T (2000) FEBS Lett 484:207
14. Noda Y, Kneyuki T, Igarashi K, Mori A, Packer L (2000) Toxicology 148:119
15. Bertuglia S, Malandrino S, Colantuoni A (1995) Pharmacol Res 31:183
16. Borissova P, Valcheva S, Belcheva A (1994) Acta Physiol Pharmacol Bulg 20:25–30
17. Joseph JA, Shukitt-Hale B, Denisova NA, Bielinski D, Martin A, McEwen JJ, Bickford PC (1999) J Neurosci 19:8114
18. Thibault O, Gant JC, Landfield PW (2007) Aging Cell 6:307

19. Youdim KA, Shukitt-Hale B, Martin A, Wang H, Denisova N, Joseph JA (2000) Nutr Neurosci 3:383
20. Martin S, Favot L, Matz R, Lugnier C, Andriantsitohaina R (2003) Biochem Pharmacol 65:669
21. Sato M, Bagchi D, Tosaki A, Das DK (2001) Free Radic Biol Med 31:729
22. Frigo DE, Duong BN, Melnik LI, Schief LS, Collins-Burow BM, Pace DK, McLachlan JA, Burow ME (2002) J Nutr 132:1848
23. Joseph JA, Denisova NA, Arendash G, Gordon M, Diamond D, Shukitt-Hale B, Morgan D (2003) Nutr Neurosci 6:153
24. Bartosz G (1996) Acta Biochim Pol 43:645
25. Galli RL, Shukitt-Hale B, Youdim KA, Joseph JA (2002) Ann N Y Acad Sci 959:128
26. Lau FC, Shukitt-Hale B, Joseph JA (2007) Subcell Biochem 42:299
27. Joseph JA, Shukitt-Hale B, Lau FC (2007) Ann N Y Acad Sci 1100:470
28. Colantuoni A, Bertuglia S, Magistretti MJ, Donato L (1991) Arzneimittelforschung 41:905
29. Renaud S, de Lorgeril M (1992) Lancet 339:1523
30. Renaud S, de Lorgeril M (1993) Acta Cardiol 48:446
31. Frankel EN, Kanner J, German JB, Parks E, Kinsella JE (1993) Lancet 341:454
32. Kinsella JE, Frankel E, German B, Kanner J (1993) Food Technol 47:85
33. Bakker J, Timberlake CF (1985) J Sci Food Agric 36:1315
34. Bakker J, Timberlake CF (1985) J Sci Food Agric 36:1325
35. Timberlake CF, Henry BS (1986) Endeavour 10:31
36. Brouillard R, Cheminat A (1988) Prog Clin Biol Res 280:93
37. Figueiredo P, Elhabiri M, Toki K, Saito N, Dangles O, Brouillard R (1996) Phytochemistry 41:301
38. Sanchez-Moreno C, Satue-Gracia MT, Frankel EN (2000) J Agric Food Chem 48:5581
39. Pawlowicz P, Wilczynski J, Stachowiak G, Hincz P (2000) Ginekol Pol 71:848
40. Andriambeloson E, Magnier C, Haan-Archipoff G, Lobstein A, Anton R, Beretz A, Stoclet JC (1998) J Nutr 128:2324
41. Favot L, Martin S, Keravis T, Andriantsitohaina R, Lugnier C (2003) Cardiovasc Res 59:479
42. Zafra-Stone S, Yasmin T, Bagchi M, Chatterjee A, Vinson JA, Bagchi D (2007) Mol Nutr Food Res 51:675
43. Sato M, Sato H, Ogawa A, Nomura R, Takashima S, Bang HJ, Matsuoka H, Imaizumi K (2007) J Agric Food Chem 55:8967
44. van Jaarsveld H, Kuyl JM, Schulenburg DH, Wiid NM (1996) Res Commun Mol Pathol Pharmacol 91:65
45. Boniface R, Robert AM (1996) Klin Monatsbl Augenheilkd 209:368
46. Cohen-Boulakia F, Valensi PE, Boulahdour H, Lestrade R, Dufour-Lamartinie JF, Hort-Legrand C, Behar A (2000) Metabolism 49:880
47. Perossini M (1987) Ann Ottalmol Clin Ocul 12:1173
48. Gray AM, Abdel-Wahab YH, Flatt PR (2000) J Nutr 130:15
49. Gray AM, Flatt PR (1999) Brit J Nutr 81:203
50. Letiner G, Westmoreland D, Knapp M, Spencer K, Merback J, Kuzik V, Weger M, Pfannhauser W, Porta S (2000) Magnesium Bull 22:72
51. Jayle GE, Aubert L (1964) Therapie 19:171
52. Jayle GE, Aubry M, Gavini H, Braccini G, Baume C. de la (1965) Ann Ocul (Paris) 198:556
53. Nakaishi H, Matsumoto H, Tominaga S, Hirayama M (2000) Altern Med Rev 5:553
54. Zadok D, Levy Y, Glovinsky Y (1999) Eye 13:734

55. Muth ER (2000) Altern Med Rev 5:164
56. Scharrer A, Ober M (1981) Klin Monatsbl Augenheilkd 178:386
57. Meiers S, Kemeny M, Weyand U, Gastpar R, von Angerer E, Marko D (2001) J Agric Food Chem 49:958
58. Bagchi D, Sen CK, Bagchi M, Atalay M (2004) Biochemistry (Mosc) 69:75
59. Zhang YC, Albrecht D, Bomser J, Schwartz SJ, Vodovotz Y (2003) J Agric Food Chem 51:7611
60. Magistretti MJ, Conti M, Cristoni A (1988) Arzneimittelforschung 38:686
61. Cristoni A, Malandrino S, Magistretti MJ (1989) Arzneimittelforschung 39:590
62. Comoglio A, Leonarduzzi G, Carini R, Busolin D, Basaga H, Albano E, Tomasi A, Poli G, Morazzoni P, Magistretti MJ (1990) Free Radic Res Commun 11:109
63. Morazzoni P, Magistretti MJ, Giachetti C, Zanolo G (1992) Eur J Drug Metab Pharmacokinet 17:39. Erratum in: Eur J Drug Metab Pharmacokinet 17:165
64. Conti M, Malandrino S, Magistretti MJ (1992) Japan J Pharmacol 6:315
65. Wilson KE, Wilson MI, Greenberg BM (1998) Photochem Photobiol 67:547
66. Wilson KE, Thompson JE, Huner NP, Greenberg BM (2001) Photochem Photobiol 73:678
67. Cimino F, Ambra R, Canali R, Saija A, Virgili F (2006) J Agric Food Chem 54:4041
68. Ferreira D, Slade D (2002) Nat Prod Rep 19:517
69. Masquelier J (1991) Historical note on OPC. Martillac, France
70. Masquelier J, Michaud J, Laparra J, Dumon MC (1979) Int J Vitam Nutr Res 49:307
71. Buz'Zard AR, Lau BH (2007) Phytother Res 21:579
72. Ray SD, Parikh H, Bagchi D (2005) Mutat Res 579:81
73. Rong Y, Li L, Shah V, Lau BH (1994–1995) Biotechnol Ther 5:117
74. Virgili F, Kim D, Packer L (1998) FEBS Lett 431:315
75. Packer L, Rimbach G, Virgili F (1999) Free Radic Biol Med 27:704
76. Maffei Facino R, Carini M, Aldini G, Calloni MT, Bombardelli E, Morazzoni P (1998) Planta Med 64:343
77. Nuttall SL, Kendall MJ, Bombardelli E, Morazzoni P (1998) J Clin Pharm Ther 23:385
78. Costantini A, De Bernardi T, Gotti A (1999) Minerva Cardioangiol 47:39
79. Yang YS, Ahn TH, Lee JC, Moon CJ, Kim SH, Jun W, Park SC, Kim HC, Kim JC (2008) Food Chem Toxicol 46:380
80. Bagchi D, Garg A, Krohn RL, Bagchi M, Bagchi DJ, Balmoori J, Stohs SJ (1998) Gen Pharmacol 30:771
81. Dauer A, Hensel A, Lhoste E, Knasmuller S, Mersch-Sundermann V (2003) Phytochemistry 63:199
82. Bagchi D, Ray SD, Bagchi M, Preuss HG, Stohs SJ (2002) Indian J Exp Biol 40:717
83. Ray SD, Kumar MA, Bagchi D (1999) Arch Biochem Biophys 369:42
84. Zhang B, Shen X, Zhang Y, Yao G (2007) Wei Sheng Yan Jiu 36:295
85. Bagchi D, Bagchi M, Stohs SJ, Das DK, Ray SD, Kuszynski CA, Joshi SS, Pruess HG (2000) Toxicology 148:187
86. Cossins E, Lee R, Packer L (1998) Biochem Mol Biol Int 45:583
87. Bagchi M, Balmoori J, Bagchi D, Ray SD, Kuszynski C, Stohs SJ (1999) Free Radic Biol Med 26:992 and Erratum in: (1999) Free Radic Biol Med 26:1599
88. Fremont L, Belguendouz L, Delpal S (1999) Life Sci 64:2511
89. Fitzpatrick DF, Bing B, Rohdewald P (1998) J Cardiovasc Pharmacol 32:509
90. Virgili F, Kobuchi H, Packer L (1998) Free Radic Biol Med 24:1120
91. Putter M, Grotemeyer KH, Wurthwein G, Araghi-Niknam M, Watson RR, Hosseini S, Rohdewald P (1999) Thromb Res 95:155
92. Yamakoshi J, Kataoka S, Koga T, Ariga T (1999) Atherosclerosis 142:139

93. Ursini F, Sevanian A (2002) Ann N Y Acad Sci 957:200
94. Natella F, Belelli F, Gentili V, Ursini F, Scaccini C (2002) J Agric Food Chem 50:7720
95. Ursini F, Tubaro F, Rong J (1999) Nutr Rev 57:241
96. Ursini F, Zamburlini A, Cazzolato G, Maiorino M, Bon GB (1998) Free Radic Biol Med 25:250
97. Sato M, Maulik G, Ray PS, Bagchi D, Das DK (1999) J Mol Cell Cardiol 31:1289
98. Das DK, Sato M, Ray PS, Maulik G, Engelman RM, Bertelli AA, Bertelli A (1999) Drugs Exp Clin Res 25:115
99. Bomser J, Madhavi DL, Singletary K, Smith MA (1996) Planta Med 62:212
100. Bomser JA, Singletary KW, Wallig MA, Smith MA (1999) Cancer Lett 135:151
101. Tamagawa K, Fukushima S, Kobori M, Shinmoto H, Tsushida T (1998) Biosci Biotechnol Biochem 62:1483
102. Ye X, Krohn RL, Liu W, Joshi SS, Kuszynski CA, McGinn TR, Bagchi M, Preuss HG, Stohs SJ, Bagchi D (1999) Mol Cell Biochem 196:99
103. Dauer A, Metzner P, Schimmer O (1998) Planta Med 64:324
104. Dauer A, Rimpler H, Hensel A (2003) Planta Med 69:89
105. Stich HF, Ohshima H, Pignatelli B, Michelon J, Bartsch H (1983) J Nat Cancer Inst 70:1047
106. Stich HF (1992) Prev Med 21:377
107. Maffei Facino R, Carini M, Aldini G, Calloni MT, Bombardelli E, Morazzoni P (1998) Planta Med 64:343
108. Carini M, Maffeifacino R, Aldini G, Calloni MT, Bombardelli E, Morazzoni P (1998) Int J Cosmetic Sci 20:203
109. Deters A, Dauer A, Schnetz E, Fartasch M, Hensel A (2001) Phytochemistry 58:949
110. Yamakoshi J, Sano A, Tokutake S, Saito M, Kikuchi M, Kubota Y, Kawachi Y, Otsuka F (2004) Phytother Res 18:895
111. Erdelmeier CA, Cinatl J Jr, Rabenau H, Doerr HW, Biber A, Koch E (1996) Planta Med 62:241
112. Meunier MT, Villie F, Bastide P (1994) J Pharm Belg 49:453
113. Takahashi T, Kamiya T, Hasegawa A, Yokoo Y (1999) J Invest Dermatol 112:310
114. De Bruyne T, Pieters L, Witvrouw M, De Clercq E, Vanden Berghe D, Vlietinck AJ (1999) J Nat Prod 62:954
115. Baek NI, Chung MS, Shamon L, Kardono LB, Tsauri S, Padmawinata K, Pezzuto JM, Soejarto DD, Kinghorn AD (1993) J Nat Prod 56:1532
116. Rosenkranz HS, Liu M, Cunningham A, Klopman G (1996) SAR QSAR Environ Res 5:79
117. Linseisen J, Radtke J, Wolfram G (1997) Z Ernährungswiss 36:403

Top Heterocycl Chem (2008) 15: 49–65
DOI 10.1007/7081_2008_124

Published online: 30 April 2008

Bioactive Mechanism of Interaction Between Anthocyanins and Macromolecules Like DNA and Proteins

Seetharamappa Jaldappagari[1] (✉) · Noboru Motohashi[2] · Mamatha P Gangeenahalli[3] · James H. Naismith[4]

[1]Department of Chemistry, Karnatak University, 580 003 Dharwad, India
jseetharam@yahoo.com

[2]Meiji Pharmaceutical University, 2-522-1 Noshio, Kiyose-shi, 204-8588 Tokyo, Japan

[3]Department of Chemistry, AVK College for Women, 577 002 Davanagere, India

[4]Centre for Biomolecular Sciences, University of St. Andrews, St. Andrews KY16 9ST, UK

Abstract Anthocyanins are the largest group of naturally occurring phytochemicals, and impart the rich colors ranging from red to violet and blue to fruits, vegetables and other plants. These are the glycosides of polyhydroxy and polymethoxy derivatives of 2-phenylbenzopyrylium or flavylium salts. The interest in anthocyanins has increased immensely during the past decade due to their array of healthily beneficial phytochemicals. Anthocyanins can protect against health damage by some types of harmful oxidants through different mechanisms. The purpose of this article is to review the biological activities of anthocyanins and the interactions of anthocyanins with DNA and protein.

Keywords Anthocyanins · Biological properties · Interactions · Macromolecules

1 Introduction

Anthocyanins (in Greek, anthos means flower and kyanos means blue) are one of the most important plant pigments visible to the human eye. Anthocyanins are the largest group of colorful plant pigments and are responsible

for colors ranging from red to violet and blue [1]. These plant pigments accumulate richly in the epidermal or subepidermal cell vacuoles of flowers, fruits, vegetables and foliage. Generally, anthocyanins belong to the widespread class of (poly)phenolic compounds, which are collectively named flavonoids. Flavonoids belong to a group of phytochemicals as naturally functional substances with variable phenolic structures and are recognized as the colorful pigments responsible for the color of leaves or petals [2]. Now, more than 4000 varieties of flavonoids have been identified, many of which are responsible for the attractively unique colors of flowers, fruits, vegetables and leaves [3]. Flavonoids are easily found in citrus fruits, apples, olive oil, grapes, tea, red wine and other fruits and vegetables. The dietary flavonoids are the focus of increasing attention as potential protectors against a variety of human diseases, in particular, age-related diseases such as cardiovascular disease [4–6] and cancer [7–12]. A large number of the action mechanisms have been attributed to the diverse functions of the flavonoids, including antioxidant properties [13–15] and effects on enzymes and signal transduction pathways. However, it is also known that flavonoids inhibit the activities of many enzymes such as calcium phospholipid-dependent protein kinase, tyrosine protein kinase from rat lung, phosphorylase kinase, phosphatidylinositol 3-kinase and DNA topoisomerases.

Anthocyanins are the glycosides of flavonoids with polyhydroxy and polymethoxy derivatives of 2-phenylbenzopyrylium or flavylium cation (Fig. 1). Anthocyanins are conjugated aromatic systems, which are often positively charged. Anthocyanins can absorb in the visible range, hence each anthocyanin can be represented by their unique color. Generally, anthocyanin itself has a carbohydrate (sugar, usually glucose) esterified at the 3 position (Table 1). An anthocyanidin, termed the aglycone, does not have a sugar at the 3 position. Glucose (glc), galactose (gal), arabinose (arab), rhamnose (rham) and xylose (xyl) are the most common sugars that are bonded to anthocyanidins as mono-, di- or trisaccharide forms. Except for the 3-deoxyanthocyanidins, such as luteolinidin and apigeninidin in sorghum [16], aglycones are rarely found in fresh plant materials. There are about 17 anthocyanidins found in nature (Fig. 2 and Table 2), whereas only six anthocyanidins, cyanidin (Cy), delphinidin (Dp), petunidin (Pt), peoni-

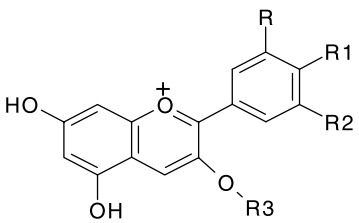

Fig. 1 Chemical structure of anthocyanins

Table 1 Anthocyanins

	R	R1	R2	R3
Cyanidin 3-*O*-glycoside	OH	OH	H	Sugar
Delphinidin 3-*O*-glycoside	OH	OH	OH	Sugar
Malvidin 3-*O*-glycoside	OCH_3	OH	OCH_3	Sugar
Peonidin 3-*O*-glycoside	OCH_3	OH	H	Sugar
Petunidin 3-*O*-glycoside	OH	OH	OCH_3	Sugar

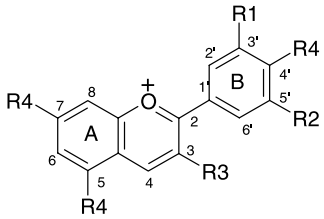

Fig. 2 Structure of anthocyanidins: *R1* and *R2* are H, OH or OCH_3; *R3* is a glycosyl or H; and *R4* is OH or a glycosyl

Table 2 Naturally occurring anthocyanidins

Name	Abbreviation	Substitution pattern							Color
		3	5	6	7	3′	4′	5′	
Apigeninidin	Ap	H	OH	H	OH	H	OH	H	Orange
Aurantinidin	Au	OH	OH	OH	OH	H	OH	H	Orange
Capensinidin	Cp	OH	OMe	H	OH	OMe	OH	OMe	Bluish-red
Cyanidin	Cy	OH	OH	H	OH	OH	OH	H	Orange-red
Delphinidin	Dp	OH	OH	H	OH	OH	OH	OH	Bluish-red
Europinidin	Eu	OH	OMe	H	OH	OMe	OH	OH	Bluish-red
Hirsutidin	Hs	OH	OH	H	OMe	OMe	OH	OMe	Bluish-red
6-Hydroxycyanidin	6OHCy	OH	OH	OH	OH	OH	OH	H	Red
Luteolinidin	Lt	H	OH	H	OH	OH	OH	H	Orange
Malvidin	Mv	OH	OH	H	OH	OMe	OH	OMe	Bluish-red
5-Methylcyanidin	5-MCy	OH	OMe	H	OH	OH	OH	H	Orange-red
Pelargonidin	Pg	OH	OH	H	OH	H	OH	H	Orange
Peonidin	Pn	OH	OH	H	OH	OMe	OH	H	Orange-red
Petunidin	Pt	OH	OH	H	OH	OMe	OH	OH	Bluish-red
Pulchellidin	Pl	OH	OMe	H	OH	OH	OH	OH	Bluish-red
Rosinidin	Rs	OH	OH	H	OMe	OMe	OH	H	Red
Tricetinidin	Tr	H	OH	H	OH	OH	OH	OH	Red

din (Pn), pelargonidin (Pg) and malvidin (Mv), are ubiquitously distributed. For example, the distribution of anthocyanidins in the edible parts of plants are: Cy (50%), Pg (12%), Pn (12%), Dlp (12%), Pt (7%) and Mv (7%). The presence of sugar in anthocyanins is important for water solubility; if their sugar(s) are hydrolyzed or lost, their solubility might decrease or be lost and the anthocyanin molecules will be destabilized and lost. The differences in function between the individual anthocyanins relate to the number of hydroxyl groups, the kinds and number of sugars attached to the molecule, the position of the attachment, and the kinds and number of aliphatic or aromatic acids attached to the sugars in the anthocyanin molecule.

Anthocyanidins of the sugar-free core structure are also the salt derivatives with a 2-phenylchromenylium cation such as a flavylium cation. The following four classes of anthocyanidin glycosides (anthocyanins) are very common: 3-monosides, 3-biosides, 3,5-diglycosides and 3,7-diglycosides. 3-Glycosides occur about two and half times more frequently than 3,5-diglycosides. The most widespread anthocyanin is cyanidin 3-glucoside. Three non-methylated anthocyanidins of cyanidin (Cy), delphinidin (Dp) and pelargonidin (Pg) are the most widespread in the plant kingdom, being present in 80% of pigmented leaves, 69% of fruits and 50% of flowers.

More than 600 naturally occurring anthocyanins have been reported [17]. It is known that anthocyanins are very changeable for following the reasons: (i) the number and position of reactive hydroxyl and methoxyl groups on the basic anthocyanidin skeleton; (ii) the decomposition, number and positions of the sugar group, and (iii) the extent of sugar acylation and the decomposition of the acylating anthocyanins [18]. Thus, changes in the chemical structure of anthocyanins might significantly depend on the extent of glycosylation and acylation. The molecular weight of anthocyanins might be around 400 to 1200.

In solution, the anthocyanins actually might exist in equilibrium with essentially four molecular forms – the flavylium cation, the quinoidal base, the hemiacetal base and chalcone [19]. The relative amounts of the four structure forms depends on both the pH and the difference in structure of the anthocyanins [20–22]. Generally, anthocyanins exist primarily as the stable flavylium cation above pH 2. This uniqueness in the chemical structure is one of the important key factors affecting their absorption, metabolism, bioavailability and, consequently, the biological responses of the human body to anthocyanins.

2
Stability and Catabolism of Anthocyanins in Plants

Very little is known about the stability and catabolism of anthocyanins in plants. A few studies have traced the turnover of anthocyanins in living

plant tissues. Anthocyanin metabolism was followed in mustard seedlings by pulse chase treatment with radioactive phenylalanine and showed a turnover of about 6% per day when anthocyanin levels reached a high and steady level [23]. Aminooxyphenylpropionic acid (AOPP) of a specific phenylalanine ammonia-lyase (PAL) enzyme inhibitor was found to inhibit anthocyanin synthesis effectively in petunia detached flower buds and in carrot cell suspensions. The stability of accumulated anthocyanin in suspension-cultures of the parental line and in high and low accumulating subclones of wild carrot was studied [24]. Even though very few studies have dealt with anthocyanin degradation, it is clear that degradation does occur in plants. The anthocyanin concentration in young photosynthetic leaves decreased according to either the leaf maturation or changing environmental conditions [25–27]. A study on the effect of temperature on aster flower pigmentation has shown that the fading changes of flower color due to high growth temperatures could be partially prevented by stabilizing the pigments with magnesium ions, and that the flowers themselves might be protected from the high temperature changes [28]. These findings suggested that anthocyanin degradation might play a crucial role in the control of pigment concentrations under any temperature conditions when the anthocyanin synthesis rates are low. The anthocyanin degradations might be caused by active enzymatic or chemical reactions. A typical oxidase of anthocyanins in fruit extracts is polyphenol oxidase (PPO), followed by peroxidases [29]. Unlike PPO, peroxidases exist in cell vacuoles, and therefore might be the more important candidates for plant anthocyanin degradations.

Anthocyanins are soluble in polar solvents, and can normally be extracted from common plant materials by methanol containing small amounts of HCl or formic acid. Addition of the acid lowers the pH value of the solution and safely protects against degradation of their structures with the non-acylated anthocyanin pigments. However, when anthocyanins from red grapes were extracted, the use of solvents containing up to 0.12 M HCl caused the partial hydrolysis of acylated anthocyanins [30]. Acetone has also been used to extract the anthocyanins from the diverse plant sources [31, 32]. The other analytical techniques [33] employed for analysis and identification of anthocyanins include solid-phase extraction (SPE), nuclear magnetic resonance (NMR), fluorescence and fast atom bombardment–mass spectroscopy (FAB-MS), liquid chromatography–mass spectrometry (LC-MS), liquid chromatography–electrospray ionization mass spectrometry (LC-ESIMS), liquid chromatography–electron impact ionization–mass spectrometry (LC-EI-MS), LC-MS with an atmospheric pressure-ionization ionspray interface, LC-MS system equipped with an ESI interface, LC-MS system equipped with an APCI interface, MALDI-MS, MALDI-TOF-MS, capillary zone electrophoresis (CZE), micellar electrokinetic chromatography (MEKC), and other analytical methods.

3 Biological Acitivities of Anthocyanins

Interest in anthocyanins has increased immensely during the past decade. For example, the extraction, analysis and biological activities of anthocyanins have been reported by Kong et al. [33]. In recent years, numerous studies have shown that anthocyanins display a wide range of biological activities including antioxidant, antiinflammatory, antimicrobial and anticarcinogenic activities, improvement of eye vision, induction of apoptosis, and neuroprotective effects [34]. Anthocyanins play a definite role in the attraction of animals for pollination and seed dispersal. Therefore, anthocyanins are of considerable importance in the coevolution of these plant–animal interactions. Anthocyanins such as 3-deoxyanthocyanidins in flowering plants can act as antioxidants, phytoalexins or as antibacterial agents. Anthocyanins might act as important factors, along with other flavonoids, in the resistance of plants against insect attacks [35]. The intake of fruit extracts rich in anthocyanins might be effective in an improvement of the reversing of age-related deficits in several neural and behavioral parameters [36].

A report on the antitumor activity of anthocyanins was published by Kamei et al. [37]. The anthocyanins in red wine could suppress the growth of HCT-15 cells, which are derived from a human colon cancer, or AGS cells from human gastric cancer. Anthocyanin with a purple color in corn was anticarcinogenic against 2-amino-1-methyl-6-phenylimidazo[4,5-*b*]pyridine-associated colorectal carcinogenesis in male F344 rats pretreated with 1,2-dimethylhydrazine [38]. The antioxidant activity of fractions of an Italian red wine showed that the anthocyanin fraction was the most effective both as a scavenger of reactive oxygen species, and as an inhibitor of lipoprotein oxidation and platelet aggregation [39]. This result suggested that anthocyanins could be a key component in red wine, which might protect against cardiovascular disease. The aglycones such as cyanidin (Cy) and delphinidin (Dp) are the most abundant anthocyanins in daily foods and might possess the ability to inhibit the growth of human tumor cells in vitro in the micromolar range [40]. Anthocyanins first showed high inhibition against NO production [41]. Furthermore, anthocyanins also possess antiulcerative activity [42] and protect against UV radiation [43].

4 Antioxidant Properties and Free Radical Scavenging Properties

The antioxidant potential of anthocyanins might depend on their substituents [44, 45]. The glycosidic forms (glycosides) generally have decreased antioxidant capacity when compared to their corresponding aglycone [46] because the glycosides are probably sterically hindered by the bulky sugar

molecules [47]. In studies on the antioxidative, radical scavenging and inhibitory effects of three anthocyanin pigments, viz., pelargonidin 3-*O*-β-D-glucoside (P3G), cyanidin 3-*O*-β-D-glucoside (C3G), and delphinidin 3-*O*-β-D-glucoside (D3G) (isolated from the *Phaseolus vulgaris* L. seed coat) and their aglycones (such as pelargonidin chloride, cyanidin chloride and delphinidin chloride) on the lipid peroxidation of UV light irradiation, all anthocyanins and anthocyanidins were highly antioxidative against the liposomal system and reduced the formation of malondialdehyde by the UVB (320–290 nm) irradiation. Additionally, the extent of the antioxidative activity in a rat liver microsomal system, and the scavenging effect of hydroxyl radicals and superoxide anion radicals, could be influenced by their individual structures.

Studies on the antioxidant properties of anthocyanins on human low-density lipoprotein (LDL) and lecithin liposome systems in vitro showed that the inhibition of oxidation increased dose-dependently with antioxidant concentration. The oxidation was catalyzed by copper in the LDL system and the effects of the anthocyanins were explained by several antioxidant mechanisms including hydrogen donation, metal chelation and protein binding [33]. Anthocyanins also prevented the oxidation of ascorbic acid (vitamin C), through chelate formation with the metal ions, and finally by the formation of an ascorbic (copigment)–metal–anthocyanin complex [49].

An anthocyanin of delphinidin-3-(*p*-coumaroylrutinoside)-5-glucoside (nasunin) with the purple colored crystals from eggplant skins, *Solanum melongena* L. "Chouja" could directly scavenge the O^{2-} with a potency of 143 ± 8 SOD-equivalent units mg^{-1} [50]. The order of the antioxidative efficiency of three fruit anthocyanins from chokeberry, honeysuckle and sloe was chokeberry > sloe > honeysuckle by using a thiobarbituric acid-reactive substance assay against an UV radiation-induced lipid oxidation in the liposome membrane [51].

Cyanidin 3-*O*-β-D-glucoside (C3G) of a typical anthocyanin pigment could lower the serum thiobarbituric acid-reactive substance concentration and increase the oxidation resistance of the serum to lipid peroxidation in rats [52]. In vitro enzymatic and non-enzymatic polyunsaturated fatty acid per oxidation was significantly inhibited in a dose-dependent manner by anthocyanin [53], a deep-red color pigment from carrot cell cultures.

The antioxidant activity of anthocyanins in the fruits and leaves from different cultivars of the thornless blackberry (*Rubus* sp.), red raspberry (*Rubus idaeus* L.), black raspberry (*Rubus occidentalis* L.) and strawberry (*Fragaria* × *ananassa* D.) was reported [54]. Studies on the ability of endothelial cells (EC) to incorporate anthocyanins and on the potential benefits against various oxidative stressors showed that the enrichment of EC with elderberry anthocyanins gave significant protective effects in the endothelial cells against the oxidative stressors, hydrogen peroxide, 2,2′-azobis(2-amidinopropane) dihydrochloride, and iron(II) sulfate/ascorbic acid [55].

The daily intake of anthocyanins (34.5 mg day^{-1}) from chokeberry juice could lower the redox status in the blood of boat rowers who performed a physical exercise during a 1-month training camp. After the chokeberry supplementation period, the concentrations of thiobarbituric acid-reactive substances in the blood samples collected 1 min after the exercise test and following a 24-h recovery period were significantly lower in the rowers receiving chokeberry juice than those in the control group. This means that anthocyanins could enhance the endogenous antioxidant defense system [56].

An indomethacin-induced gastric mucosal damage in the rat was accompanied by the development of oxidative stress, as evidenced by the accumulation of malondialdehyde. The pretreatment of rats with *Aronia melanocarpa* fruit juice (5, 10 and 20 mL kg^{-1}) rich in anthocyanins decreased the risk of the gastric lesions caused by indomethacin [57]. Studies on the peripheral circulation during rest and during typing work has shown that the intake of blackcurrant anthocyanins might improve the shoulder stiffness caused by typing work because of the increase of the peripheral blood flow and the reduction of muscle fatigue [58].

Anthocyanins from litchi fruit pericarp strongly inhibited linoleic acid oxidation and exhibited dose-dependent free-radical-scavenging activity against the 1,1-diphenyl-2-picrylhydrazyl radical (DPPH), superoxide anions and hydroxyl radicals. The degradation of deoxyribose by hydroxyl radicals was likely used for the inhibition by anthocyanins acting mainly as indirect chelators of iron ions rather than directly scavenging the hydroxyl radicals, suggesting that anthocyanins in litchi fruit pericarp might be beneficial as a scavenger against the free radicals or as a reducing agent against production of the lipid peroxidation [59].

The electrochemical and antioxidant properties of delphinidin, cyanidin, pelargonidin, kuromanin and callistephin were studied [60]. Antioxidant activities of the anthocyanins were evaluated using the 1,1-diphenyl-2-picrylhydrazyl (DPPH) radical-scavenging method. The order of antioxidant activity of the five anthocyanins was delphinidin > cyanidin > pelargonidin > kuromanin > callistephin.

5
Interactions of Anthocyanins with Biomolecules

5.1
Mechanism of Interaction of Anthocyanins with DNA

Human gene DNA is composed of a series of polymerized nucleotides, joined by phosphodiester bonds between the 5′ and 3′ carbons of deoxyribose units. A double helix is formed between the two strands, which run in opposite

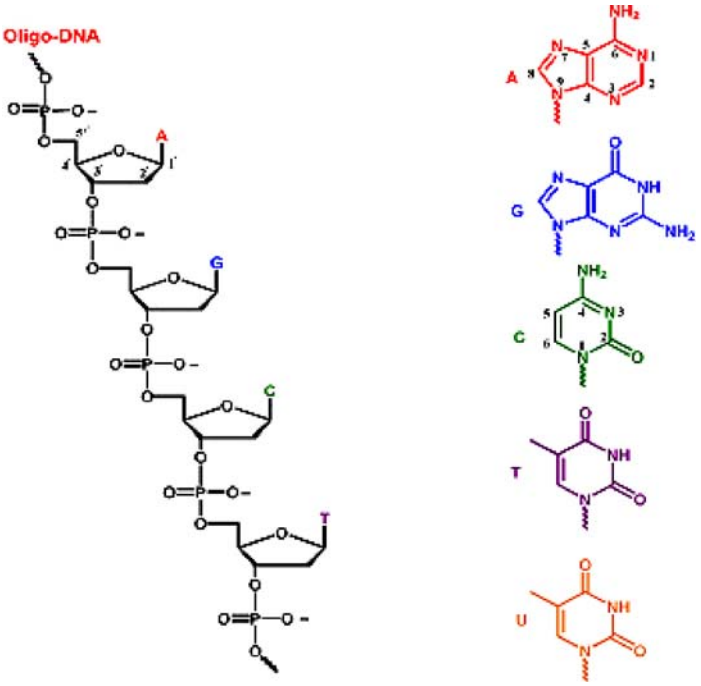

Fig. 3 Structures of oligo-DNA and bases

directions [61] (Fig. 3). The nucleotide bases form the hydrogen bonds to maintain the DNA structure, with two bonds between adenine and thymine bases (A = T) and three bonds between cytosine and guanine (C ≡ G) residues. These DNA bases always exist in the center of the double helix, with the deoxyribose and phosphate groups on the outside of the DNA.

The most common form of the DNA double helix is referred to as B type-DNA. The B-DNA helix contains two grooves, the major groove and the minor groove. The major groove is wider and deeper. There is a greater opportunity for the molecules to interact in the major groove due to its larger size. In addition, there is potential for the hydrogen bonds between the DNA base pairs in these grooves, as there is access to both sides of DNA. A type-DNA is a helical form that is generated when the duplex is dehydrated. A-DNA's helix is wider and shorter than that of B-DNA, and has a narrower major groove and almost no minor groove. A third DNA species is the Z type-DNA, which is a form that consists of a left-handed helix (A- and B-DNA are right handed). This zigzag Z-DNA has only a single groove and is present in oligonucleotides with alternating pyrimidine and purine bases. Most physiological DNA in human gene is present in the B-form.

The ligands could interact with DNA, primarily, in the following ways (Fig. 4 [62]): (i) Surface binding by interionic interactions with the positively

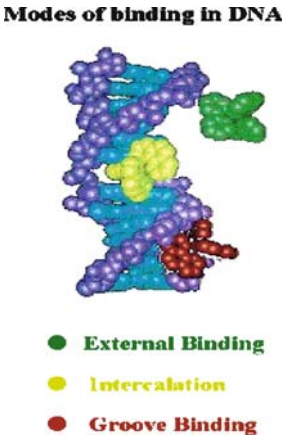

Fig. 4 Modes of binding in DNA

charged species, (ii) intercalation of the polycyclic aromatic (arene) rings in between the base stacks, and (iii) specific recognition in major and minor grooves via hydrophobic and hydrogen-bonding interactions.

Among the three basic components of DNA, viz. sugars, phosphate and heterocyclic bases (nucleic acid bases), the (deoxy) sugar and phosphate provide centers for non-specific hydrophobic and electrostatic interactions, respectively. The aza-arene bases of purines and pyrimidines in DNA are responsible for the specific hydrogen-bonding interactions in the major and minor grooves. Many biomolecules such as cytokines in the human body might form complicated combinations by the above three modes to generate their high sequence-specificity in DNA binding. If the ligand has an extended aromatic portion, it itself could be put between the two base pairs in a sandwich-like complex. This phenomenon, called intercalation [63–65], was first described by Lerman to explain the interaction binding of aminoacridines with DNA [66]. The intercalation is generally brought out by a (few) π–π interaction(s) between the molecule and the aromatic heterocyclic bases (aza-arene bases) of DNA. Interestingly, the intercalation could increase the separation of adjacent base–base pairs and the resulting helix distortions are compensated by adjustments in the sugar phosphate backbone, generally by an unwinding of the duplex. Ethidium bromide (EtBr) is a typical example of a DNA intercalator [64, 65].

DNA plays a major role in the life process because it carries human genetic information and instructs the biosynthesis of proteins and enzyme through the two processes of replication and transcription of genetic information. The exact recognition and exploration of duplex DNA through binding molecules might be a promising approach to the developments of novel reagents, which could recognize binding sites and probe the structure and function of DNA. Moreover, an understanding of how molecules bind to DNA could be poten-

tially useful in the design of new drugs such as anticancer agents, and in new treatments for genetic and other diseases. Many anticancer, antibiotic and antiviral drugs have exerted their primary treatment effects by the reversible interaction of a DNA targeting drug, such as actinomycin D, with DNA. Therefore, DNA could be a major target for the production of next-generation therapeutics, especially for age-related diseases such as cancer, hypertension and diabetes.

Anthocyanins have very similar structures to potent intercalating agents such as actinomycin D and mitomycin C, which are clinically used [67]. Nucleic acids such DNA and RNA have also been proved to act as highly reactive copigments for the natural anthocyanins [66]. In this case, the copigmentation effect was attributed to an intercalating phenomenon between two closely adjacent base pairs, which represent the intercalation between both proper sites for their $\pi-\pi$ hydrophobic stacking. The interaction of anthocyanins with calf thymus DNA (ctDNA) was reported by Sarma and Sharma [69]. The addition of DNA to cyanidin solution resulted in a 15–20 nm bathochromic shift in the λ_{max} of the cyanidin derivative, revealing that a charge-transfer complex DNA (ctDNA) could be formed as a copigmentation complex [69] of the cyanidin molecule with DNA (Fig. 5). The individual exposure of either cyanidin or ctDNA to hydroxyl radicals (OH) obtained in a Fenton reaction caused severe oxidative damage. However, the formation of the cyanin–DNA complex prior to exposure to the hydroxyl radicals could protect both the cyanidin and ctDNA from the oxidative damage. Based on these facts, the cyanidin–DNA copigmentation might be a possible defense mechanism against oxidative damage to DNA and might have normal physiological functions in vivo. The antiradical property of anthocyanin extracted from black chokeberry, black-thorn, and strawberry was reported by Espin et al. [70]. The DNA triplex stabilization property of seven natural anthocyanins (five monoglucosides and two diglucosides) has been determined by triplex denaturation experiments [33, 69]. It was believed that the difference between the diglucosides and monoglucosides could be due to the supplementary sugar moiety at the 5 position for the diglucosylated compounds, which would make the anthocyanins too crowded and close together to allow their interactions with the triplex. Further, the most active compounds among the monoglucoside series are the only anthocyanins to embody a catechol B-ring in their structure, which could be important for such an interaction.

Hordeumin, a purple anthocyanin–tannin pigment, was extracted from barley bran-fermented broth and was shown to scavenge superoxide radicals in a concentration-dependent manner. Hordeumin had also an antimutagenicity effect [71, 72]. Endothelial cells enriched with elderberry anthocyanins exhibited significant protective effects against oxidative stressors such as hydrogen peroxide, 2,2′-azobis(2-amidinopropane) dihydrochloride, and iron(II) sulfate/ascorbic acid [55].

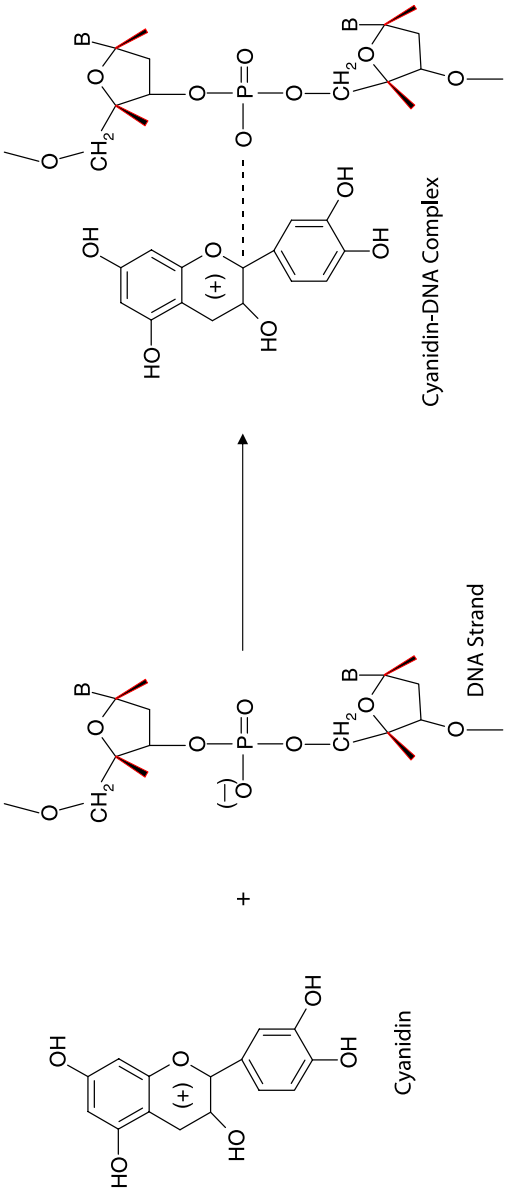

Fig. 5 Formation of cyanidin–DNA complex

The potential of a natural anthocyanin with purple corn color (PCC) has been tested against colorectal carcinogenesis, using male F344/DuCrj rats that were initially treated with 1,2-dimethylhydrazine (DMH). 2-Amino-1-methyl-6-phenylimidazo[4,5-*b*]pyridine (PhIP) exerted promoting effects on

the DMH-induced colorectal carcinogenesis, and this could be reduced by adding PCC (5.0%) to the rat's diet [73]. The acylated anthocyanins had strong, maltase inhibitory activities with IC50 values of $< 200\ \mu M$, whereas no sucrase inhibition was observed [74, 75]. Since the deacylated anthocyanins reduced the iAGH (maltase) inhibitory activity, the acylation of anthocyanin with caffeic or ferulic acid was shown to be an important factor in the inhibition of iAGH (maltase) expression [73].

The interaction of DNA with delphindin (Dp) was studied by FTIR and UV-visible difference spectroscopic methods. At low Dp concentration, a major interaction of Dp with the backbone phosphate group of DNA was observed. This interaction was between the positively charged Dp (oxy) and the PO_2 group; the ctDNA complex led to phosphate charge neutralization and helix stabilization. The evidence for the complex formation was evident from IR spectrum. These spectral changes were attributed to the indirect interaction of Dp (via OH and O+) with guanine, adenine and thymine bases. The observed shifting of the sugar–phosphate bands at $837\ cm^{-1}$ and $1710\ cm^{-1}$ was assigned to a partial reduction of the B-DNA towards A-DNA upon Dp complexation [76].

5.2 Mechanism of Interaction of Anthocyanin with Protein

The word "protein" describes molecules or those parts of molecules that are composed entirely of α-amino acid residues, covalently united head-to-tail by peptide linkages to form the long, unbranched polymers. Serum albumins are one of the most studied proteins [77, 78]. Human serum albumin (HSA) is the principal extracellular protein, with a high concentration in the blood plasma [77, 79] ($40\ mg\ mL^{-1}$ or $0.6\ mM$). The HSA helps to maintain the normal colloid osmotic blood pressure and is mainly responsible for the maintenance of blood pH. HSA is a globular protein and the crystallographic analyses of HSA have revealed that the protein is a 585-amino acid residue monomer containing three homologous α-helical domains (I–III), each containing two subdomains (A and B), stabilized by 17 disulfide bridges [77, 79] (Fig. 6).

Aromatic and heterocyclic ligands were found to bind within two hydrophobic pockets in subdomains IIA and IIIA, which are site I and site II of HSA [77, 79]. HSA contains a single tryptophan (Trp 214). Seven binding sites in HSA are localized for fatty acids in subdomains IB, IIIA, IIIB and on the subdomain interfaces [80]. HSA also has a high affinity metal binding site at the N-terminus [79]. Moreover, HSA is known to play an important role for the transport and disposition of the endogenous and exogenous ligands present in blood [79, 81]. The remarkable capacity of HSA to bind a variety of drugs could be an important key for the expression of the extensive role of HSA in HSA–drug pharmacokinetics and pharmacodynamics.

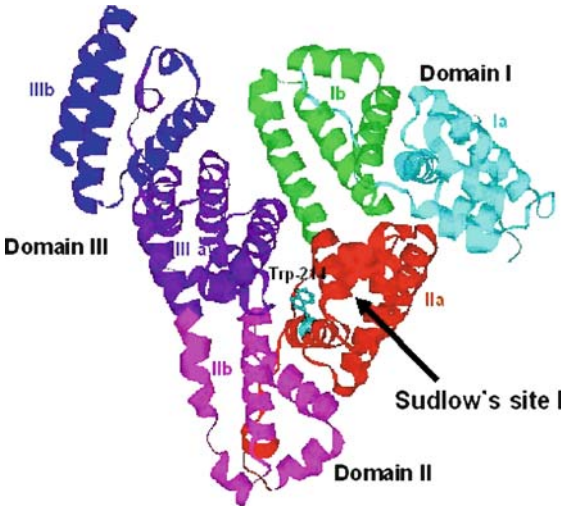

Fig. 6 Structure of human serum albumin

Protein binding is a rapid and reversible process, where the concentrations of the drug and the protein might easily reach the equilibrium state. Generally, the reversible binding of a ligand (L) to a protein (P) can be described by a simple equilibrium expression: $P + L \rightleftharpoons PL$. The unbound drug in the plasma can transfer freely to the target organ to produce the pharmacological effect, whereas the bound drug will not pass easily through the blood capillary walls to reach the action site because of its bigger molecular weight. The effectiveness of drugs depends on their binding ability to proteins. Generally, weak binding to proteins leads to a short lifetime or poor distribution, while strong binding to proteins decreases the concentrations of free drug in plasma. Many pharmaceutical firms have their own developed and standardized screens for HSA binding in the first step of new drug design. Therefore, studies on the interactions of a bioactive compound with HSA could easily assume significance in chemistry, biochemistry, life sciences and clinical medicine [82–84].

An interaction of HSA with Dp was studied by spectroscopic methods [85]. Infrared spectroscopic results gave evidence on Dp–HSA complex formation. The observed spectral changes were assigned to the interaction of Dp with the protein C = O and C – N groups. On Dp complex formation, the α-helix structure was reduced from 55% to 42–46%, whereas the β-sheet increased from 15% to 17–19% and the β-anti also increased from 7% to 10–20% at high Dp concentration. Furthermore, it is interesting to note that no major alterations of the protein secondary structure occurred upon the interaction at low concentration of Dp. The absorption spectrum revealed a major reduction of the intensity and a shifting of the characteristic UV absorption bands of Dp at 572 nm upon HSA interaction. The binding constant *K* was evaluated

by the double reciprocal plot of $1/A–A_0$ versus 1/[drug], and it was found to be 4.71×10^5 M^{-1} from the ratio of the intercept to the slope. The stability of the Dp–HSA complex might be attributed to the presence of a positive charge on the polyphenolic ring, which interacted with the protein negative charges and stabilized the Dp–HSA complex. This could be the reason for the decrease in the absorption intensity of Dp [85].

6 Conclusions

Anthocyanins are the largest group of phytochemical pigments in the plant kingdom and exhibit antioxidant properties. These anthocyanins are common in human daily foods. Though several papers have been published on anthocyanins, there are still fewer studies than on other flavonoids. Spectroscopic studies have indicated interactions of anthocyanins with DNA. Both base and phosphate groups in DNA could interact with the higher concentrations of Dp. Structural modeling and spectroscopic results reveal the moderate binding for the Dp–HSA complexes. Dp might mainly locate in the vicinity of the protein subdomain IIA, having both hydrogen bonding and ionic interactions with DNA.

References

1. van Tunen AJ, Mol JNM (1991) Plant Biotechnol 2:94
2. Middleton EJ (1998) Adv Exp Med Biol 439:175
3. de Groot H, Rauen U (1998) Fundam Clin Pharmacol 12:249
4. Middelton E, Kandaswami C, Theoharides TC (2000) Pharmacol Rev 52:673
5. Yang CS, Landau JM, Huang MT, Mewmark HL (2001) Annu Rev Nutr 21:381
6. Ren W, Qiao Z, Wang H, Zhu L, Zhang L (2003) Med Res Rev 23:519
7. Halliwell B, Aeschbach R, Loliger J Arouma OI (1995) Food Chem Toxicol 33:617
8. Ferguson LR (2001) Mutat Res 475:89
9. Sakihama Y, Cohen MF, Grace SC, Yamasaki H (2002) Toxicol 177:67
10. Amic D, Davidovic-Amic D, Beslo D, Trinajstic N (2003) Croatica Chim Acta 76:55
11. Fleschin S, Fleschin M, Nita S, Pavel E, Magearu V (2003) Roun Biotechnol Lett 5:479
12. Blackburn GM, Gait MJ (1996) Nucleic acids in chemistry and biology. Oxford University Press, New York, chap. 8
13. Husain SR, Cillard J, Cillard P (1987) Phytochemistry 26:2489
14. Afanas'ev IB, Osttrachovitch EA, Abramova NE, Korkina LG (1995) Biochem Pharmacol 50:627
15. Jagetia GC, Venkatesha VA, Reddy TK (2003) Mutagenesis 18:337
16. Wu X, Prior RL (2005) J Agric Food Chem 53:3101
17. Anderson OM (2002) Anthocyanin occurrences and analyses. In: Proceedings of the international workshop on anthocyanins: research and development of anthocyanins. Adelaide, Australia, 17–19 April 2002. pp 17–19

18. Prior RL (2004) Absorption and metabolism of anthocyanins: potential health effects. In: Meskin M, Bidlack WR, Davies AJ, Lewis DS, Randolph RK (eds) Phytochemicals: mechanisms of action. CRC, Boca Raton, pp 1–19
19. Cooke D, Steward WP, Gescher AJ, Marczylo T (2005) Eur J Cancer 41:1931
20. Mazza G, Miniati E (1993) Anthocyanins in fruits, vegetables, and grains. CRC, Boca Raton, p 362
21. Brouillard R, Delaporte B (1977) J Am Chem Soc 99:8461
22. Brouillard R (1982) Chemical structure of anthocyanins. In: Markakis P (ed) Anthocyanins as food colors. Academic, New York, pp 1–40
23. Zenner K, Bopp M (1987) J Plant Physiol 126:475
24. Jonsson LM, Donker-Koopman WE, Schram AW (1984) Plant Cell Tiss Org 8:113
25. Nissim-Levi A, Kagan S, Ovadia R, Oren-Shamir M (2003) J Hortic Sci Biotechnol 78:61
26. Oren-Shamir M, Levi-Nissim A (1997) J Hortic Sci 72:425
27. Oren-Shamir M, Nissim-Levi A (1999) J Hortic Sci Biotechnol 74:355
28. Shaked-Sachray L, Weiss D, Moshe R, Nissim-Levi A, Oren-Shamir M (2002) Physiol Plant 114:559
29. Calderon AA, Garciaflorenciano E, Munoz R, Barcelo AR (1992) Vitis 31:139
30. Revilla E, Ryan JM, Martin-Ortega G (1998) J Agric Food Chem 46:4592
31. Giusti MM, Luis ERS, James R (1998) J Food Sci 63:219
32. Garcia-Viguera C, Zafrilla P, Tomas-Barberan FA (1998) Phytochem Anal 9:274
33. Jin MK, Lian SC, Ngoh KG, Tet FC, Brouillard R (2003) Phytochemistry 64:923
34. Prior RL, Wu X (2006) Free Radic Res 40:1014
35. Harborne JB (1988) Introduction to ecological biochemistry, 3rd edn. Academic, London
36. Joseph JA, Shukitt HB, Denisova NA, Bielinski D, Martin A, McEwen JJ, Bickford PC (1999) J Neurosci 19:8114
37. Kamei H, Hashimoto Y, Koide T, Kojima T, Hasegawa M (1998) Cancer Biother Radiopharmacol 13:447
38. Akihiro H, Kayoko M, Takumi N, Masashi S, Seiko T, Tadaomi K, Takatoshi K, Mikio N, Katsumi I, Nobuyuki I, Tomoyuki S (2001) Cancer Lett 171:17
39. Ghiselli A, Nardini M, Baldi A, Scaccini C (1998) J Agric Food Chem 46:361
40. Meiers S, Kemeny M, Weyand U, Gastpar R, von Angerer E, Marko D (2001) J Agric Food Chem 49:958
41. Wang J, Mazza G (2002) J Agric Food Chem 50:850
42. Cristoni A, Magistretti MJ (1987) Ed Prat 42:29
43. Sharma R (2001) Impact of solar UV-B on tropical ecosystems and agriculture. Case study: effect of UV-B on rice. Proceedings of Seawpit98 and Seawpit2000 1:92. Available at http://phototropism.tripod.com/UV-B.pdf. Last visited 18 March 2008
44. Rice ECA, Miller NJ, Paganga G (1996) Free Radical Biol Med 20:933
45. Kähkönen MHMP (2003) J Agric Food Chem 51:628
46. Satué-Gracia MT, Heinonen IM, Frankel EN (1997) J Agric Food Chem 45:3362
47. Kim DO, Lee CY (2004) Crit Rev Food Sci 44:253
48. Tsuda T, Horio F, Osawa T (1998) Lipids 33:583
49. Sarma AD, Sreelakshmi Y, Sharma R (1997) Phytochemistry 45:671
50. Noda Y, Kaneyuki T, Igarashi K, Mori A, Packer L (1998) Res Commun Molecul Pathol Pharmacol 102:175
51. Gabrielska J, Oszmianski J, Komorowska M, Langner M (1999) Z Naturforsch C 54:319
52. Tsuda T, Horio F, Kitoh J, Osawa T (1999) Arch Biochem Biophy 368:361

53. Narayan M, Naidu K, Ravishankar G, Srinivas L, Venkataraman L (1999) Prostaglandins Leukot Essent Fatty Acids 60:1
54. Wang SY, Lin HS (2000) J Agric Food Chem 48:140
55. Youdim KA, Martin A, Joseph JA (2000) Free Radical Biol Med 29:51
56. Pilaczynska-Szczesniak L, Skarpanska-Steinborn A, Deskur E, Basta P, Horoszkiewicz-Hassan M (2005) Int J Sport Nutr Exerc Metab 15:48
57. Valcheva KS, Marazova K, Krasnaliev I, Galunska B, Borisova P, Belcheva A (2005) Exp Toxicol Pathol 56:385
58. Matsumoto H, Takenami E, Iwasaki KK, Osada T, Katsumura T, Hamaoka T (2005) Eur J Appl Physiol 94:36
59. Xuewu D, Yueming J, Xinguo S, Zhaoqi Z, John S (2007) Food Chem 101:1365
60. de Lima AA, Eliana MS, Wagner F De Giovani (2007) Croatica Chim Acta 80:34
61. Watson JD, Crick FH (1953) Nature 171:737
62. http://www.photobiology.com/photoiupac2000/pierard/Interactionmain.html
63. Neidle S, Abraham Z (1984) Crit Rev Biochem 17:73
64. Wang JC (1974) J Mol Biol 89:783
65. Wang A (1992) Current Opin Struct Biol 361:361
66. Lerman LS (1961) J Mol Biol 3:18
67. Mas T, Susperregui J, Berké B, Chèze C, Moreau S, Nuhrich A, Vercauteren J (2000) Phytochemistry 53:679
68. Mistry TV, Cai Y, Lilley TH, Haslam E (1991) J Chem Soc Perkin Trans 2:1287
69. Sarma AD, Sharma R (1999) Phytochemistry 52:1313
70. Espin JC, Soler RC, Wichers HJ, Garcia VC (2000) J Agric Food Chem 48:1588
71. Deguchi T, Ohba R, Ueda S (2000) J Agric Food Chem 48:3198
72. Deguchi T, Yoshimoto M, Ohba R, Ueda S (2000) Biosci, Biotech Biochem 64:414
73. Hagiwara A, Miyashita K, Nakanishi T, Sano M, Tamano S, Kadota T, Koda T, Nakamura M, Imaida K, Ito N, Shirai T (2001) Cancer Lett 171:17
74. Matsui T, Ueda T, Oki T, Sugita K, Terahara N, Matsumoto K (2001) J Agric Food Chem 49:1948
75. Matsui T, Ueda T, Oki T, Sugita K, Terahara N, Matsumoto K (2001) J Agric Food Chem 49:1952
76. Kanakis CD, Tarantilis PA, Polissiou MG, Diamantoglou S, Tajmir RHA (2005) Biomol Str Dyn 22:739
77. Carter D, Chang B, Ho JX, Keeling K, Krishnasami Z (1994) Eur J Biochem 226:1052
78. Brown JR, Shockley P (1982) Lipid–protein interactions, vol 1. Wiley, New York
79. Peters T (1996) All about albumin biochemistry, genetics and medical application. Academic, San Diego
80. Carter DC, Ho JX (1994) Adv Protein Chem 45:153
81. Doumas BT, Peters T (1997) Clin Chim Acta 258:3
82. Jianniao T, Jiaquin L, Hu Z, Xingguo C (2005) Bioorg Med Chem 13:4124
83. Jiaquin L, Jianniao T, Wenying H, Jianping X, Hu Z, Xingguo C (2004) J Pharm Biomed Anal 35:671
84. Kandagal PB, Seetharamappa J, Shaikh SMT, Manjunatha DH (2007) J Photochem Photobiol Part A 185:239
85. Kanakis CD, Tarantilis PA, Polissiou MG, Diamantoglou S, Tajmir-Riahi HA (2006) J Mol Str 798:69

Top Heterocycl Chem (2008) 15: 67–132
DOI 10.1007/7081_2007_108

Published online: 29 April 2008

Antibacterial Activity of Artificial Phenothiazines and Isoflavones from Plants

Asish Dasgupta[1,2] · Sujata G. Dastidar[1] (✉) · Yoshiaki Shirataki[3] · Noboru Motohashi[4]

[1] Division Microbiology, Department of Pharmaceutical Technology, Jadavpur University, Kolkata 700032, India
jumicrobiol@yahoo.co.in

[2] *Present address:*
Microbiology Section, Herbicure Healthcare Bio-Herbal Research Foundation, Kolkata 700 104, India

[3] Faculty of Pharmaceutical Sciences, Josai University, 1-1 Keyakidai, Sakado, 350-0295 Saitama, Japan

[4] Meiji Pharmaceutical University, Kiyose, Tokyo, Japan

Abstract Significant antimicrobial action was detected in vitro and in vivo in phenothiazines that are applied to humans as neuroleptics or antihistamines. Both Gram-positive and Gram-negative bacteria were equally sensitive, with the MIC varying between 25 and 100 μg/ml with most agents. Some phenothiazines were bactericidal, while others were bacteriostatic in action. Similar activity could be observed in isoflavonones obtained from the plants *Sophora* spp. Trifluoperazine and methdilazine exhibited antimycobacterial properties as well, and in experimental animals the latter showed definite healing properties. Chlorpromazine and thioridazine were able to eliminate R-plasmids in drug-resistant bacteria. Artificially synthesized Benzo[α]phenothiazines could effectively suppress adenovirus oncogene expression. Phenothiazines have now been shown to inhibit efflux pumps in multidrug-resistant bacteria.

Keywords Adenovirus · Antimycobacterial · Efflux pumps · Isoflavonones · Phenothiazines · R-plasmid

1 Introduction

Chemotherapy based on selective toxicity was first conceived by Paul Ehrlich. It relied on the principle that the drug should be more toxic and harmful for the invading microorganism than for the host. This understanding rendered the phenolic compounds and alcohols unsatisfactory as chemotherapeutic agents, since they caused considerable damage to the eukaryotic cells and their natural defense mechanisms.

Ehrlich's extensive studies with the vital dye, methylene blue, showed that this was readily taken up, or could bind itself to/by the malaria parasites in the blood. In 1904, salvarsan, a specific antimicrobial agent with low toxicity for humans, came into use [14]. In 1908, Ehrlich was instrumental in synthesizing it and used it as an antisyphilitic drug [14]. Mietzsch and Klarer [14] conducted a systematic synthesis of a series of azo dyes as possible antimicrobials; in 1935, Gerhard Domagk reported that another dye, prontosil, led to a remarkable curing of experimental streptococcal infection in mice [32]. Also in 1935, Trefouel et al. reported that the azo-linkage of prontosil was broken down metabolically when administered in vivo, in order to release the active antimicrobial component called sulfanilamide [99].

Conventionally, a drug is designated by its dominant or by its first recognized function. Examples include antihistamines, tranquilizers, sedatives, antihypertensives, hypnotics, anti-inflammatory agents, and many more. However, after their prolonged usage, other not necessarily toxic effects were discovered either accidentally or by systematic research. The history of development of pharmaceutical compounds has shown that a therapeutic agent may possess diverse functions and, therefore, may have a more useful activity in an entirely different field of medical treatment. The premier example of this would be prontosil, which initially served as a dye, but ultimately turned out to be highly successful antibacterial agent in vivo, thus, paving the way for

the discovery of a new class of antimicrobial compounds, the sulfonamides. Similarly, an anabolic stimulant and antihistamine is now found to be endowed with antimicrobial properties. A more recent example is that of the much used antipyretic analgesic, aspirin, which is now being recommended for cardiovascular diseases.

Drug discovery gradually became an exercise of detailed scientific knowledge, wisdom, and research. This resulted in drug explosion over the past 70 years in which minimum contribution has been made by the antimicrobial chemotherapeutic substances.

With the advent of antibiotics, the hit and miss discovery of the antimicrobial chemotherapeutic compounds became less important and less lucrative, since a large number of antibiotics that were discovered in a short period of time acted as magic bullets against various types of infections.

A major problem with antibiotics is that their overuse and improper use have led to the development of drug resistant bacteria and thus an increased number of infections with opportunistic bacteria, such as enterococci, coliforms, pseudomonads, streptococci which are versatile and capable of becoming multidrug resistant. With this background, it may be said that searching for newer antimicrobial substances would be a promising line of research in the field of clinical microbiology.

Although the field of chemotherapy had been dominated by antibiotics, efforts were continuing to widen the range of antimicrobial agents by investigating such actions in a host of compounds hitherto known only to possess completely different chemical or pharmacological activities. In this regard, during the period between 1950 and 1958, varying degrees of antibacterial action were obtained in the bactericidal agent, phenanthraquinone; the local anesthetic, amylocaine; the psychotropic agent, stelazine; and the anthelminthic drug, aspidin.

Since the 1970s, several groups of workers [26, 70] independently undertook a systematic study of the antimicrobial action of drugs belonging to various pharmacological classes not recognized as antimicrobials. This resulted in the accumulation of a large amount of evidence on many types of drugs possessing moderate to powerful antimicrobial action. All such drugs with antimicrobial activity have been grouped together under the common title “non-antibiotics”. The word non-antibiotic, which had been coined earlier for an antiseptic or a disinfectant, came into much wider usage and was applied in a large connotation to include all those compounds that were not known to be either antibiotics or antimicrobial chemotherapeutics, yet still possessed unmistakable antimicrobial effects.

The accumulated studies on the antimicrobial activity of non-antibiotics carried out by various groups of scientists revealed that such activities could be detected in increasing numbers among drugs from different pharmacological groups.

The first report of the distinct antimicrobial potentiality was made by Prof. Joseph Molnar and his associates in 1975 [71]. The drug was chlorpromazine, a phenothiazine discovered in 1950 for its antipsychotic property [14].

2 Phenothiazines

The word "phenothiazine" is used to describe the largest of five main classes of antipsychotic drugs. Although these drugs are generally effective, many serious side effects, including tardive dyskinesia and sedation, are observed especially in the early stages of treatment. In 1891, Paul Ehrlich observed the antimalarial effects of methylene blue, a phenothiazine derivative [55]. Later, the phenothiazines were developed for their antihistaminic properties [98]. In 1951, Laborit and Huguenard administered the aliphatic phenothiazine, chlorpromazine, to patients for its potential anesthetic effects during surgery [61]. Shortly thereafter, Hamon et al. [44] and Delay et al. [30] extended the use of this treatment in psychiatric patients and they serendipitously uncovered its antipsychotic activity.

A phenothiazine has a three-ring structure, in which a sulfur atom and a nitrogen atom link two benzene rings. If a carbon atom replaces the nitrogen atom at position 10 with a double bond to the side chain, the compound becomes a thioxanthene. Phenothiazines are classified into three groups.

Aminoalkyl compounds, such as chlorpromazine and promazine, antagonize α_1-adrenoreceptors, histamine H_1-receptors and muscarinic cholinergic receptors. The blockade of α_1-adrenoreceptors and histamine H_1-receptors gives chlorpromazine a sedating profile, while α_1-adrenoreceptor blockage also causes hypotension. The anticholinergic activity may cause dry mouth, urinary difficulties, and constipation, while, on the other hand, offsetting the liability to produce extra pyramidal effects.

Piperidine compounds, such as thioridazine, are similar to chlorpromazine, because they are very potent muscarinic antagonists with correspondingly low incidences of movement disorders.

Piperazine compounds, such as trifluoperazine or fluphenazine, are the most selective dopamine receptor antagonists. They have the least sedating action and they are the most likely producer of extra pyramidal effects.

2.1 Basic Phenothiazine Structure

Butyrophenones

Butyrophenones, such as haloperidol and droperidol, have a different structure but are clinically similar to the thioxanthenes. They are potent dopamine

Table 1 Basic structures of phenothiazine and related compounds

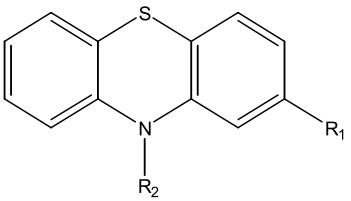

Type of compound	Example	R_1	R_2
Aminoalkyl compound	Chlorpromazine	–Cl	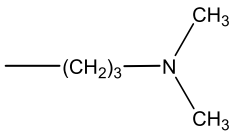
Piperidine	Thioridazine	$-SCH_3$	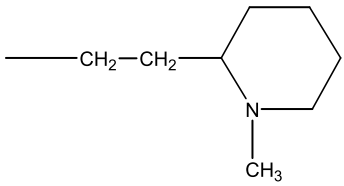
Piperazine	Trifluperazine	$-CF_3$	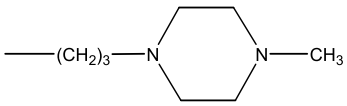
	Fluphenazine	$-CF_3$	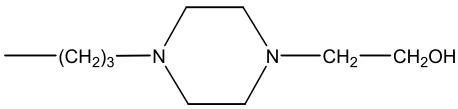

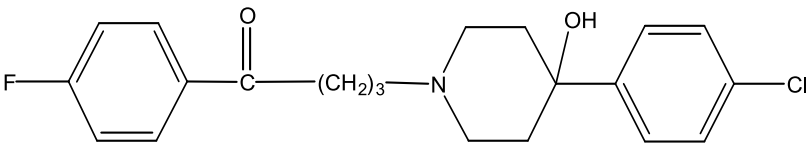

Haloperidol (butyrophenone compound)

receptor antagonists with few effects on other neurotransmitter receptors. They are not sedating but have a high propensity to cause extra pyramidal effects.

Thioxanthenes

Thioxanthenes differ from the phenothiazines by having a carbon atom instead of a nitrogen atom in the central ring. The thioxanthenes can be represented as two geometric stereo-isomers: *Cis*(Z)- and *trans*(E)- compounds. Only the *cis*(Z)- compounds have been shown to be neuroleptically active [83].

Thioxanthenes, such as flupenthixol and clopenthixol, are similar in structure to the phenothiazines. The therapeutic effects are similar to those of the piperazine group. Antipsychotic thioxanthenes are thought to benefit psychotic conditions by blocking postsynaptic dopamine receptors in the brain. They also produce an alpha-adrenergic blocking effect and depress the release of most hypothalamic and hypophyseal hormones. However, the concentration of prolactin is increased due to blockade of prolactin inhibitory factor (PIF), which inhibits the release of prolactin from the pituitary gland.

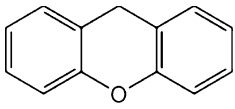

Thioxanthene molecule

3 Antimicrobial Potentiality of Phenothiazines

A phenothiazine compound with potent antimicrobial action was first noticed by Prof. Joseph Molnar and his team in Szeged, Hungary, in 1976 [70]. They observed that chlorpromazine was antibacterial against *Bacillus anthracis* following the agar dilution technique. The minimum inhibitory concentrations (MIC) varied between 12 and 25 μg/ml for this bacterium. Molnar et al. then studied the effect of chlorpromazine along with levomeprazine and promethazine against *Staphylococcus aureus*, *Diplococcus pneumoniae*, *Corynebacterium hofmanni* as the test bacteria. Chlorpromazine turned out to be equally potent against these microorganisms; however, the other two phenothiazines were less effective, since the MIC values were much higher. With respect to *Escherichia coli*, *Proteus vulgaris* and *Klebsiella pneumoniae*, the MIC values of chlorpromazine and levomeprazine varied between 100 and 125 μg/ml, but the MIC of promethazine against all the bacteria was between 125 and 250 μg/ml. Strains of *Pseudomonas aeruginosa* were found to be resistant to all tested phenothiazines. Molnar et al. [70] could further determine that chlorpromazine possessed bactericidal activity against both *Escherichia coli* and *Staphylococcus aureus* at 100 μg/ml. They reported that all three phenothiazines could exert a bacteriostatic effect on Gram-positive

bacteria at 20–40 μg/ml and on Gram-negative bacteria at 130–180 μg/ml concentrations of the three compounds. Chlorpromazine had a marked bactericidal effect on cultures of *Bacillus anthracis* growing in minimal medium. In addition, this compound had a significant bactericidal effect on the resting cells of *Escherichia coli* suspended in saline.

3.1 Antimicrobial Properties of Chlorpromazine

Molnar, Beladii, and Foldes [69] studied antimycobacterial activity of five phenothiazine derivatives including chlorpromazine, levomeprazine, promazine, promethazine, and diethazine. The growth of *Mycobacterium tuberculosis*, *Mycobacterium bovis*, and *Mycobacterium butyricum* was found to be inhibited by chlorpromazine at practically identical concentrations. The minimum inhibitory concentrations for *Mycobacterium tuberculosis* were: chlorpromazine and levomeprazine 10 μg/ml; diethazine and promethazine 20 μg/ml; whilst chlorpromazine sulphoxide was ineffective even at 100 μg/ml. Chlorpromazine and promethazine exerted a measurable bactericidal activity on *Mycobacterium tuberculosis* at 50 μg/ml; total destruction of the organism and loss of acid fastness in part of the cells were shown at 300 μg/ml. Preliminary studies in mouse experiments revealed that phenothiazine derivatives were ineffective.

In 1979, Jette E. Kristiansen of Copenhagen, Denmark, performed extensive experiments to elaborate the effect of chlorpromazine on the permeability of the bacterial cell wall [55]. In vitro experiments were carried out with *Staphylococcus aureus* under the influence of chlorpromazine. Depigmentation and bacteriostatic/bactericidal effects of chlorpromazine on the microorganisms were observed. It has been shown that concentrations of chlorpromazine near the bacteriostatic value, in combination with bacterial haemolysins, could alter erythrocyte membranes of horse and rabbit blood in such a way that they become resistant to haemolysis. It was further realized that chlorpromazine in bacteriostatic concentration probably changed the transport of potassium through the bacterial membrane in the same manner as described for mammalian muscle tissue [54].

In 1981, Kristiansen and Blom studied the effect of chlorpromazine on the ultrastructure of *Staphylococcus aureus* [56]. Their study centered around the growth of *Staphylococcus aureus* on plates containing chlorpromazine at concentrations up to the bacteriostatic level (150 μg/ml). They observed that high concentrations of chlorpromazine induced large Mesosome-like structure and an asymmetrical cell division in a considerable number of cells.

Kristiansen and Blom [56] examined various types of phenothiazines for antibacterial effect on 61 Gram-positive and Gram- negative bacterial strains in vitro; the investigated phenothiazines were two neuroleptic drugs, fluphenazine and chlorpromazine, and an antihistaminic drug, prometha-

Table 2 List of phenothiazines tested for antimicrobial action

Compound	Obtained from	Refs.
Promazine	Wyeth, Bombay, India	[20]
Methdilazine	Glaxo Laboratories, India	[16]
Promethazine	May and Baker, Bombay, India	[15]
Fluphenazine	Sarabhai Chemicals, India	[21]
Trimeprazine	Sarabhai Chemicals, India	[24]
Thioridazine	Sun Pharma, India	[88]
Trifluoperazine	Smitkline Beecham Pharmaceuticals (India) Ltd. India	[64]
Triflupromazine	Sarabhai Chemicals, India	[22]
Prochloperazine	Rallis India Limited, Mumbai, India	[5]
Flupenthixol	Lundbeck Pvt. Ltd, Bangalore, India	[50]

Table 2 shows the phenothiazine compounds tested by Dastidar, Chakrabarty and their group for detection of antimicrobial action along with the names of industries which supplied these compounds in pure, dry powder form. The table also provides specific references.

zine. All three drugs had antibacterial effects in vitro, with the phenothiazines being more potent against Gram-positive microorganisms. The antibacterial potency of drugs was measured as IC50: fluphenazine 29 μM (15 μg/ml), alimunzaine 49 μM (37 μg/ml), promethazine 88 μM (28 μg/ml), and chlorpromazine 92 μM (29 μg/ml). The antibacterial potency of drugs was linked neither to the neuroleptic nor to the antihistaminic potency of drugs, which appeared in agreement with the results of earlier stereoisomeric investigations. Therefore, these phenothiazines potentially represented a pool of new antimicrobial drugs. However a therapeutic application of these results have remained unexplained [56].

Since 1977, Dastidar, Chakrabarty, and their team of students have made significant contributions in this field [14]. They were able to determine moderate to highly powerful antibacterial and antimycobacterial properties in several phenothiazines. The list of drugs studied by these authors is presented in Table 2.

4 Materials and Methods

4.1 Bacteria

The source of bacterial strains used by Dastidar and co-workers are described in Table 3. The number of test bacteria against each phenothiazine varied be-

Table 3 Names, sources and numbers of bacterial strains

Name of the bacteria	No. of strains	Source
Staphylococcus aureus ML 2, ML 6, ML 9, ML 11	118	Dr. M. R. Lahiri, Calcutta
Staphylococcus aureus NCTC 6571, NCTC 8530, NCTC 8531, NCTC 8532	4	Dr. S. P. Lapage, London
Staphylococcus aureus ATCC 6538, ATCC 29737, ATCC 25923	3	Central Drugs Laboratory, Calcutta
Staphylococcus aureus SA 1, SA 3, SA 6, SA 15, SA 17, SA 18, SA 36, SA 99, SA 379, SA 467	10	Prof. S. G. Dastidar, Jadavpur University, Calcutta
S. aureus BDC 1	1	Prof. B. D. Chatterjee, Ruby General Hospital, Calcutta
Streptococcus lactis 309	1	Prof. A. N. Chakrabarty, Calcutta University College of Medicine, Calcutta
Staphylococcus aureus Bang 18, Bang 25, Bang 43, Bang 44, Bang 46	6	Dr. N. Gupta, Bangur Hospital, Calcutta
Staphylococcus aureus PS 29, PS 40, PS 42, PS 52, PS 53	17	Prof. A. N. Chakrabarty, Calcutta
PS 84, PS 85, PS 94, PS HK 2, VS 14, WS 2, WS 75, Pathogenic 2/01, MLPS 301, PGI/01		University College of Medicine, Calcutta
Staphylococcus aureus UT 0002, UT 0007	2	Dr. Roglsky, USA
Bacillus brevis NCTC 7096	1	Dr. S. Ghosh, London
Bacillus cereus ATCC 11778	1	Central Drugs Laboratory, Calcutta
Bacillus cereus ATCC 11778 var. mycoides	1	Dr. S. Ghosh, London
Bacillus licheniformis NCTC 10341	1	Dr. S. Ghosh, London
Bacillus polymyxa NCTC 4747	1	Dr. S. P. Lapage, London
Bacillus pumilus NCTC 8241	1	Dr. S. P. Lapage, London
Bacillus subtilis ATCC 6633, MP 1	1	Dr. S. P. Lapage, London
Bacillus subtilis UC 564	2	Upjhon laboratory USA
Bacillus sphaericus NCTC 431	1	Prof. A. N. Chakrabarty, Calcutta University College of Medicine, Calcutta
Micrococcus detolia 1/01	2	Central Drugs Laboratory, Calcutta
Micrococcus luteus ATCC 9341		
Streptococcus faecalis ATCC 29212	1	Central Drugs Laboratory, Calcutta
St. pneumoniae S 1, S 2	2	Prof. S. G. Dastidar, Jadavpur University, Calcutta
Escherichia coli K_{12} Row	1	Dr. J. D. Abbott, UK
E. coli 14, 306, 320, 334, 357, 383, 397, C 1, C 21, C22, DH 5 α, 54B-10 A,18/9	13	Prof. S. G. Dastidar, Jadavpur University, Calcutta

Table 3 (continued)

Name of the bacteria	No. of strains	Source
Escherichia coli 721, 798, 817, 870, 871, 872, 10536	7	Dr. Pratip Kundu, National Medical Medical College, Calcutta
Escherichia coli 478, C 600, MA 140, 517	4	Dr. S. Palchaudhuri, Detroit, USA
Escherichia coli K 88, K 99, K88 Ac	2	Staten's Serum Institute, Denmark
Escherichia coli ES 2 A, ETEC	2	Prof. A. N. Chakrabarty, Calcutta University College of Medicine, Calcutta
Escherichia coli ATCC 25922, ATCC 25938	2	Central Drugs Laboratory, Calcutta
Escherichia coli R 122, R 224, R 239	3	Dr. Krishna Bhattacharya, Woodlands Nursing home, Calcutta
Klebsiella pneumoniae 1, 14, 57, J 14, J/1/4, R 114, 725	7	Prof. A. N. Chakrabarty, Calcutta University College of Medicine, Calcutta
Klebsiella pneumoniae SSKM/1/01	1	Prof. K. Karak, Institute of Post Graduate Medical Education and Research (IPGMER), Calcutta
Klebsiella pneumoniae ATCC 10031	1	Central Drugs Laboratory, Calcutta
Salmonella berta 69	1	Dr. Joan Taylor, Salmonella Reference Laboratory, London
Salmonella choleraesuis NCTC 36, NCTC 37	2	Dr. Joan Taylor, Salmonella Reference Laboratory, London
Salmonella london 76	1	Dr. Joan Taylor, Salmonella Reference Laboratory, London
Salmonella paratyphi A NCTC 1, A NCTC 2, B NCTC 5	3	Dr. Joan Taylor, Salmonella Reference Laboratory, London
Salmonella typhi NCTC 57, NCTC 59, NCTC 62	3	Dr. Joan Taylor, Salmonella Reference Laboratory, London
Salmonella typhimurium NCTC 11, 74	2	Dr. Joan Taylor, Salmonella Reference Laboratory, London
Salmonella viballerup 1	1	Dr. Zia Uddin Ahmed, ICDDR, Dhaka, Bangaladesh
Salmonella typhi ATCC 3/4	1	Dr. Satadal Das, Peerless Hospital & B.K Roy Research Institute, Calcutta
Proteus mirabilis 7, 10, 21, 34, 175, 800	6	Prof. A. N. Chakrabarty, Calcutta University, College of Medicine, Calcutta
Proteus mirabilis C/6/5	1	Prof. A. N. Chakrabarty, Calcutta University, College of Medicine, Calcutta
Proteus vulgaris	1	Prof. A. N. Chakrabarty, Calcutta University, College of Medicine, Calcutta

Table 3 (continued)

Name of the bacteria	No. of strains	Source
Proteus vulgaris SSKM 1/01	1	Prof. K. Karak, IPGMER, Calcutta
Providencia spp.	1	Prof. A. N. Chakrabarty, Calcutta University, College of Medicine, Calcutta
Citrobacter spp.	1	Prof. A. N. Chakrabarty, Calcutta University College of Medicine, Calcutta
Enterobacter cloaca	1	Prof. A. N. Chakrabarty, Calcutta University College of Medicine, Calcutta
Shigella boydii 5 NCTC 541/60, 7 NCTC 315/61, 8 NCTC 254/66, 10 NCTC 386/66	4	Dr. K. Patricia Carpenter, London National Institute of Cholerae and Enteric Diseases, Calcutta
Sh. boydii BCH 937, D 13624, 9 E 16552	3	National Institute of Cholera and Enteric Diseases (NICED), Calcutta
Shigella dysenteriae 1	1	Dr. K. Patricia Carpenter, Dysentery Reference Laboratory, London
Shigella dysenteriae 2 NCTC 566/61, 3 NCTC 102/65, 5 NCTC 230/63, 6 NCTC 100/54, 7 NCTC 519/66, 8 NCTC 599/52, 9 NCTC 7919, 10 NCTC 2050/52	8	Dr. K. Patricia Carpenter, London
Sh. flexneri 6 NCTC 396/63	1	Dr. K. Patricia Carpenter, Dysentery Reference Laboratory, London
Sh. flexneri 2a NK 307, 3b NK 331, 2a 33220, 2a D00213, 3a 30903, DN 13, 5a B 18630, 5a BCH 511, BCH 995, BCH 895, 3b NK 331, BCH 995, BCH 999, 6 NK 126, F 20570	10	National Institute of Cholerae and Enteric Diseases, Calcutta
Sh. floxneri 6 BDC 1	1	Prof. B. D. Chatterjee, Ruby General Hospital, Calcutta
Sh. sonnei 1 NCTC 9774, 2	2	Dr. J. D. Abbott, Manchester U.K.
Sh. sonnei B 22461, BCH 217, DN 3, E 08869, F 11001, KS 1, NK 29	11	National Institute of Cholerae and Enteric Diseases, Calcutta
Arizona spp.	1	Prof. A. N. Chakrabarty, Calcutta University College of Medicine, Calcutta
Hafnia spp.	1	Prof. A. N. Chakrabarty, Calcutta University College of Medicine, Calcutta
Bordetella bronchiseptica 76	1	Prof. A. N. Chakrabarty, Calcutta University College of Medicine, Calcutta

Table 3 (continued)

Name of the bacteria	No. of strains	Source
Pasturella septica 136	1	Prof. A. N. Chakrabarty, Calcutta University College of Medicine, Calcutta
Vibrio cholerae ATCC 14033, 14035 9, 10, 12, 33, 39, 40, 42, 46, 53, 55, 56, 57, 58, 59, 64, 65, 67, 69, 71, 74, 83, 92, 97, 113, 117, 133, 141/69, 142, 142/69, 148, 154, 243/76, 288/75, 293, 423/75, 426	38	Dr. S. Mukerjee, International Vibrio Reference Center, Calcutta
Vibrio cholerae 522, 530, 538, 540, 546, 547, 550, 552, 553, 557, 564, 575, 583, 584, 585, 588, 590, 593, 728, 730, 734, 735, 752, 754, 756, 764, 765, 783, 792, 810, 811, 813, 817, 820, 824, 851, 852, 854, 856, 860, 862, 865, 914, 941, 945, 955, 976, 978, 1002, 1003, 1004, 1010, 1012, 1021, 1023, 1033, 1037, 1039, 1311, 1313, 1315, 1317, 1341, 1342, 1343, 1345, 347, 1348, 1351, 1363, 1363/75, 1392	72	Dr. Ranjit Sen, All India Institute of Hygiene and Public Health, Calcutta
Vibrio cholerae 569 B	1	Dr. N. K. Dutta, Haffkine Institute, Bombay
Vibrio cholerae DN 6, DN 7, DN 8, DN 16, DN 26	5	National Institute of Cholera and Enteric Diseases, Calcutta
V. cholerae Kathmandu 2, K9, K13, K22	4	Dr. Ranjit Sen, All India Institute of Hygiene and Public Health, Calcutta
Vibrio cholerae NG 8/69, NG 226/01, NG 44	3	Dr. S. Mukerjee, International Vibrio Reference Center (IVRC), Calcutta
Vibrio cholerae VRC 85, 106, 110/76, 242, 244, 293, 295, 369/76, 410, 418, 419, 423/75, 426, 440,475, 476/76, 1720, 2002/75, 2077, 2080, 2004/75, 2069/75, 2290/75, 2292, 2458/75	25	Dr. S. C. Pal, National Institute of Cholera and Enteric Diseases, Calcutta
Vibrio parahaemolyticus 5, P 3, P 4, P 5, P 7	5	Prof. A. N. Chakrabarty, Calcutta University College of Medicine, Calcutta
Vibrio parahaemolyticus P 8, 732, 734,916, 4379, 4750, 5507, 8742, 8848, 8942, 9166, 9331, 9369, 9379, 9580, 9601, 9602, 9603, 9606, 9639, 9750, 72003, 72008, 72016, 72026, 72027, 72040, 72172	28	Dr. Y. Miyamoto, Tokyo, Japan

Table 3 (continued)

Name of the bacteria	No. of strains	Source
Pseudomonas aeruginosa ATCC 25619, 27853	2	Central Drugs Laboratory, Calcutta
Pseudomonas aeruginosa APC/PS, C/1/7, Kr/12/3, 61, W 82, 71, 81, 1006	8	Prof. A. N. Chakrabarty, Calcutta University, College of Medicine, Calcutta
Pseudomonas aeruginosa AGD3	1	Prof. S. G. Dastidar, Jadavpur University, Calcutta
Pseudomonas putida 61	1	S. Palchaudhuri, Detroit, USA

tween 350 to 500; many of these strains have been obtained from international reference centers, while others were clinical isolates in various parts of India and preserved in a freeze-dried state and also as stab slant agar.

4.2 Tests for Identification of Different Bacteria

All the bacterial strains were identified on the basis of their morphology [85] (modification of Gram's method as described by [34]), motility [17], biochemical tests [4, 7, 8, 10, 11, 17, 35, 38, 39, 47, 53, 68, 96]), and serological tests [35, 47].

4.3 Media

4.3.1 Liquid Media

These included peptone water (bacteriological peptone, Oxoid 1.0%, Analar NaCl 0.5%, pH 7.2–7.4), nutrient broth (Oxoid), and Mueller–Hinton broth (Oxoid).

4.3.2 Solid Media

These included nutrient agar (Oxoid), Mueller–Hinton Agar (Oxoid), Desoxycholate Citrate Agar (Oxoid), and MacConkey Agar (Oxoid).

4.3.3 Blood Agar

This medium was prepared by adding sterile defribrinated sheep blood (10%) to sterile molten nutrient agar (Oxoid) at 55 °C.

4.4 Preparation of Standard Solutions

Stock solutions of 1 mg/ml and 10 mg/ml were prepared for antibiotics and chemotherapeutic agents, by dissolving a suitable quantity in an appropriate diluent. These were preserved at 4 °C; the solutions were used over a period not more than 3 months from the date of preparation.

4.5 Bacterial Inoculum

All organisms were grown overnight on nutrient agar/Mueller–Hinton agar/blood agar plates at 37 °C and harvested during the stationary phase. The suspension was standardized by diluting with saline or broth to a density visually equivalent to the McFarland standard 0.5% (a turbidity standard prepared by adding 0.5 ml of a barium chloride solution to 99.5 ml of 1% H_2SO_4), corresponding approximately to 5×10^5 CFU/ml [63]. The inoculations of the plates were made within 15 min of diluting the broth culture, so that the standardization was maintained throughout the study.

4.6 Determination of the Minimum Inhibitory Concentration (MIC) of Different Phenothiazines with Respect to Various Bacteria

The MIC of the phenothiazines was determined by agar dilution method [79], by adding the phenothiazines individually at concentrations of 0 (control), 2, 5, 10, 25, 50, and 100 μg/ml. For the MIC of these drugs, the final concentrations in 1.0 ml of medium were 0 (control), 5, 10, 25, 50, 100, 200, and 400 μg. The volume of nutrient agar medium poured in 80 mm Petri dishes was 20 ml. The organisms were grown in peptone water, and the inoculum was matched to a McFarland standard of 0.5 and spot-inoculated on nutrient agar plates, such that each inoculum contained approximately 5×10^5 CFU/ml. The plates were incubated at 37 °C, examined after 24 h, and incubated further for 72 h, if necessary. The MIC was defined as the lowest concentration of an antibiotic or phenothiazine that completely inhibited the growth of the organism [79].

The MIC determinations were performed in triplicate for each organism, and experiments were repeated when necessary.

4.7
Determination of Bacteriostatic/Bactericidal Action of Phenothiazines

For this purpose, an 18-hour-old nutrient broth culture of a bacterium sensitive to a particular phenothiazine was used. 2 ml of this 18-hour-old broth culture was added to 4 ml of a fresh broth. This was incubated at 37 °C for 2 h, so that the bacterial culture could attain the logarithmic growth phase. At this point, the number of viable cells in the culture was determined by the colony forming unit (CFU) count, as described by Miles and Misra [65]. The drug was added at a concentration higher than the respective MIC value at the logarithmic growth phase of the culture. The CFU counts were determined at intervals of 2 h, 6 h and then after 18 h.

4.8
In Vivo Experimentation

4.8.1
Selection and Maintenance of Experimental Animals

A Swiss strain of male white mice weighing 18–20 g was used for in vivo studies. Animals were maintained following standard conditions at 21 ± 1 °C and 50–60% relative humidity, with a photo period of 14:10 hours of light and dark cycles. A water and a dry pellet diet were given ad libitum [26, 28, 49]. The mice exhibited genetic homogeneity and were susceptible to the test organisms *Salmonella typhimurium* NCTC 11 and 74. These strains were the challenge bacteria used for all the in vivo experiments, as these are known to be naturally virulent and pathogenic to mice. The male mice were selected for the tests, as the female mice are reported to be more resistant to different pathogens [66, 99].

These mice, kept in cages of 20, were inspected daily . Temperature, humidity, light, space, and ventilation in the animal house were satisfactory [66].

4.8.2
Determination of Median Lethal Dose (MLD or LD_{50})

Salmonella typhimurium 11 and NCTC 74 were selected as the challenge strains for this study. They were sensitive to phenothiazines, to all of the test antibiotics, and to most of the chemotherapeutic agents in vitro. Attempts to increase virulence of this strain were made through repeated mouse passages, by administering intraperitoneally and recovering from the heart blood. The median lethal dose (MLD or LD_{50}) of any of the passaged mouse strains was determined by using graded challenges on five batches of mice having six mice in a batch and recording mortality up to 100 h [26, 61, 99]; this strain was then preserved by freeze drying. In this method [66, 94] it was assumed that

animals dying at a stated dose would also have been killed by greater amounts of challenges and, conversely, those surviving animals would have survived smaller doses. An accumulated value for the mice affected was obtained by adding the number of dying animals at a certain dilution to the number of animals killed by lesser doses; a similar addition, but in the reverse direction, was made for the survivors.

$$\text{MLD or } LD_{50} = \frac{\%\ \text{Mortality above 50} - 50\%}{\%\ \text{Mortality above 50\%} - \text{Mortality below 50\%}}$$

4.8.3
Detection of Antibacterial Activity of Phenothiazines In Vivo

In this experiment, a 50 LD_{50} challenge dose, corresponding to 0.95×10^9 CFU of *Salmonella typhimurium* 74 and *Salmonella typhimurium* 11, was suspended in 0.5 ml sterile peptone water. Reproducibility of the challenge dose was ensured by standardization of its optical density at 640 nm in a Klett Summerson colorimeter and by standardization of the desired number of CFU on nutrient agar [65]. The phenothiazines were administered intraperitoneally in graded doses, 3 h before the challenge (50 LD_{50}). The drug effects were assessed in experiments (i) where both the drug and challenge were given; (ii) where the drug was injected but the challenge bacterium was replaced by 0.5 ml of sterile peptone water; and (iii) where the challenge was used but 0.1 ml of saline replaced the test drug.

4.8.4
Elucidation of Bacterial Counts (CFU/ml) in Heart Blood and Organs of Phenothiazine Treated Mice

This was done by using a 50 LD_{50} challenge dose suspended in 0.5 ml sterile peptone water of the infecting bacterium *Salmonella typhimurium* 11 or 74, as stated earlier. In this experiment, two groups of five mice each were used. Group 1 was given a definite dose of a phenothiazine while group 2 was given 0.1 ml sterile saline. After 3 h, both groups were given a 50 MLD challenge of *Salmonella typhimurium* NCTC 11 or 74. After 18 h, groups 1 and 2 were sacrificed. Their heart blood was collected aseptically. The serum was separated and the bacterial load was determined. Their livers and spleens were also removed under aseptic conditions, homogenized in tissue homogenizer, and preserved at –20 °C for determination of CFU/ml counts. Statistical analysis of the in vivo data was done using the Student's *t*-test.

The homogenized livers and spleens of the autopsied animals were diluted ten-fold in 4.5 ml sterile peptone water and the blood samples were tested in undiluted condition. Prior to inoculation, the plates containing solid medium

were over-dried at 37 °C to facilitate quick absorption of inoculum by the agar surface. The inoculum from each dilution was deposited as a drop from a calibrated Pasteur pipette [65]. Each drop (0.02 ml in volume) was allowed to fall from a height of 2.5 cm on the medium, where it could spread over an area of 1.5 to 2.0 cm diameter. The plates were divided into six sectors and each of the six sectors in the plates received one drop of each dilution. Bacterial counts were made in the drop areas, showing the largest number of colonies without confluence (up to 20 or more); the mean of the six counts was taken to determine the viable counts per ml of the dilution [1, 21, 65].

5 Antibacterial Activity of Promazine

A systematic search for antibacterial activity among the currently widely used tranquilizers showed that promazine, a routinely used phenothiazine, possessed antibacterial activity. The result of the study is presented in Table 4.

In vitro screening of bacteria by promazine (Table 5) indicate that strains of *Bacillus Staphylococcus aureus* and *Vibrio cholerae* were most sensitive to the compound, while strains of *Proteus*, *Klebsiella*, *Pasteurella*, and *Pseudomonas* were resistant. The other bacteria were moderately sensitive to the drug.

Table 4 In vitro antibacterial activity of promazine

Bacteria	No. tested	Number of strains inhibited by promazine (μg/ml) 5	10	25	50	100	200	400
Bacillus spp.	3	1	1	1				
Staphylococcus aureus	59	4	7	18	30			
Streptococcus faecalis	1						1	
Escherichia coli	35			1	4	12	6	12
Salmonella spp.	16			2	6	6		2
Providencia spp.	4						3	1
Proteus spp.	31				11	12	6	2
Shigella spp.	66		6	10	30	12	6	
Pasteurella spp.	1							1
Bordetella bronchoseptica	1				1			
Klebsiella spp.	4					1	1	2
Vibrio cholerae	61	14	6	21	12	8		
Pseudomonas spp.	9							9
Yersinia pseudotuberculosis	1							1

Table 5 Protective capacity of promazine in infected mice

Dose (μg/g of mice) in 0.1 ml distilled water	Challenge (3.5×10^7 CFU in 0.5 ml peptone water)	No. of animals Tested	Died
8	Yes	20	6[a]
8	No (control)	20	4
4	Yes	20	6[a]
4	No	20	1
2	Yes	20	9[a]
2	No	20	3
1	Yes	20	12[b]
1	No	20	1
0.1 ml saline	Yes	66	57

[a] Highly significant at 1% level of significance.
[b] Insignificant at 5% level of significance according to χ^2 test after elimination of the toxic effects due to the drug along (test-control), which were particularly manifested in the higher dosage schedules.

5.1
Effect of Promazine on Mouse Challenged with *Salmonella typhimurium* 11

In the test group, batches of animals received 1, 2, 4, or 8 μg/g body weight of mouse of promazine hydrochloride, while in the control group they received only 0.1 ml saline. All animals were challenged with 3.5×10^7 CFU (50 LD_{50}) of *Salmonella typhimurium* 11; mortality was recorded up to 100 h. For every test batch there was a control batch which received the drug, but not the challenge. This was done for evaluating the toxic effect of promazine.

Thus, the results of protection tests with promazine on challenged mice, in comparison with control animals not receiving any drug, revealed highly sensitive data (Table 5).

Antihistamines are used in various allergic reactions/conditions with or without associated effective diseases and act chiefly by antagonizing histamines.

6
Antimicrobial Potentiality of Methdilazine

In 1988, Chattopadhyay et al. analyzed nine different antihistaminic Drugs [16]. All chemically pure forms of these drugs were procured from their respective manufacturers and screened primarily with the help of eight indicator bacteria, which were known to be highly sensitive to different antibiotics. The results showed that methdilazine inhibited the growth of most of the test bac-

teria and the MIC of the drug ranged from 25 to 50 μg/ml with respect to these organisms.

In a detailed study comprising 367 different strains of bacteria, methdilazine proved to be a very potent antibacterial agent (Table 6). Different groups of bacteria could be arranged in order of their decreasing sensitivity towards methdilazine, as follows: *Staphylococcus aureus*, *Vibrio cholerae*, *Escherichia coli*, and *Shigella* spp. Their MIC varied between 25 and 200 μg/ml in most cases, although a few strains were sensitive even at 10 μg/ml of the compound (Table 6).

Table 6 Inhibitory spectra for methdilazine hydrochloride

Bacteria	No. of strains tested	No. of strains inhibited my methdilazine (μg/ml)							
		10	25	50	100	200	400	1000	>1000
Staphylococcus aureus	92	6	19	39	15	6	4	3	
Streptococcus pneumoniae	1		1						
Bacillus pumilus	1				1				
Bacillus subtilis	1		1		4	3	2	2	
Salmonella spp.	12								
Shigella spp.	39		4		21	11	2	1	
Klebsiella spp.	9		3		2	3	1		
Escherichia coli	32		8	3	5	8	7	1	
Vibrio cholerae	125	5	17	33	29	31	3	6	
Vibrio parahaemolyticus	38			7	13	15	3		
Pseudomonas aeruginosa	9								9
Providencia spp.	7				2	1	1	3	
Bordetella bronchoseptica	1						1		

7
Antimicrobial Activity of Promethazine

Chakrabarty et al. (1989) selected several antihistamines for detection of antibacterial action [15]. According to them, promethazine was the most powerful and significant antimicrobial. The authors observed that in staphylococci, shigellae, and vibrios the MIC of promethazine varied between 100 and 200 μg/ml. Although one strain of *Escherichia coli* was sensitive at 50 μg/ml, the others were resistant. With respect to *Pseudomonas aeruginosa*, *Proteus vulgaris*, and *Providencia* spp., the MIC of promethazine was always >200 μg/ml (Table 7).

Table 7 Determination of minimum inhibitory concentration (MIC) of promethazine against various bacterial strains

Bacterial strains	No.	No. showing MIC of promethazine at (μg/ml)				
		50	100	150	200	>200
Staphylococcus aureus	42		3	13	16	10
Bacillus spp.	2		1		1	
Escherichia coli	8	1	3		4	
Shigella boydii	11		2	3	2	4
Salmonella spp.	8				8	
Arizona spp.	1					1
Anaerobic Gram positive cocci[a]	6		2		4	
Pseudomonas aeruginosa	5					5
Proteus vulgaris	9					9
Providencia spp.	3		1			2
Vibrio cholerae	6		2	4		
Vibrio parahaemolyticus	29		5	24		
Anaerobic Gram positive bacilli[b]	7		1		5	1

[a] Anaerobic Gram positive cocci were 1 strain each of *Acidaminococcus fermentans*, *Peptococcus magnus* and 3 strains of *Peptostreptococcus anaerobius*.

[b] Anaerobic Gram positive bacilli included 2 strains each of *Bacteroid oralis* and 1 strain each of *Bacteroid capillosus*, *Bacteroid melaniogenicus* var *intermedius*, *Bifidobacterium infantis*, *Eubacterium cylindroids* and *Propionibacterium avidus*.

8
Antibacterial Property of Fluphenazine

Recognizing the multiple functions of pharmaceutical compounds, Dastidar et al. (1995) proceeded to determine antimicrobial property in a psychotherapeutic drug, fluphenazine [21]. Since preliminary screening showed that fluphenazine was highly powerful antimicrobial agent, the dilutions of the same made in nutrient agar were 10, 40, 80, 100, and 200 μg/ml. In a total of 482 strains, fluphenazine was found to have pronounced antimicrobial action against both Gram-positive and Gram-negative bacteria. From Table 8, it can be seen that five of six strains of *Bacillus* spp. were inhibited, while 95 of 164 staphylococci were killed at 20–40 μg/ml of fluphenazine. *Vibrio cholerae* was the most sensitive of all Gram-negative organisms tested, as 138 of 153 strains yielded the MIC that ranged from 10 to 80 μg/ml of the drug. Fluphenazine also stopped the growth of 13 out 18 *Vibrio parahaemolyticus* at concentrations ranging from 10–80 μg/ml. This also showed moderate activity with respect to some strains of *Shigella*, *Salmonella*, and *Escherichia coli*. *Salmonella typhimurium* NCTC 74 was found to have the MIC at 80 μg/ml (Table 8).

Table 8 Antimicrobial activity of fluphenazine in vitro

Bacteria	No. of strains tested	No. of strains inhibited by fluphenazine (μg/ml) 10	20	40	80	100	200	>200
Bacillus spp.	6	1	1	1	2		1	
Staphyloccus aureus	159	8	18	21	30	36	14	32
Staphylococcus spp.	5		2		3			
Escherichia coli	45	2	8	10	6	2	6	11
Salmonella typhi	4			2		2		
Salmonella typhimurium	2			1	1			
Salmonella paratyphi B	1			1				
Salmonella spp.	7			1	2	3	1	
Shigella dysenteriae	10	1	5	1		2		2
Shigella flexneri	20		4	3	3	4	2	3
Shigella boydii	4							4
Shigella sonnei	2							2
Klebsiella pneumoniae	8				1	2	5	
Proteus mirabilis	14				1	6	2	5
Providencia spp.	4			1		1	2	
Pseudomonas aeruginosa	18	1	3	1		1		12
Pseudomonas putida	2	1						
Vibrio cholerae	153	10	17	12	23	45	25	21
Vibrio parahaemolyticus	18	2	10	1			5	
Total	482	26	68	56	72	104	64	92

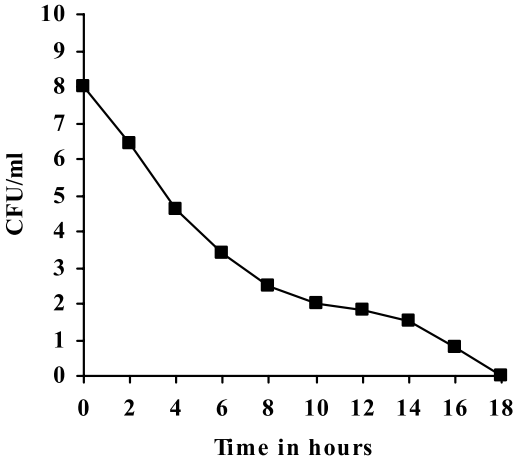

Fig. 1 Action of fluphenazine on *Staphylococcus aureus* ML 281

The MIC of fluphanazine against *Staphylococcus aureus* ML 281 was found to be 20 μg/ml. When 40 μg/ml was added to the nutrient broth containing *Staphylococcus aureus* ML 281 after 0 h of the logarithmic growth phase, the CFU count was determined to be 3.5×10^8. After 6 h, the count came down to 5.5×10^3, while at the end of 18 h the CFU count became 0 (Fig. 1), proving the bactericidal nature of the drug.

8.1 In Vivo Antibacterial Property of Fluphenazine

Fluphenazine was then administered to eight batches of animals, four of which were test batches and four of which were control batches, with each batch having 18 mice (Table 9). There was a separate batch (control) with 54 animals that were only administered the challenge.

The results presented in Table 9 show that in doses of 3 μg/g body weight only three out of 18 mice died in the test proper, whereas in the control group, which received only the drug, two mice expired. With fluphenazine at 1.5 μg/g level, four animals died and at 0.75 μg/g five mice died in the test groups. In the control series, which received the challenge only, 41 out of 54 mice died. The protection test turned out to be highly statistically significant ($p < 0.001$ in χ^2 test) at both 3 and 1.5 μg/g doses of fluphenazine compared to the control (without drug).

Fluphnazine significantly reduced the CFU/ml of bacteria in organ homogenates of animals at both 2 h and 18 h challenge compared with the control (statistically, both showed significant reduction in cell counts in treated animals). The free drug concentrations in the sera of the challenged animals at

Table 9 Effects of fluphenazine on survival of mice challenged with *Salmonella typhimurium* NCTC 74

Drug	Dose (μg/g)	Challenge 0.95×10^9 CFU in 0.05 ml peptone water	No. of animals Tested	Died	Type of expt.
Fluphenazine	3	Yes	18	3[a]	T
	3	No	18	2	C
	1.5	Yes	18	4[a]	T
	1.5	No	18	1	C
	0.75	Yes	18	5	T
	0.75	No	18	0	C
Nil	0.1	Yes	54	41	C
	0.1 ml of saline				

[a] $p \leq 0.001$ according to χ^2 test after elimination of the toxic effects due to drug alone (test-control); T, Test: C, Control.

0 h and 2 h varied from 0.5 to 1.5 μg/ml and those at 18 h varied from 0.2 to 0.6 μg/ml.

9 Antibacterial Spectrum of Trimeprazine

In 1997, Dastidar et al. conducted experiments to determine the antibacterial spectrum of trimeprazine tartrate, which was tested against 249 strains of Gram-positive and Gram-negative bacteria [24]. The susceptibility of these organisms to trimeprazine was assessed by determining the MIC of the drug, which lied between 10 and 100 μg/ml. Nineteen strains of staphylococci were inhibited within a range of 10–50 μg/ml of the drug. For most of strains belonging to *Bacillus* spp. and *Salmonella* spp., the MIC was 100 μg/ml; this could also inhibit many strains of *Shigella* spp., *Vibrio cholerae*, and *Vibrio parahaemolyticus* (MIC 10–100 μg/ml). Strains of klebsiellae, proteus, and citrobacter appeared to be moderately sensitive to trimeprazine; of nine strains of *Pseudomonas* spp., which were highly antibiotic resistant, five were inhibited at 100 to 200 μg/ml of this drug (Table 10). In tests to determine the nature of antibacterial action of this drug with respect to a strain of *Staphylococcus aureus* (Fig. 2) it was observed that like fluphenazine, there was a sharp decline in the CFU of the culture in the log phase, till it dropped to nearly zero at the end of 18 h, indicating that trimeprazine also had a similar bactericidal mode of action [24]. Figure 2

Table 10 Inhibitory spectrum of trimeprazine

Bacteria	No. inhibited by trimeprazine at (μg/ml)						
	Tested	10	25	50	100	200	400
Staphylococcus aureus	20	2	10	4	4		
Staphylococcus spp.	3		1	2			
Bacillus spp.	5	1		2	2		
Salmonella spp.	8	1			4	3	
Salmonella typhimurium	2	1			1		
Shigella spp.	26	5	6	5	5	5	
Escherichia coli	70						70
Klebsiella spp.	7						7
Proteus mirabilis	6						6
Citrobacter freundii	2						2
Vibrio cholerae	54		15	15	5	8	4
Vibrio parahaemolyticus	26		8	7	2		
Pseudomonas spp.	20				8	5	7

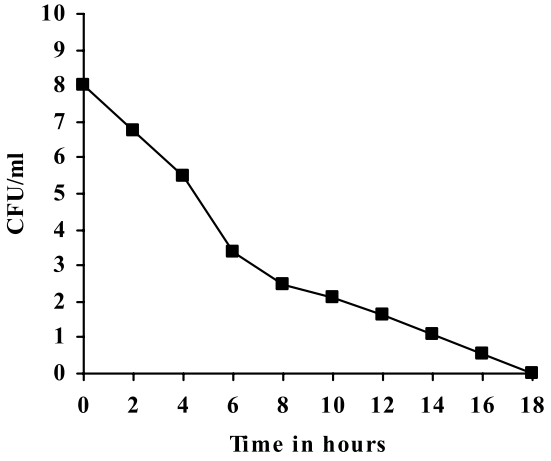

Fig. 2 The action of trimeprazine on *Staphylococcus aureus* ML 275

shows the bactericidal action of 50 μg/ml of trimemprazine on *Staphylococcus aureus* ML 275.

Two strains of *Salmonella typhimurium* were used for in vivo experiments, however, the results with respect to *Salmonella typhimurium* NCTC 74 is being presented.

9.1 In Vivo Antibacterial Activity of Trimeprazine

1.5 μg/g trimeprazine proved to be toxic. Table 11 shows that 0.75 μg/g and 0.4 μg/g trimeprazine given 3 h before the challenge reduced the mortality of mice. The effect proved to be significant according to χ^2 test.

In order to determine whether trimeprazine can reduce the bacterial counts in organ homogenates of challenged animals, ten mice were divided into two groups. All the mice received a challenge dose of 0.95×10^9 CFU/ml

Table 11 Effects of trimeprazine on survival of mice challenged with *Salmonella typhimurium* NCTC 74

Treatment	Mice dying
Trimeprazine 0.75 μg/g	8 out of 20
Trimemprazine 0.4 μg/g	7 out of 20
Saline (control experiment)	49 out of 60

Infecting dose (0.95×10^9 CFU of *Salmonella typhimurium* NCTC 74) was given 3 hour after treatment.

Table 12 Viable counts (CFU/ml) of *Salmonella typhimurium* NCTC 74 in organ homogenates of trimeprazine treated mice

Time of sampling	Mouse No.	Drug (μg/g)	CFU counts in Liver	Spleen
18 hour	1	Trimeprazine (0.75)	1.1×10^7	2.1×10^7
	2		1.8×10^7	3.9×10^7
	3		2.7×10^7	8.2×10^7
	4		3.5×10^7	4.4×10^7
	5		4.0×10^7	6.0×10^7
18 hour	1	Saline (control)	0.31×10^9	1.5×10^9
	2		1.0×10^9	0.9×10^9
	3		1.9×10^9	1.2×10^9
	4		1.9×10^9	1.1×10^9
	5		0.3×10^9	1.3×10^9

Statistical analysis of counts of 18 hour and spleen homogenates was performed by *t*-test.

of *Salmonella typhimurium* NCTC 74. Five mice received 0.75 μg/g trimeprazine 3 h before the challenge, while the remaining five received only saline. The mice were autopsied 18 h after the challenge; homogenates of their liver and spleen were prepared for viable counts. Table 12 shows that the viable counts of trimeprazine administered animals were considerably lower than that observed in mice that did not receive the drug. A similar protection by trimeprazine was observed when *Salmonella typhimurium* 11 was used instead of *Salmonella typhimurium* NCTC 74.

10 Antibacterial Effectivity of Thioridazine

In 1999, Radhakrishnan et al. observed that thioridazine, which is therapeutically used in psychiatric patients, was also an effective antibacterial agent [88]. When tested against thioridazine, a total of 316 bacteria, comprising 70 Gram-positive and 246 Gram-negative bacteria, showed that staphylococci and vibrios were highly sensitive to this drug (Table 13). Among others *Bacillus* spp. salmonellae and shigellae were moderately sensitive, being inhibited in the range of 200 to 400 μg/ml of the agent.

The MIC of thioridazine with respect to *Staphylococcus aureus* ML 322 was 200 μg/ml. At the logarithmic growth phase of the culture, when CFU count was 7.6×10^8, 400 μg/ml of the drug was added. After 2 h there were no live cells in the culture, proving severe bactericidal action of thioridazine on *Staphylococcus aureus* (Fig. 3). Similar action was observed when the drug

Table 13 Minimum inhibitory concentration (MIC) of thioridazine with respect to different bacteria

Bacteria	No. tested	No. of bacteria inhibited by thioridazinne (μg/ml) 50	100	200	400	800	1000	>1000
Staphylococcus aureus	62	5	1	14	31	11		
Staphylococcus spp.	3			1	1	1		
Bacillus spp.	5				2	1	1	1
Salmonella typhi	6				2			4
Salmonella typhimurium	2					1		1
Salmonella spp.	9				1	1		7
Shigella spp.	20	2	2	3	3			10
Escherichia coli	44		2	1	2			39
Klebsiella spp.	5			1				4
Providencia spp.	1							1
Bordetella bronchoseptica	1		1					
Arizona spp.	1							1
Vibrio cholerae	125	2	6	12	35	36	11	23
Vibrio parahaemolyticus	22		2	1	5	12	2	2
Pseudomonas spp.	9				2		1	6

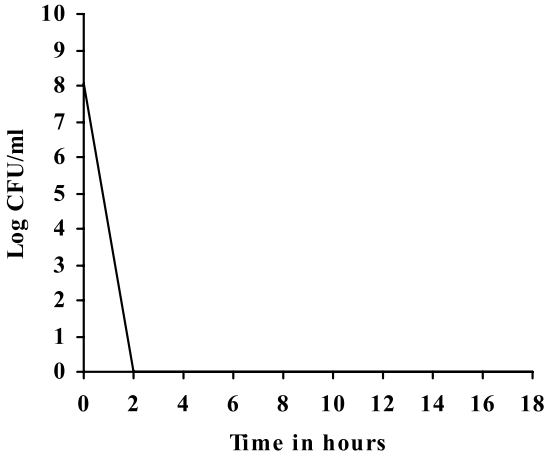

Fig. 3 Action of thioridazine on *Staphylococcus aureus* ML 322

was tested against other Gram-positive bacteria. However, the Gram-negative bacteria behaved quite differently. The MIC of thioridazine against *Shigella boydii* 10 NCTC 386/67 was 400 μg/ml; when the CFU count at the logarithmic growth phase was 1.1×10^8, 800 μg/ml of the drug was added and after 4 h CFU was 7.5×10^4, after 6 h 5.0×10^4 and at the end of 18 h it became 3.0×10^3, showing the bacteriostatic action thioridazine against this

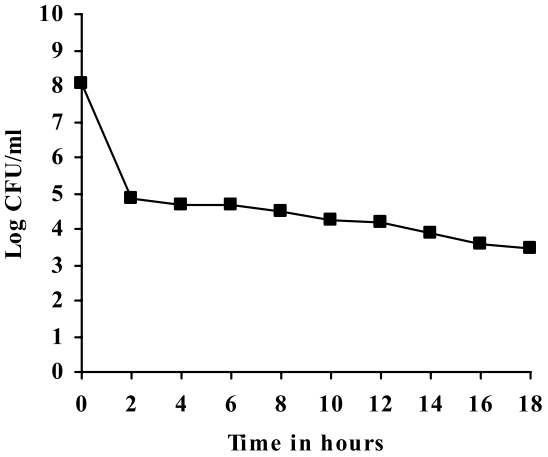

Fig. 4 Action of thioridazine on *Shigella boydii* 10 NCTC 386/67

bacterium (Fig. 4). The strains of *Escherichia coli*, *Salmonella typhimurium*, and *Vibrio cholerae* exhibited identical bacteriostatic character.

Since salmonellae were found to be rather resistant to the drug, animal experiments were not carried out with this drug.

11
Antibacterial Activity of Trifluoperazine

Studies on antipsychotic phenothiazine triflupromazine [64] based on 322 bacteria belonging to both Gram-positive and Gram-negative species, showed that this drug also possessed distinct antibacterial activity; the MIC of the drug (determined by agar dilution technique) varied between 50 and 100 μg/ml with respect to most of the test bacteria. Strains of *Vibrio cholerae* and *Staphylococcus aureus* were highly sensitive, while *Escherichia coli* and *Proteus mirabilis* were fairly resistant to this agent (Table 14). When tested for the mode of action against *Shigella dysenteriae*, this drug proved to be bactericidal (Fig. 5).

11.1
In Vivo Antimicrobial Potentiality of Trifluoperazine

In the in vivo studies this compound offered significant protection to Swiss albino mice at a concentration of 30 μg/mouse ($p > 0.001$) (Table 15). The drug was capable of reducing the number of viable bacteria in the organ homogenates of mice challenged with a virulent bacterium (Table 16).

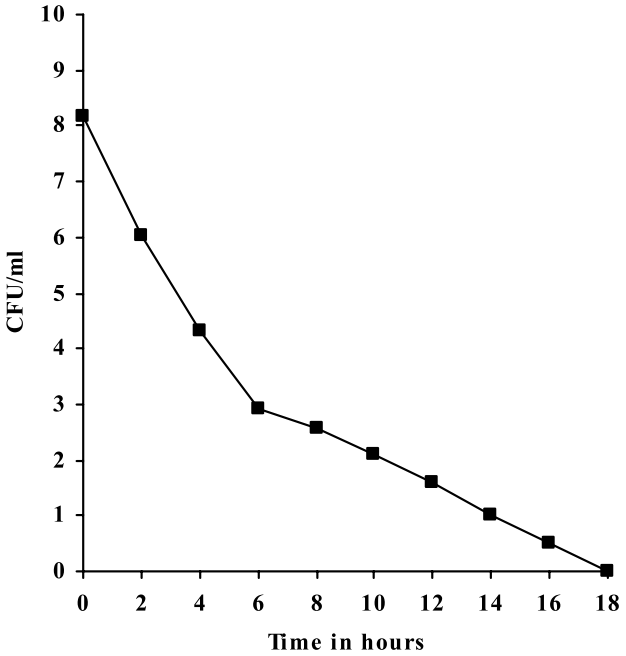

Fig. 5 Action of trifluoperazine on *Staphylococcus aureus* 8530

Table 14 Antimicrobial activity of trifluoperazine in vitro

Bacteria	No. tested	No. of strains inhibited by trifluoperazine (μg/ml) 10	25	50	100	200	400	800	>800
Staphylococcus aureus	55	5	17	22	2	8			1
Staphylococcus spp.	2				1		1		
Bacillus spp.	7			4	1	1	1		
Escherichia coli	35				2		1	3	29
Salmonella typhi	4							4	
Salmonella typhimurium	2				2				
Salmonella spp.	5			2		2			1
Shigella dysenteriare	13		7	6					
Shigella flexneri	13		5	6					2
Shigella boydii	6		1	4					1
Shigella sonnei	2		1						1
Enterobacter spp.	2							2	
Klebsiella pneumoniae	4	1							3
Proteus mirabilis	15				1	1			13
Vibrio cholerae	87	4	14	40	13	9			7
Vibrio parahaemolyticus	23			12		1	3	6	1
Pseudomonas spp.	18	1	4	3		1			9

Table 15 Effect of trifluoperazine on survival of mice challenged with *Salmonella typhimurium*

Test groups[a] Drug (μg/mouse)	Mice died	Control groups[b] Drug (μg/mouse)	Mice died
15	10[c]	15	0
30	8[d]	30	2
60	20	60	13

[a] Received challenge dose of 0.95×10^9 CFU *Salmonella typhimurium* NCTC 74 3 hr after administration of trifluoperazine.
[b] Received the drug but no challenge. In the group that received challenge and saline (in place of drug), 49 of 60 mice died.
[c] $P < 0.05$.
[d] $P < 0.001$ according to χ^2 test, after elimination of effect due to the drug alone.

Table 16 Variation of CFU/ml *Salmonella typhimurium* NCTC 74 in blood and other organs of trifluoperazine treated and untreated mice[a]

Time of sampling	Treated with	Mouse no.	CFU/ml Blood	Liver	Spleen
18	Trifluoperazine	1	3.3×10^3	3.5×10^3	5.5×10^3
		2	6.6×10^3	4.5×10^3	8.2×10^3
		3	1.1×10^5	9.0×10^4	8.5×10^4
		4	5.0×10^4	2.8×10^4	6.5×10^4
		5	9.5×10^5	1.5×10^5	2.0×10^5
18 h	Saline	1	6.3×10^8	9.5×10^7	5.6×10^8
		2	2.0×10^8	7.5×10^8	8.9×10^7
		3	4.8×10^8	5.8×10^8	6.6×10^8
		4	5.6×10^8	6.8×10^8	4.5×10^8
		5	2.5×10^8	8.5×10^8	9.2×10^7

[a] Variable counts between two groups significant, $p < 0.001$ (Student's *t*-test).

12 Antibacterial Property of Triflupromazine

Dastidar et al. [22] reported that the antipsychotic phenothiazine triflupromazine possesses powerful antibacterial property. The drug exhibited significant antibacterial activity against 279 strains of Gram-positive and Gram-negative bacteria. According to the agar dilution method, the MIC of the drug was between 2 and 50 μg/ml for *Staphylococcus aureus*, and 5 and 100 μg/ml for shigellae and vibrios (Table 17). Triflupromazine, when injected intraperitoneally into Swiss albino mice at a concentration of 30 μg/mouse (weighing 20 g each), manifested a significant protection to the animals ($p < 0.001$) when

Table 17 Inhibitory spectrum of triflupromazine

Bacteria	No. tested	Minimum inhibitory concentration (μg/ml) 2	5	10	25	50	100	200	400	>400
S. aureus	58	2	4	26	26					
S. aureus	17[a]					16	1			
Bacillus spp.	4				2					2
E. coli	7				6	1				
E. coli	29[b]						1		2	26
Salmonella spp.	5		1	2	2					
Salmonella spp.	10[b]					3	2	2	2	1
Shigella spp.	8		4		4					
Shigella spp.	16[b]					4			3	9
Klebsiella spp.	5[b]									5
V. cholerae	59	4	8	35	12					
V. cholerae	33[c]					18	13			2
V. parahaemolyticus	14				14					
V. parahaemolyticus	6[c]					5	1			
Pseudomonas spp.	8				2		1			5
Total	279	6	17	63	68	47	19		7	50

The MIC of trifluopromazine with respect to *Salmonella typhimurium* NCTC 74 was 5 μg/ml.

[a] 16 strains were resistant to penicillin-G, ampicillin, amoxycillin, methicillin, cloxacillin and azithromycin, whereas the remaining one was simultaneously resistant to vancomycin as well.

[b] Resistant to tetracycline, fluoroqunolones, cotrimoxazole.

[c] Resistant to tetracycline, chloramphenicol and cotrimoxazole.

Pseudomonas starins were resistant to amikacin, mezlocillin and piperacillin.

they were challenged with 50 median lethal dose (MLD) of *Salmonella typhimurium* NCTC 74 (Table 18).

13
Antibacterial Property of Prochlorperazine

In 2005, Basu et al. reported the antibacterial property of the antipsychotic agent, prochlorperazine [5]. The drug was screened in vitro against 157 different strains of bacteria belonging to various types. Out of eight strains of *Bacillus* spp., one was inhibited by prochlorperazine at 100 μg/ml and the remaining seven at 200 μg/ml. Among the 28 strains of staphylococci tested, 19 were inhibited within 50 μg/ml, eight strains at 100 μg/ml and the one remaining strain at 200 μg/ml. Strains of *Escherichia coli*, *Salmonella*, *Klebsiella*, and *Pseudomonas* were either moderately sensitive

Table 18 Determination of protective capacity of triflupromazine

Test batch Triflupromazine (μg) injected per mouse	Mice died (out of 20)	Control batch Triflupromazine (μg) injected per mouse	Mice died (out of 20)
60	0[a]	60	4
30	4[a]	30	0
15	8[b]	15	0

Test Batch received the challenge dose of 0.95×10^9 CFU in 0.5 ml nutrient broth culture of *S. typhimurium* NCTC 74. Control Batch received no challenge. In the batch thatreceived the challenge and 0.1 ml saline (in place of drug) 41 out of 54 animals died. In the other batch of mice that received 0.1 ml of heat-killed *S. typhimurium* cells, none of the animals died.

[a] $p < 0.001$.

[b] p, 0.01 according to Chi-square test.

(MIC 50–400 μg/ml) or resistant (800 or >800 μg/ml) to the drug. Out of 17 strains of *Shigella* spp., seven stopped growing at 25 μg/ml, two at 50 μg/ml, five strains at 400 μg/ml and the remaining three strains at 800 μg/ml. For the vibrios, the MIC of prochloperazine ranged from 25 to 200 μg/ml for most of the strains. Certain enterobacteria like *Proteus*, *Providencia*, *Citrobacter*, *Bordetella*, and *Arizona* were less sensitive to prochlorperazine (MIC 400–800 μg/ml), while *Hafnia* and *Pasteurella* were more sensitive (Table 19).

14 Antibacterial Property of Flupenthixol

In 2006, Jeyaseeli et al. reported that the antipsychotic thioxanthene, flupenthixol, possessing a trifluoromethyl substituent at position 2, exhibited a distinct antibacterial property against 352 strains of bacteria taken from three Gram-positive and 13 Gram-negative genera [50]. The MIC of flupenthixol was determined by the National Committee for Clinical Laboratory Standard's agar dilution method; MICs ranged from 10–100 μg/ml in most of the strains, whilst some strains were inhibited at even lower concentrations (Table 20). The mode of action of this drug was found to be bacteriostatic against *Staphylococcus aureus* (Fig. 6) and *Vibrio cholerae* (Fig. 7). In the in vivo experiments, the drug was capable of contributing significant protection ($p < 0.001$) to a Swiss strain of white mice challenged with 50 median lethal dose of mouse-virulent strain at a concentration of 15 μg/mouse (Table 21). In addition, flupenthixol remarkably reduced the number of viable bacteria in organ homogenates and blood of mice (Table 22).

Table 19 Antibacterial activity of prochlorperazine by in vitro screening

Bacteria	No. of strains	Growth in nutrient agar containing different concentration of prochlorperazine								
		0	10	25	50	100	200	400	800	>800
Bacillus spp.	8		1			1	7			
Staphylococcus aureus	28			10	8	8	1			
Micrococcus spp.	1					1				15
Escherichia coli	16				1				1	10
Salmonella spp.	13			7	2				3	
Shigella spp.	17			2	2			5	1	
Vibrio cholerae	34				10	8	11	2	3	2
Vibrio parahaemolyticus	13				2	3	8		1	4
Klebsiella spp.	7					1		1		1
Proteus spp.	5								1	
Providencia spp.	1									
Citrobacter spp.	1							1	1	
Bordetella bronchoseptica	1								1	
Arizona spp.	1							1		
Hafnia spp.	1									
Pasteurella spp.	1							2	6	1
Pseudomonas spp.	9									
Total	157		1	19	27	22	27	27	17	33

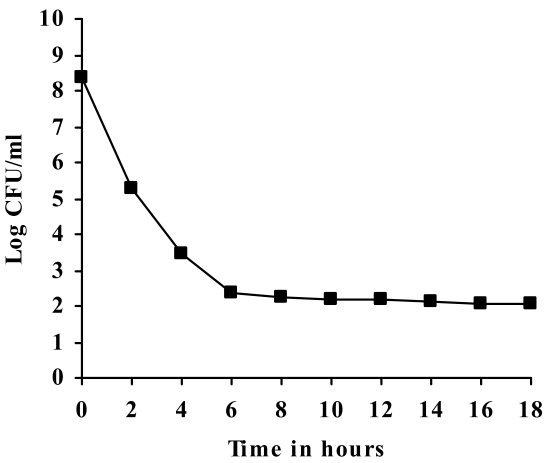

Fig. 6 Action of flupenthixol on *Staphylococcus aureus* NCTC 6571

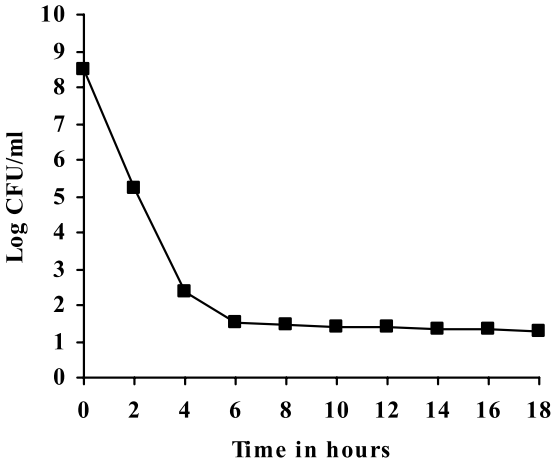

Fig. 7 Action of flupenthixol on *Vibrio cholerae* 1347

Table 20 In vitro antibacterial activity of flupenthixol

Bacteria	No. tested	Concentration of flupenthixol (μg/ml) 5	10	25	50	100	200	>200
Bacillus spp.	6		1	5				
Staphylococcus aureus	84	9	30	31	12	2		
Streptococcus spp.	4		1	2	1			
Escherichia coli	47		1	2	4	5	3	29
Salmonella spp.	15		1		5		1	8
Arizona spp.	1			1				
Providencia spp.	1		1					
Proteus spp.	4						1	3
Shigella spp.	26	2	11	1	1			11
Pseudomonas spp.	12			1	2			9
Pasteurella spp.	1						1	
Bordetella bronchoseptica	1			1				
Hafnia spp.	1			1				
Klebsiella spp.	5							5
Vibrio cholerae	111	5	9	23	26	5	4	39
Vibrio parahaemolyticus	33	1	1	9		1	5	16
Total	352	17	56	80	51	13	15	120

15
Antimicrobial Property of Prenylflavanones

Dastidar et al. [21] determined the antimicrobial activities of eight prenylflavanones isolated from the root of genus *Sophora* of Leguminosae family

Table 21 Determination of the in vivo protective capacity of flupenthixol in mice receiving a challenge dose 1.85×10^9 CFU units of *Salmonella typhimurium* NCTC 74 in 0.5 ml nutrient broth

Group	Drug injected per mouse	Mice died
Group (N = 60)	0.1 ml sterile saline	48
Group (N = 20)	15 μg flupenthixol	3[a]
Group (N = 20)	30 μg flupenthixol	10[b]

N = number of animals tested.
Note: None of the animals died when 15 μg of the drug alone was injected to two separate groups of mice (10 mice in each).
[a] $p < 0.001$ according to χ^2 test.
[b] $p < 0.05$ according to χ^2 test.

Table 22 Reduction in colony-forming units (CFUs) of *Salmonella typhimurium* NCTC 74 at 18 h following treatment with flupenthixol in blood and organ homogenates of mice

Group	No. of mice tested	Drug (μg/ml)	CFU/ml[a] Heart blood	Liver	Spleen
I	5	Flupenthixol 15 μg	1.2×10^3 to 4.4×10^4	6.5×10^3 to 7.3×10^4	3.2×10^3 to 7.5×10^4
II	5	Saline (Control)	5.3×10^8 to 7.4×10^9	8.5×10^8 to 5.0×10^9	1.8×10^8 to 8.0×10^9

[a] Viable counts between two groups significant $p < 0.01$ in 18 h samples (Student's *t*-test).

and two flavanones both by in vitro and in vivo tests. Among two flavanones [YS01 and YS02] and eight prenylflavanones [YS03-YS10], during preliminary screening with 15 known sensitive bacterial strains, it was noted that YS06 was the most active agent. Subsequently, YS06 exhibited highly significant antimicrobial action when tested against 228 bacterial strains comprising two Gram-positive and six Gram-negative genera (Table 23). The in vitro susceptibility test was carried out by determining the MIC of YS06 by agar dilution technique. Twenty-two out of 50 strains of *Staphylococcus aureus* were inhibited at 25 to 50 μg/ml of the agent; YS06 also inhibited the strains of *Salmonella*, *Shigella*, and very few strains of *Escherichia coli* were also highly sensitive to YS06, while *Klebsiella* spp. and *Pseudomonas aeruginosa* were less sensitive (Table 24). The compound exhibited a bactericidal action when tested against *Staphylococcus aureus* 8530.

Table 23 Antimicrobial activity of prenylflavanones [YS01–YS10]

Bacterial strains	MIC (μg/ml) of YS01–YS10		
	YS01	YS03	YS07
	YS02	YS04	YS08
		YS05	YS09
		YS06	YS010
Staphylococcus aureus 6571, 8530, 8531	25–100	10–100	10–100
Bacillus subtilis VP1			
Shigella sonnei 2			
Salmonella typhi 57, 59			
Salmonella typhimurium 74	50–100[1]	10–100[1]	100-200[1]
Escherichia coli K_{12} Row			
Klebsiella spp. 14			
Providencia spp. 1			
Shigella dysenteriae 1			
Escherichia coli 832	50–100[2]	10–100[2]	100–200[2]
Vibrio cholerae 865, 14033			

Table 24 Bacterial inhibitory spectra of a prenylflavanone [YS06]

Bacterial strain	No. tested	No. of bacteria inhibited by YS06 at concentrations (μg/ml)				
		25	50	100	200	>200
Staphylococcus aureus	50	15	7	11	17	
Bacillus spp.	10		2	4	4	
Salmonella spp.	7	2	2	2		1
Shigella spp.	34	3	8	12	9	2
Escherichia coli	30	2	6	9	12	1
Klebsiella spp.	2			7	1	4
Vibrio cholerae	4	16	14	25	19	
Pseudomonas aeruginosa	11				9	2

15.1 In Vivo Antibacterial Study on YS06

During in vivo study, YS06 offered significant protection ($p < 0.001$ according to chi-square test) to Swiss albino mice challenged with 50 MLD of the virulent bacterium at concentrations of 160 and 80 μg/mouse (Table 24).

Table 25 Determination of protective capacity of YS06 in vivo

YS06[a] (μg/mouse)	Mice died (out of 20)
0.1 ml saline (control)	16
160	4[b]
80	8[b]
40	11
20	13

[a] All mice received a challenge dose of 0.95×10^9 CFU in 0.5 ml nutrient broth of *Salmonella typhimurium* NCTC 74. For each of the test batches, there was a control that received only the compound YS06; none of the animals died in these batches proving that the compound was totally free from toxicity upto 160 μg/mouse.
[b] $p < 0.001$, according to Chi-square test, after elimination of the toxic affects due to the drug dose.

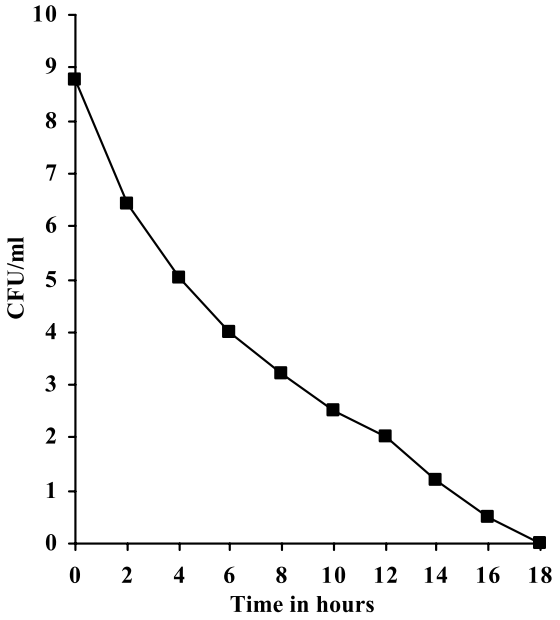

Fig. 8 The action of prenylflavanone YS06 on *Staphylococcus aureus* 8530

16
Studies on the Antimicrobial Potentiality of Isoflavonoid Compounds

In 2004, Dastidar et al. [27] extracted and studied the isoflavonoid phenollic compounds from the roots of *Sophora* genus for their antimicrobial activity. The isoflavonoid compounds "YS11–YS21" were screened for possible antimicrobial property against 12 known Gram-positive and Gram-negative

Table 26 CFU/ml of *Salmonella typhimurium* 74 in organ homogenates and blood of experimental animals (each with 5 mice/group)[a1]

Group Saline (control) YS06 (160 μg/mouse)	Time of sampling of organs (hr)	CFU/ml in Liver	Spleen	Heart blood
I (YS06)	2	1.2×10^4	6.2×10^3	3.1×10^4
	2	2.1×10^3	2.5×10^4	5.6×10^3
	2	3.0×10^3	4.3×10^3	2.3×10^3
	2	1.1×10^3	1.2×10^3	2.1×10^3
	2	6.5×10^4	4.6×10^2	2.5×10^5
II (Saline)	2	4.6×10^6	5.4×10^5	4.0×10^5
	2	2.8×10^6	8.8×10^6	5.7×10^6
	2	6.0×10^6	5.4×10^6	5.8×10^6
	2	7.0×10^6	1.2×10^5	6.9×10^6
	2	8.5×10^5	0.6×10^5	7.8×10^6
III (YS06)	18	2.3×10^4	3.4×10^4	1.1×10^3
	18	7.3×10^4	4.0×10^4	2.6×10^3
	18	3.8×10^4	7.8×10^5	3.6×10^4
	18	5.8×10^3	3.5×10^3	4.5×10^4
	18	7.1×10^4	7.2×10^3	7.0×10^3
IV (Saline)	18	8.0×10^3	1.8×10^8	6.8×10^8
	18	5.2×10^9	5.0×10^8	5.4×10^8
	18	3.9×10^8	8.2×10^9	7.2×10^9
	18	5.8×10^8	5.4×10^9	4.7×10^9
	18	2.7×10^9	4.9×10^8	5.6×10^9

[a] All mice received a challenge dose of 0.95×10^9 CFU of *Salmonella typhimurium* NCTC 74 and YS06 was administered 3 hours before this challenge. The mice were killed 2 hours and 18 hours before the challenge, their livers and spleens were homogenized and the blood was aseptically collected for determination of CFU/ml. Statistically analysis of CFU counts of 2 hours and 18 hours.

Table 27 Antibacterial spectra of YS 19

Bacterial strains	No. tested	Minimum inhibitory concentrations (mg/ml) 25	50	100	200	>200
Staphylococcus aureus	39	4	11	11	10	3
Salmonella spp.	31	4	5	8	8	6
Shigella spp.	35	3	7	8	10	7
Klebsilella spp	9			2	6	1
Pseudomonas spp.	11		1	2	8	
Vibrio cholerae	69	3	10	12	39	5
Vibrio parahaemolyticus	20	2	5	3	10	
Total	214	16	39	46	91	22

Table 28 Antibacterial spectra of YS 21

Bacterial strains	No. tested	Minimum inhibitory concentrations (mg/ml) 25	50	100	200	>200
Staphylococcus aureus	39	4	5	9	10	3
Salmonella spp.	31	6	8	6	12	4
Shigella spp.	35			5	10	6
Klebsilella spp	9		1	2	5	2
Pseudomonas spp.	11		1	3	7	
Vibrio cholerae	69	6	8	24	24	7
Vibrio parahaemolyticus	20	2	5	5	8	
Total	214	23	39	54	76	22

Table 29 Determination of mouse protective capacity of YS19 and YS19

Control group[a] Drug injected per mouse	Mice died (out of 60)	Test group[b] YS19 (μg) injected per mouse	Mice died (out of 20)	YS21 (μg) injected per mouse	Mice died (out of 20)
0.1 ml saline	48	30	8	30	4
		60	0	60	0

$p < 0.001$ using Chi-square test.

[a] Received a challenge dose of 0.95×10^9 CFU in 0.5 ml NB of *S. typhimurium* NCTC 74.

[b] None of the animals died when 30 or 60 μg of YS19 and YS21 was injected to separate groups of mice (20 mice each), i.e. YS19 and YS21 were found to be non-toxic to mice.

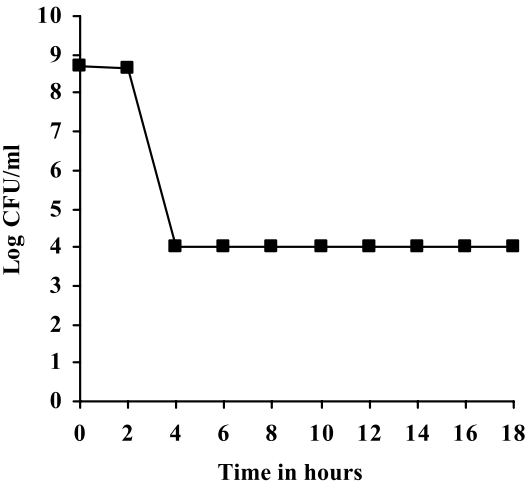

Fig. 9 Mode of action of YS19 against *Staphylococcus aureus* NCTC 8530

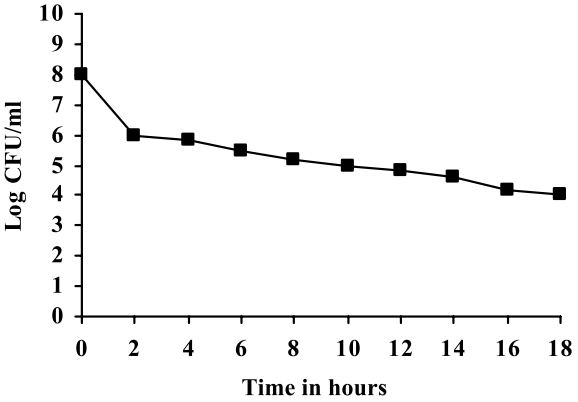

Fig. 10 Mode of action of YS21 against *Staphylococcus aureus* NCTC 8530

sensitive bacteria. YS11 and YS16 failed to show antimicrobial activity and YS12, 13, 14, 15 17, 18, and 20 had moderate antimicrobial action. Compounds YS19 and YS21 showed antimicrobial property. YS19 and YS21 were then tested in vitro against 214 strains of bacteria from one Gram-positive and six Gram- negative genera. The MIC of YS19 and YS21 was determined by agar dilution method and ranged from 25 to 200 μg/l in most strains (Tables 27, 28). At concentrations of 30 and 60 μg/mouse these compounds offered significant protection to mice challenged with 50 median lethal dose (MLD) of a virulent strain of *Salmonella typhimurium* (Table 29). These compounds also reduced the number of viable cells in the organ homogenates of mice challenged with a virulent bacterium (Table 30).

Table 30 Reduction in the CFU/ml of *S. typhimurium* NCTC 74 in organ homogenates of mice treated with YS19 and YS21

Time of sampling (each five mice)[a] h	Group	Mouse no.	Agent/mouse	CFU/ml counts in Heart Blood	Liver	Spleen
18	1	1–5	YS19, 60 μg	1.5×10^4 to 7.2×10^5	1.6×10^5 to 3.5×10^6	2.2×10^5 to 5×10^6
18	2	1–5	YS21, 60 μg	4.8×10^3 to 2.2×10^4	3.1×10^3 to 6.5×10^4	2.4×10^3 to 3.2×10^4
18	3	1–5	Control, 0.1 ml saline	2×10^8 to 6.3×10^8	5.8×10^8 to 9.5×10^7	4.5×10^8 to 9.2×10^7

[a] Viable count between two groups significant.
$p < 0.01$ in 18 h samples.

17
Antimycobacterial Properties of Phenothiazines

Multidrug-resistant tuberculosis has been reported during the last 20 years. Failure to cure this infection with the currently available antitubercular drugs has resulted in the spread of this deadly infection in the community. Hence, there has been an urgent need to discover new and potent drugs to treat such cases, thereby preventing an emerging multidimensional problem. Inhibition of the causative pathogen *Mycobacterium tuberculosis* by phenothiazines was considered as one of the alternative approaches to combat this infection [96]. In 1977, Molnar et al. reported the antitubercular action of five phenothiazines in vitro [69]. In this study, phenothiazine derivatives (chlorpromazine, levomepromazine, diethazine, promethazine, and chlorpromazine sulfoxide) were tested for their antimycobacterial activity. The growth of *Mycobacterium tuberculosis*, *Mycobacterium bovis* and *Mycobacterium butyricum* was inhibited by chlorpromazine practically at identical concentrations. The MICs for *Mycobacterium tuberculosis* were: 10 μg/ml for chlorpromazine and levopromazine; 20 μg/ml for diethazine and promethazine; whilst chlorpromazine sulphoxyde was ineffective even at the concentration of 100 μg/ml. Chlorpromazine and promethazine exerted a measurable bactericidal activity on *Mycobacterium tuberculosis* at 50 μg/ml; total destruction of the organism and loss of acid fastness in part of the cells were exhibited at 300 μg/ml. Earlier studies showed the presence of calmodulin-like proteins in mycobacteria and their regulatory effects on lipid metabolism and growth, and hence calmodulin antagonists were considered for inhibiting the growth of mycobacteria [91]. A calmodulin antagonist, trifluoperazine, was studied by Selvakukmar and Kumar [96] to determine its inhibitory activity against mycobacteria.

Along with *Mycobacterium tuberculosis* $H_{37}Rv$, several clinical isolates of *Mycobacterium tuberculosis* were employed in this work. The MIC was defined as the lowest concentration of the drug in mg/L, which inhibited more than 99% of the population in the control culture on the seventh day.

The minimal bactericidal concentration (MBC) was defined as the lowest concentration of the drug in mg/L, which killed more than 99 percent of the population in the initial inoculum.

The bactericidal activity (BA) was measured as the average reduction in $\log_{10}$ CFU/ml/day when exposed to the respective concentration of the drug.

These were determined separately for sensitive and resistant clinical isolates.

These authors observed that MIC and MBC of trifluoperazine against the *Mycobacterium tuberculosis* $H_{37}Rv$ were 8 and 32 mg/L, respectively. The BA was found to be 0.33 with 32 mg/L on the third day and it was 0.27 and 0.16, respectively, with 32 and 16 mg/L on the seventh day (Table 31). However, all these values were found to be much higher with respect to the clinical isolates.

Table 31 Activity of trifluoperazine against *Mycobacterium tuberculosis* $H_{37}Rv$

Conc. (mg/L)	Viable	Counts (log_{10} CFU/ml) 3	On day 7
0	4.60	6.16	8.39
32	4.60	3.60 (0.33)[a]	2.66 (0.27)
16	4.60	4.94	4.23 (0.16)
8	4.60	5.58	6.03

[a] Bactericidal activity is given in the parentheses.

The MIC/MBC ratio was 1:4 for sensitive isolates, while it was 1:2 for drug-resistant *Mycobacterium tuberculosis* isolates. The BA values against the sensitive isolates were 0.19 and 0.50, respectively, for days 7 to 32.

Chakrabarty et al. [13] carried out an extensive study on the antimycobacterial property of methdilazine.

Fourteen different reference strains of mycobacteria from Central JALMA Institute of Leprosy, Agra, India, isolated from clinical specimens, have been screened for the in vitro studies. Among these were several members of slow-growing atypical mycobacteria, e.g., *Mycobacterium marinum* 50, *Mycobacterium scrofulaceum* 1323, *Mycobacterium gordonae* 1324, *Mycobacterium terrae* 1450, *Mycobacterium tuberculosis* $H_{37}Rv$ 16, and $H_{37}Rv$ (102, K1, K2). Two other strains, known as the "ICRC" [41] and "Skinsnes" bacillus [31], which had been isolated from human leproma and found to be the members of the *Mycobacterium avium-intracellulare-scrofulaceum*, were also included in this study.

17.1 Determination of Minimum Inhibitory Concentration of Antibiotics and Non-Antibiotics by Tube Dilution of Different Strains of Mycobacteria

In these tests, MIC represented the smallest concentration of antibiotic/non-antibiotic that completely inhibited growth. Fourteen strains of mycobacteria were used for this study (Table 32). The drugs, namely, Streptomycin and Rifampicin, were used at the following concentrations (μg/ml) in Kirchner's liquid medium [51]: 0.12, 0.25, 0.5, 1.0, 1.5, and 2.0, with one drug-free control; for methdilazine the concentrations (μg/ml) was: 1, 2.5, 5.0, 7.5, 10.0, 12.5, and 15.

Table 32 Determination of the minimum inhibitory concentration (MIC) of methdilazine (Md), streptomycin (Sm) and rifampicin (Rf) on *Mycobacterium* spp.

Mycobacterium	Md	Sm	Rf
M. smegmatis 789	15.0	2.0	2.0
M. smegmatis 1546	15.0	2.0	2.0
M. fortuitum 1529	10.0	2.0	1.5
M. scrofulaceum 1323	12.5	2.0	1.0
M. gordonae 1324	5.0	2.0	2.0
M. marinum 50	12.5	2.0	2.0
M. flavescens 1541	12.5	2.0	1.0
M. terrae 1450	12.5	2.0	2.0
M. tuberculosis			
H_{37} Ra 16	5.0	1.0	1.0
H_{37} Rv 102	10.0	2.0	1.0
K1	10.0	2.0	1.0
K2	10.0	2.0	1.0
ICRC bacillus	12.5	2.0	1.0
"Skinsnes" bacillus	12.5	2.0	2.0

17.2 The Inoculum for Susceptibility Tests

The inoculum for the in vitro screening tests (tube dilution, as well as filter paper diffusion) was prepared by homogenizing the fluid Kirchner's liquid medium culture with glass beads, spinning down the large particles, and matching the supernatant against McFarland's standard (1%, [81]). 0.1 ml of a standard suspension was used to inoculate a tube, or 0.5 ml to apply over a thin dry film of mycobacterial culture on the Lowenstein Jenson Medium plates, on which the antibiotic-impregnated discs (Whatman no.1) or filter paper strips were then placed [91]. Incubation was carried out at 37 °C for ten days.

17.3 In Vitro Tests for Sensitivity to Antimicrobial Agents

In sensitivity tests based on disc diffusion methods, the clear zone of inhibition around each individual disc was measured in three different directions to obtain the mean value of each set.

17.3.1 In Vivo Susceptibility Tests

Systemic infection was produced in groups of 20 inbred Swiss albino mice (18–20 g), by administering intraperitoneally 0.05 ml of a suspension containing 0.5 mgm homogenized Kirchner Liquid Medium culture having $<9 \times 10^9$ CFU. Of these mice, ten were protected by methdilazine (dose 10 μg/gm body weight/day × 6 weeks), whilst the other ten did not receive any drug and served as the control. Six weeks after the infection, the viscera from the animals autopsied were obtained, taking strict precaution, respecting sterility, and examining for macroscopic lesions of systemic infections (e.g., tubercles and caseation), for both treated and untreated groups [103]. Portions of each organ were processed for histological study of the lesions. The remainders were homogenized aseptically in sterile homogenizers in saline, examined under the microscope as stained smears for presence of acid-fast bacilli/and contaminants, and inoculated onto nutrient/blood agar plates to determine rapid growth, if any. Sterile specimens (as well as contaminated specimens after adequate decontamination by Petrov's method) were placed out on a Lowstein Jenson medium in 0.1 ml amounts and examined for growth of the infecting *Mycobacterium tuberculosis*.

17.4 Results

17.4.1 In Vitro Tests

Table 32 shows the MIC of methdilazine with different strains tested. In general, the MIC of this drug was much higher than that of streptomycin and rifampicin. The MBC of these agents with respect to the above strains was determined by subculturing 0.1 ml amounts from the respective MIC dilution of each series on drug-free medium and incubating at 37 °C for three weeks for colonies to develop. A similar culture inoculum from drug-free medium provided the control. The MBC values were 2–8 times higher than the MIC values for complete killing of the inoculum by the drugs.

17.4.2 In Vivo Assessment

Table 33 showed that of the ten animals in the untreated group, eight developed minute tubercles in the liver, five in the spleen and lungs, and nine in the peritoneum and intestines; microscopic necrosis suggestive of caseation was found in the liver of three animals and in the spleen, peritoneum, and intestine each in one animal. Smears of acid-fast bac-

Table 33 Effect of Md[a] on HV_{37} Rv 102[b] infection in mice

	Liver (10)	Spleen (10)	Peritoneum/ intestine (10)	Lungs (10)	Cumulative values	Recovery of AFB (no. of animals) Smears	Cultures
Untreated (10)							
Smears AFB (+)	10/10	10/10	10/10	10/10	40/40		
Tubercles	8/10	5/10	9/10	5/10	27/40	10[c]	5
Caseation	3/10	1/10	1/10	0/10	5/40		
Treated (10)							
Smears AFB (+)	0/10	2/10	2/10	0/10	4/40		
Tubercles	2/10	3/10	3/10	0/10	8/10	4[d]	1
Caseation	0/10	0/10	0/10	0/10	0/40		

[a] 10 μg/gm body weight/day.
[b] 4.5×10^9 CFU/mouse intraperitoneally.
[c] From the last one viscera of 10 animals, all viscera did not yield (+) culture; the viable counts (CFU) varied: 10^3–10^6/ml.
[d] Only from 4 animals, recovery from even a single organ being counted as positive, other organs did not yield any growth; CFU: 10^1–10^3/ml in positive samples.

teria by Ziehl–Neelsen stain, from centrifuged deposits (for 100 fields) of tissue homogenates, showed all ten animals to be smear-positive at the time of autopsy, which suggested successful infections in these animals. In contrast, macroscopic examination of the treated group (ten animals) showed tiny tubercles to be present only in some liver specimens and in the spleen, peritoneum, as well as in the intestines (three each), but not in the lungs. Ziehl–Neelsen stained smears showed the presence of acid fast bacili (AFB) only in four cases. In 10 animals of the untreated group, *Mycobacterium tuberculosis* $H_{37}Rv$ could actually be recovered on subculture, in comparison with only one of the treated groups, which appeared to be significant ($p < 0.01$). The failure to recover $H_{37}Rv$ in other untreated animals was probably due to a non-viability of these bacilli, although these could readily be detected in smears in all cases.

In 2001, Amaral et al. reviewed the in vitro and in vivo activity of phenothiazines against antibiotic susceptible and resistant *Mycobacterium tuberculosis* and malaria parasites [2]. The scientific rationale for the potential use of many phenothiazines for the management of infections would be a worthy goal of clinical research, given the fact that pulmonary tuberculosis and malaria are major causes of death in developing countries, that both of these infections continue to escalate their resistance to antibiotics, that the cost of management of these infections is beyond affordable by many developing nations, and, lastly, that new and effective agents are not forthcoming from the pharmaceutical industries.

Amaral et al. [3] prepared a review providing cogent evidence that both intracellular multidrug-resistant tuberculosis (MDRTB) and intracellular methicillin-resistant *Staphylococcus aureus* (MRSA) can be killed by concentrations of thioridazine in the medium that is below that present in the plasma of the patients treated with this agent. Although thioridazine has been claimed to cause arrhythmias and even sudden death, the frequencies of those episodes are rare and, when present, they are related to a patient's underlying cardiac status, as opposed to the direct effect of the agent itself.

18
Synergism, Antagonism and Indifference

Antimicrobial combination therapy can be a powerful tool in the treatment of bacterial infections. Antimicrobial combinations are considered to be synergistic if the effect of the combination is greater than the effect of either agent alone or greater than the sum total of the effects of the individual agents. Antagonism results if the combination provides a lesser effect than the effect of either agent alone or lesser than the sum of the effects of the individual agents. Indifference results if the combination provides an effect equal to the effect of either agent alone [36].

Combination therapy is often used when dealing with infections caused by both aerobic and anaerobic bacteria [50, 80]. Combination of metronidazole with either gentamicin or ciprofloxacin appeared to be effective in preventing infection of abdominal trauma [101]; when combined with ciprofloxacin, metronidazole was affective as a preoperative antibiotic in colorectal surgery and appeared equal in efficacy to impipenem/cilastin for the treatment of complicated intraabdominal infections [103]. Combination therapy is not always indicated for the treatment of polymicrobial infections. New antibiotics, whose spectrum includes multiple classes of microorganisms (e.g., imipenem), may often preclude combination therapy.

Synergism between antimicrobials is most likely to occur when the two antimicrobials kill bacteria through independent mechanisms (e.g., an aminoglycoside coupled with a β-lactam) or through sequential pathways towards the same target [36, 95]. Four well-established mechanisms of synergism are known to exist. They include sequential inhibition of a common pathway by the combination of two bacteriostatic drugs. Their combined effect may result in bactericidal activity, by inhibition of a destructive enzyme (e.g., β-lactamase [39]). Inhibition of cell wall synthesis has been observed in penicillin-vancomycin combination [36]. Inhibition of a destructive enzyme, by combination of clavulanic acid with amoxicillin, was reported by [92]. Finally, facilitation of entry of antimicrobial agents through cell walls could produce synergism between β-lactams and aminoglycosides [67].

Table 34 List of bactericidal and bacteriostatic drugs

Bactericidal drugs	Bacteriostatic drugs
Penicillin	Tetracyclines
Cephalosporins	Chloramphenicol
Aminoglycosides	Erythromycin
Bacitracin	Novobiocin
Vancomycin	Lincomycin
Polymyxins	
Gramicidines	
Tyrocidins	
Co-trimoxazole	

The synergistic effects of fluorinated quinolones plus aminoglycosides has been reported in *Pseudomonas aeruginosa* [36]. A synergistic effect in the treatment of gingivitis and periodontal disease could be seen in both dogs and cats when metronidazole was combined with spiramycin [44].

Antagonism usually occurs when a bacteriostatic agent is combined with a bactericidal agent, e.g., combination of chlortetracycline with penicillin in the treatment of pneumococcal meningitis. A grouping of these bactericidal and bacteriostatic drugs proposed by Jawetz and Gunnison [49] and Rahal [86] is given above (Table 34). Combination effects are usually as follows:

1. Bactericidal plus bactericidal may be synergistic.
2. Bactericidal plus bacteriostatic may be antagonistic.
3. Bacteriostatic plus bacteriostatic may be additive.

Antagonism may also occur when two drugs acting at the same site are combined with one another, resulting in competition for the same binding sites, e.g., macrolides, lincosamides, and chloramphenicol [102]. Combinations of β-lactams containing one agent that induce β-lactamase production (e.g., selective cephalosporins, particularly cefoxitin) with another β-lactam can result in antagonistic actions [40]. The β-lactams which target the same penicillin binding proteins can result in antagonistic action.

The additive effect of a combination of antibiotics is one in which the effect of the combination is equal to that of the sum of the effects of the individual components. Additive effects probably occur when active metabolites are produced from an active parent compound, such as metabolism of enrofloxacin to ciprofloxacin [59].

18.1 Materials and Methods for Determination of Synergism

18.1.1 Bacteria

The strains used in this study have been described earlier (Table 3).

18.1.2 Media

The liquid media consisted of peptone water (1.0% bacteriological peptone, Oxoid, plus 0.5% Analar NaCl), Mueller–Hinton broth (Oxoid), and nutrient broth (Oxoid). The solid media were peptone agar, nutrient agar, and Mueller–Hinton agar, which were prepared by solidifying liquid media by adding 1.3% agar (Oxoid No. 3). Peptone agar and nutrient agar were used respectively for the assay involving Gram-negative and Gram-positive bacteria, while Mueller–Hinton broth was used to determine the fractional inhibitory concentration (FIC) index.

18.1.3 Drugs

The antibiotics were procured commercially as pure dry powders, while the phenothiazines were obtained from their respective manufacturers in India in pure dry powder form.

18.2 Synergism In Vitro

Determination of combined effects of phenothiazines with antibiotics was carried out by disc diffusion technique, which was based on the method described by Garrod and O' Grady [39]. Sterile filter paper discs (7.25 mm, Whatman No. 1) containing the agent(s) were prepared according to Cruickshank et al. [19]; an 18 h liquid culture of bacteria was flooded on agar plates in triplicate [16]; the plates were dried well at 37 °C. For individual effects, two discs (containing two different drugs) were placed apart on the agar surface at a wide distance, so that each disc could produce a clear-cut zone of inhibition. Plates were then incubated at 37 °C for 18 h and the mean diameters of zones of inhibition across each disc were measured in three directions, and the mean value was taken. In subsequent tests for determination of combined effect of two such drugs, the discs were placed on the agar plates at a predetermined distance, so that their inhibitory circles would touch each other tangentially, when uninfluenced by each other [16], i.e., when the drug

actions resulted in indifference. In the case of antagonism between them, the touching circles receded away from each other, while merger and enlargement of inhibition circles signified synergism.

18.3 Calculations

Apart from diameters of the inhibition zones, increase/decrease in the surface areas (πr^2), if any, due to the combined effects vis-a-vis their individual effects were evaluated statistically by χ^2 test, for gauging the level the significance [6]. The combined effects were further evaluated by a "checkerboard" dilution test for determination of FIC according the Krogstad and Moellering [59], using doubling dilutions of the pair of test drugs in Mueller–Hinton broth with an inoculum size of about 10^5 CFU of a sensitive bacterium.

18.4 Synergism Between Streptomycin (Sm) and Methdilazine (Md)

In an elaborate study based on different test strains sensitive to methdilazine (Md) (Table 35), Chattopadhyay et al. [16] reported that methdilazine

Table 35 Minimum inhibitory cencentration (MIC) of various antibiotics and methdilazine with respect to test bacteria

Strains	Minimum inhibitory concentration (MIC) μg/ml									Source
	Pc	Ap	Tc	DMTC	Cm	Er	Sm	Km	Md	
Staphylococcus aureus 8530	5	5	5	10	5	10	10	10	25	S.P Lapage, London
Staphylococcus aureus 8531	5	5	5	10	5	10	10	10	25	S.P Lapage, London
Staphylococcus aureus ML 316	10	10	10	10	10	25	10	20	25	M.L. Lahiri, Calcutta
Salmonella typhi-murium 74	8	8	10	10	8	10	8	8	50	J. Taylor, London
Shigella boydii 8 254/66	5	5	5	10	15	10	10	10	25	K.P. Carpenter, London
Vibrio cholerae 154	5	20	8	10	8	10	4	2	100	S. Mukhrejee, Calcutta
Vibrio cholerae 14033	4	8	50	50	2	10	8	8	100	S. Mukhrejee, Calcutta

Pc, penicillin; Ap, ampicillin; Tc, tetracycline; DMTC, dimethyl-chlortetacycline; Cm, chloramphenicol; Er, erythromycin; Sm, streptomycin; Km, kanamycin; Md, methdilazine.

Table 36 Percent increase in activities of streptomycin (Sm) and methdilazine (Md) compared with individual activities on the basis of their surface area of their inhibition zones

Strains	Mode of action	Inhibition due to Sm in terms of diameter in mm (2r)	Surface area (πr^2)	Inhibitions due to Md in terms of diameter in mm (2r)	Surface area (πr^2)
Staphylococcus aureus ML 316	Singly	19.8	(A) 308.03 mm^{2a}	23.2	(A) 422.90 mm^2
	In combination % increase	22.7	(B) 404.87 mm^2 31.44[b]	24.9	(B) 487.15 mm^2 15.19
Salmonella typhimurium 74	Singly	20.1	(A) 317.44 mm^2	15.9	(A) 198.64 mm^2
	In combination % increase	23.6	(B) 437.61 mm^2 37.86	18.4	(B) 266.01 mm^2 33.92

[a] Mean surface area of the inhibition zone (mm^2) was calculated as (πr^2) on the basis of its mean diameter (2r).
[b] Percent increase was calculated as B-A/A X 100. Sm, streptomycin; Md, methdilazine.

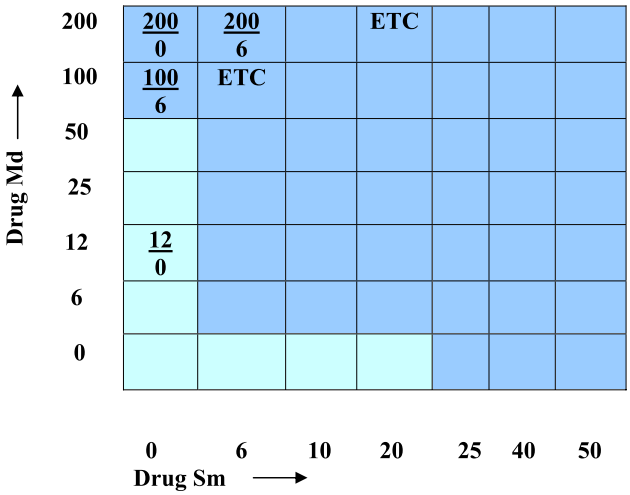

Fig. 11 Assessment of antibacterial combinations of Sm and Md by checkerboard on *Salmonella typhimurium* 74

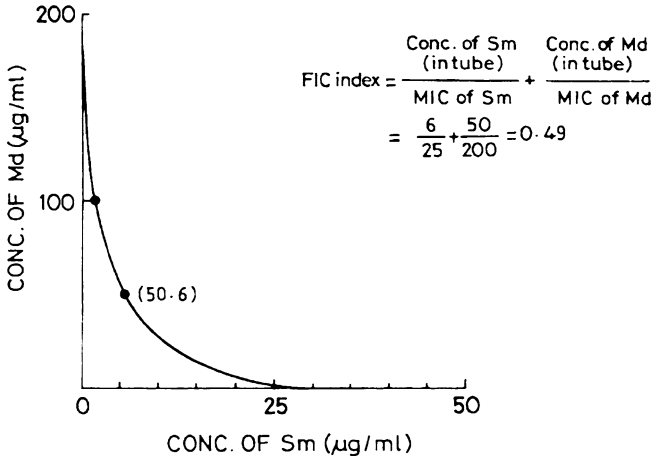

Fig. 12 Isobologram plotted from results of checkerboard test

in combination with streptomycin (Sm) enhanced its antibacterial effects, suggesting a synergism of their activities (Table 36).

The determination of the area of inhibition zones for the degree of synergism between methdilazine and streptomycin showed the increase to be statistically significant ($P \leq 0.01$) when compared with their individual effects. These could also be corroborated by FIC index 0.49 (Figs. 11 and 12) for the Sm–Md combination.

18.5 Synergism Between Promazine and Tetracycline

Dastidar et al. [23] reported synergistic activity between the "antimicrobial tranquilizer" promazine (Pr) and tetracycline (Tc). Studies on the combined action of Pr and Tc were carried out on three highly sensitive strains of *Staphylococcus aureus* NCTC 8530, 8531, and ML 316, *Salmonella typhimurium* NCTC 74, *Shigella boydii* 8 254/66, and two strains of *Vibrio cholerae* 154 and ATCC 14033. The data presented in Table 37 shows that when Tc (10 μg) disc and Pr (200 μg) discs were placed individually on a plate containing *Staphylococcus aureus* 8530, the average zones of inhibition were 16.0 and 18.0 mm, respectively, which increased to 17.3 mm and 20.0 mm, respectively, when the discs were placed for combined effects. A similar synergistic effect was noted with other *Staphylococcus* spp., and the zones of inhibition observed when the drug discs were placed separately varied from 16.0 mm to 17.3 mm for Tc and 16.0 mm to 18.0 mm for Pr. However, the zones due to the combined effect varied from 14.6 mm to 17.7 mm for Tc and 16.5 mm to 20.0 mm for Pr. In tests with *Salmonella typhimurium* 74 the inhibition zones were 15.0 mm against Tc and 16.6 mm against Pr when the discs were placed

alone, while in combination they were 15.3 mm and 16.7 mm, respectively. In case of *Shigella boydii* 8 254/66 the zones of inhibition were 18.0 mm and 18.0 mm individually with respect to Tc and Pr; their combination produced 18.6 mm and 18.2 mm wide zones of inhibition, respectively. When the tests were carried out with two strains of vibrios, the individual inhibition zones

Table 37 Effect of tetracycline (Tc) and promazine (Pr) on bacteria by disc diffusion technique

Bacteria	Zone of inhibition in mm			
	Individual effect		Combined Effect	
	Tc	Pr	Tc	Pr
	10[a]	200[a]	10	200
Staphylococcus aureus 8530	16.0	18.0	17.3	20.0
Staphylococcus aureus 8531	14.0	16.0	14.6	16.5
Staphylococcus aureus Ml 9	17.3	16.0	17.7	17.6
Salmonella typhimurium 74	15.0	16.6	15.3	16.7
Shigella boydii 8 254/66	18.0	18.0	18.6	18.2
Vibrio cholerae 540	16.0	15.9	16.3	16.6
Vibrio cholerae 14033	13.0	15.0	13.2	17.2

[a] μg/disc.
Tc, tetracycline, Pr, promazine.

Table 38 Synergism between trimethoprim (Tm) and trimeprazine (Tz) with respect to Gram- positive and Gram-negative bacteria

Strain	Diameter of the inhibition zone in mm				Percentage increase on the basis of πr^2	
	Single (A)		Combined (B)			
	Tm 400[a]	Tz 300	Tm 400	Tz 300	Tm 400	Tz 300
Staphylococcus aureus 8530	26.2	28.3	28.6	32.8	19.15	34.24
Shigella dysenteriae 7	15.6	19.7	19.7	22.4	40.6.3	29.28
Shigella boydii 10	17.8	21.3	21.3	24.6	31.35	33.38
Shigella sonnei 17	14.6	18.5	18.5	20.2	42.03	19.22
Vibrio cholerae 14033	13.4	16.2	16.2	18.5	28.67	30.32
Salmonella typhimurium 74	15.1	19.2	19.2	23.6	26.69	33.81

[a] Amount (μg) of the drug/disc.
Mean surface area of the inhibition zones (mm^2) was calculated as πr^2 on the basis of their mean diameter (2r) and % increase was calculated as B-A/A x 100, which was highly significant ($p < 0.01$).

produced by Tc varied from 13.0 mm to 16.0 mm, while, with Pr discs, the zones were 15.0 mm to 15.9 mm. Here also the enhancement of inhibitory circles around both discs were observed in the combined test with Tc plus Pr, in which the values ranged from 13.2 to 16.3 mm for Tc and 16.6 mm to 17.2 mm for Pr, thus, exhibiting a state of mutual synergism among these drugs.

18.6 Synergism Between Trimethoprim and Trimeprazine

Guha-Thakurta et al. [43] reported that the antihistaminic antimicrobial agent trimeprazine with trimethoprim was a significant synergistic combination. The degree of synergism between trimeprazine and trimethoprim showed a statistically significant value ($p < 0.001$) when compared with their individual effects (Table 38). The protective capacity of this combination was then assessed in the Swiss strain of white mice by using *Salmonella typhimurium*. The statistical analysis of the data by Student's *t*-test finally proved that a combination of trimeprazine with trimethoprim was highly synergistic (Table 39).

18.7 Activities of Ciprofloxacin Alone and in Combination with Flupenthixol Against Both Gram-Positive and Gram-Negative Bacteria

The test bacteria, which were found suitable in the earlier studies, were now used to assess the activity against ciprofloxacin (Cf) and Flupenthixol (Fp) in combination.

The Cf and Fp discs placed separately on a lawn of *S. aureus* strains gave an average inhibition zones measuring from 19.7 to 20.9 mm and 22.4 to 23.3 mm, respectively; these increased to a range of 22.8 to 25.1 mm and 23.9 to 27.6 mm, respectively, when tested for combined effects. The synergism obtained between Cf and Fp was analyzed statistically to determine the increase in surface area (πr^2) caused by these combinations, vis-a-vis those due to single effects, and percent increase in the diameters of the inhibition zones for the level of significance were also determined. The percent increase observed for *Staphylococcus aureus* were 19.01 to 30.61 due to Cf and 11.38 to 16.72 due to Fp.

On plates having *Bacillus pumilus* 8241, Cf (5 μg) and Fp (200 μg) discs when placed separately and independently, the zones of inhibition were 23.1 mm and 18.0 mm, respectively, which increased to 25.9 mm with Cf and 22.0 mm with Fp, when the discs were placed for the elicitation of combined effect. The percent increase in surface area towards Cf was found to be 25.71%, while for Fp it was 49.38%, thereby enhancing the activity between the drugs and establishing a state of synergism (Table 40).

Table 39 CFU/ml of *Salmonella typhimurium* 74 in organ homogenates and blood samples of mice

No. of mouse	Drug/ mouse	CFU/ml Blood	Liver	Spleen
1	Tz(30)	2.0×10^6	2.5×10^6	1.5×10^6
2		3.5×10^6	2.8×10^6	2.0×10^6
3		1.8×10^5	9.0×10^5	8.5×10^5
4		7.6×10^5	8.7×10^5	7.0×10^5
5		8.5×10^5	9.5×10^5	7.5×10^5
6		8.5×10^5	1.5×10^5	6.9×10^5
1	Tm(30)	8.0×10^5	7.6×10^5	2.2×10^5
2		3.0×10^5	8.1×10^5	8.0×10^5
3		9.5×10^5	2.4×10^6	4.5×10^6
4		7.5×10^5	6.5×10^5	6.5×10^5
5		6.8×10^5	7.5×10^5	5.8×10^5
6		5.8×10^5	3.1×10^6	6.8×10^6
1	Tz(30)	8.8×10^3	2.5×10^4	8.5×10^3
2	+	3.5×10^4	3.8×10^3	9.5×10^3
3	Tm(30)	5.0×10^4	6.7×10^3	4.5×10^4
4		9.6×10^3	7.8×10^3	4.0×10^4
5		7.9×10^3	6.5×10^3	5.5×10^4
6		2.5×10^5	1.5×10^4	5.8×10^4
1	Saline	6.5×10^7	4.5×10^7	1.2×10^8
2		7.0×10^7	2.5×10^7	6.8×10^7
3		7.5×10^5	1.1×10^8	4.5×10^7
4		1.2×10^8	9.5×10^6	7.2×10^7
5		4.8×10^7	5.0×10^7	2.1×10^8
6		5.5×10^7	5.5×10^7	8.5×10^7

All mice received a challenged dose of 8.5×10^9 CFU of *Salmonella typhimurium* 74, 3 hour after administration of the drug(s) or saline. Animals were killed after 18 hour after challenge, their blood samples taken and livers, spleens homogenized and checked for viable bacteria. Statistical analyses of combined affect (Tm + Tz) versus single effect (Tm or Tz) when compared by *t*-test revealed $p < 0.01$.

Tests when performed with Gram-negative bacteria, such as *Escherichia coli* 25922, revealed a large zone of inhibition of 18.9 mm around the Cf discs, while a 17.8 mm zone of inhibition around Fp discs when placed individually. These on combination became a 20.0 mm zone of inhibition for Cf and a 18.9 mm zone of inhibition for Fp, respectively. The surface area of inhibition due to Cf was 11.98%, while that due to Fp was 12.74% (Table 40).

The diameters of the individual zones of inhibition of Cf and Fp against *Salmonella typhimurium* 74 were 21.8 mm and 17.0 mm, respectively, which enhanced to 22.4 mm and 17.7 mm, respectively, in the test for combined ef-

Table 40 Synergism between ciprofloxacin (Cf) and flupenthixol (Fp) by disc diffusion test

Bacterial strains tested	Diameter of the inhibition zone in mm					
	Single (A) effect		Combined (B) drug effect		% Increase on the basis of πr^2	
	Cf[a]	Fp[b]	Cf[a]	Fp[b]	Cf[a]	Fp[b]
Staphylococcus aureus ML 324	20.9	22.4	22.8	24.2	19.01	16.72
Staphylococcus aureus NCTC 8530	20.3	22.5	23.2	23.9	30.61	12.81
Staphylococcus aureus NCTC 8531	19.7	23.3	25.1	27.6	24.22	11.38
Bacillus pumilus NCTC 8241	23.1	18.0	25.9	22.0	25.71	49.38
Salmonella typhimurium 74	21.8	17.0	22.4	17.7	6.94	8.40
Shigella dysenteriae 7 NCTC 519/66	21.8	19.0	26.9	23.5	52.23	52.98
Escherichia coli ATCC 25922	18.9	17.8	20.0	18.9	11.98	12.74
Vibrio cholerae 865	23.1	21.8	25.8	23.4	24.74	15.22
Vibrio cholerae ATCC 14033	28.5	18.1	31.5	23.8	22.16	72.90
Vibrio cholerae ATCC 14035	24.9	19.8	28.8	23.0	33.78	34.94

Cf, ciprofloxacin; Fp, Flupenthixol.

[a] 5 μg of the drug/disc.

[b] 200 μg of the drug/disc.

Mean surface area of the inhibition zone (mm^2) was calculated as πr^2 on the basis of their mean diameter (2r) and % increase was calculated as (B-A)/A x 100, which was highly significant ($p < 0.01$).

The zones of inhibition formed singly with respect to Cf and Fp and those formed multiply against the same compounds were larger in size. These were calculated statistically by determining Student's "*t*" test based on the values of standard deviation and standard error obtained which showed the differences to be highly significant ($p < 0.001$) with respect to all the test bacteria.

fect of the two drugs. Surface areas of inhibition zones increased by 6.94% for Cf and 8.40% for Fp.

The inhibitory circles produced by Cf in case of *Shigella dysenteriae* 7 when the discs were kept far apart from one another was 21.8 mm and by Fp was 19.0 mm. These increased in size to 26.9 and 23.5 mm, respectively, in combination studies; the percent increase was 52.23 in case of Cf and 52.98 in case of Fp.

The area of inhibition zone displayed by Cf when the drug discs were kept independently on three strains of *Vibrio cholerae* was between 23.1 and 28.5 mm and that by Fp varied from 18.1 to 21.8 mm. In the tests for joint effect, their diameters became wider and varied from 25.8 to 31.5 mm against Cf and 23.0 to 23.8 mm against Fp. The percent increase in surface area observed with Cf varied from 22.16 to 33.78% and with Fp was from 15.22 to 72.90% (Table 40).

The zones of inhibition formed singly with respect to Cf and Fp and those formed in combination against the same compounds were larger in size.

These were calculated statistically by determining the Student's *t*-test based on the values of standard deviation and standard error, which showed the

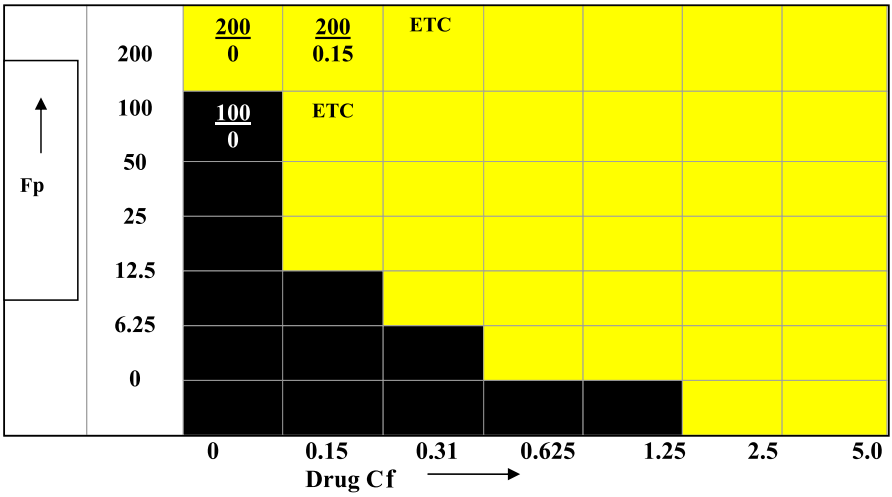

Fig. 13 Determination of FIC index by checkerboard test on *Shigella dysenteriae* 7

$$\text{FIC Index} = \frac{\text{Conc. of Cf (in tube)}}{\text{MIC of Cf}} + \frac{\text{Conc. of Fp (in tube)}}{\text{MIC of Cf}}$$

$$= \frac{1.25}{5.0} + \frac{25}{200} = 0.375$$

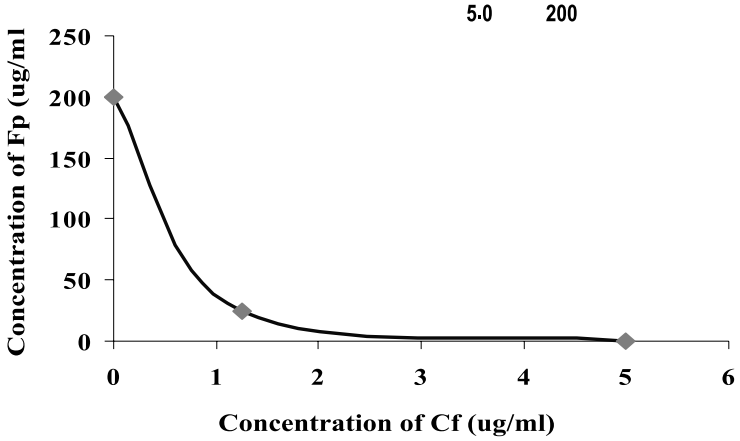

Fig. 14 Isobologram plotted from the results of the checkerboard

differences to be highly significant ($p < 0.0001$) with respect to all the test bacteria.

To substantiate this claim, the data were further corroborated by in vitro checkerboard dilution studies to determine the FIC index of the combination of Cf plus Fp in *Shigella dysenteriae* 7 (Figs. 13 and 14).

19
Curing Effects of Phenothiazines

Plasmids are extrachromosomal dispensable cloud circular DNA elements found in bacterial cells. There are several types of plasmids.

Of these, R plasmids carry various antibiotic resistant genes singly or in different combinations. These genes can be eliminated in vitro with the help of various chemical and physical agents. Such a process has been defined as "curing" and the chemical compounds as "curing agents". Many of the phenothiazines have been found to possess such an activity. For this purpose, the preliminary study includes isolation and recognition of multiple resistant bacteria followed by treatment of these organisms with varying concentrations of a curing agent. The bacteria are found to have at least one or many of the resistance plasmid.

In 1975, Mandi et al. reported that chlorpromazine, levopromazine and promethazine, possessed bacteriostatic action on various Gram-positive and Gram-negative bacteria at 130–180 μg/ml concentration [71]; chloropromazine had bactericidal activity on resting cells of *Escherichia coli* suspended in saline. An effective R-plasmid eliminating property was observed with chlorpromazine at concentration of 50 μg/ml in multidrug-resistant *Escherichia coli*. The same group of workers [71] observed that chlorpromazine and the other phenothiazines at sub-bacterial amount efficiently cured an *Escherichia coli* F′lac+ strain of its plasmid. Curing was found to be most effective at high pH and in complex medium when 70% or more of the bacteria were plasmid free after overnight growth of the cultures in the presence of the drug.

Molnar et al. [69] studied antibacterial effect and plasmid curing property of several phenothaizines and tried to correlate these functions with respect to their chemical structure. They observed that diethazine, amitriptyline, and impipramine showed bacteriostatic and bactericidal effect on different bacteria. Chlorpromazine sulfoxide and fluorescein were ineffective even at 1000 μg/ml. The antibacterial compounds deleted at 40–70% frequency the F′lac+ plasmid of *Escherichia coli* K_{12} Le-140. Similar plasmid elimination potentiality by phenothiazines was reported by the same group of authors in 1982 [72].

In 1999, Radhakrishnan et al. [88] reported the plasmid curing effect of thioridazine on 12 multiple antibiotic and thioridazine resistant bacteria.

Table 41 Distribution pattern of multiple antibiotic resistance in test bacteria

Bacteria	Multiple Resistance Pattern[a]							
Staphylococcus aureus ML 178	Pc_{200}	Ap_{200}	Ax_{100}	Sm_{200}	Er_{200}	Tc_{200}	Cm_{200}	Th_{800}
Staphylococcus aureus SA 18	Pc_{10}	Ap_{50}		Sm_{300}	Er_{10}	Tc_{200}	Cm_{100}	Th_{800}
Escherichia coli 38B	Pc_{400}	Ap_{400}	Ax_{400}	Sm_{400}	Er_{200}	Tc_{200}	Cm_{200}	Th_{1500}
Escherichia coli 54B	Pc_{1500}	Ap_{1500}	Ax_{25}	Sm_{500}	Er_{200}	Tc_{500}	Cm_{1000}	Th_{1500}
Escherichia coli 870	Pc_{400}	Ap_{400}	Ax_{400}	Sm_{400}	Er_{400}	Tc_{400}	Cm_{400}	Th_{1500}
Escherichia coli 871	Pc_{400}	Ap_{400}	Ax_{400}	Sm_{200}	Er_{200}	Tc_{200}	Cm_{50}	Th_{1500}
Escherichia coli 872	Pc_{400}	Ap_{400}	Ax_{400}	Sm_{200}	Er_{400}	Tc_{400}	Cm_{400}	Th_{1500}
Escherichia coli TG1	Pc_{400}	Ap_{400}	Ax_{400}	Sm_{200}	Er_{200}	Tc_{200}	Cm_{400}	Th_{800}
Shigella flexneri 6 B4	Pc_{400}	Ap_{200}	Ax_{400}	Sm_{10}	Er_{200}	Tc_{100}	Cm_{10}	Th_{400}
Vibrio cholerae 14033	Pc_{200}	Ap_{100}		Sm_{10}	Er_{200}	Tc_{100}	Cm_{25}	Th_{200}
Vibrio cholerae 1033	Pc_{200}	Ap_{100}		Sm_{10}	Er_{200}	Tc_{25}	Cm_{2}	Th_{100}
Vibrio cholerae 811	Pc_{200}	Ap_{100}		Sm_{10}	Er_{200}	Tc_{25}	Cm_{2}	Th_{800}

[a] Pc, penicillin; Ap, ampicillin; Ax, amoxycillin; Sm, streptomucin; Er, erythromycin; Tc, tetracycline; Cm, chlorampehicol; Th, thioridazine. Subscripted number denotes levels of corresponding antibiotic resistance in μg/ml.

After determination of the MIC of thioridazine in 12 test bacteria, the curing test was performed by taking 75%, 50%, and 25% of the MIC of thioridazine with respect to each bacterium and inoculating the tube with approximately 300 CFU. A loopful of growth from each of these tubes was plated out on nutrient agar containing the corresponding concentration of thioridazine, so as to produce numerous isolated colonies. At least 100 colonies of a single culture were tested for single or multiple losses of antibiotic resistance(s) at 25% MIC of a particular antibiotic with respect to the given type (untreated). It was observed that elimination of R plasmids was facilitated by choice of optimal concentration of thioridazine, so as to produce numerous isolated colonies. At least 100 colonies of a single culture were tested for single or multiple loss of antibiotic resistance(s) at 25% MIC of a particular antibiotic with respect to the given type (untreated).

The result suggested that thioridazine was able to eliminate different antibiotic resistances singly or jointly in *Escherichia coli* strains and *Shigella flexneri* 6 BDC1 quite efficiently, but had a much weaker effect on *Vibrio cholerae* (Table 42). The pattern of elimination further indicated that penicillin, ampicillin, and amoxicillin were determined by a single plasmid in these bacteria. It seems that effective elimination depended on the curing concentrations, which were close to the MIC value of thioridazine for any

Table 42 Effect of thioridazine on elimination of antibiotic resistance

Strain	Wild type of resistance pattern	Curing agent	Resistance eliminated
Escherichia coli 38B	Pc_{400} Ap_{400} Ax_{400} Sm_{400} Er_{200} Tc_{200} Cm_{200} Th_{1500}	Th	PcApAx(10) Ser(48) Sm(47) Tc(44) Cm(11)
		Spontaneous	Cm(4) Tc(2)
Escherichia coli 871	Pc_{400} Ap_{400} Ax_{400} Sm_{200} Er_{200} Tc_{200} Cm_{50} Th_{1500}	Th	PcApAx(11), Ap(48), Ax(2) Sm(43), Er(11) Tc(22) Cm(97)
		Spontaneous	Tc(2)
Shigella flexneri 6 BDC1	Pc_{400} Ap_{200} Ax_{400} Sm_{10} Er_{25} Tc_{100} Cm_{10} Th_{200}	Th	PcApAx(18), Pc(70) Ap(72) Sm(22) Er(32) TcCm(60) Cm(8)
		Spontaneous	0
Vibrio cholerae 14033	Pc_{200} Ap_{100} Ax_{400} Sm_{10} Er_{100} Tc_{25} Cm_{25} Th_{400}	Th	PcSmTc(60), TcCm(41) SmEr(6), Tc(34)
		Spontaneous	0

Pc, penicillin; Ap, ampicillin; Sm, streptomycin; Er, erythromycin; Tc, tetracycline; Cm, chloramphenicol; Th, thioridazine.

Numbers within parentheses indicate number of colonies cured of resistances out of 100 colonies tested; broth cultures after treatment with Th were plated out for isolated colonies which were then transferred to different antibiotic agar and nutrient agar plates. These plates contained 25% of the MIC of a particular antibiotic with respect to the given type (untreated).

particular bacterium. Thus, most of the cured clones came from 75% concentration series as determined with respect to MIC of thioridazine for a given strain. These elimination studies suggest that the antibiotic resistance determinants in *Escherichia coli* and *Shigella flexneri* 6 BDC1 were probably plasmid linked.

Intracellular efflux pumps have been largely the research focus in multidrug-resistant (MDR) Gram-positive and Gram-negative microorganisms and parasites, including malaria. However, drug-efflux mechanisms, other than pumps per se, have been observed, supported by the effects of isomeric, non-antibiotic depressants (DPRs), phenothiazines and thioxanthenes, and antidepressant (ADPR) phenylpiperidine neurotropic drugs, alone or in combination with classical antimicrobials on MDR *Staphylococcus aureus*, *Stapylococcus epidermidis*, *Enterobacter faecalis*, *Streptococcus pyogenes* and *Streptococcus pneumoniae*. Of the non-antibiotics investigated by Kristiansen et al. [57] the DPR 1-thioridazine, trams-clopenthixol and isomers of phenylpiperidines NNC20-4962 and NNC-7052 were potent antimicrobials.

20
Phenothiazines as Anticancer/Antitumor and Antiviral Agents

Clinical applications of the first phenothiazines date back to 1940 [14]. The antineoplastic properties of these agents emerged almost simultaneously. Certain phenothiazines and benzo[α]phenothiazines possess an inhibitory action for the growth of cancer cells. Benzo[α]phenothiazines revealed remarkable antitumor activity against human myelogenous leukemia cell lines. This is a distinctive property of benzo[α]phenothiazines. Such an action was possibly reflected due to the relationship between anticancer activity and π electron density of benzo[α] phneothiazines [73].

Some of the derivatives of phenothiazines and benzo[α]phenothiazines display antitumor and anticancer activity as well [72]. Coleman et al. [17] reported that cases of metastatic brain tumors could be detected in patients suffering from stomach cancer, breast cancer, and small cell lung carcinoma. According to them, the continuous exposure to the treatment could have significantly enhanced the risk period of the metastases of the central nervous system. The mechanism of complex formation between chlorpromazine and DNA was investigated using high performance liquid chromatography (HPLC) [76]. Their results portrayed that DNA-nucleotides and non-nucleosides could form a chlorpromazine-DNA or a chlorpromazine-nucleotide complex that produced anticancer and antitumor actions. Some phenothiazines were found to exert antiproliferative effects on different membrane bound chemical events, such as H_2O_2 formation and peroxide generated chemiluminescence of polymorphonuclear leukocytes [73]. In 1992, Molnar et al. further observed that

phenothiazines could significantly inhibit the endotoxin of heat killed *Staphylococcus aureus* induced tumor necrosis factor produced by human mononuclear cells [73]. Several phenothiazines revealed ability to induce apoptosis in case of tumor or cancer cells. The substituent at the second position on the phenothiazine and the alkylene number (n) of the side chain on the nitrogen of the phenothiazine ring might have played a role in antitumor activity against AIDS-related leukemia and lymphomas [76].

Apoptosis had been acknowledged as a distinct pathological mechanism in tumor responding to anticancer therapies [29]. It was further noted that the main purpose of anticancer chemotherapy was to kill the tumor cells by inducing apoptosis and triggering the specific apoptotic pathway, rather than by affecting cellular metabolism. Phenothiazines in combination therapy with caffeine were reported to be potent to cure cancer.

Mucsi et al. [78] reported that trifluoperazine, chlorpromazine, and promethazine were effective against herpes simplex virus. Certain benzo[α]-phenothiazines also produced identical results against herpes virus [78]. Some structurally related phenothiazines exhibited photodynamic activity against the pseudorabies virus [33]. The inhibitory effect of the phenothiazines was investigated on the multiplication of several viruses.

Chlorpromazine reduced the multiplication of influenza virus in chick embryo cell culture [57]. It was found that this inhibitory effect was due to the interaction of phenothiazines with cellular calmodulin. Chlorpromazine and trifluoperazine could also inhibit the budding of measles virus at the intermediate stage in plasma membrane of Hela cells. The antiviral effect of trifluoperazine on the influenza virus multiplication was also observed in cell culture, even if the drug was added at a later stage of infection [82]. Trifuoperazine caused a reversible inhibition of influenza virus morphogenesis by disturbing a cellular calmodulin function. However, the budding of the virus was not affected. Candurra et al. noted inhibitory effect on the multiplication of arena virus in Vero cells [10]. Based on these results, it was thought that chlorpromazine could block early stage junin virus replication at the viral entry, while trifluoperazine caused interference with the penetration, and hence inhibition at the viral maturation stage.

Although the phenothiazines and benzo[α]phenothiazines failed to inhibit the HIV replication, they could block attachment of HIV to CD4 molecules, possibly due to dipole-dipole interactions [77]. Depending on the position of different substituents in benzo[α]phenothiazines, increasing or decreasing effect on the adenovirus oncogene expression were exerted within concentration range between 0.005 and 0.5 μg/ml [86]. A possible mechanism of the inhibition of T-antigen expression suggested that the phenothiazine derivatives were able to stabilize the structure of DNA, reducing viral yields or inducing expression of the antioncogenes. The antigen-oncogene binding affinity could result in the shift of an antigen conformation from a resulting

stage. This observation may explain the antiproliferative action of the phenothiazines. The enhancing effect of phenothiazine derivatives on T-antigen expression requires further chemical and biological studies for testing of the antiviral effect of these compounds [73].

21 Conclusion

The World Health Organization has estimated that there are at least 17 million infection-related deaths every year and that up to half of the approximately 5.8 billion people on earth are at risk of many endemic diseases. Infections which caused ravages in the 19th century, such as tuberculosis and plague, are once again resurging with vehemence. Newly emerging pathogens capable of human diseases, such as the human immunodeficiency virus (HIV), bovine-spongiform encephalitis related Creutzfeldt–Jacob Disease and Ebola haemorrhagic fever, continue to surface. The steady progression in the longevity of the population at large will be associated with a rising number of transplantations being performed and a concurrent increase in the incidence of opportunistic infections. Antibiotic resistant nosocomial infections remain significant. Some infections are now so resistant to drug therapy that they are almost untreatable. Multi-drug resistance will predictably persist as a major problem even in the 21st century. Many leading experts are openly concerned about a post-antibiotic era. The struggle to control infectious diseases is far from being over, and it has acquired a new poignancy. International, governmental, and private institutions concerned with public health will have to face up to the challenges posed by existing and emerging microbial infections. Therefore, novel concepts acting as adjunct to established therapies are urgently needed.

The accumulated studies on the antimicrobial activity of phenothiazines carried out by various groups of scientists, as presented above, reveal that such actions could be detected in increasing numbers among drugs of different pharmacological groups, of which phenothiazines are the most prominent. The phenothiazines are primarily antipsychotic and neuroleptic; however, some of them are antihistamines. Antimicrobial potentiality has been reported in all the pharmacologically varied types of phenothiazines. These were active both in vitro and in vivo in remarkable ways and could form synergistic combinations among themselves and also with antibiotics and other chemotherapeutic agents. The problem of drug resistance, as well as the means of ridding many of the plasmid mediated resistances due to curing or eliminating effects exerted by some of these phenothiazines, have been presented above. The antimicrobial activity of these drugs was seen against many genera, starting from enterbacteria, staphylococci, and mycobacteria. Side-by-side activity of several phenothiazines against viruses, tumors, and cancer cells has also been reported. All such studies clearly indicate that

phenothiazines have a great potential in clinical therapy. Thus, the phenothiazines which were developed initially as antimicrobial agents, on subsequent research proved to be a rich source of anticancer drugs. Many such drugs possibly have offshoots again as sedatives, hypnotics, or antidepressants. Therefore, this reveals the multi-functional nature of drugs used in medicine and the potential to generate desired drugs by tailoring them to our needs.

References

1. Asok Kumar K, Ganguly K, Mazumdar K, Dutta NK, Dastidar SG, Chakrabarty AN (2003) Acta Microbiol Polonica 52(3):285–292
2. Amaral L, Viverios M, Kristiansen JE (2001) Trop Med Int Health 6(12):1016–1022
3. Amaral L, Viverios M, Kristiansen JE (2006) Curr Drug Target 7(7):887–891
4. Baritt MM (1936) J Path Bacteriol 42:441
5. Basu LR, Mazumdar K, Dutta NK, Karak P, Dastidar SG (2005) Microbiol Res 160(1):95–100
6. Bhattacharya GK, Johnson RA (1977) Statistical Concept and Methods. John Wiley and Sons, New York, p 425
7. Braun H, Guggenheim K (1932) Zbl Bakt 127:97
8. Brown R, Collee JG, Poxton IR, Fraser AG (1996) In: Collee JG, Fraser AG, Marmion BP, Simons A (eds) Mackie & McCartney's Practical Medical Microbiology. Churchill Livingstone, New York, p 561
9. Bushby SRM (1973) J Infect Dis 128:442–462
10. Candurra et al. (1996) Antiviral Res 31:44–55
11. Cappuccino JG, Sherman N (1983) A Laboratory Manual. Addison-Wesley Publishing Company, USA
12. Chakrabarty AN, Adhya S, Pramanik MK (1970) J Appl Bacteriol 33:397
13. Chakrabarty AN, Bhattacharya CP, Dastidar SG (1993) APMIS 101:449–454
14. Chakrabarty AN, Molnar J, Dastidar SG, Motohashi N (1998) Non Antibiotics – A New Class of Unrecognised Antimicrobics, National Institute of Science Communication (CSIR), New Delhi, India
15. Chakrabarty AN, Neogi D, Acharya DP, Dastidar SG (1989) Indian J Med Res 89:233–237
16. Chattapadhyay D, Dastidar SG, Chakrabarty AN (1988) Arzneim-Forsch/Drug Res 38(11):869–872
17. Coleman MP et al. (eds) (1993) Trends in Cancer Incidence and Mortality. IARC Scientific Publications, vol 121. International Agency for Research on Cancer, Lyon
18. Collee JG, Miles RS, Watt B (1996) In: Collee JG, Fraser AG, Marmion BP, Simons A (eds) Mackie and Mc Cartney's Practical Medical Microbiology. Churchill Livingstone, New York, pp 131–149
19. Cruickshank R (1965) In: Cruickshank R, Duguid JP, Marmion BP, Swain RHA (eds) Medical Microbiology, vol 2. Churchill Livingstone, Edinburg, London and New York, p 113
20. Dash SK, Dastidar SG, Chakrabarty AN (1977) Indian J Exp Biol 15:324
21. Dastidar SG, Chaudhury A, Annadurai S, Roy S, Mookerjee M, Chakrabarty AN (1995) J Chemother 7:201–206
22. Dastidar et al. (2004) Acta Microbiol Immunol Hung 51:75–83

23. Dastidar SG, Chakrabarty P, Mookerjee M, Ganguly M, Chakrabarty AN (1994) Acta Microbiol Immunol Hung 41:41–49
24. Dastidar SG, Jairaj J, Mookerjee M, Chakrabarty AN (1997) Acta Microbiol Immun Hung 44:241–247
25. Dastidar SG, Mahapatra SK, Ganguly K, Chakrabarty AN, Shirataki Y, Motohashi N (2001) In vivo 15:519–524
26. Dastidar SG, Saha PK, Sanyamat B, Chakraborty AN (1976) J Appl Bacteriol 41:209
27. Dastidar SG, Manna A, Asok Kumar K, Mazumdar K, Dutta NK, Chakrabarty AN, Motohashi N, Shirataki Y (2004) Int J Antimicrob Agents 23:99–102
28. Dastidar SG, Mahapatra SK, Ganguly K, Chakrabarty AN, Shirataki Y, Motohashi N (2001) in vivo 15:519–524
29. David EF (1994) Apoptosis in Cancer therapy: Crossing the threshold. Cell 78:539–542
30. Delay J, Deniker P, Harl JM, Grasset A (1952) Ann Med Psychol 110(2):112–117
31. Dharmendra S (1985) Leprosy, vol 2. Samant & Company, Bombay, p 771
32. Domagk G (1935) Dtsch Med Wochenschr 61:280
33. Domonkos K, Molnar J, Musci I, Béládi I, Manian AA (1982) Kisérletes Orvostudomány 34:574–580
34. Duguid JP (1996) In: Collee JG, Fraser AG, Marmion BP, Simons A (eds) Mackie & McCartney's Practical Medical Microbiology. Churchill Livingstone, New York
35. Edwards PR, Ewing WH (eds) (1972) Identification of Enterobacteriaceae. Burgers Publishing Company, Minneapolis
36. Eliopoulos GM, Moellering RC Jr (1996) In: Lorian V (ed) Antibiotics in laboratory medicine. The Williams & Wilkins Co., Baltimore, MD, pp 330–396
37. Falkow S (1958) Am J Clin Path 29:598
38. Farmer JJ III, Fanning GR, Davis BR, O'Hara CM, Riddle C, Hickman-Brenner FW, Asbury MA, Lowery VA III, Brenner DJ (1985) J Clin Microbiol 21(1):77–81
39. Garrod LP, O'Grady F (1971) Antibiotics and Chemotherapy, 3rd ed. Churchill Livingstone, Edinburgh and London, p 468
40. Gillespie EH (1943) Month Bull Emerg Publ Health Laborat Serv 2:19
41. Gootz TD, Sanders CC, Goering RV (1982) J Infect Dis 146(1):34–42
42. Grosskinsky CM, Jacobs WR, Clark-Curtiss J, Bloom BR (1989) Infect Immun 58:2821–2827
43. Guha-Thakurtha A, Mandal SK, Ganguly K, Dastidar SG, Chakrabarty AN (2000) Acta Microbiol Immunol Hung 47(1):21–28
44. Hamon J, Paraire J, Vallux J (1952) Ann Med Psychol 110:331–335
45. Hennet PR, Harvey CE (1991) J Vet Dent 8(2):18–21
46. Hewlette et al. (1997) J Acquired Immunodeficiency Syndromes Human Retrovirology 15:16–20
47. Hickman FW, Farmer JJ III (1978) Am J Med Technol 44:1149–1159
48. Hugh R, Leifson E (1953) J Bacteriol 66:24
49. Jawetz E, Gunnison JB (1952) J Am Med Assoc 150:693
50. Jeyaseeli L, Dasgupta A, Asok Kumar K, Mazumdar K, Dutta NK, Dastidar SG (2006) Int J Antimicrob Agents 21:58–62
51. Kapusnik JE, Hackbarth CJ, Chambers HF (1988) J Infect Dis 158:7–12
52. Kirchner O (1932) Zentralblatt Bakt 124:403–413
53. Kidd SE, Nelson MJ, Epstein M, Aszalós A, Pine S, Molnár J (1997) Antiinfect Drugs Chemother 15:71–77
54. Kovacs N (1956) Nature 178:703
55. Kristiansen JE (1979) Acta Path Microbiol Scand 87:317–319

56. Kristiansen JE, Blom J (1981) Acta Pathol Microbiol Scand B 89(6):399–405
57. Kristiansen JE, Hendricks O, Delvin T, Butterworth TS, Aagaard L, Christensen JB, Flores VC, Keyzer H (2007) J Antimicrob Chemother 59(6):1271–1279
58. Krizanova et al. (1982) Acta Virol 26:209–216
59. Krogstad DJ, Moellering RC (1980) In: Lorian V (ed) Antibiotics in Laboratory Medicine. Williams and Wilkins, Baltimore, London, pp 298–313
60. Kubalski A, Martinac B, Ling YK, Alder J, Kung C (1993) J Membrane Biol 131:151–160
61. Laborit H, Huguenard P (1951) Press Med 58:416
62. Lorian V (1986) Program Abst International Congress on Bacterial and Parasitic Drug Resistance (Bangkok), p 57
63. McFarland J (1907) J Am Med Assoc 49:1176–1178
64. Mazumdar R, Ganguli K, Dastidar SG, Chakrabarty AN (2001) Int J Antimicrob Agents 18(4):403–406
65. Miles AA, Misra SS (1938) J Hyg (Cambridge) 38:732–749
66. Mitruka BM, Rawnsle HM, Vadehra DV (eds) (1976) Animals for Medical Research, vol 341. John Wiley & Sons, Inc. USA, pp 145–150
67. Moellering RC Jr, Wennersten C, Weinberg AN (1971) J Lab Clin Med 77:821
68. Moeller V (1955) Acta Pathol Microbiol Scand 36:158
69. Molnar J, Beladi I, Foldes I (1977) Zbl Bakt Hyg I Abt Orig A 239:521–526
70. Molnar J, Mandi Y, Kiraly J (1976) Acta Microbiol Acad Sci Hung 23:45–54
71. Mandi Y, Molnar J, Holland IB (1975) Genet Res Camb 26:109–111
72. Molnar J, Mandi Y, Boda K, Foldeak S (1982) Neoplasia 29:215–222
73. Molnar J, Tarodi B, Galfi M (1992) Anticancer Res 12:273–280
74. Morell A, Preston NW (1962) J Pathol Bacteriol 84:241
75. Motohashi N (1998) Antitumour activities of phenothiazines (Phenothiazine Oncology). In: Gupta RR (ed) Phenothiazines and 1,4-benzothiazines. Chemical and biological aspects. Biological Molecules, vol 4, Elsevier, London, pp 705–770
76. Motohashi N, Sakagami H, Molnar J (1998) Non-antibiotics: A New Class of Unrecognised Antimicrobics. In: Chanrabarty AN, Molnar J, Dastidar S, Motohashi N (eds) Non-Antibiotics. NISCOm, New Delhi, India, pp 70–77
77. Motohashi N, Molnar J, Burian I (1995) Antiviral activity of phenothiazine derivatives. In: Barbe J, Keyzer H, Soyfer J (eds) Biological and chemical aspects of thiazine and analogs. Enlight Associates, San Gabriel, California, pp 347–356
78. Mucsi I, Molnar J, Motohashi N (1998) Int J Antimicrob Agents 18(1):67–72
79. National Committee for Clinical Laboratory Standards (2003) Methods for Dilution Antimicrobial Susceptibility Tests for Bacteria That Grow Aerobically; Approved Standard, M7-A6. NCCLS, Wayne, PA
80. Neu HC (ed) (1984) Med Clin N Am 72:555
81. Oberhofer TR (1985) Manual of Practical Medical Microbiology and Parasitology. John Wiley and Sons, Toronto, p 352
82. Ochiai H, Furukawa M, Niwayama S (1991) Antiviral Res 15:149–160
83. Petersen PV, Nielsen IM, Pedersen V, Jorgensen A, Lassen N (1977) In: Usdin E, Forrest I (eds) Thioxanthenes In Psychotherapeutic drugs. Marcel Dekker, New York, pp 827–867
84. Preston NW, Morrell A (1962) J Pathol Bact 84:241
85. Pusztai R, Motohashi N, Párkányi C, Aaron JJ, Kesava BR, Molnar J (1996) Anticancer Res 16:2961–2964
86. Rahal BD (1978) Chemotherapy 24:166
87. Raleigh GW, Youmans GP (1948) J Infect Dis 82:197–204

88. Radhakrishnan V, Ganguly K, Ganguly M, Dastidar SG, Chakrabarty AN (1999) Indian J Exp Biol 37:671–675
89. Rahal BD (1978) Chemotherapy 24:166
90. Ray S, Chattopadhay D, Dastidar SG, Chakrabarty AN (1990) Indian J Exp Biol 28:253–258
91. Ratnakar P, Murthy PS (1992) FEM Microbiol Lett 76:(1–2):73–76
92. Reading C (1977) Augmentin Proc Int Symp (Montreux, Switzerland), pp 5–21
93. Reed LV, Muench H (1938) Am J Hyg 27:493–497
94. Richards RM, Xing DK (1993) J Pharm Pharmacol 45(3):171–175
95. Sanyal et al. (1968) Indian Exp Biol 6:112
96. Selvankumar N, Kumar V (1998) Inhibitory activity of trifluoperazine against *Mycobacterium tuberculosis* in Non Antibiotics – A New Class of Unrecognized Antimicrobics. NISCOM, New Delhi, pp. 176–182
97. Shen WW (1999) Comp Psychiatr 40(6):407–414
98. Spooner DF, Sykes G (1972) In: Norris JR, Ribbons DW (eds) Methods in Microbiology, vol 78. Academic Press, New York, pp 211–276
99. Trefouel J, Nitti F, Bovet D (1935) Compt Rev Sec Biol 23:209
100. Tyburski JG, Wilson RF, Warsow KM, McCreadie S (1998) Arch Surg 133(12):1289–1296
101. Weisblum B (1967) Lancet 151(7494):843–844
102. Wilson SG, Miles SA (1979) In: Wilsen G, Dick HH (eds) Topley and Wilson's Principles of Bacteriology, Virology and Immunity, 5th ed, vol 1. Edward Arnold Publishers, London
103. Solonkin JS, Dellinger EP et al. (1990) Ann Surg 212:581–591

Top Heterocycl Chem (2008) 15: 133–159
DOI 10.1007/7081_2008_120

Published online: 29 April 2008

Multidrug Resistance Reversal on Cancer Cells by Selected Carotenoids, Flavonoids and Anthocyanins

Joseph Molnár[1] · Helga Engi[1] · Nóra Gyémánt[1] · Zsuzsanne Schelz[1] · Gabriella Spengler[1] · Imre Ocsovski[1] · Miklós Szücs[1] · Judith Hohmann[2] · Margaret Szabo[3] · Lajos Tanács[4] · Péter Molnár[5] · Joseph Deli[6] · Liselotte Krenn[7] · Masami Kawase[8] · Hidetsugu Wakabayashi[9] · Teruo Kurihara[9] · Yoshiaki Shirataki[10] · Hiroshi Sakagami[11] · Noboru Motohashi[12] (✉) · Remigijus Didiziapetris[13]

[1]Institute of Medical Microbiology and Immunology, University of Szeged, Dóm tér 10, 6720 Szeged, Hungary

[2]Department of Pharmacognosy, University of Szeged, Eötvös u. 6., 6720 Szeged, Hungary

[3]Department of Plant Physiology, University of Szeged, Egyetem u.2., 6722 Szeged, Hungary

[4]Department of Food Chemistry, Faculty of Engineering, University of Szeged, Mars tér 7, 6725 Szeged, Hungary

[5]Department of Pharmacognosy, University of Pécs, Medical School, Rókus u. 2, 7624 Pécs, Hungary

[6]Department of Biochemistry and Medical Chemistry, University of Pécs, Medical School, Szigeti út 12, 7624 Pécs, Hungary

[7]Department of Pharmacognosy, PharmaCenter Vienna, University of Vienna, Althanstr. 14, 1090 Vienna, Austria

[8]Faculty of Pharmaceutical Sciences, Matsuyama University, 4-2 Bunkyo-cho, Matsuyama-shi, 790-8578 Ehime, Japan

[9]Faculty of Sciences, Josai University, 1-1 Keyakidai, Sakado-shi, 350-0295 Saitama, Japan

[10]Faculty of Pharmaceutical Sciences, Josai University, 1-1 Keyakidai, Sakado-shi, 350-0295 Saitama, Japan

[11]Division of Pharmacology, Department of Diagnostic and Therapeutic Sciences, Meikai University School of Dentistry, 1-1 Keyakidai, Sakado-shi, 350-0283 Saitama, Japan

[12]Meiji Pharmaceutical University, 2-522-1 Noshio, Kiyose-shi, 204-8588 Tokyo, Japan
noborumotohashi@jcom.home.ne.jp

[13]Pharma Algorythms, Inc., Mickeviviaus 29, 08117 Vilnius, Lithuania

Abstract The multidrug resistance (MDR) proteins which belong to the ATP-binding cassette superfamily are present in a majority of human tumors and are an important final cause of therapeutic failure. Therefore, some compounds which inhibit the function of the MDR-efflux proteins may improve the cytotoxic action in cancer chemotherapy. The mechanism of action was believed to be a competition between their resistance modifiers and the cytotoxic agents for the same binding site of MDR P-glycoprotein (P-gp) due to a complementarity with a hypothetic receptor site with unknown structure. In the absence of the crystal structures of the P-gp, a receptor fitting was not available. Therefore, we tried to indirectly define the receptor structure or mapping of human MDR1-encoded P-gp in the presence of the structurally unrelated carotenoids, flavonoids, isoflavones and terpenoids.

The inhibition of the efflux activity was measured by the increase of rhodamine 123 (R123) uptake by cancer cells. The effects of flavonoids, carotenoids and anthocyanins were studied on the activity of the MDR-1 gene-encoded efflux pump system. The effective flavonoids were rotenone, chrysin, phloretin and sakuranetin, which could inhibit the MDR efflux pump in the mouse lymphoma and colon cancer cells. The carotenoids isolated from paprika and other vegetables were tested on the increase of R123 accumulation of human MDR-1 gene-transfected L1210 mouse lymphoma cells and human breast cancer cells MDA-MB-231 (HTB-26). Capsanthin and capsorubin enhanced the R123 accumulation 30-fold relative to the nontreated lymphoma cells. Lycopene, lutein, antheraxanthin and violaxanthin had moderate effects, whereas α- and β-carotene had no effect on the reversal of MDR in the cancer cells. The MDR reversal of anthocyanins such as callistephin chloride, pelargonin chloride, ideaninchloride and pelargonidin chloride were studied. Cyanin chloride slightly increased the activity of P-gp; however, all other flavonoids were ineffective as resistance modifiers. Their biological ineffectivity is possibly related to the differences on the polarities of their compounds and permanent positive charge.

Keywords Anthocyanins · Flavonoids · Carotenoids · Isoflavones · Multidrug resistance reversal

1 Introduction

The data suggest the potential importance of carotenoids as possible resistance modifiers in cancer chemotherapy. By our transport inhibition hypothesis, these multidrug resistance (MDR) modulators might bind into the transmembrane domains in three different ways: (1) as competitive inhibitors binding at the same site as the drug substrates, (2) allosteric binding means a modification of the active configuration of P-gp molecule far from the substrate binding site (also called noncompetitive inhibition) and (3) the similarly noncompetitive inhibition of P-gp activity could be reached as the consequence of the modification of the cellular membrane bilayer in which the P-gp is embedded. Two other binding sites for the resistance modifiers could be considered at the extra-membrane domains as follows: (4) the intracytoplasmic ATP-binding sites are sensitive to some flavonoids and (5) the polylactosamine moiety located on the first extracellular do-

main could be modified by tomato lectin specifically binding to the first loop.

The transport activity of P-gp could slow down depending on the conformational changes induced by the resistance modifiers. When the transporter activity-related currents are modified by semiconductors or particular charged molecules, the transporter activity might consequently be modified by the induced electronic changes via the modification of active protein conformation. Their areas of charging currents may increase along with the inhibitor concentrations, which can reflect the extent of their inhibition. When the modified direction of charge flow resulted in a switching from active conformation of the MDR P-glycoprotein (P-gp), which could bind the substrate to an inactive conformation, which does not bind the substrate.

Paprika was imported to European countries from the Far East such as China and India. The first blossoming of paprika in science was in 1930 when the Nobel Prize winner, Albert Szent-Györgyi of Hungary discovered vitamin P (mixture of flavonoids hesperidin and rutin) with the antiscorbutic substance ascorbic acid, vitamin C [1–3].

Soon after this great finding, rutin of vitamin P could prevent the fragility of the capillaries, and was also found from paprika in the same laboratory [4, 5].

Many bioactive phytochemicals were systematically studied after their fractionation and characterization from many vegetables and fruits. New biological effects such as the differentiation-inducing activity of carotenoids—particularly vitamin A—were described in the 1930s. In addition, several experimental results suggested that various carotenoids might serve as dietary chemopreventive agents [6] because of their ability to quench excited molecules and excess radicals.

Phytochemicals may express their antitumor effects through diverse mechanisms such as direct antiproliferation, suppression of oncogene expression, the inhibition of angiogenesis and induction of differentiation. However, a therapeutic effect was only observed in precancerous conditions and promyelocytic leukemia [7]. The risk reduction of age-related diseases was ascribed to the effect of carotenoids such as β-carotene in vegetable intakes [8]. Indeed, the higher intake of carotenoid-rich foods is apparently associated with a reduced risk of developing the age-related diseases such as coronary sclerosis, cancer and cataract formation [9]. In animal experiments, a carrot-rich diet reduced tumor incidence in rats and mice treated with carcinogenic chemicals [10]. In these studies, both β- and α-carotene showed significantly anticancer activity in their two-stage carcinogenesis models [11].

Carotene complexes might restore electrical conductivity [12] in several subcellular compartments. Recently, carotene-containing paprika extracts were fractionated by Motohashi and his coworkers and some of the fractions could apparently reverse the MDR of tumor cells [13].

Based on also our result [14], the ATP-binding cassette (ABC) transporter might be a promising transmembrane protein to determine the responsibility for the MDR reversal of cancers by selected flavonoids and carotenoids, which are abundantly contained in daily various vegetables and fruits including also paprika.

2 Materials and Methods

2.1 Materials

Carotenoids: 8′-Apo-β-caroten-8′-al, semi-β-carotenon-epoxide, 5,6-epoxy-5,6-dihydro-8′-apo-β-caroten-8′-al, β-citraurin-acetate, (3*S*,5*S*,6*R*)-β-citraurine-epoxide, (3*S*,5*R*,6*S*)-β-citraurin-epoxide, rhodoxanthin, apo-10′-violaxanthal, β-carotene-5,6-monoepoxide and its oxidation products, β-citraurin, vitamin A (retinol), vitamin A aldehyde (retinal), vitamin A acetate, 8′-apo-β-carotenoic acid ethylester, phytoxanthins from peach, phytoxanthins from Valencia orange peel, lycopene (*Lycopersicon esculentum*, tomato), capsanthin, capsorubin (*Capsicum annuum*, red paprika), antheraxanthin, violaxanthin (yellow flowers of *Viola tricolor*), β-carotene, α-carotene (*Daucus carota*, carrot), β-cryptoxanthin, α-cryptoxanthin (yellow paprika, Valencia orange peels), zeaxanthin (*Lycium halimifolium*), lutein (*Caltha palustris*, Marsh Marigold) and lycophyll (*Solanum dulcamara*), isolated and identified earlier by our group [13–16], were taken from our store. Stock solutions were prepared in DMSO.

Flavonoids: rotenone, catechin, neohesperidin, naringin, chrysin, robinin, phloretin, phloridzin, robinetin, dihydrorobinetin, kaempferol, dihydrophysetin, dihydroquercetin, sakuranin and sakuranetin (Prof. Sándor Antus, Debrecen, Hungary), formononetin, amorphigenin, afrormosin, 6a,12a-dehydroamorphigenin, (+)-12a-hydroxyamorphigenin (Prof. Judith Hohmann, Szeged, Hungary), and epigallocatechin purchased from SIGMA (St Louis, MO, USA) were dissolved in DMSO.

Anthocyanins: cyanidin chloride, callistephin chloride, pelargonin chloride, ideanin chloride, cyanin chloride and pelargonidin chloride (Prof. Liselotte Krenn, Vienna, Austria) were dissolved in DMSO.

Cell cultures: L5178Y (parent) mouse T-cell lymphoma drug-sensitive cells and the transformed subline with MDR (MDR1/A) were used. The cells were grown in McCoy's 5A medium supplemented with 10% heat-inactivated horse serum [17]. The breast cancer MDA MB 231/MRP (HTB-26), MCF7/KCR/MDR and colon cancer (colo320/MDR) drug-resistant cell lines were also used. These cells were grown in Leibovitz's L-15 medium in the

presence of 10% fetal bovine serum (fbs). All media was supplemented with 2 mM L-glutamine and antibiotics.

Assay for reversal of MDR in mouse lymphoma cells: the L5178 MDR and L5178Y parent cell lines were grown in McCoy's 5A medium containing 10% heat-inactivated horse serum, L-glutamine and antibiotics. The tumor cells were adjusted to a density of 2×10^6 /mL, resuspended in serum-free McCoy's 5A medium and distributed in 0.5 mL aliquots into Eppendorf centrifuge tubes. The compounds used in this study were added at various concentrations in different volumes (2.0–20.0 L) of the 1.0–10.0 mg/mL stock solutions and the samples were incubated for 10 min at room temperature. Next, 10 L (5.2 M final concentration) of the indicator rhodamine 123 (R123) (Sigma, St. Louis, MO, USA) was added to the samples and the cells were incubated for a further 20 min at 37 °C, washed twice and resuspended in 0.5 mL phosphate-buffered saline (PBS) for analysis. The fluorescence of the cell population was measured with a Beckton Dickinson FACScan flow cytometer. Verapamil (EGIS, Hungarian Pharmaceutical Company, Budapest, Hungary) was used as a positive control in R123 exclusion experiments [17]. The percentage mean of the fluorescence intensity was calculated for the carotenoids- or anthocyanins-treated MDR and parental cell lines as compared to the untreated cancer cells. An activity ratio (R) was calculated via the following equation [14] on the basis of the measured fluorescence values:

$$R = \frac{\text{MDR treated/MDR control}}{\text{parental treated/parental control}} .$$

Assay for reversal of MDR drug-resistant subline of breast cancer MCF7 cells: the same method was used as in the case of mouse lymphoma, above.

Reversal of multidrug resistance related protein (MRP) in the MDA-MB-231 (HTB-26) cell line: the cells were distributed onto a six-well plate, each well containing 2.5×10^5 cells in 5 mL of culture medium. The cells were grown for 72 h for the experiment. The culture medium was then changed to 1 mL of serum-free medium per well and two carotenoids and flavonoids in this study were added in various amounts (4–40 μL) from a 1.0 mg/mL stock solution, and the cells were incubated for 10 min at room temperature. Next, 10 L of 2′,7′-bis(2-carboxyethyl)-5(6)-carboxy-fluorescein acetoxymethyl ester (BCECF-AM) (Sigma) was added to the samples, to give a final concentration of 2.6 μM, and the cells were then incubated for a further 20 min at 37 °C, and washed in PBS and detached with trypsin-versen solution [0.25% (w/v) trypsin, 0.03% (w/v) EDTA] to harvest the cells from the six-well plate. The cells from each well were transferred to Eppendorf centrifuge tubes and washed once in culture medium and PBS. The samples were resuspended in 0.5 mL of PBS for measurement. The fluorescence of the cell population was analyzed by flow cytometry using a Beckton Dickinson FACScan instrument.

Indomethacin (Sigma) in a final concentration of 20 μM was used as a positive control in the experiments. The fluorescence activity was determined as the ratio of the fluorescence activities of the treated and untreated samples.

A checkerboard microplate method: this method was applied to study the effects of drug interactions between the resistance modifiers and the cytotoxic compound on cancer cells. Both the effects of the anticancer drug of epirubicin and the resistance modifiers in their combination were studied on various cancer cell lines. The dilutions of epirubicin (A) were made in a horizontal direction, and the dilutions of resistance modifiers (B) vertically in microtiter plate of 100 μL volume. The cell suspension in the tissue culture medium was distributed into each well in 100 μL containing 5×10^4 cancer cells. The plates were incubated for 72 h at 37 °C under a CO_2 incubator. The cell growth rate was determined after minimal-trypton-yeast extract (MTT) staining and the intensity of the blue color was measured on a micro-ELISA reader. The drug interactions of carotenoids or flavonoids with cancer cells were evaluated according to the following system:

$$FIC_A = IC_{50A \text{ in combination}}/IC_{50A \text{ alone}}$$

$$FIC_B = IC_{50B \text{ in combination}}/IC_{50B \text{ alone}}$$

IC = inhibitory concentration
FIC = fractional inhibitory concentration

$$FIX = FIC_A + FIC_B$$

$0.5 < FIX < 1$	Additive effect
$FIX < 0.5$	Synergism
$1 < FIX < 2$	Indifferent effect
$FIX > 2$	Antagonism

FIX = fractional inhibitory index

The prediction of P-gp substrate specificity was also evaluated [16].

2.2 Results

Many fractions of red and green paprika extracts had reversed the MDR of cancer cells [13, 16] in our previous experiments. The effectiveness of hexane and acetone fractions of paprika on the ABC transporter responsible for MDR reversal, made it worth studying the effects of carotenoids and flavonoids on the drug accumulation of cancer cells.

By comparing the drug uptake by the MDR gene-transfected mouse lymphoma cells in the presence of some selected carotenoids, the carotenoids were classified into three different groups based on MDR reversal activity: inactive, moderately active and very active. As shown in Table 1, the

α- and β-carotene were without effect in the first group. The most effective carotenoids were capsanthin, lycophyll and capsorubin. There were some moderately effective carotenoids, such as violaxanthin, lycopene, lutein, zeaxanthin and antheraxanthin. The cell size decreased by less than 5% in the

Table 1 The effects of carotenoids on reversing multidrug resistance (MDR) in human *MDR1* gene-transfected mouse lymphoma cells

Sample	Conc. (μg/mL)	FSC[a]	SSC[b]	FL-1[c]	Fluorescence activity ratio[d]
Parental control	–	586	223	935	–
Multidrug-resistant control	–	621	215	17	–
Control					
Verapamil	5	622	217	99	5.73
Lycopene	2	618	205	19	1.10
	20	622	200	168	9.70
β-Carotene	2	597	215	11	0.66
	20	612	191	9	0.56
α-Carotene	2	575	213	13	0.76
	20	612	187	13	0.81
β-Cryptoxanthin	2	607	195	76	4.41
	20	598	212	167	9.65
α-Cryptoxanthin	2	589	187	16	0.93
	20	571	289	76	4.42
Zeaxanthin	2	594	180	90	5.21
	20	529	307	167	9.67
Lutein	2	597	183	149	8.61
	20	529	242	174	10.06
Antheraxanthin	2	591	163	193	11.13
	20	556	233	176	10.17
Violaxanthin	2	582	165	15	0.90
	20	574	206	103	5.97
Capsanthin	2	538	255	727	30.98
	20	476	340	647	27.59
Capsorubin	2	494	329	793	33.78
	20	441	366	574	24.46
Lycophyll	2	514	177	26	1.4
	20	449	123	471	25.2
DMSO control	20	485	625	25	1.10

[a] FSC: forward scatter analysis;
[b] SSC: side scatter analysis;
[c] FL-1: fluorescence 1 (green fluorescence) analysis;
[d] Fluorescence activity ratio (FAR): FAR means fluorescence ratio for treated/untreated samples

cases of β-cryptoxanthin, lutein and lycophyll. Shrinkage was observed in the presence of zeaxanthin (Table 1). It is concluded that the carotenoids have a MDR-reversing effect on the human MDR-1 gene-transfected mouse lymphoma cells. The drug-sensitive human breast carcinoma cells did not increase the drug accumulation in the presence of carotenoids.

The MDR reversing action of carotenoids depended on the chemical structure of the carotenoids tested on the different cell lines. The different sensitivity of cancer cells to various carotenoids could be explained by the differences in their membrane passing properties or electronic distribution (semiconductor properties of the carotenoids).

Besides the mouse lymphoma cells, the R123 accumulation was also studied in the human breast cancer HTB-26 cells in the presence of carotenoids. The R123 accumulation could not be modified in these cells after carotenoid treatment (Table 2). Because these cancer cells do not contain a MDR efflux pump because the cells have only MDR-related protein (MRP). It is concluded that some carotenoids exert their MDR reversing effect in the human MDR-1 gene-transfected mouse lymphoma cells. However, the same carotenoids did not modify the drug accumulation in the drug-sensitive human breast carcinoma cells (data not shown). It is interesting

Table 2 The MDR reversal effects of carotenoids on MDA-MB231 (HTB-26) multidrug resistance related protein (MRP)-expressing human breast cancer cells

Sample	Conc. (μg/mL)	FSC[a]	SSC[b]	FL-1[c]	Fluorescence activity ratio[d]
HTB-26 CONT	–	558	202	9.21	–
HTB-26 + R123	–	557	197	1406	–
Verapamil	10	554	209	1376	0.978
Lycopene	4	560	218	1245	0.885
β-Cryptoxanthin	4	544	212	1197	0.851
α-Cryptoxanthin	4	551	212	1349	0.959
Zeaxanthin	4	560	225	1210	0.860
Lutein	4	562	222	1318	0.936
Antheraxanthin	4	563	214	1338	0.951
Violaxanthin	4	548	200	1330	0.945
Capsanthin	4	557	215	1252	0.890
Capsorubin	4	547	213	1202	0.855
DMSO control	4	548	208	1306	0.928

[a] FSC: forward scatter analysis;
[b] SSC: side scatter analysis;
[c] FL-1: fluorescence 1 (green fluorescence) analysis;
[d] Fluorescence activity ratio (FAR): FAR means fluorescence ratio for treated/untreated samples

that the MDR reversing effects of the carotenoids tested in these experiments against the two different cell lines might be apparently related to the chemical structures of carotenoids. The majority of carotenoids with hydroxylation on the right six-membered ring revealed a moderate effect on the MDR reversal. In addition to the hydroxylation on the left ring in case of capsanthin and capsorubin, a hydroxylation on the right five-membered ring possibly is responsible for the very high resistance reversal effects.

Some rare types of carotenoids, such as mutatochrome and aurochrome, diepoxy-β-carotene were moderately active for the reversal of MDR (Table 3). Flavoxanthin plus chrysanthemaxanthin, (5*R*,8*R*)-capsochrome, (5*R*,8*S*)-capsochrome, (5*S*,8*S*)-capsochrome, and (5*S*,8*R*)-capsochrome had significantly high fluorescence activity ratios on their reversals of MDR. 15,15-

Table 3 The effects of carotenoids in reversing MDR of *mdr1* gene-transfected mouse lymphoma cells

Sample	μg/mL	Fluorescence activity ratio [a]
Verapamil	10	15.70
Mutatochrome	4	2.02
	40	7.47
Aurochrome	4	0.94
	40	3.34
Flavoxanthin + chrysanthemaxanthin	4	4.12
	40	30.27
(5*R*,8*R*)-Capsochrome	4	11.03
	40	37.92
(5*R*,8*S*)-Capsochrome	4	14.04
	40	56.81
(5*S*,8*S*)-Capsochrome	4	40.13
	40	41.52
(5*S*,8*R*)-Capsochrome	4	23.25
	40	53.54
Monoepoxy-β-carotene	4	9.54
	40	37.59
Diepoxy-β-carotene	4	1.44
	40	5.72
15,15′-Dehydro-diepoxy-β-carotene	4	0.75
	40	0.58
Monoepoxy-β-carotene	4	0.72
	40	0.56
DMSO control		0.74

[a] Fluorescence activity ratio (FAR): FAR means fluorescence ratio for treated/untreated samples

Dehydro-diepoxy-β-carotene and mono-epoxy-α-carotene were ineffective in the same concentrations as were applied for other carotenoids (Table 3).

Luteochrome was hardly effective at all as a reversing agent, when compared to (8′*R*)- and (8′*S*)-luteoxanthin, (13*Z*)-zeaxanthin, (13*Z*)-lutein, (9*Z*)-zeaxanthin, (9*Z*)-violaxanthin and (9′*Z*)-neoxanthin and their high fluorescence activity ratios on the mouse lymphoma cells (Table 4).

Much less inhibition was found in the MCF7/MDR1 drug-resistant human breast cancer cell line in the presence of same carotenoids as were investigated earlier on the human MDR1 gene-transfected mouse lymphoma cells. As Table 5 shows the, rhodamine accumulation was enhanced only moderately from 1.1 to 2.2 fluorescence activity ratio, which means that the rhodamine uptake was enhanced from 10% to 120% in the human breast cancer cells. On the other hand, some carotenoids such as (9′*Z*)-neoxanthin, mono-epoxy-α-carotene and 15,15-dehydro-diepoxy-β-carotene were inactive (Table 5).

The comparison of the sensitivity of mouse lymphoma and human breast cancer MCF7 cell lines shows that the same human MDR1 gene-encoded P-gp

Table 4 The effects of carotenoids on MDR reversal in human *mdr1* gene-transfected mouse lymphoma cell line

Sample	μg/mL	Fluorescence activity ratio [a]
Verapamil	10	19.29
Luteochrome	4	1.54
	40	2.83
(8′*R*)-Luteoxanthin	4	56.90
	40	61.95
(8′*S*)-Luteoxanthin	4	35.94
	40	63.57
(13*Z*) + (13′*Z*)-Lutein	4	11.64
	40	31.42
(13*Z*)-Zeaxanthin	4	3.58
	40	35.24
(9*Z*)-Zeaxanthin	4	4.86
	40	20.54
(9*Z*)-Violaxanthin	4	34.01
	40	57.74
(9′*Z*)-Neoxanthin	4	51.21
	40	59.55
DMSO control		0.72

[a] Fluorescence activity ratio (FAR): FAR means fluorescence ratio for treated/untreated samples

Table 5 The effects of carotenoids on MDR reversal in doxorubicin-resistant MCF7/KCR MDR1-expressing human breast cancer cell line

Sample	μg/mL	Fluorescence activity ratio [a]
Verapamil	5	11.9
Luteochrome	4	2.1
	40	1.3
(8′*R*)-Luteoxanthin	4	1.2
	40	1.9
(8′*S*)-Luteoxanthin	4	1.1
	40	2.1
(13*Z*) + (13′*Z*)-Lutein	4	1.2
	40	2.0
(13*Z*)-Zeaxanthin	4	1.1
	40	2.0
(9*Z*)-Violaxanthin	4	1.7
	40	2.2
(9′*Z*)-Neoxanthin	4	0.89
	40	0.69
(5*S*,8*R*)-Capsochrome	4	1.27
	40	1.38
(5*S*,8*S*)-Capsochrome	4	1.77
	40	1.99
(5*R*,8*S*)-Capsochrome	4	1.34
	40	1.67
(5*R*,8*R*)-Capsochrome	4	1.43
	40	1.95
Monoepoxy-α-carotene	4	0.94
	40	0.69
15,15′-Dehydro-diepoxy-β-carotene	4	0.89
	40	0.62
Diepoxy-β-carotene	4	1.07
	40	2.08
Monoepoxy-β-carotene	4	1.17
	40	2.37
DMSO control		0.6

[a] Fluorescence activity ratio (FAR): FAR means fluorescence ratio for treated/untreated samples

efflux pump had a different rate of expression because the two tumor cells had different sensitivities to carotenoids, despite the fact that the drug accumulation in the verapamil control was similar to the comparable range in both cell lines. We suppose that the cell membrane structures with their P-gp are different in each cell line and have the different sensitivity to the

Table 6 Checkerboard microplate method for the two drug-resistant cell lines

Sample	L5178 Mouse lymphoma MDR1 resistent cell line		Drug resistant subline of MCF7 breast cancer cell	
	FIX	Interaction	FIX	Interaction
Monoepoxy-β-carotene	0.678	Additive	1.512	Indifferent
(5*S*,8*S*)-Capsochrome	0.467	Synergism	2.855	Antagonism
(8′*S*)-Luteoxanthin	0.448	Synergism	0.803	Additive
(9*Z*)-Violaxanthin	0.568	Additive	0.279	Synergism
(9*Z*)-Zeaxanthin	0.239	Synergism	0.976	Additive
(13*Z*)-Zeaxanthin	0.494	Synergism	0.426	Synergism

extremely hydrophobic carotenoids. The MDR reversal was enhanced by the combination of doxorubicin and some carotenoids were synergistic in the antiproliferative action on both cell lines in vitro (Table 6).

The majority of carotenoids tested in this study increased the rhodamine accumulation of the Colo 320 MDR/MRP human colon cancer cells by the inhibition of the MDR1-mediated efflux pump activity. The cell size and the intracellular or subcellular structures of carotenoid-treated cells were not modified during the short period of the flow cytometric experiments. The mean fluorescence and the shift of the fluorescence peak increased to various extents in the presence of carotenoids. The most active compounds were antheraxanthin, violeoxanthin, apple peel phytoxanthin, lutein and violaxanthin, while the luteoxanthin, neoxanthin and β-cryptoxanthin were only moderate in their inhibition of the efflux pump (Tables 7, 8).

Anthocyanins isolated from plants were studied for their possible inhibitory action on the MDR1 efflux pump. Among anthocyanins tested in this study, only cyanidin chloride showed a slight inhibition on P-gp function (Table 9). The chlorides of callistephin, pelargonin, ideanin, cyanin and pellargonidin slightly enhanced the activity of the efflux pumps.

Two drug accumulations in the human *mdr1* gene-transfected mouse lymphoma and human breast cancer (HTB26) cell line carrying MRP were compared in the presence of naturally occurring plant-derived flavonoids and isoflavonoids including isoflavones and rotenoids based on our former results [4, 18]. The presence of MRP in MDA-MB 231 cells was detected by their immunocytochemistry analysis with MRPm6 of monoclonal antibody. The antibody MRPm6 reacted with an internal epitope of MRP, however, it did not cross-react with human *mdr1* and *mdr3* gene products. A high level of P-gp expression was also detected in the membrane of L5178Y human *mdr1*-transfected mouse lymphoma cells by the NCL-PGLYm mouse monoclonal antibody, which reacts with the human P-gp

Table 7 Effects of selected carotenoids on MDR reversal in human *MDR1* gene-transfected mouse lymphoma cells

	Sample	μg/mL	FSC[a]	SSC[b]	FL-1[c]	Fluorescence activity ratio[d]	Peak Ch[e]
1	PAR + R123	–	507.80	150.12	948.12	–	938
2	PAR + R123	–	511.04	149.63	942.36	–	956
3	MDR + R123	–	560.76	150.01	13.32	–	10
	MDR mean	–	512.78	140.17	10.09	–	–
4	Verapamil	10	562.61	153.21	*66.74*	*6.61*	17
5	8′-Apo-β-Caroten-8′-al	8	557.34	174.79	8.96	0.88	7
6		40	557.22	181.65	8.49	0.84	7
7	Semi-β-Carotenon-epoxide	8	545.14	165.19	*237.01*	23.49	286
8		40	545.33	166.66	524.62	51.99	385
9	5,6-Epoxy-5,6-dihydro-8′-apo-β-caroten-8′-al	8	533.46	177.63	6.99	0.69	6
10		40	493.38	246.12	8.05	0.79	7
11	β-Citraurin-acetate	8	514.90	149.65	13.77	1.36	8
12		40	509.72	165.78	*47.02*	4.66	12
13	(3*S*,5*S*,6*R*)-β-Citraurin-epoxide	8	474.09	153.95	17.90	1.77	10
14		0	426.83	161.73	19.84	1.96	10
15	(3*S*,5*R*,6*S*)-β-Citraurin-epoxide	8	464.22	151.10	22.33	2.21	12
16		40	438.83	169.91	26.00	2.57	14
17	Rhodoxanthin	8	486.47	139.43	7.89	0.78	8
18		40	483.68	141.93	9.09	0.90	7
19	Apo-10′-violaxanthal	8	378.98	169.40	80.09	7.93	55
20		40	385.69	312.58	–	Toxic	–
21	DMSO 100% 10 μL	2%	477.82	133.82	7.36	0.72	6
22	MDR	–	464.79	130.33	6.87	–	6

[a] FSC: forward scatter analysis;
[b] SSC: side scatter analysis;
[c] FL-1: fluorescence 1 (green fluorescence) analysis;
[d] Fluorescence activity ratio (FAR): FAR means fluorescence ratio for treated/untreated samples;
[e] Peak Ch: fluorescence peak channel.

G-terminal cytoplasmic domain. Among isoflavonoids, the rotenoid, amorphigenin and isoflavone formononetin were proved to have the highest MDR reversal effects. Afrormosin, (+)-12a-hydroxyamorphigenin and 6a,12a-dehydroamorphigenin were moderately effective against the human *mdr1* gene-transfected mouse lymphoma cells (Table 10).

When the same isoflavonoids were tested on MRP, the carboxyfluorescein accumulation of the MDA-MB-231 breast cancer cells was measured. BCECF-AM, a fluorescent dye used as an intracellular pH indicator, is an especially good MRP substrate [12]. The MRP expression and its func-

Table 8 Effects of some selected carotenoids on MDR reversal in human *MDR1* gene-transfected mouse lymphoma cells

	Sample	μg/mL	FSC[a]	SSC[b]	FL-1[c]	Fluorescence activity ratio[d]	Peak Ch[e]
1	PAR +R123	–	492.16	136.85	911.11	–	1175
2	PAR +R123	–	520.79	145.65	933.83	–	1018
3	MDR + R123	–	582.25	170.11	11.89	–	10
	MDR mean	–	541.92	158.8	10.77	–	–
4	Verapamil	10	581.92	171.07	115.75	10.74	35
5	*β*-Carotene-5,6-monoepoxide	8	581.66	170.61	12.86	1.19	11
6	and its oxidation products	40	578.55	164.40	14.42	1.33	11
7	*β*-Citraurin	8	564.94	181.43	13.66	1.26	11
8		40	514.73	248.75	83.52	7.75	16
9	Vitamin A (retinol)	8	490.17	126.14	*363.91*	33.78	392
10		40	380.57	277.30	–	Toxic	–
11	Vitamin A aldehyde (retinal)	8	483.81	138.50	*166.77*	15.48	224
12		40	325.25	323.01	–	Toxic	–
13	Vitamin A acetate	8	550.44	169.12	*184.25*	17.11	186
14		40	529.36	155.04	*139.84*	12.98	64
15	8′-Apo-*β*-carotenoic-	8	536.48	165.89	10.65	0.98	8
16	acid-ethylester	40	538.79	202.55	11.64	1.08	10
17	Phytoxanthins from peach	8	521.63	161.69	*153.38*	14.24	42
18		40	511.97	183.30	*429.24*	39.85	352
19	Phytoxanthins from	8	502.81	161.52	*173.51*	16.11	77
20	Valencia orange peel	40	513.13	181.69	*352.32*	32.71	271
21	DMSO 100% 10 μL	2%	502.81	139.66	10.85	1.00	9
22	MDR	-	501.59	147.49	9.65	–	9

[a] FSC: forward scatter analysis;
[b] SSC: side scatter analysis;
[c] FL-1: fluorescence 1 (green fluorescence) analysis;
[d] Fluorescence activity ratio (FAR): FAR means fluorescence ratio for treated/untreated samples;
[e] Peak Ch: fluorescence peak channel.

tion were calculated by flow cytometry [13], although the sensitivity of this method was lower than the R123 exclusion test against the mouse lymphoma cells. Formononetin increased the drug accumulation in both cell lines, when compared to the control. Afrormosin was only moderately effective on the MRP reversal in the tumor cells. 6a,12a-Dehydroamorphigenin and

Table 9 Effect of anthocyanins on MDR efflux pump of human *MDR1* gene-transfected mouse lymphoma cells

Sample	μg/mL	Dye	FSC[a]	SSC[b]	FL-1[c]	FAR[d]	Peak Ch[e]
1 PAR	–	R123	400.13	154.28	943.39	–	763
2 PAR	–	R123	403.41	152.32	1081.89	–	991
3 MDR	–	R123	509.75	233.97	45.04	–	38
MDR mean	–	R123	451.54	230.60	40.15	–	32
4 Verapamil	10	R123	501.93	233.20	*433.18*	10.78	268
5 Cyanidin-chloride	4	R123	497.99	228.33	41.96	1.04	39
6	40	R123	500.08	231.55	43.54	1.08	34
7 Callistephin-chloride	4	R123	496.35	229.18	32.14	0.80	17
8	40	R123	493.57	224.25	31.57	0.78	27
9 Pelargonin-chloride	4	R123	486.32	226.03	23.58	0.58	14
10	40	R123	477.30	215.86	22.51	0.56	14
11 Ideanin-chloride	4	R123	473.95	220.80	26.07	0.64	22
12	40	R123	463.78	213.72	25.58	0.63	22
13 Cyanin-chloride	4	R123	459.60	201.65	34.31	0.85	28
14	40	R123	429.49	190.98	13.87	0.34	10
15 Pelargonidin-chloride	4	R123	461.00	219.97	29.30	0.73	21
16	40	R123	462.32	190.41	23.80	0.59	19
23 DMSO	–	R123	388.76	223.39	37.78	0.94	29
24 MDR	–	R123	393.34	227.24	35.27	–	26

[a] FSC: forward scatter analysis;
[b] SSC: side scatter analysis;
[c] FL-1: fluorescence 1 (green fluorescence) analysis;
[d] Fluorescence activity ratio (FAR): FAR means fluorescence ratio for treated/untreated samples;
[e] Peak Ch: fluorescence peak channel.

(+)-12a-hydroxyamorphigenin had only marginal effects, when compared with indomethacin-treated MRP cells (Table 11).

The flavonoids were tested for the drug accumulation in the HTB26 breast cancer cells; three groups of compounds could be distinguished. In the first group, chrysin, robinin, kaempferol, dihydroquercetin and epigallocatechin were as effective as the indomethacin control elevating the BCECF-AM accumulation by 20–60%. In the second group, neohesperidin, naringin, phloretin, phloridzin, robinetin, dihydrorobinetin and dihydrofisetin were practically ineffective. In the third group, rotenone, catechin and sakuranin reduced the drug accumulation in the cells (Table 12).

Table 10 Effects of isoflavonoids on rhodamine 123 accumulation in human *mdr1* gene-transfected mouse lymphoma cell line

Compound	μg/mL	Fluorescence activity ratio[a]
Verapamil	5	17.1
Formononetin	4	0.8
	40	18.3
Amorphigenin	4	12.4
	40	46.4
Afrormosin	4	0.5
	40	3.1
6a,12a-Dehydroamorphigenin	4	1.1
	40	3.0
(+)-12-Hydroxyamorphigenin	4	0.4
	40	2.8
DMSO control		0.9

[a] Fluorescence activity ratio (FAR): FAR means fluorescence ratio for treated/untreated samples

Table 11 Effects of isoflavonoids on BCECF-AM accumulation of MDA-MB-231 (HTB-26) MRP-expressing cell line

Compound	μg/mL	Fluorescence activity ratio[a]
Indomethacin	10	2.4
Formononetin	4	1.0
	40	1.5
Amorphigenin	4	1.0
	40	1.0
Afrormosin	4	1.3
	40	1.4
6a,12a-Dehydroamorphigenin	4	1.0
	40	1.2
(+)-12-Hydroxyamorphigenin	4	1.1
	40	1.1
DMSO control		1.0

[a] Fluorescence activity ratio (FAR): FAR means fluorescence ratio for treated/untreated samples

When the same flavonoids were tested on the mouse lymphoma cells, rotenone, chrysin, phloretin and epigallocatechin displayed a dose-dependent increase in the fluorescence activity ratio (FAR). These flavonoids caused

Table 12 Effects of flavonoids on BCECF-AM accumulation in MDA-MB-231 (HTB-26) MRP-expressing cell line

Compound	μg/mL	Fluorescence activity ratio[a]
Indomethacin	10	1.3
Rotenone	4	0.3
	40	0.3
Catechin	4	0.6
	40	0.6
Neohesperidin	4	0.8
	40	0.9
Naringin	4	1.0
	40	0.8
Chrysin	4	1.0
	40	1.2
Robinin	4	1.4
	40	1.6
Phloretin	4	0.7
	40	1.0
Phloridzin	4	0.8
	40	0.9
Robinetin	4	0.8
	40	0.9
Dihydrorobinetin	4	0.8
	40	1.1
Kaempferol	4	0.9
	40	1.3
Dihydrofisetin	4	1.0
	40	1.0
Dihydroquercetin	4	0.9
	40	1.3
Sakuranin	4	0.8
	40	0.7
Sakuranetin	4	0.8
	40	0.8
Epigallocatechin	4	1.1
	40	1.3
DMSO control		0.9

[a] Fluorescence activity ratio (FAR): FAR means fluorescence ratio for treated/untreated samples

a much higher drug accumulation than that of the verapamil control. Catechin, neohesperidin, naringin, robinin and sakuratin had moderate effects. Dihydroquercetin, dihydrofisetin, dihydrorobinetin and phloridzin reduced the R123 accumulation in the cells. Kaempferol and robinetin had no effect

on the R123 accumulation in the human *mdr1* gene-transfected mouse lymphoma cell line (Table 13).

Table 13 Effect of flavonoids on rhodamine 123 accumulation in human *mdr1* gene-transfected mouse lymphoma cell line

Compound	μg/mL	Fluorescence activity ratio [a]
Verapamil	5	8.9
Rotenone	4	27.7
	40	28.6
Catechin	4	2.7
	40	2.9
Neohesperidin	4	2.3
	40	2.8
Naringin	4	2.6
	40	2.3
Chrysin	4	3.7
	40	14.6
Robinin	4	2.0
	40	1.5
Phloretin	4	0.8
	40	4.9
Phloridzin	4	0.7
	40	0.6
Robinetin	4	0.7
	40	0.7
Dihydrorobinetin	4	0.8
	40	0.7
Kaempferol	4	0.8
	40	0.8
Dihydrofisetin	4	0.7
	40	0.5
Dihydroquercetin	4	0.7
	40	0.6
Sakuranin	4	0.7
	40	0.8
Sakuranetin	4	0.8
	40	2.4
Epigallocatechin	4	0.6
	40	36.1
DMSO control		0.8

[a] Fluorescence activity ratio (FAR): FAR means fluorescence ratio for treated/untreated samples

The effects of different flavonoids on the drug accumulation of Colo320 human colon cancer cells was studied (Table 14). Rotenone and sakuranetin were most effective in the inhibition of MDR efflux pump. Dihydrorobinetin, phloridzin, naringin and neohesperidin had only moderate effects, while dihydrophysetin, kaempferol, dihydroquercetin and sakuranin were ineffective.

Furthermore, the enhanced antiproliferative activity by the combinations of the tested compounds with epirubicin was examined. Among the resistance modifiers (formononetin, amorphigenin, rotenone, chrysin and epigallocatechin), chrysin and amorphigenin enhanced the antiproliferative activity

Table 14 The effects of various flavonoids on the drug accumulation (rhodamine 123) in MDR1/LRP-expressing human colon cancer cells (Colo 320)

Compound	Final concentration μg/mL	Fluorescence activity ratio	Peak channel
Verapamil	10	21.62	598
DMSO	–	1.09	18
Rotenon	4	13.58	881
	40	40.04	1433
Catechin	4	1.48	41
	40	1.57	59
Neohesperidin	4	1.60	35
	40	1.55	50
Naringin	4	1.91	44
	40	1.18	16
Robinin	4	1.43	36
	40	1.18	18
Phloridzin	4	1.26	24
	40	2.81	27
Robinetin	4	1.10	26
	40	0.83	15
Dihydrobinetin	4	2.01	52
	40	1.48	40
Dihydrofisetin	4	1.32	57
	40	1.21	21
Kampferol	4	0.46	9
	40	0.81	14
Dihydroquercetin	4	0.69	16
	40	0.91	15
Sakuranin	4	0.59	12
	40	0.52	11
Sakuranetin	4	0.60	11
	40	5.2	27

of epirubicin against mouse lymphoma cells. Although rotenone significantly increased the R123 drug accumulation, it had only a marginal additive antiproliferative effect in combination with epirubicin. On the MDA-MB-231 breast cancer cell line, formononetin and kaempferol were synergetic. Some compounds such as afrormosin and robinin also had their weak effects in the combination with epirubicin. Interestingly, afrormosin and robinin were ineffective against the human *mdr1*-transfected mouse lymphoma cell line. Amorphigenin treatment also showed different effects against the two cell lines (Table 15).

Table 15 Antiproliferative activity of selected flavonoids and epirubicin against resistant mouse lymphoma and human breast cancer cells. Epi* = Epirubicin

Cell line	Sample	ID_{50} (μg/mL)	FIX	Interaction
L5718-MDR mouse lymphoma	Chrysin	15.51		
	Epirubicin control	1.4		
	Chrysin + Epi*	0.606	0.471	Synergism
	Rotenone	0.01		
	Epirubicin control	1.4		
	Rotenone + Epi	0.006	0.604	Additive effect
	Amorphigenin	1.04		
	Epirubicin control	3.46		
	Amorphigenin + Epi	0.18	0.120	Synergism
	Formononetin	19.7		
	Epirubicin control	3.46		
	Formononetin + Epi	3.64	1.230	No interaction
MDA-MB-231 human breast cancer	Amorphigenin	0.01		
	Epirubicin control	0.11		
	Amorphigenin + Epi	0.01	1.090	No interaction
	Formononetin	17.54		
	Epirubicin control	0.11		
	Formononetin + Epi	0.02	0.181	Synergism
	Afrormosin	20.5		
	Epirubicin control	0.11		
	Afrormozin + Epi	0.06	0.548	Additive effect
	Robinin	18.6		
	Epirubicin control	0.04		
	Robinin + Epi	0.02	0.501	Additive effect
	Epigallocatechin	26.01		
	Epirubicin control	0.05		
	Epigallo. + Epi	0.05	1.001	No interaction
	Kaempferol	55.47		
	Epirubicin control	0.05		
	Kaempferol + Epi	0.02	0.440	Synergism

2.3 Discussion

The results show that the MDR reversing effect might depend on the chemical structure. The explanation can be approached from submolecular biology and molecular chemistry. In the case of vitamins and hormones, there are special structural conditions to be fulfilled in order that the absorbed energy (e.g., light energy quanta) will be given off in a form of fluorescent light. A light transformer can act as a catalyst. In this case, an aliphatic carotenoid (or acridine) with conjugated unsaturated rings with a conjugated system had a marked propensity for resonance. The essential role of such compounds can be easily understood if we consider that flavones and chlorophylls are capable of undergoing the subsidiary valency cyclization with foreign atoms or molecules such as Zn or chlorophyll. Here is an example of light absorption and emission which depends on raising the molecule from the ground state to an excited state, with a subsequent emission of energy when the molecule returns to the ground state.

Apparently, there is no relationship between chemical structure and fluorescence; however, the absorption of light alone could not be responsible for the signal transmission. By their absorption of the light quanta, the molecules are raised to excited states from the ground state; after absorption of energy, the excited molecules returned again to their first excited state, then the transition of molecules from their first excited state to the ground state occurred with the emittance of fluorescent light, which was dependent on their different energy quanta. What is the meaning of such an interaction in carotenoids? One possibility might be that carotenoids might provide a network for well-organized conduction. Furthermore, the conductance and semiconductors might play an important role in their signal transductions at subcellular compartments, such as the restructuralization of the differentiated state by the induction or reorganization of normal subcellular compartments in the presence of carotenoids. Indeed, carotenoids could form charge transfer complexes (CTCs) with high conductivity or the strong ESR signals [19]. Their spectral data show that carotene could form CTCs with iodine, due to a special CT transition between the CT ground state and excited state [19]. In addition, the carotene protein complex exhibits high conductivity with low activation energy [15].

Epidemiological studies have indicated that high consumption of vegetables and fruits rich in both flavonoids and carotenoids could reduce the risk of various cancers. Common fruits and vegetables contain approximately 40–50 carotenoids, and many of these could be selected as nutraceuticals with diverse functionalities [20].

Apart from β- and α-carotene, rare carotenoids such as prenigroxanthin [21] from red paprika and cycloviolaxanthin [18] and capsoneoxanthin from *Asparagus falcatus* [21] have been chemically well characterized; how-

ever some biological effects are still not clearly defined. Because carotenoids are extremely hydrophobic, and are sensitive to oxidation or photooxidation, their investigation is laborious and time-consuming [21–23]. Therefore, their complex formations with cyclomalto-oligosaccharides such as water-soluble micelles have been recommended as both convenient and inexpensive solubilizing agents [24, 25]. Such a solvent was used in the investigation of the antiproliferative effects of the tomato carotenoid lycopene against various prostate cancer cells [24]. It turned out that the major tomato carotenoid had an antitumor effect against prostate cancer. The growth inhibition was accompanied by slowing down the cell cycle progression through the G1-S phase in the mammary cancer MCF7 via the reduction of cycline-D1 [25]. Interestingly, the lycopene inhibits the cell growth by interference with the growth factor signal transduction with the insulin-like growth factor (IGF) in breast cancer MCF7 and endometrial cancers [26, 27], because of the reduction of the IGF-induced tyrosine phosphorylation of the insulin receptor substrates.

The carotenoids have multiplex targets for the oncogenes [21, 28–42], apoptosis induction and protection from membrane damage. The immunomodulatory effects of carotenoids are a result of complex mechanisms for the immunostimulation, in which generated as their antioxidative activity, that is, the singlet oxygen quenching capacities of carotenoids having nine or more conjugated double bonds in the molecule may be involved.

The absorption and bioavailability of both lutein and zeaxanthin were studied and their epimeric isomers were found in human serum. Much evidence shows that a high intake of carotenoids in fruits and vegetables might be associated with a reduction in the risk of lung cancer, and in particular that α-carotene rather than β-carotene may be associated with that reduced risk.

It has been shown that numerous carotenoids can exert their inhibitory action on the excess harmful free-radical generation in leukocytes. These findings could explain why the daily intake of colorful vegetables and fruits, such as green yellow, blue and other colors, might be strongly associated with diverse cancer preventions. The carotenoids like capsanthin isolated from the fruits of red paprika *Capsicum annum* L. significantly enhanced anticancer-promoting activity by the inhibition of the early tumor antigen expression of Epstein–Barr virus (EBV) after 12-*O*-tetradecanoylphorbol 13-acetate (TPA) induction, showing that paprika carotenoids might have anticancer effects of both in vitro and in vivo. Other structurally related carotenoids such as lycopene from tomato were also studied in vivo on human cervical, breast, ovarian and colorectal cancers. The results show that the high serum carotenoid concentrations might be associated with a decreased risk of cancer recurrence. There are data that the increased consumption of carotenoids could reduce their risk of the cancers, especially the upper respiratory tract and digestive tract cancers. A carotenoid-rich diet could suppress

the prostate cancer by inducing apoptotic cell death with the process of Bcl-2 and Bax. Carotenoids could reduce the growth factor that induced the cell cycle progression from G1 to S phase. Generally, it is known that diets rich in vegetables and fruits with a natural mixture of carotenoids are effective for the promotions of their anticancer effects by phytoestrogens and other phytochemicals. Epidemiologically, these carotenoids in the diet could reduce the occurrence of various types of cancer, including the hormone-induced breast cancer in the menopausal women.

A number of plant extracts and chemically characterized plant components have previously been tested for MDR reversal in our laboratory [16].

We have examined the effects of flavonoids and isoflavonoids on the P-gp- and MRP- mediated MDR mechanisms in both mouse lymphoma and human breast cancer cell lines. The interactions of the drug transporters P-gp or MRP with flavonoids or isoflavonoids might be worth their use as anticancer agents, such as a single administration or a combination cancer therapy with cytotoxic agents such as mitomycin C (MMC). Differences in the activities of the P-gp and the MRP-mediated efflux pump could be found in the presence of flavonoids and isoflavonoids.

Both a short-term intracellular drug accumulation and a long-term viability assay have been used to understand the anticancer properties of the effects of flavonoids against tumor cells [14, 16].

In the drug accumulation studies, the P-gp inhibition of carotenoids was apparently higher than the MRP inhibition for each compound in the sensitivities against the two different efflux proteins. Furthermore, some compounds in combination with epirubicin were more effective than expected in the MRP-expressing human breast cancer cell line because the efflux activity of P-gp was much higher than the activity of MRP. Thus, the MTT assay was used in an assessment of "antiproliferative or cytotoxic" cellular effects in both single administration of the carotenoid alone and the combination administration of the carotenoids with anticancer agents. The differences might also be explained by structural and functional mechanisms that might be related to the different sensitivities against the simultaneously applied anticancer drugs.

One of the differences between the two efflux systems is that the P-gp has been shown to bind directly to the transported drug to which P-gp confers the MDR, whereas the MRP pumps out some compounds through a cotransport mechanism with reduced glutathione (GSH) and compounds with anionic character. Other studies have demonstrated that some dietary flavonoids could modulate organic anion and GSH transport, ATPase and their drug resistances. The soybean isoflavone genistein was found to act as an inhibitor of drug accumulation in MRP-overexpressing cells, and also to interact with P-gp and inhibit the P-gp-mediated drug transport.

However, contradictory results on the MDR-modulating activity of the flavonoid polyphenols kaempferol and quercetin have been reported that

these polyphenols stimulated the P-gp-mediated efflux of doxorubicin in the adriamycin-resistant subline of the MCF-7 breast cancer cell line.

In our experiments, kaempferol was ineffective in P-gp inhibition; however, chrysin had a significant inhibitory effect. The rotenoid derivatives, amorphigenin and rotenone, had their MDR-modulating activity because of their structural difference of a hydroxyl (-OH) group at the position of C-8′. The concentrations of flavonoids tested in this study had greater effects on the experimental results, then, a low concentration of quercetin activated the activity of P-gp, whereas a high concentration of quercetin inhibited the Pgp. A similar biphasic effect has been found for kaempferol.

It is concluded that the sensitivities of the MDR- and MRP-mediated drug resistance mechanisms by the inhibitory flavonoids and isoflavonoids might differ because of selective activity based on their chemical structures; this is in good agreement with other studies.

The effects of many kinds of flavonoids on drug accumulation was also studied on the human colon cancer cells with MDR and on drug-sensitive colon cancer cells. It was found that rotenone is an effective inhibitor of the drug efflux, but that flavonoids such as catechin, neohesperidin, naringin, robinin or phloridzin had only small effects on the rhodamine accumulation.

In other experiments, the effects of 16 flavonoids and 5 isoflavones on the drug accumulation were compared in human MDR1 gene-transfected mouse lymphoma cells and MRP-expressing human breast cancer cells. The expression of P-gp 170 and P-gp 190 was confirmed by an immunocytochemical method [14, 16].

Based on the FAR values and the chemical structures of the compounds tested, it was found that there are some good relationships between the resistance modifier actions and the physicochemical parameters of the compounds tested. It could be proposed that the majority of carotenoids might have a special binding which is not yet characterized in the P-gp inhibition, whereas the flavonoids could have multiple targets, but only the ATPase binding site is now thought to contribute in P-gp binding. Moreover, the direct membrane effect cannot be ignored in case of the resistance modifier effects.

The transporters shifted the electrical charges, while the transporters might be carried away through use of their transporter cycle. This shift might originate either from the movement of the charged substrates, or from the movements of the protein moieties carrying charges. Then, the transporter-related currents could be modified after the incorporation of the resistance modifiers into the P-gp, or into the membrane bilayer around the P-gp, in which the P-gp might be embedded. The P-gp or other membrane proteins could turn into a capacitor. After the surface modification has been taken place in an aqueous solution, as a consequence the surface of target(s) might become hydrophilic: sticky against the membrane fragments. The transporter activity could be slowed down by the conformational changes induced by the resistance modulator.

Electrogenic properties could keep the functionally active conformation of ABC transporters within their native or artificially modified environment: for example, the P-gp protein subcompartments might be easily adsorbed at the hydrophilic or hydrophobic target within the surface binding site by forming microcavities, which were electrically isolated from the surrounding molecular compartments within the membrane. The isolation might enable some rapid solution exchanges above the target binding site by the inserted drug molecule.

Naturally, the areas of the current changes increased along with the concentrations of substrate or inhibitor, at the same time reflecting the extents of activity or inhibition.

After the transporter activity-related currents were modified by their charged molecules or semiconductors, the transporter activity itself could be modified by the induced electrogenic changes via the modification of active protein conformation.

After switching from the active conformation that might be concerned in the binding of the substrate of the MDR P-gp to an inactive conformation, the transient charging-current of the capacitor-like P-gp could be neutralized, or the direction of charge flow could be modified in the system.

The MDR efflux pump was inhibited by isoflavonoids such as formononetin, amorphigenin, rotenone and chrysin. The MRP-mediated carboxyfluorescein efflux was reduced by afrormosin, formononetin, amorphigenin, rotenone, chrysin, robinin, kaempferol and epigallocatechin [38].

In the antiproliferative effects of the MDR mouse lymphoma cells, a combination of flavonoids and epirubicin was studied. The interaction of chrysene or amorphigenin with epirubicin was synergistic and the interaction of rotenone with epirubicin was additive. On the MRP-carrying human breast cancer cells, formononetin and kaempferol revealed their good antiproliferative effects with synergistically epirubicin, whereas afrormosin and robinin had only an additive type of interaction.

Acknowledgements The study was supported by Szeged Foundation for Anticancer Research, by Grants from OTKA K 60121 (Hungarian National Research Foundation) and NKFP 1-00012/2005.

References

1. Szent-Györgyi A (1933) Nature 131:225
2. Szent-Györgyi A (1933) Nature 131:24
3. Banga I, Szent-Györgyi A (1934) Biochem J 28:1625
4. Szent-Györgyi A, Foreword MR (1936) Paprika from foodtechnical and dietetical point of view. Leipzig, Barth [III]. Nature, p 1939
5. Szent-Györgyi A (1939) US Patent 2 152 827
6. Molnár J, Szabó D, Pusztai R, Mucsi I, Berek L, Ocsovszki I, Kawata E, Shoyama Y (2000) Anticancer Res 20:861

7. Bollag W (1994) Pure Appl Chem 66:995
8. Nishino H, Tokuda H, Satomi Y, Masuda M, Bu P, Onozuka M, Ymaguchi S, Ichiishi E, Murakoshi M, Kato T, Misawa N, Narisawa T, Takasuka N, Yano M (1999) Pure Appl Chem 71:2273
9. Mayne ST (1999) In: Abstracts of the 12th international carotenoid symposium, Cairns, Australia, 18–23 July 1999
10. Manoharan K, Som S, Chatterjee M, Banerjee MR (1984) Carcinogenesis 5:937
11. Murakoshi M, Nishino H (1992) Cancer Res 52:6583
12. Smaller B, Isenberg I, Baird SL (1961) Nature 191:168
13. Motohasi N, Kurihara T, Wakabayashi H, Yaji M, Mucsi I, Molnár J, Maruyama S, Sakagami H, Nakasima H, Tani S, Shirataki Y, Kawase M (2001) In Vivo 15:437
14. Gyémánt N, Tanaka M, Molnár P, Deli J, Mándoky L, Molnár J (2006) Anticancer Res 26:367
15. Eley DD, Snart RS (1965) Biochim Biophys Acta 102:379
16. Molnár J, Gyémánt N, Tanaka M, Hohmann J, Bergrmann-Leitner E, Molnár P, Deli J, Didiziapetris R, Ferreira MJU (2006) Curr Pharm Design 12:287
17. Cornwell MM, Pastan I, Gottesmann MM (1987) J Biol Chem 262:2166
18. Deli J, Molnár P, Tóth G, Baumeler A, Eugster CH (1991) Helv Chim Acta 74:819
19. Huggins CM, Le Blanc OH (1960) Nature 186:552
20. Motohashi N, Wakabayashi H, Kurihara T, Takada Y, Maruyama S, Sakagami H, Nakashima H, Tani S, Shiratakim Y, Kawase M, Wolfard K, Molnár J (2003) Phytotherapy Res 17:348
21. Deli J, Molnár P, Matus Z, Traber B, Pfander H (2001) Tetrahedron Lett 42:1395
22. Khachik F, Nir Z, Ausich RL (1997) In: Ohigashi H (ed) Proceedings of the 2nd international conference on food factors: chemistry and cancer prevention. Springer, Tokyo, p 204
23. Deli J, Molnár P, Õsz E, Tóth G (2000) Tetrahedron Lett 41:8153
24. Mele A, Mendichi R, Selva A, Molnár P, Tóth G (2002) Carbohydrate Res 337:1129
25. Van Breemen RB, Xu X, Wang Y, Constantinou A, Bowen PE (1999) In: Abstracts of the 12th international carotenoid symposium, Cairns, Australia, 18–23 July 1999
26. Nahum A, Amir H, Danilenko M, Karas M, Giat Y, Levy J, Sharoni Y (1999) In: Abstracts of the 12th international carotenoid symposium, Cairns, Australia, 18–23 July 1999
27. Sharoni Y, Karas M, Amir H, Giat J, Danilenko M, Levy J (1996) In: Abstracts of the 11th International Symposium on Carotenoids, Leiden, The Netherlands, August 18–23 1996
28. Kleinman D, Karas M, Roberts CT Jr, LeRoith D, Phillip M, Segev Y, Levy J, Sharoni Y (1995) Endocrinol 136:2531
29. Nishino H (1999) In: Abstracts of the 12th international carotenoid symposium, Cairns, Australia, 18–23 July 1999
30. Simoni D, Roberti M, Invidiata FP, Rondanin R, Baruchello R, Malagutti C, Mazzali A, Rossi M, Grimaudo S, Capone F, Dusonchet L, Meli M, Raimond MV, Landino M, D'Alessandro N, Tolomeo M, Arindam D, Lu S, Benbrook DM (2001) J Med Chem 2308
31. Lowe GM, Booth LA, Young AJ, Bilton RF (1999) In: Abstracts of the 12th international carotenoid symposium, Cairns, Australia, 18–23 July 1999
32. Bendich A (1989) In: Krinsky NI, Mathews-Roth MM, Taylor RF (eds) Carotenoids: chemisty and biology. Plenum, New York London, p 323
33. Khachik F, Steck A, Pfander H (1977) In: Ohigashi H, Osawa T, Terao J, Watanabe S, Yoshikawa T (ed) Food factors for cancer prevention. Springer, Tokyo, p 542

34. Knekt P, Järvinen R, Teppo L, Aromaa A, Seppänen R (1999) J Natl Cancer Inst 91:182
35. Murakami A, Nakashima M, Koshiba T, Maoka T, Nishino H, Yano M, Sumida T, Kim OK, Koshimizu K, Ohigashi H (2000) Cancer Lett 149:115
36. Maoka T, Mochida K, Kozuka M, Ito Y, Fujiwara Y, Hashimoto K, Enjo F, Ogata M, Nobukuni Y, Tokuda H, Nishino H (2001) Cancer Lett 172:103
37. Diwadkar-Navsariwala V, Novotny JA, Gustin DM, Sosman JA, Stacewicz-Sapuntzakis M, Murray JL, Tiller PA, Bowen PE (2002) In: Abstracts of the 13th international carotenoid symposium, Honolulu, USA, 6–11 January 2002
38. Bobrowska-Hägerstrand M, Wróbel A, Rychlik B, Bartosz G, Söderström T, Shirataki Y, Motohashi N, Molnár J, Michalak K, Hägerstrand H (2001) Blood Cells Mol Dis 27:894
39. Mayne ST (2002) 13th International Carotenoid Symposium January 6–11, Honolulu, USA, abstracts, p 10
40. Kim HS, Christov K, Chen L, Ghosh L, Duncan C, Sharifi R, Bowen P (2002) In: Abstracts of the 13th international carotenoid symposium, Honolulu, USA, 6–11 January 2002
41. Hirsch K, Sharoni Y, Danilenko M, Giat Y, Kirilov E, Nahum A, Levy J (2002) In: Abstracts of the 13th international carotenoid symposium, Honolulu, USA, 6–11 January 2002
42. Ugocsai K, Varga A, Molnár P, Antus S, Molnár J (2005) In Vivo 19:433

Top Heterocycl Chem (2008) 15: 161–171
DOI 10.1007/7081_2007_102

Published online: 18 January 2008

Changes in Polyamine Levels During Cell Death Induced by Heterocycles

Masaki Kobayashi[1] (✉) · Hiroshi Sakagami[1] · Masami Kawase[2] · Noboru Motohashi[3]

[1]Division of Pharmacology, Department of Diagnostic and Therapeutic Sciences, Meikai University School of Dentistry, Sakado, 350-0283 Saitama, Japan
kobamasa@dent.meikai.ac.jp

[2]Faculty of Pharmaceutical Sciences, Matsuyama University, Matsuyama, 790-8578 Ehime, Japan

[3]Meiji Pharmaceutical University, Kiyose, 204-8588 Tokyo, Japan

Abstract Natural polyamines (putrescine, spermidine, spermine) are aliphatic amines containing 2 or more amino groups, and play an important role in regulating cell growth and differentiation. Depletion of polyamine in cells has been known to inhibit cell proliferation or induce cell death. This review summarizes changes in polyamine levels during cell death induced by the selective properties of various heterocycles.

Keywords Apoptosis · Cell death · Heterocycles · Polyamine

Abbreviations

ODC	Ornithine decarboxylase
PAO	Polyamine oxidase
SAMDC	*S*-adenosylmethionine decarboxylase
Spd-Syn	Spermidine synthase
Spm-Syn	Spermine synthase
SSAT	Spermidine/spermine N1-acetyltransferase

1 Introduction

The polyamines (spermine, spermidine) and diamine (putrescine) are present in all mammalian cells [1–7]. Putrescine is synthesized from ornithine via the reaction catalyzed by a key regulatory enzyme, ornithine decarboxylase (ODC). Spermidine and spermine are synthesized from putrescine by the action of *S*-adenosyl methionine decarboxylase (SAMDC) as well as spermidine and spermine synthases [1, 8]. This synthetic pathway is coupled to the degradation pathway, and the first step is the acetylation of spermidine and spermine by spermidine/spermine acetyltransferase (SSAT) [9]. The acetylated spermine and spermidine are then converted to spermidine and putrescine, respectively, by polyamine oxidases (PAO) [10]. Despite the fact that the total intracellular concentration of the polyamines is in the millimolar range, their functions in the cellular physiology are not still well understood. Polyamines could play important roles in various cellular processes such as the regulation of cell growth, cell survival and ion-channel transport, the maintenance of chromatin and membrane integrity, the association with nucleic acids, the scavenging of radicals and the synthesis of eukaryotic translation initiation factor 5A (IF5A) [11–17]. This evidence suggests that the alteration of the cell functions by bioactive components might in turn change the intracellular polyamine concentration. The bioactive heterocycles with nitrogen or oxygen atoms were investigated for their potential to change the intracellular polyamine levels in relation to their cell death-induction activity.

2 *N*-Heterocycles

2.1 Mitomycin C (MMC)

The mitomycins are a family of aziridine-containing antibiotics isolated from *Streptomyces lavendulae*. One of these antibiotics, mitomycin C (MMC), is an antitumor antibiotic frequently used for the treatment of breast, lung, stomach, intestinal, testicular, cholioepithelial, seminal and oral carcinoma [18–20]. When human oral squamous cell carcinoma cell lines (HSC-2, HSC-4) were treated with MMC, the viable cell number was dose-dependently reduced (CC_{50} of MMC against HSC-2, HSC-3 and HSC-4 cells: 3.5, 9.7 and 18 μM, respectively, determined 24 hours after treatment). The rapid decline of polyamines (measured at 3 hours after MMC treatment) was observed prior to the expression of early apoptosis markers such as the production of annexin-positive cells and caspase activation (Table 1) [21]. The interactions

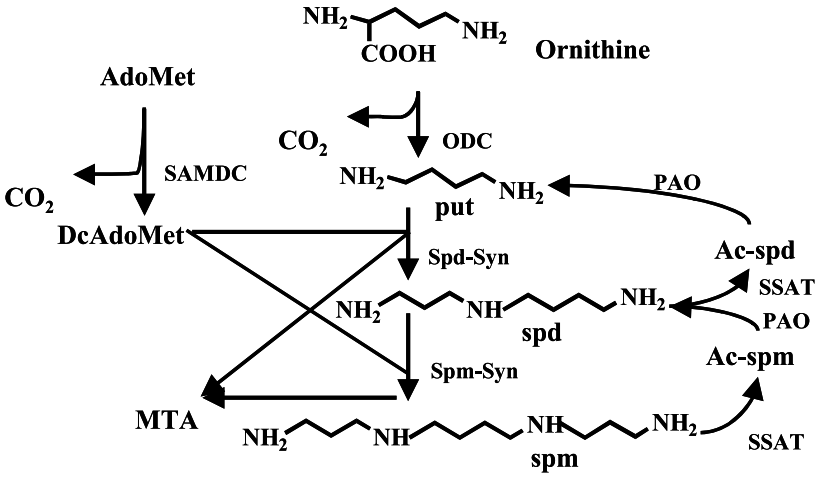

Fig. 1 Metabolic pathway of polyamines

Table 1 Changes in polyamine levels during cell death induced by 3 hours of MMC treatment

Mitomycin C	Tumor	μM	Putrescine	Spermidine	Spermine
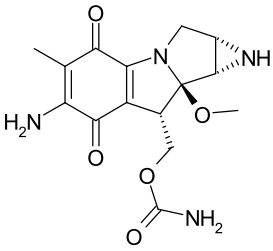	HSC-2	0	0.22 ± 0.09	1.2 ± 0.12	1.31 ± 0.33
		300	0.04 ± 0.03	0.62 ± 0.05	1.08 ± 0.09
	HSC-4	0	0.56 ± 0.09	1.02 ± 0.47	1.34 ± 0.59
		300	0.34 ± 0.13	0.91 ± 0.11	1.12 ± 0.12

of polyamines with many bio-components are known. Generally, polyamines are ionically bound to various anionic high molecular weight cellular components such as DNA, RNA, proteins and phospholipids. This fact suggests some connections between the reduced polyamine levels and the on-set of cell death signaling. However, the causal correlation and effect relationships are unclear.

2.2 5-Fluorouracil

5-Fluorouracil (5-FU), a pyrimidine analog, has been clinically used as a popular antitumor agent for the treatment of various malignant tumors such as head and neck [22], gastric [23], esophageal [24], ovarian [25] and lung can-

Table 2 Changes in polyamine levels during cell death induced by 24 hours of 5-FU treatment

5-FU	Tumor	μM	Polyamine concentration (μmol/10^5 cells) Putrescine	Spermidine	Spermine
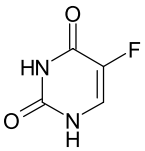	HSC-2	0	0.67	2.16	1.91
		30	0.25	0.55	0.20
	HSC-3	0	1.12	2.16	2.88
		25	0.11	1.50	1.53
	HSC-4	0	0.76	1.12	1.49
		60	0.32	0.74	0.32

cer [26]. 5-FU has usually been used in a combined treatment with cisplatin. 5-FU requires an enzymatic conversion to nucleotide (ribosylation and phosphorylation) to exert its cytotoxic activity. The 5-fluoro-2′-deoxyuridine-5′-monophosphate (F-dUMP) of the 5-FU metabolite is a potent inhibitor of thymidylate sythesis. The incorporation of 5-fluorouridine-5′-triphosphate (FUTP) into RNA caused toxicity as the result of major effects on both the enzymatic processing and functions of RNA [27]. In 5-FU-treated cells, both 5-fluoro-2′-deoxyuridine-5′-triphosphate (FdUTP) and dUTP are incorporated into DNA, and finally the DNA strand breaks [28].

Cells treated with 5-FU undergo cell cycle arrest or apoptosis by inhibition of DNA synthesis. When human oral squamous cell carcinomas (HSC-2, HSC-3, HSC-4) were treated with 5-FU, viable cell numbers declined dose-dependently (CC_{50} determined after 24 hours treatment: 3.4, 6.9 and 1.7 μM, respectively). The intracellular putrescine concentration slightly declined (Table 2) [29]. The combination treatment of 5-FU with N(1),N(11)-diethylnorspermine (DENSPM), which is an inducer of spermidine/spermine N(1)-acetyltransferase (SSAT) that depletes polyamine, has been reported to augment the cytotoxic activity of 5-FU, suggesting possible clinical application [30].

2.3 Codeinone

Codeinone is an oxidation product of codeine, and has been used to relieve pain as a narcotic analgesic [31]. In both humans and animals, the metabolites of codeine are codeine 6-glucuronide, morphine and norcodeine [32]. However, in the presence of nicotinamide adenine dinucleotide (NAD), the 9000 xg supernatant of guinea pig liver homogenate can transform codeine into codeinone [33]. Codeinone has been reported to show two interesting biological activities such as analgesic action and weak apoptosis-inducing activity [34, 35]. In conditions in which codeinone reduced the viable cell num-

Table 3 Changes in polyamine levels during cell death induced by 3 hours of codeinone treatment

Codeinone	Tumor	μM	Polyamine concentration (μmol/g protein) Putrescine	Spermidine	Spermine
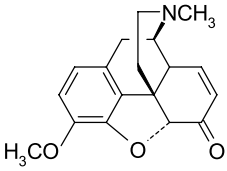	HSC-3	0	0.28 ± 0.04	1.59 ± 0.10	1.44 ± 0.13
		80	0.27 ± 0.03	0.50 ± 0.06	0.68 ± 0.10
	HSC-4	0	0.58 ± 0.06	1.73 ± 0.09	1.75 ± 0.24
		80	0.70 ± 0.05	1.27 ± 0.10	1.96 ± 0.18

ber of human oral squamous cell carcinoma cell lines (HSC-3) by approximately 50%, the intracellular polyamine level was slightly reduced. In HSC-3 cells, spermidine and spermine were considerably reduced by codeinone (Table 3). This could be caused by the weak apoptosis-inducing activity of codeinone.

2.4 Phenoxazine Derivatives

Phenoxazine derivatives have demonstrated diverse biological activities such as MDR modulation, inhibition of Akt signaling, inhibition of human plasma cholinesterase, and photo-sensitized chemotherapeutic activity (see Chapt. 8). Among twenty-four phenoxazine derivatives, **WM7** (CC_{50} against HSC-3 and HSC-4 cells: 38 and 28 μM, respectively) and **WM8** (CC_{50} against HSC-3 and HSC-4 cells: 31 and 17 μM, respectively) showed the highest tumor-specific cytotoxic activity [36]. However, the two phenoxazines apparently did not change polyamine levels, even at cytotoxic concentrations (Table 4). Additionally, the **WM7** and **WM8** didn't induce of apoptotic cell death, and didn't reduced the polyamine levels [36], suggesting the occurrence of other types of cell death.

3 *O*-Heterocycles (flavonoids)

3.1 (–)-Epigallocatechin Gallate (EGCG)

Similar to the antioxidant properties of other low molecular weight polyphenols, (–)-epigallocatechin gallate, a main component of green teas, has been known to be a potent antioxidant and reduce free radical-induced lipid perox-

Table 4 Changes in polyamine levels during cell death induced by 3 hours of phenoxazine derivatives (**WM7**, **WM8**)

	Tumor	μM	Polyamine concentration (μmol/g protein) Putrescine	Spermidine	Spermine
WM7 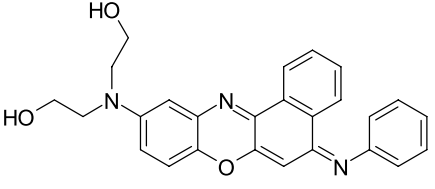	HSC-3	0	0.28 ± 0.04	1.59 ± 0.10	1.44 ± 0.13
		20	0.25 ± 0.06	1.59 ± 0.10	1.47 ± 0.08
	HSC-4	0	0.58 ± 0.06	1.73 ± 0.09	1.75 ± 0.24
		20	0.55 ± 0.03	1.68 ± 0.17	1.76 ± 0.12
WM8 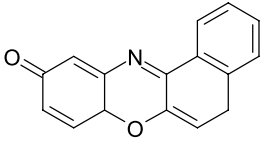	HSC-3	0	0.28 ± 0.04	1.59 ± 0.10	1.44 ± 0.13
		20	0.26 ± 0.08	1.75 ± 0.07	1.55 ± 0.13
	HSC-4	0	0.58 ± 0.06	1.73 ± 0.09	1.75 ± 0.24
		20	0.75 ± 0.03	1.89 ± 0.11	1.99 ± 0.05

Table 5 Changes in polyamine levels during cell death induced by 3 hours of EGCG treatment

EGCG	Tumor	μM	Polyamine concentration (% of control) Putrescine	Spermidine	Spermine
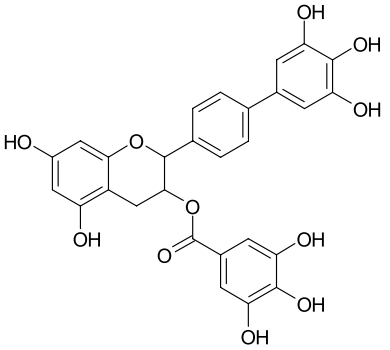	HL-60	0	100	100	100
		500	8	40	60

idation [37–39]. It has recently been shown that EGCG inhibited hippocampal neuronal damage in the gerbil model of global ischemia [40]. On the other hand, many investigators have reported the apoptosis-inducing activity of EGCG in various human tumor cell lines [41–43]. During the apoptosis induced by EGCG in HL-60 cells, both the viable cell number (approx 50% of control) and intracellular concentrations of some substances, especially putrescin, declined (Table 5) [44].

3.2 Naringenin

Naringenin is present in some fresh grapefruit, and known as a CYP3A4 inhibitor [45]. Naringenin lowered plasma cholesterol in vivo [46], and displayed anti-atherogenic effects via the reduction of hepatic acyl-CoA cholesterol acyltransferase (ACAT) [47]. Naringenin exhibits neuroprotection via its antioxidant properties [48]. Moreover, naringenin is known to have antiproliferative properties. The significant inhibition of cell proliferation in HT-29 colon cancer has been reported [49]. Naringenin inhibited the proliferation of the transfected human hepatoma Hep G2 and colon adenocarcinoma DLD-1 cell lines via estrogen receptor-dependent mechanisms [50], suggesting a new potential chemopreventive action against cancer growth. It has recently been reported that naringenin reduced the viable cell number (approx 50% of control) and induced the down-regulation of polyamine levels (spermidine, spermine) in B16-F10 melanoma cells [51] (Table 6). The administration of naringenin to B16-F10 bearing C57BL/N mice demonstrated that they could

Table 6 Changes in polyamine levels during cell death induced by 24 hours of naringenin treatment

Naringenin	Tumor	μM	Polyamine concentration (μmol/g protein) Putrescine	Spermidine	Spermine
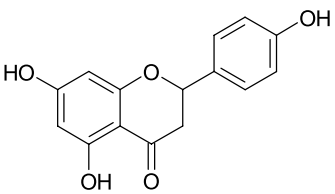	B16-F10	0	0.06	0.91	0.76
		10	0.05	0.40	0.10

survive significantly longer than the control mice (50% of the naringenin-treated mice died 38±3.1 days after tumor cell injection, while 50% of control mice died 18±1.5 days thereafter) [51]. These data suggest the chemopreventive effects of naringenin.

3.3 Procyanidin Oligomers

A mixture of procyanidin oligomers has been produced from apple juice extract. The procyanidin oligomers induced an apoptosis in human colon cancer-derived metastatic cells (SW620) [52]. Procyanidin oligomers reduced viable cell numbers (approx 80% of control) and intracellular polyamine levels (Table 7), possibly due to their suppressive effect on ornithine decarboxylase and *S*-adenosyl-L-methioninedecarboxylase activities and the induction of spermidine/spermine N1-acethyltransferase. Procyanidin oligomers were non-toxic, and are therefore a highly promising new drug, particularly in colon cancer chemoprevention.

4 Conclusion

This review demonstrates some relationships between the decline of polyamines and the decline of cell proliferation or induction of cell death triggered by *N*- and *O*-heterocycles. Many heterocycles including flavonoids reduced the polyamine levels in various cell culture systems. Studies of polyamine synthase inhibitors indicate that the down-regulation of polyamine might trigger cell growth, or induce cytotoxicity. Hydrogen peroxide generated during polyamine catabolism might induce apoptotic cell death. This

Table 7 Changes in polyamine levels during cell death induced by 24 hours of procyanidin oligomers treatment

Apple procyanidin	Tumor	μg/mL	Polyamine concentration (μmol/g protein) Putrescine	Spermidine	Spermine
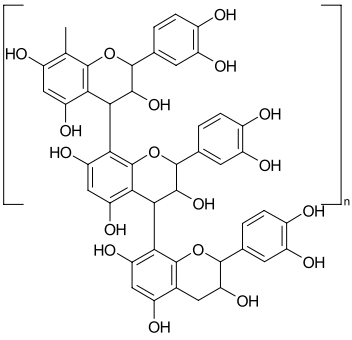	SW620	0	0.33	0.80	0.66
		50	0.41	0.71	0.47

Table 8 Effect of inducers on the type of cell death and the intracellular polyamine levels

Inducers	Target cells	Type of cell death	Changes in intracellular level of Putrescine	Spermidine	Spermine	Incubation time (hours)	Refs.
Sodium ascorbate	HL-60	Apoptosis	↓↓↓	–	–	2	[53]
Benzylidene ascorbate	HL-60	Apoptosis	↓↓↓	–	–	2	[53]
EGCG	HL-60	Apoptosis	↓↓↓	↓	↓	0.2	[44]
Gallic acid	HL-60	Apoptosis	↓↓	↓	–	0.6	[44]
Etoposide	HL-60	Apoptosis	↓↓	↓	↓	3	[44]
UV	HL-60	Apoptosis	↓↓	↓	↓	3	[44]
Doxorubicin	HL-60	Non-apoptosis	–	–	–	3	[44]
Cisplatin + 5-FU	HSC-2	Apoptosis	↓	–	–	72	[29]
Trichloro-acetylazulene	HSC-4	Non-apoptosis	–	–	–	4	[54]
Water pressure	HGF	Non-apoptosis	–	–	–	3	[55]

The extent of decrease: ↓↓↓ potently; ↓↓ modestly; ↓ weakly

suggests that polyamine level is a useful marker for detecting cytotoxicity induction.

We have reported the changes of polyamine levels during cell death induction by sodium ascorbate, sodium 5,6-benzylidene-L-ascorbate [53], EGCG, gallic acid, etoposide, ultraviolet irradiation, doxorubicin [44], cisplatin + 5-FU [29], chloroacetylazulene [54] and water pressure [55] in various cell systems. It seems likely that the decrease of the putrescine concentration might be the most prominent phenomenon during the apoptotic cell death. However, more rigorous experiments with many anticancer drugs might be necessary to generalize this finding.

References

1. Williams-Ashman HG, Canellakis ZN (1979) Perspect Biol Med 22:421
2. McCann PP, Pegg AE, Sjoerdama A (1987) Biological Significance and Basis for New Therapies, pp 1–371
3. Pegg AE, McCann PP (1982) Am J Physiol 243:C212
4. Janne J, Holtta E, Kallio A, Kapyaho K (1983) Spec Top Endocrinol Metab 5:227
5. Tabor CW, Tabor H (1984) Annu Rev Biochem 53:749
6. Pegg AE (1986) Biochem J 234:249
7. Porter CW, Sufrin J (1986) Anticancer Res 6:525
8. Thomas T, Thomas TJ (2001) J Cell Mol Life Sci 58:244
9. Casero RA Jr, Pegg AE (1993) Faseb 7:653
10. Morgan DM (1999) Mol Biotechnol 11:229
11. Feuerstein BG, Williams LD, Basu HS, Marton LJ (1991) J Cell Biochem 46:37
12. Frydman B, Westler WM, Samejima K (1996) J Org Chem 61:2588
13. Ha HC, Sirisoma NS, Kuppusamy P, Zweier JL, Woster PM, Casero RA Jr (1998) Proc Natl Acad Sci USA 95:11140
14. Hobbs CA, Gilmour SK (2006) In: polyamine cell signaling: Physiology, Phamacology, and Cancer Research. Humana Press, Totowa, p 75
15. Kurata HT, Marton LJ, Nichols CG (2006) J Gen Physiol 127:467
16. Park MH (2006) J Biochem (Tokyo) 139:161
17. Park JH, Aravind L, Wolff E C, Kaevel J, Kim YS, Park MH (2006) Proc Natl Acad Sci USA 103:51
18. Kanamori H, Shima T, Morita C, Hata T (1957) J Antibiot (Tokyo) 10:120
19. Umezawa H (1967) Gan No Rinsho 13:735 (in Japanese)
20. Okamoto H, Morimoto H, Haneji T (2001) Oral Oncol 37:379
21. Sasaki M, Okamura M, Ideo A, Shimada J, Suzuki F, Ishihara M, Kikuchi H, Kanda Y, Kunii S, Sakagami H (2006) Anticancer Res 26:3373
22. Andreadis C, Vahtsevanos K, Sidiras T, Thomaidis I, Antoniadis K, Mouratidou D (2003) Oral Oncol 39:380
23. Kin R, Togo T (2002) Hematol Oncol 44:154
24. Lee J, Lee KE, Im YH, Kang WK, Park K, Kim K, Shim YM (2005) Ann Thorac Surg 80:1170
25. Braly PS, Berek JS, Blessing JA, Homesley HD, Averette H (1995) Gynecol Oncol 56:164
26. Itoh Y, Fuwa N, Matsumoto A, Asano A, Morita K (2002) Am J Clin Oncol 25:230

27. Danenberg PV, Shea LCC, Danenberg K (1990) Cancer Res 50:1757
28. Mauro DJ, DeRiel JK, Tallarida RJ, Sirover MA (1993) Mol Pharmacol 43:854
29. Okamura M, Kobayashi M, Suzuki F, Shimada J, Sakagami H (2007) Anticancer Res 27:3331
30. Choi W, Gerner EW, Ramdae L, Dupart J, Proctor L, Huang P, Zhang W, Hamilton SR (2005) J Biol Chem 280:3295
31. Morgan GE, Mikhail MS, Murray MJ, Larson CP Jr (1983) Clinical Anesthesiology LANGE: Medical Students Science, p 342
32. Willman DG, Hatch DJ, Howard RF (2001) Br J Anaesth 86:413
33. Nagamatsu K, Terao T, Toki S (1985) Biochem Pharmacol 34:3143
34. Takeuchi R, Hoshijima H, Onuki N, Nagasaka H, Chowdhury SA, Kawase M, Sakagami H (2005) Anticancer Res 25:4037
35. Kawase M, Sakagami H, Furuya K, Kikuchi H, Nishikawa H, Motohashi N, Morimoto Y, Varga A, Molnar J (2002) Anticancer Res 22:211
36. Suzuki F, Hashimoto K, Ishihara M, Westman G, Samuelsson K, Kawase M, Motohashi N, Sakagami H (2007) Anticancer Res 27:4233
37. Valcic S, Muders A, Jacobsen NE, Liebler DC, Timmermann BN (1999) Chem Res Toxicol 12:382
38. Nakagawa K, Ninomiya M, Okubo T, Aoi N, Juneja LR, Kim M, Yamanaka K, Miyazawa T (1999) J Agric Food Chem 47:3967
39. Ishino A, Mita S, Watanabe S, Sakagami H (1999) Anticancer Res 19:4343
40. Lee S, Suh S, Kim S (2000) Neurosci Lett 287:191
41. Hibasami H, Achiwa Y, Fujikawa T, Komiya T (1996) Anticancer Res 16:1943
42. Ahmad N, Feyes DK, Nieminen AL, Agarwal R, Mukhtar H (1997) J Natl Cancer Inst 89:1881
43. Paschka AG, Butler R, Young CY (1998) Cancer Lett 130:1
44. Nakamura C, Yasumoto E, Nakano K, Nakayachi T, Hashimoto K, Kusama K, Fukuda M, Sakashita H, Shirahata A, Sakagami H (2003) Anticancer Res 23:4797
45. Ho PC, Saville DJ, Coville PF, Wanwimolruk S (2000) Pharm Acta Helv 74:379
46. Wilcox LJ, Borradaile NM, de Dreu LE, Huff MW (2001) J Lipid Res 42:725
47. Lee CH, Jeong TS, Choi YK, Hyun BH, Oh GT, Kim EH, Kim JR, Han JI, Bok SH (2001) Biochem Biophys Res Commun 284:681
48. Zbarsky V, Datla KP, Parkar S, Rai DK, Aruoma OI, Dexter DT (2005) Free Radic Res 39:1119
49. Frydoonfar HR, McGrath DR, Spigelman AD (2003) Colorectal Dis 5:149
50. Totta P, Acconcia F, Leone S, Cardillo I, Marino M (2004) IUBMB Life 56:491
51. Lentini A, Forni C, Provenzano B, Beninati S (2007) Amino Acids 32:95
52. Gosse F, Roussi S, Guyot S, Schoenfelder A, Mann A, Bergerat JP, Seiler N, Raul F (2006) Int J Oncol 29:423
53. Sakagami H, Fujiwara E, Yokote Y, Akahane K, Asano K, Kochi M, Hara E, Shirahata A (2000) Anticancer Res 20:265
54. Sekine T, Takahashi J, Nishishiro M, Arai A, Wakabayashi H, Kurihara T, Kobayashi M, Hashimoto K, Kikuchi H, Katayama T, Kanda Y, Kunii S, Motohashi N, Sakagami H (2007) Anticancer Res 27:133
55. Chien C-H, Otsuki S, Chowdhury SA, Kobayashi M, Takahashi K, Kanda Y, Kunii S, Sakagami H, Kanegae H (2006) In Vivo 20:849

Top Heterocycl Chem (2008) 15: 173–199
DOI 10.1007/7081_2007_103

Published online: 17 January 2007

Tumor Specificity and the Type of Cell Death Induced by Heterocycles

Hiroshi Sakagami[1] (✉) · Masaki Kobayashi[1] · Mariko Ishihara[2] · Hirotaka Kikuchi[3] · Yukio Nakamura[3] · Masami Kawase[4] · Noboru Motohashi[5]

[1]Division of Pharmacology, Department of Diagnostic and Therapeutic Sciences, Meikai University School of Dentistry, Sakado, 350-0283 Saitama, Japan
sakagami@dent.meikai.ac.jp

[2]Division of Basic Chemistry, Meikai University School of Dentistry, Sakado, 350-0283 Saitama, Japan

[3]Division of Endodontics, Meikai University School of Dentistry, Sakado, 350-0283 Saitama, Japan

[4]Faculty of Pharmaceutical Sciences, Matsuyama University, Matsuyama, 790-8578 Ehime, Japan

[5]Meiji Pharmaceutical University, Kiyose, 204-8588 Tokyo, Japan

Abstract Considering the presence of multiple types of cell death induced by chemicals, it is important to determine a definitive strategy for the exploration of new highly tumor-selective compounds. The screening of highly selective compounds should be performed before the identification of the type of cell death (either apoptosis, autophagy, or necrosis) and the cell death induction mechanism. The tumor specificities of heterocyclic compounds and the type of cell death induced by them are summarized.

Keywords Heterocyclic compounds · Tumor specificity · Type of cell death

1 Introduction

1.1 Factors That Affect the Type of Cell Death Induced by Chemicals

There are at least three types of cell death: apoptosis (type I programmed cell death), autophagy (type II programmed cell death), and necrosis. Apoptosis is involved in destroying many unnecessary or harmful cells and tissues during development, and is characterized by condensation of the cytoplasm and chromatin, DNA fragmentation, and cell fragmentation into apoptotic bodies, which are then removed and degraded by phagocytosis [1]. Autophagy is a proteolytic system ubiquitously distributed in eukaryotic cells that transports and degrades cellular constituents (cytoplasmic proteins and organella) in its own endogenous lysosomal machinery. Autophagy is morphologically characterized by the accumulation of autophagic vesicles (autophagosomes and autophagolysosomes) and is often observed when massive cell elimination is demanded or when phagocytes do not have easy access to the dying cells [2]. It is unclear whether autophagy directly executes cell death or exhibits the secondary effect of apoptosis [3]. Necrosis is induced by the extracellular environment and is characterized by swelling of the cells, membrane disruption, leakage of cellular components, and inflammation.

Among these three types of cell death, apoptosis-inducing activity has been considered by many researchers to be an essential criterion for antitumor agents, since many chemotherapeutic agents have induced apoptosis-associated characteristics. On the other hand, human glioblastoma cell lines (M059J, M059K, U373-MG, T98G) have been recently reported to be committed to autophagy upon exposure to radiation [4, 5], arsenic trioxide [6, 7], ceramide [8], or temozolomide (a new alkylating agent) [9]. Autophagy is characterized by autophagosome formation, the accumulation of Agp8p/Aut7p and LC3 (ATG 8 homolog) in autophagosome, and the susceptibility to 3-methyladenine, an autophagy inhibitor. We have also reported previously that vitamin C, hydrogen peroxide, etoposide, TNF, hyperthermia (43 °C, 30–60 min) and UV irradiation (6 J/m^2) induced internucleosomal DNA fragmentation in human myelogenous leukemic cell lines (HL-60, ML-1, U-937, THP-1) (group I), but not in human erythroleukemia (K-562), T-cell leukemia (MOLT4) [10], glioblastoma (T98, U87MG) or human glioma cell lines (KG-1-C) (group II) [11]. This may partially result from the higher sensitivity of chromatin DNA of group I cells to endonuclease attack in the isolated nucleus system than that of group II cells [12]. These data suggest that the commitment of the cells toward apoptotic or non-apoptotic cell death [13] (such as autophagy) depends on the type of target cells, which possibly have different drug sensitivities.

The other factor that may determine the type of cell death is the chemical structure of inducing agents [14]. We have recently found that α,β-unsaturated ketones such as 4,4-dimethyl-2-cyclopenten-1-one, α-methylene-γ-butyrolactone, 5,6-dihydro-2*H*-pyran-2-one [15], codeinone [16], and morphinone [17]; and α-hydroxylketones such as 3,3,3-trifluoro-2-hydroxy-1-phenyl-1-propanone induced caspase-independent cell death [18], induced vacuolization or autophagosome formation engulfing organelles, but without induction of apoptosis markers.

1.2 In Vitro Assay System to Monitor Tumor-Specific Cytotoxicity

The presence of multiple types of cell death suggests the importance of determining a definitive strategy for the exploration of new highly selective compounds for tumor cells. The screening of highly selective compounds should be performed before the identification of the type of cell death (either apoptosis, necrosis, or autophagy) and the elucidation of the cell death induction mechanism. However, there are few investigations on the relative toxicity of antitumor agents to both normal and malignant cells. This is true for polyphenols [19, 20], despite the vast literature on their antioxidant and apoptosis-inducing activities.

Considering this background, we have initiated the investigation of the selective toxicity and type of cell death induced in oral squamous cell carcinoma (OSCC) by a total of 500 natural and synthetic compounds. Flavonoids, coumarins, tannins, ketones, and other synthetic compounds showed low to moderate tumor-specific cytotoxicity against human OSCC cell lines as compared with normal human oral cells (gingival fibroblast, pulp cell, periodontal ligament fibroblast), whereas anthracyclines, nocobactins, and cyclic α,β-unsaturated compounds showed much higher tumor-specific cytotoxicity. No strict relationship was found between the tumor-specific cytotoxicity and apoptosis induction. There was a considerable variation in drug sensitivity among five OSCC cell lines. OSCC cell lines were generally resistant to apoptosis induction. The cytotoxic activity of antitumor agents is affected by various factors related to the compounds themselves, the cells, and their environments. Systematization of the relationship between these factors and tumor specificity may contribute in the quest for more active compounds [21].

This article is a summary of our recent extensive study of tumor specificity (TS) and the type of cell death induced by *N*-containing heterocycles such as 4-trifluoromethylimidazole [22] and phenoxazine derivatives [23], by *O*-containing heterocycles such as 3-formylchromone [24] and coumarin derivatives [25, 26], and by other compounds such as vitamin K_2 and prenylalcohols [27].

Normal cells used in this study are human gingival fibroblast (HGF), pulp cell (HPC), and periodontal ligament fibroblast (HPLF). Tumor cell lines we

have used are human squamous cell carcinoma (HSC-2, HSC-3, HSC-4, NA, Ca9-22), glioblastoma (T98G, U87MG), hepatocellular carcinoma (HepG2), and lung carcinoma (A-539). The tumor-specific cytotoxicity index (TS) of each test compound was determined by the ratio of the mean 50% cytotoxic concentration (CC_{50}) against normal human oral cells to that against human oral tumor cell lines. The apoptosis induction was monitored via the internucleosomal DNA fragmentation and the activation of caspase-3, caspase-8, and caspase-9. Autophagy was monitored by determining autophagosome formation observed under transmission electron microscopy and fluorescent microscopy after staining with acridine orange.

2
N-Containing Heterocycles

2.1
4-Trifluoromethylimidazoles

Among 14 4-trifluoromethylimidazole derivatives (Fig. 1), 4-trifluoromethyl-1,2-diphenylimidazole (**IM5**) showed the highest cytotoxicity, followed by 5-[1-ethoxy-2,2,2-trifluoro-1-(trifluoromethyl)ethyl]-1-methyl-2-phenyl-1*H*-imidazole (**IM12**) and 1-benzyl-4-trifluoromethyl-2-phenylimidazole (**IM7**), whereas other compounds showed much lower cytotoxicity (Table 1). The

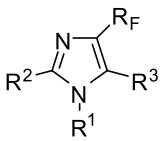

IM1-14

	R^1	R^2	R^3	R_F
IM1	CH_3	C_6H_5	H	CF_3
IM2	CH_3	$C_6H_5CH_2$	H	CF_3
IM3	CH_3	tert-Butyl	H	CF_3
IM4	C_6H_5	CH_3	H	CF_3
IM5	C_6H_5	C_6H_5	H	CF_3
IM6	$C_6H_5CH_2$	CH_3	H	CF_3
IM7	$C_6H_5CH_2$	C_6H_5	H	CF_3
IM8	$C_6H_5CH_2$	OH	$C_6H_5CH_2$	CF_3
IM9	CH_3	C_6H_5	H	C_2F_5
IM10	CH_3	C_6H_5	H	C_3F_7
IM11	CH_3	C_6H_5	CHO	H
IM12	CH_3	C_6H_5	$C(OEt)(CF_3)_2$	H
IM13	C_6H_5	H	H	H
IM14	H	C_6H_5	H	CH_3

Fig. 1 Structure of 4-trifluoromethylimidazoles

Table 1 Cytotoxic activity of 4-trifluoromethylimidazoles (**IM1–14**) against human tumor and normal cells

Compound	50% Cytotoxic concentration (CC_{50}, μM)							TS
	Tumor cell lines				Normal cells			
	HSC-2	HSC-3	HSC-4	HL-60	HGF	HPC	HPLF	
IM1	>395 ± 9.2	>400	>381 ± 32	255 ± 42	>400	>371 ± 30	>310 ± 148	>< 1.0 ± 0.1
IM2	>389 ± 12	>400	>383 ± 30	149 ± 54	368 ± 19	344 ± 21	319 ± 86	< 1.0 ± 0.1
IM3	>400	>400	>400	>354 ± 79	>400	>400	>370 ± 51	>< 1.0 ± 0.0
IM4	325 ± 16	294 ± 5.5	>341 ± 61	31 ± 18	323 ± 3.1	303 ± 22	310 ± 24	< 1.3 ± 0.1
IM5	70 ± 9.7	38 ± 4.4	43 ± 6.5	3.0 ± 2.9	147 ± 30	134 ± 6.1	>221 ± 155	4.3 ± 1.2
IM6	>354 ± 41	>399 ± 2.3	>380 ± 35	31 ± 27	>389 ± 19	328 ± 31	299 ± 145	>< 1.2 ± 0.2
IM7	115 ± 38	86 ± 12	115 ± 25	8.1 ± 6.6	196 ± 60	15331	>251 ± 130	>2.5 ± 0.9
IM8	251 ± 37	262 ± 10	276 ± 169	145 ± 63	285 ± 15	256 ± 20	302 ± 38	1.4 ± 0.3
IM9	325 ± 66	320 ± 30	>310 ± 156	102 ± 36	>393 ± 13	357 ± 37	>350 ± 87	>< 1.5 ± 0.3
IM10	241 ± 20	215 ± 30	>236 ± 150	27 ± 19	338 ± 25	293 ± 19	331 ± 29	1.9 ± 0.4
IM11	>400	>400	>400	122 ± 37	>400	>400	>305 ± 165	>< 1.2 ± 0.1
IM12	77 ± 5	83 ± 13	67 ± 34	11 ± 5	182 ± 48	118 ± 13	>233 ± 145	>3.0 ± 1.9
IM13	>371 ± 41	230 ± 90	>281 ± 119	29 ± 16	361 ± 22	305 ± 26	374 ± 44	< 1.6 ± 0.2
IM14	>400	>400	>400	>367 ± 58	>400	>400	>400	>< 1.0 ± 0.1
Melphalan	10 ± 5.7	31 ± 5.5	40 ± 3.2	< 2.6 ± 0.9	176 ± 23	>322 ± 135	>236 ± 46	>12 ± 1.7
5-FU	< 118 ± 151	< 57 ± 29	< 156 ± 144	< 24 ± 7.6	>4000	>4000	>4000	>49 ± 16

Each value represents the mean ± S.D. from three independent experiments

cytotoxicity of 1,2-diphenylimidazole (**IM5**) was much more than that of 1-methyl-2-phenylimidazole (**IM1**) and 2-methyl-1-phenylimidazole (**IM4**), suggesting that the presence of two aromatic rings at both N-1 and C-2 positions was beneficial. 1-Benzyl-2-phenylimidazole (**IM7**) also showed potent cytotoxicity against tumor cells. The 1,2-diphenylimidzole framework of **IM5** might serve as the basis for development of a new series of more tumor-specific cytotoxic compounds. Among these three compounds, **IM5** showed the highest tumor specificity (*TS* = 4.3), followed by **IM12** (*TS* > 3.0) and then **IM7** (>2.5).

A slight difference in drug sensitivity was found among cell lines. The sensitivity to **IM5** was in the order: HL-60 (CC_{50} = 3 μM) (most sensitive) > HSC-3 (38 μM) > HSC-4 (43 μM) > HSC-2 (70 μM) > HPC (134 μM) > HGF (147 μM) > HPLF (>221 μM) (most resistant) (Table 1). The sensitivity to **IM12** was in the order: HL-60 (CC_{50} = 11 μM) (most sensitive) > HSC-4 (67 μM) > HSC-2 (77 μM) > HSC-3 (83 μM) > HPC (118 μM) > HGF (182 μM) > HPLF (>233 μM) (most resistant). The sensitivity to **IM7** was in the order: HL-60 (8 μM) (most sensitive) > HSC-3 (86 μM) > HSC-2, HSC-4 (115 μM) > HPC (153 μM) > HGF (196 μM) > HPLF (>251 μM) (most resistant) (Table 1). The sensitivities of HSC-2 and HSC-4 cells against **IM5**, **IM7** and **IM12** were found to be comparable with each other.

Treatment of HL-60 cells for 6 h with 172 μM (four times higher concentration of CC_{50}) of **IM5** induced internucleosomal DNA fragmentation in HL-60 cells (Fig. 2a). When the treatment time was prolonged to 24 h, even lower concentrations (43 μM) of **IM5** induced DNA fragmentation (Fig. 2b). **IM5** (43–172 μM) induced DNA fragmentation in HSC-2 cells only after 24 h, without a clear-cut laddering pattern of DNA fragmentation (Fig. 2b). On the other hand, **IM5** did not induce any trace of DNA fragmentation in HSC-4 cells. Transmission electron microscope analysis demonstrated various profiles of lysosomes in the cells cultured with **IM5** for 6 and 24 h (Fig. 3). The number of lysosomes increased over 18 h (from 6 to 24 h) of culture period in the cells incubated with 43 and 86 μM of **IM5**. Lysosomes observed in the cells cultured with **IM5** contained small vesicular and/or lamellar structures, suggesting the digestion of organelles (Fig. 3j,k). In these cells, enlarged mitochondria accompanying electron-lucent matrices were also found with the lysosomes. Moreover, rod-shaped lysosomes were observed surrounding small vesicles and/or lucent materials (Fig. 3k, arrowheads). Therefore, these lysosomes could be identified as the secondary lysosomes digesting the broken organelles. It should be noted that disappearance of cell surface microvilli, one of the morphological marker of apoptosis, was not observed in **IM5**-treated cells [22].

We found that **IM5** induced different types of cell death in HSC-2, HSC-4, and HL-60 cells. **IM5** induced apoptotic characteristic in HL-60 cells. **IM5** also induced DNA fragmentation, but no clear-cut laddering pattern in HSC-2 cells. On the other hand, **IM5** induced the formation of secondary lysosomes without induction of apoptosis markers in HSC-4 cells, even though HSC-2

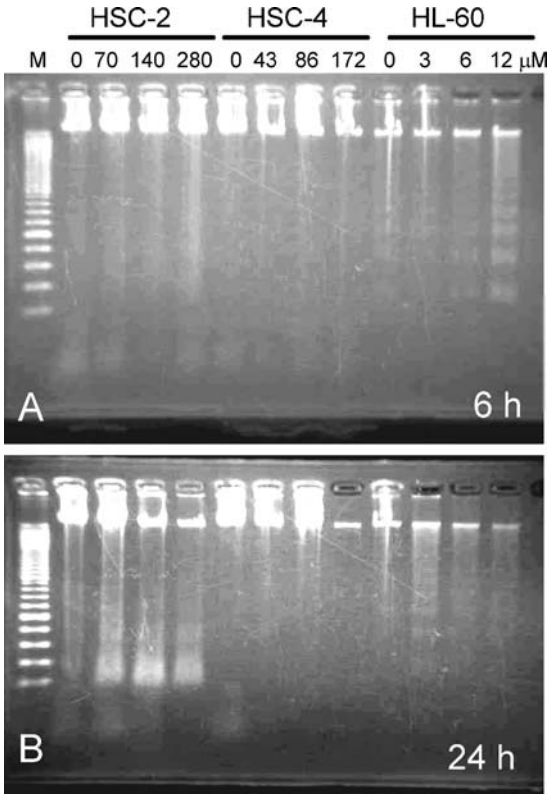

Fig. 2 Effect of 4-trifluoromethylimidazoles on DNA fragmentation for **A** 6 h and **B** 24 h (assayed by agarose gel electrophoresis). *M* DNA size marker

and HSC-4 cells showed comparable sensitivity to **IM5**. This suggests that the type of cell death may be determined by the type of target cells, but not by the drug sensitivity of the cells.

Compounds with imidazole ring systems have many pharmacological properties and play important roles in biochemical processes [28]. Many substituted imidazoles are known as inhibitors of p38 MAP kinase, anti-inflammatory agents, angiotensin II receptor antagonists, fungicides, and herbicides [29]. Some imidazole derivatives have been reported to induce apoptosis in Ehrlich ascites tumor cells [30]. Vicinal diaryl-substituted five-membered heteroaromatic rings (including imidazole, oxazole, isoxazole, thiazole, pyrazole, and tetrazole) have been considered to be the bioisosteric replacement of the olefinic double bond of combretastatin A-4, a potent antimitotic agent isolated from the stem wood of the South African tree *Combretum caffrum* [31, 32]. The 1,2-diphenylimidazole scaffold thus appear to be appropriate for the development of more potent anticancer agents with a tumor-specific cytotoxicity. The semiempirical method can be applicable to

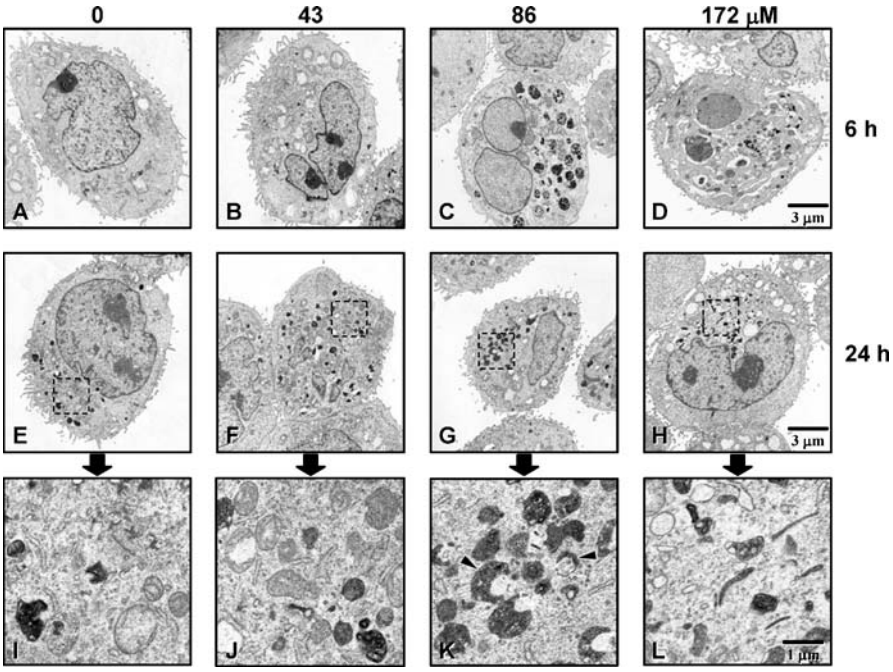

Fig. 3 Electron microscopy of control and **IM5**-treated HSC-4 cells. Areas surrounded by *dotted lines* in **E**, **F**, **G**, and **H** are magnified in **I**, **J**, **K** and **L**, respectively. *Arrowhead* indicates rod-shaped lysosomes surrounding small vesicles and/or lucent materials

estimate the biological activity of novel imidazole derivatives (Ishihara et al., unpublished results).

2.2 Phenoxazine Derivatives

Actinomycin D has been clinically used for the treatment of many cancers and is known to be a DNA intercalator. The structure of actinomycin D is based on a phenoxazine ring bound to two cyclic pentapeptides [33]. The presence of the phenoxazine ring in the structure of actinomycin D suggests that phenoxazine derivatives may possess anticancer activity. Phenoxazine derivatives are known to be effective multidrug resistance (MDR) modulators in cancer cells [34], potent inhibitors of Akt signaling in cells [35], inhibitors of human plasma cholinesterase [36], and photo-chemotherapeutic agents in cancer cells [37]. Recent studies also show that the relatively water-soluble phenoxazines, such as 2-amino-4,4α-dihydro-4α,7-dimethyl-2*H*-phenoxazine-3-one and 2-aminophenoxazine-3-one, exert antitumor effects on various cancer cells in vitro and in vivo. [38]. We have investigated 24 phenoxazines [23, 39] (Fig. 4).

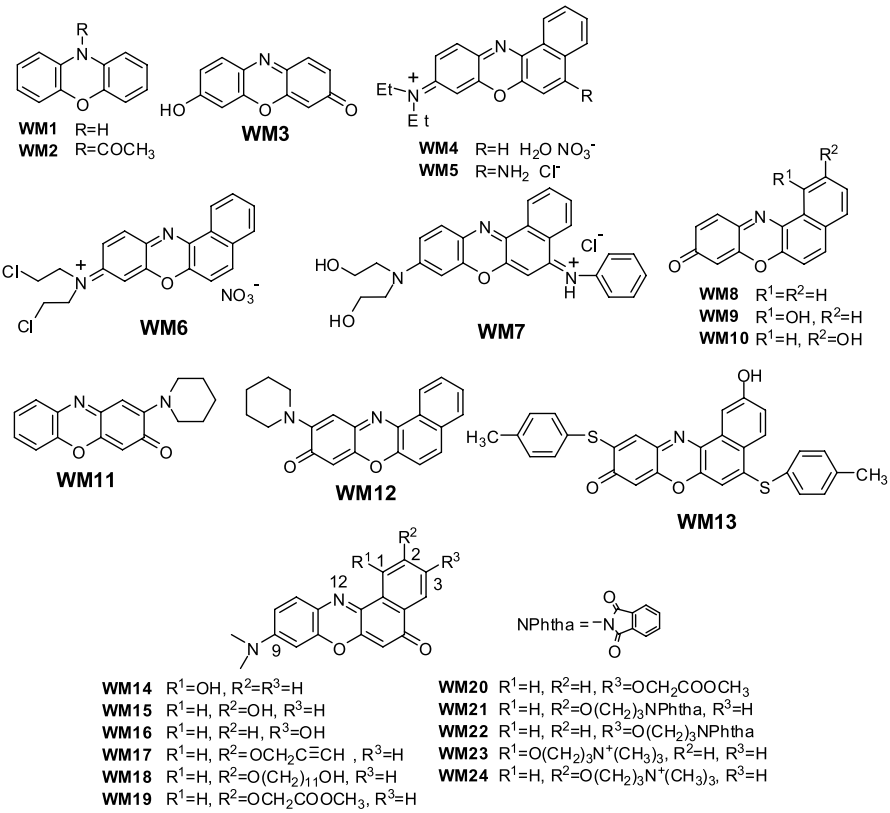

Fig. 4 Structure of phenoxazine derivatives

Among the 24 phenoxazine derivatives, **WM4** showed the highest cytotoxicity, followed by **WM5** > **WM10** > **WM7** > **WM8**, whereas the other 19 phenoxazines showed much less cytotoxic activity (Table 2). Four cationic phenoxazine dyes (**WM4–7**) were found to be cytotoxic against both tumor and normal cells. The presence of positively charged quaternary nitrogen substituents on the phenoxazine ring may be crucial to the cytotoxicity induction. Among three benzophenoxazines (**WM8**, **9** and **10**), **WM8** and **10** are cytotoxic against tumor cells. The difference in chemical structure between **WM9** and **10** is the position of the hydroxyl group in ring D. The presence of the hydroxyl group at C-1 in **WM9** is not beneficial to the cytotoxic activity, presumably due to the presence of an intramolecular hydrogen bond between *N*12 and the 1-hydroxyl group. It is therefore speculated that the electron density of the nitrogen at the 12 position plays an important role in determining the activity of the phenoxazine derivatives. The hydrogen bond reduced the density of the nitrogen and could possibly reduce its ability to interact with other molecules. Among **WM14–24**, cytostatic **WM23** and **24** have

Table 2 Cytotoxic activity of phenoxazines (**WM1–24**) against human tumor and normal cells

Comd.	MW	50% Cytotoxic concentration (CC_{50}, μM)							TS
		Tumor cell lines				Normal cells			
		HSC-2	HSC-3	HSC-4	HL-60	HGF	HPC	HPLF	
WM1	183	154	137	164	6.9	>200	>200	154	>1.6
WM2	225	181	109	157	42	184	184	170	1.5
WM3	213	40	28	115	60	>200	83	61	>1.9
WM4	383	3.5	2.6	4.4	<1.6	5.9	11	4	2.3
WM5	354	4.5	2	4.5	<1.6	4.4	4.8	2.4	1.2
WM6	434	48	56	78	16	165	183	87	2.9
WM7	462	25	3.8	28	<1.6	77	75	37	4.3
WM8	247	18	31	17	<1.6	67	133	44	4.8
WM9	263	>200	>200	>200	>200	>200	>200	>200	><1.0
WM10	263	3.2	6.9	8	1.6	16	22	12	3.4
WM11	280	>200	>200	>200	>200	>200	>200	>200	><1.0
WM12	330	>200	>200	>200	49	>200	>200	>200	><1.2
WM13	330	>200	>200	>200	>200	>200	>200	>200	><1.0
WM14	306	>200	>200	>200	147	>200	>200	>200	><1.1
WM15	306	>200	>200	>200	>200	>200	>200	>200	><1.0
WM16	306	>200	>200	>200	>200	>200	>200	>200	><1.0
WM17	344	>200	>200	>200	>200	>200	>200	>200	><1.0
WM18	476	>200	>200	>200	>200	>200	>200	>200	><1.0
WM19	378	>200	>200	>200	148	>200	>200	>200	><1.1
WM20	378	>200	153	>200	165	>200	>200	>200	><1.1
WM21	493	>200	>200	>200	>200	>200	>200	>200	><1.0
WM22	493	>200	>200	>200	>200	>200	>200	>200	><1.0
WM23	406	<1.6[a]	6.2[a]	3.1[a]	>200	9.8[a]	>200[a]	>200[a]	>2.6
WM24	406	<1.6[a]	100	19[a]	>200	25[a]	>200[a]	>200[a]	>1.8

Each value represents the mean from duplicate experiments

[a] Cell death was not observed, but growth was inhibited by 52∼60%

a tertiary amine group at the end of the side-chain. The difference in chemical structure between **WM14–22** and **WM23/24** is the presence or absence of the quaternized nitrogen on the side-chain. Thus, it is suggested that the presence of a positively charged quaternary nitrogen on the side-chain substituent of the ring is favorable for the cytostatic activity. It should be noticed, however, that the above conclusions may be limited to the relatively small set of compounds studied in the present study. To establish whether these conclusions are valid would require further studies in which larger sets of phenoxazines were used.

Phenoxazine derivatives showed low to moderate tumor-specific cytotoxicity (*TS* = 1.0 – 4.8). **WM8** showed the highest tumor-specific index (*TS* = 4.8), followed by **WM7** (*TS* = 4.3) > **WM10** (*TS* = 3.4) > **WM4** (*TS* = 2.3) > **WM5** (*TS* = 1.2). The TS values of the other 19 phenoxazines were 1.0∼2.6. **WM23**

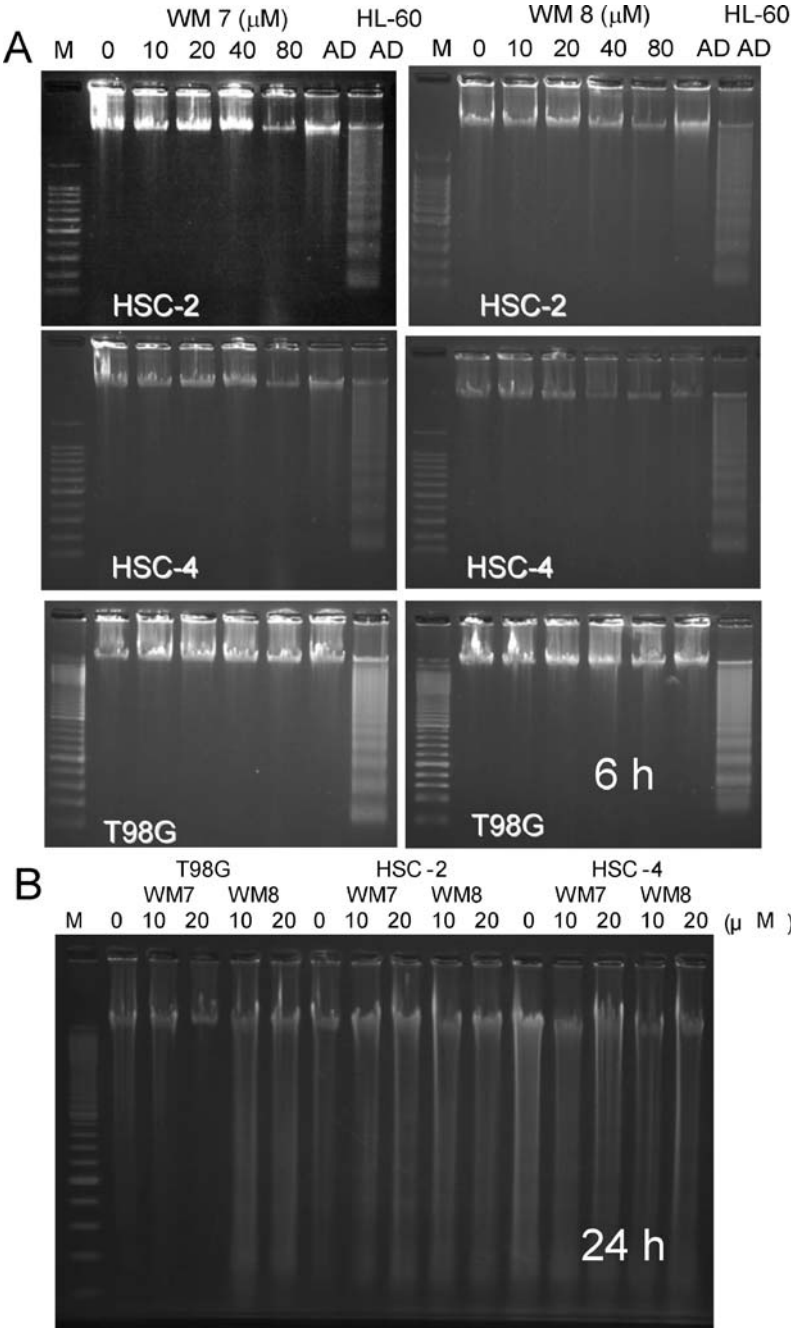

Fig. 5 Effect of **WM7** and **WM8** on DNA fragmentation in HSC-2, HSC-4, and T98G cells treated for **A** 6 h or **B** 24 h. *AD* 1 μg/mL actinomycin D, *HL-60 AD* DNA from HL-60 cells treated for 6 h with 1 μg/mL actinomycin D, *M* marker DNA

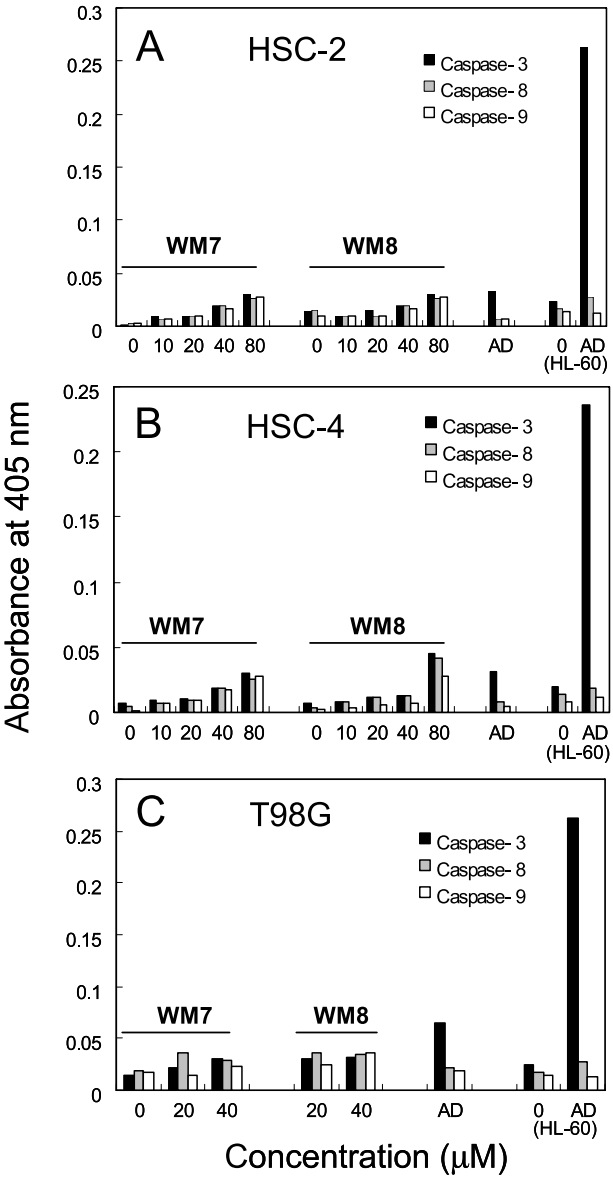

Fig. 6 Effect of **WM7** and **WM8** on caspase activity in **A** HSC-2, **B** HSC-4, and **C** T98G cells. Cells were treated for 4 h with the indicated concentrations of **WM7**, **WM8**, or 1 μg/mL actinomycin D (*AD*). *HL-60 AD* HL-60 cells treated for 4 h with 1 μg/mL actinomycin D

and **WM24** showed cytostatic effects, but did not show cytotoxic effects (data not shown). Since **WM7** and **WM8** showed the highest tumor-specific cytotoxic activity, these phenoxazines were investigated in more detail.

Considerable differences in drug sensitivity were found among these cell lines. The sensitivity to **WM7** was in the order: HL-60 (CC_{50} < 1.6) (most sensitive) > HSC-3 (3.8 μM) > HSC-2 (25 μM) > HSC-4 (28 μM) > HPLF (37 μM) > HPC (75 μM) > HGF (77 μM) (most resistant) (Table 2). Similarly, the sensitivity to **WM8** was in the order: HL-60 (CC_{50} < 1.6 μM) (most sensitive) > HSC-4 (17 μM) > HSC-2 (18 μM) > HSC-3 (31 μM) > HPLF (44 μM) > HGF (67 μM) > HPC (133 μM) (most resistant) (Table 2).

WM7 (10–80 μM) did not induce internucleosomal DNA fragmentation in three tumor cell lines (HSC-2, HSC-4, T98G), in contrast to apoptotic leukemia HL-60 induced by actinomycin D (Fig. 5). Actinomycin D induced only traces of DNA fragmentation in HSC-2, HSC-4, and T98G cells. Even when the treatment time was prolonged to 24 h, **WM7** and **WM8** did not induce DNA fragmentation in HSC-2, HSC-4, and T98 cells (data not shown). Both **WM7** and **WM8** enhanced the caspase-3, caspase-8 and caspase-9 activities only at higher concentrations (40 or 80 μM) in HSC-2, HSC-4, and T98G cells. However, the extent of caspase-3 activation by these compounds was much less than that induced by actinomycin D in HL-60 cells (positive control) (Fig. 6).

We found that treatment of HSC-4 cells with **WM7** considerably reduced the incidence of the acid organelle detected by acridine orange staining in HSC-4 cells [23]. Similarly, **WM7** did not affect the accumulation of microtubule-associated protein 1 light chain 3 (LC3)-GFP fusion protein in the autophagosome, a popular marker of autophagy [23]. We found no apparent effect of **WM8** on the autophagosome formation detected by acridine orange and LC3-GFP (data not shown). These data demonstrate that **WM7** and **WM8** failed to induce autophagy in HSC-4 cells [23]. **WM8** has α,β-unsaturated ketone structure, whereas **WM7** has imine structure. Further structure and activity studies are required to determine whether this structure is required for non-apoptotic cell death. Our finding is not consistent with the recent report that the inhibition of autophagy by 3-methyladenine enhanced the oridonin-induced apoptosis in HeLa cells [40]. It therefore seems likely that the inhibition of autophagy is not always coupled with apoptosis induction.

3
O-Containing Heterocycles

3.1
3-Formylchromone Derivatives

The chromones (4*H*-1-benzopyran-4-ones) have attracted attention from the viewpoint of both biological activity [41, 42] and organic synthesis [42, 43]. Chromone derivatives have been found to exhibit a broad range of biolog-

ical activities, including antifungal, antiviral, antimicrobial, antiallergenic, antitublin, and antitumor activity [41, 44]. In addition, many flavonoids are based on the chromone structure and have been found to possess several therapeutically interesting biological activities [45]. In our previous studies on the structure–cytotoxic activity relationship of a series of β-diketones, 3-formylchromone (**FC1**) was shown to exhibit potent cytotoxic activities against some tumor cells and tumor cell-specific cytotoxicity [46]. The presence of a formyl group at the C-3 position of the chromone seems to be responsible for such biological activity. Because compound (**FC1**) possesses a α,β-unsaturated reactive aldehyde, it could react as a Michael acceptor. It is known that 3-formylchromone derivatives show induction of the chloroplast-free mutants [47] and antiproliferative activity [48] and act as $p56^{lck}$ tyrosine kinase inhibitors [49] and modifiers of multidrug resistance in mouse lymphoma cells and in human Colo320 colon cancer cells [50]. It is also reported that some 3-formylchromone derivatives showed a relatively strong anti-anaphylactic reaction but generally had low LD_{50} [51].

In the present study, we describe the effects produced by 3-formylchromones substituted at the 6-position. We evaluated their cytotoxicity against human tumor cell lines and normal cells, and also investigated the structurally related coumarine (2*H*-1-benzopyran-2-one) derivatives [24].

The 6-substituted 3-formylchromone derivatives (**FC1–8**) screened for their tumor-specific cytotoxic potentials are shown in Fig. 7. Their CC_{50} values for the four tumor cell lines and three normal cells are summarized in Table 3. Cytotoxic data for the related chromone derivatives (**FC9–13**),

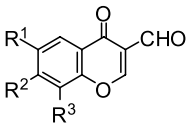

FC1-11

Compd	R^1	R^2	R^3	Calcd log P
FC1	H	H	H	0.35
FC2	CH_3	H	H	0.86
FC3	i-Pr	H	H	1.76
FC4	CH_3O	H	H	0.56
FC5	NO_2	H	H	-
FC6	F	H	H	0.60
FC7	Cl	H	H	1.17
FC8	Br	H	H	1.32
FC9	Cl	CH_3	H	1.67
FC10	Cl	H	Cl	1.91
FC11	Br	H	Br	2.21

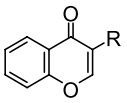

FC12, 13

Compd	R	Calcd log P
FC12	CN	0.45
FC13	H	1.01

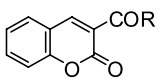

FC14-16

Compd	R	Calcd log P
FC14	CH_3	1.15
FC15	OH	1.54
FC16	OC_2H_5	1.91

Fig. 7 Chemical structures and calculated log*P* values of 3-formylchromone and coumarin derivatives (**FC1–16**)

Table 3 Cytotoxic activity of 3-formylchromones and related compounds against tumor and normal cells

Compound	50% Cytotoxic concentration (CC_{50}, μM)							TS
	Human tumor cell lines				Normal cells			
	HSC-2	HSC-3	HSG	HL-60	HGF	HPC	HPLF	
FC1	89	225	332	59	552	322	678	2.9
FC2	47	184	128	13	307	188	404	3.2
FC3	42	172	95	20	171	102	235	2.1
FC4	80	99	166	30	490	175	635	4.6
FC5	84	262	546	78	750	521	679	2.7
FC6	22	165	91	8	327	293	651	5.9
FC7	46	73	92	17	166	74	208	2.6
FC8	64	81	169	41	260	97	419	2.9
FC9	42	102	115	30	173	86	159	1.9
FC10	56	117	215	52	390	215	388	3
FC11	75	131	216	40	246	193	276	2.1
FC12	250	692	687	445	754	866	876	1.6
FC13	784	679	>1000	853	>1000	>1000	>1000	><1.2
FC14	314	469	>1000	843	945	>1000	861	><1.4
FC15	786	763	966	951	801	887	824	1
FC16	638	875	932	461	813	1000	844	1.2
Doxorubicin	9	8	37	20	>1000	>1000	>1000	>54.1
EGCG	215	375	496	83	>1000	>1000	>1000	>3.4

coumarin derivatives (**FC14–16**), doxorubicin and EGCG are also included in the table. The potency of the lead compound 3-formylchromone (**FC1**) towards four cancer cell lines is presented in Table 3. The average CC_{50} value of **FC1** to HSC-2, HSC-3, HSG, and HL-60 cells was 176 μM towards these four cell lines. 6-Substituted 3-formylchromones (**FC2–4** and **6–11**) and 6-nitro derivative (**FC5**) showed higher cytotoxicity. 6-Fluoro (**FC6**), 6-chloro (**FC7**) and 6-chloro-7-methyl (**FC9**) derivatives were the most cytotoxic. The cytotoxicities of **FC12** and **13** were much less than those of **FC1–11**, suggesting that the presence of the 3-formyl group is beneficial. In order to assess the preferential toxicity for tumor cells, the tumor-specific cytotoxicity (TS) was calculated for each compound. All 3-formylchromones (**FC1–13**) displayed preferential toxicity for malignant cells and their TS values are shown in Table 3. The normal cells exhibited a higher resistance to all of these compounds as compared with the tumor cell lines, which resulted in an elevation of the TS of some derivatives. In particular, **FC4** and **6** showed excellent selectivity (TS = 4.6 and 5.9, respectively).

The results show that all the 6-substituted 3-formylchromones, and the 6-nitro-substituted derivative **FC5**, exhibit a more potent cytotoxicity against tumor cell lines than the parent 3-formylchromone (**FC1**). However, there was no clear-cut correlation between the chemical structure of the com-

pounds tested and their cytotoxic activity. 3-Formylchromones bearing an electron-withdrawing formyl group at C-3 are highly functional molecules, capable of reacting as Michael acceptors. It seems reasonable, therefore, that the exploration of more potent or better bioavailable agents and cancer cell line-specific cytotoxic agents can be achieved through further modifications of the 3-formylchromone.

3.2 Coumarin and its Derivatives

Coumarins constitute a major class of widely distributed *O*-heterocyclic natural products isolated from citrus fruits and vegetables [52]. Naturally occurring coumarins possess a variety of biological activities, including antitumor activity [53]. 7-Hydroxycoumarin and 8-nitro-7-hydroxycoumarin were shown to be potent cytotoxic agents against the human renal cell carcinoma cell line.

We found that although coumarin itself (**C1**) and its 7-hydroxy (**C2**), 6-methoxyl-7-hydroxy (**C4**) and 5,6-dimethoxy (**C5**) derivatives were relatively non-toxic to all cell lines used, its 6,7-dihydroxy derivatives (**C3**; esculetin) revealed a tumor cell line-specific cytotoxicity of >5.1 (Table 4). These observations are in agreement with the reports that the secondary plant metabolite esculetin (**C3**) is cytotoxic to human leukemia [54] and other tumor cell lines [55] and that it is relatively non-toxic to normal human cells [56]. Among the eight 4-methylcoumarin derivatives (**C6–C13**), the most potent and tumor-specific cytotoxicity was observed in the 6,7-dihydroxylated molecule (**C8**) only. The situation was analogous for the 3,4-dimethyl- (**C15–C19**) or 3,4-cycloalkyl- (**C20–C23**) substituted coumarin derivatives. Although the TS values for all four *ortho*-dihydroxycourmarins tested were >5, such was not the case for the *ortho*-dihydroxylated reference molecule caffeic acid (or for the trihydroxylated molecule gallic acid).

These observations strongly suggest that 6,7-dihydroxycoumarins represents a specific pharmacophore moiety suitable for designing tumor-specific cytotoxic agents [25]. It is also suggested that proper substitution at the 3- and/or 4-position of the molecule makes it possible to design more cytotoxic agents. In a continuing search for potent and selective cytotoxic antitumor agents, we prepared another 22 coumarin derivatives (**C24–45**) and evaluated their cytotoxic effects against human oral tumor cells. In the present work, we also investigated the MDR reversal activities of 45 coumarins (**C1–45**) against mouse lymphoma cells transfected with human MDR 1 gene [26].

In general, 21 coumarin derivatives (**C24–44**) (see structural formulae in Fig. 8) were more cytotoxic against HSC-2 than HSC-3 cells (Table 5). Five compounds **C29**, **C39**, **C40**, **C43**, and **C44** displayed potent cytotoxic activities with CC_{50} values of 15–24 μg/mL in HSC-2 cells. Their potencies were comparable with that of gallic acid (CC_{50} = 24 μg/mL). Both **C43** and **C44**

Table 4 Cytotoxic activity of coumarin derivatives (**C1–23**) against cultured human tumor and normal cells

Compound	50% Cytotoxic concentration (CC_{50}, μg/mL)							TS
	Human tumor cell lines				Normal cells			
	HSC-2	HSC-3	A-375	HL-60	HGF	HPC	HPLF	
C1	>200	>200	>200	>200	>200	>200	>200	–
C2	166	>200	>200	142	>200	>200	>200	><1.1
C3	42	32	70	13	>200	>200	>200	><5.1
C4	>200	>200	>200	>200	>200	>200	>200	–
C5	>200	>200	>200	>200	>200	195	>200	–
C6	168	176	>200	125	>200	183	>200	>1.2
C7	124	192	177	123	>200	117	>200	>1.1
C8	33	16	34	13	>200	>200	>200	>8.3
C9	80	>200	95	49	>200	>200	>200	><1.9
C10	>200	>200	196	>200	>200	>200	>200	–
C11	156	>200	177	>200	>200	>200	>200	–
C12	40	>200	>200	>200	>200	>200	>200	–
C13	62	>200	>200	>200	>200	>200	>200	–
C14	78	157	148	133	>200	168	>200	>1.5
C15	77	128	91	150	141	161	183	1.5
C16	19	9	33	18	200	152	>200	>9.3
C17	33	46	75	>200	>200	182	200	–
C18	120	>200	>200	>200	>200	>200	>200	–
C19	39	70	106	>200	>200	133	>200	–
C20	23	19	22	9	>200	>200	>200	>11.0
C21	81	134	69	47	168	138	164	>1.9
C22	17	160	>200	>200	>200	>200	>200	–
C23	19	181	>200	>200	>200	177	>200	–
Gallic acid	20	17	55	16	38	69	48	1.9
Caffeic acid	>200	156	>200	159	158	>200	166	0

showed the highest tumor-specific cytotoxicity (TS value = 4.1 and 3.6, respectively). Among the 44 coumarins, log *P* values ranged from 0.70 to 4.79. The log *P* values of the potent **C34** and **C43** were 0.82 and 3.21, respectively.

No or only minimal cytotoxicity of most coumarins could be detected in normal cells in contrast to the positive control gallic acid. On the other hand, several of them showed concentration-dependent cytotoxicity against tumor cell lines HSC-2 and HSC-3. Among them, 6-hydroxy-7-methoxycoumarin derivatives (**C29**, **C30**, **C39**, **C40**, **C41**, **C42**, and **C43**) were cytotoxic to tumor cell line HSC-2. However, **C34** and **C38** were relatively non-toxic to all cell lines used. It is suggested that the presence of polar substituents such as ester and alcohol group at the C-3 and/or C-4 position was unfavorable for cytotoxicity. This observation confirms the recent findings that 3,4-dimethyl- (**C17**) and 3,4-cyclopentano-6-hydroxy-7-methoxycoumarin (**C22**) showed marked cytotoxic effects [25]. However, it should be noted that 4-methyl-6-hydroxy-

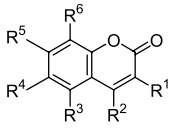

C1-44

Compd	R^1	R^2	R^3	R^4	R^5	R^6	Calcd log P
1	H	H	H	H	H	H	1.41
2	H	H	H	H	OH	H	1.61
3	H	H	H	OH	OH	H	1.21
4	H	H	H	OCH_3	OH	H	1.33
5	H	H	OCH_3	OCH_3	OH	H	0.72
6	H	CH_3	H	H	OH	H	2.11
7	H	CH_3	H	OH	H	H	2.11
8	H	CH_3	H	OH	OH	H	1.71
9	H	CH_3	OH	H	OH	H	1.64
10	H	CH_3	H	OH	OCH_3	H	1.83
11	H	CH_3	H	OCH_3	OH	H	1.83
12	H	CH_3	H	H	OCH_3	H	2.24
13	H	CH_3	H	OCH_3	H	H	2.24
14	CH_3	H	H	H	OH	H	2.11
15	CH_3	CH_3	H	H	OH	H	2.56
16	CH_3	CH_3	H	OH	OH	H	2.16
17	CH_3	CH_3	H	OH	OCH_3	H	2.28
18	CH_3	CH_3	H	OCH_3	OH	H	2.28
19	CH_3	CH_3	H	H	OCH_3	OH	2.28
20	$-(CH_2)_3-$		H	OH	OH	H	2.22
21	$-(CH_2)_3-$		OH	H	OH	H	2.15
22	$-(CH_2)_3-$		H	OH	OCH_3	H	2.35
23	$-(CH_2)_3-$		H	OCH_3	OH	H	2.35
24	$-(CH_2)_4-$		H	OH	OCH_3	H	2.91
25	-Benzo-		H	NO_2	H	H	-
26	H	CH_2CO_2H	H	H	OCH_3	H	1.01
27	NO_2	OH	H	H	H	H	-
28	$CO_2C_2H_5$	H	H	H	H	H	1.91
29	H	Ph	H	OH	OCH_3	H	3.22
30	Ph	CH_3	H	OH	OCH_3	H	3.93
31	H	CF_3	H	OH	OCH_3	H	2.25
32	H	CF_3	H	H	$N(CH_3)_2$	H	3.01
33	CH_3	CH_3	H	OR	OH	H	4.79
34	$(CH_2)_2OH$	CH_3	H	OH	OCH_3	H	0.82
35	$(CH_2)_2OH$	CH_3	H	H	OH	OH	0.70
36	$(CH_2)_2OH$	CH_3	H	OCH_3	OH	H	0.82
37	$(CH_2)_2OH$	CH_3	OH	H	OH	H	0.63
38	H	$CH_2CO_2CH_3$	H	OH	OCH_3	H	1.01
39	CH_3	CH_3	H	OH	OC_2H_5	H	2.81
40	H	C_3H_7	H	OH	OCH_3	H	2.89
41	H	$CH(CH_3)_2$	H	OH	OCH_3	H	2.76
42	C_4H_9	CH_3	H	OH	OCH_3	H	3.87
43	$CH(CH_3)_2$	CH_3	H	OH	OCH_3	H	3.21
44	C_2H_5	CH_3	H	OH	OCH_3	H	2.81

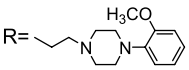

Fig. 8 Chemical structures and calculated log *P* values of courmarin derivatives (**C1–44**)

7-methoxycoumarin (**C10**) and 7-hydroxy-6-methoxycoumarin (scopoletin) (**C4**) were inactive. Furthermore, **C43** showed the highest tumor-specific cytotoxicity (TS value = 4.1), which was more potent than that of gallic acid (TS = 2.4). In the series of 3-(2-hydroxyethyl)-4-methylcoumarins (**C34-37**),

Table 5 Cytotoxic activity of coumarin derivatives (**C24–44**) against cultured human tumor and normal cells

Compound	50% Cytotoxic concentration (CC_{50}, μg/mL)					TS
	Human tumor cell lines		Normal cells			
	HSC-2	HSC-3	HGF	HPC	HPLF	
C24	75	>200	133	>200	>200	><1.3
C25	>200	>200	>200	180	>200	><1.0
C26	>200	>200	>200	>200	>200	><1.0
C27	195	150	>200	>200	>200	>1.2
C28	120	181	192	>200	179	>1.3
C29	15	85	100	133	127	2.4
C30	29	>200	>200	>200	>200	><1.7
C31	61	>200	>200	>200	>200	><1.5
C32	>200	197	>200	>200	>200	><1.0
C33	48	>200	153	154	133	<1.2
C34	100	>200	>200	>200	>200	><1.3
C35	53	78	152	>200	158	>2.6
C36	154	>200	>200	>200	>200	><1.1
C37	67	>200	>200	>200	>200	><1.5
C38	150	>200	>200	>200	>200	><1.1
C39	20	>200	>200	>200	>200	><1.8
C40	19	108	157	157	173	2.6
C41	34	157	147	162	148	1.6
C42	33	169	>200	>200	>200	>2.0
C43	19	68	161	190	188	4.1
C44	24	65	171	163	151	3.6
Gallic acid	24	38	74	76	70	2.4

enhancement of cytotoxicity was observed in the following order: 7-hydroxy-6-methoxy (**C36**) < 6-hydroxy-7-methoxy (**C34**) < 5,7-dihydroxy (**C37**) < 7,8-dihydroxy (**C35**).

4 Others

4.1 Vitamin K_2 Derivatives

Vitamin K is a dietary component essential for the normal biosynthesis of several factors required for clotting of blood. Vitamin K_1 (phylloquinone, phytonadione) is a 2-methyl-3-phytyl-1,4-naphthoquinone, and is the only natural vitamin available for therapeutic use. Vitamin K_2 represents a series of compounds (the menaquinones, MK) in which the phytyl side-

chain of phytonadione has been replaced by a side-chain built up of 1–14 isoprenyl units (MK-1∼MK-14, Fig. 9). Vitamin K_3 (menadione, 2-methyl-naphtoquinone) is a synthetic compound with the highest activity. It has been reported that vitamin K_2 (MK-4) with four isoprenyl units induced differentiation (expression of naphthol AS-D chloroacetate esterase activity, α-naphtylacetate esterase activity, Fc receptor and phagocytosis) in human myelogenous leukemia cell lines (HL-60, ML-1, U-937) [57], or apoptosis (characterized by DNA fragmentation and caspase activation) in isolated osteoclast [58] and human ovary cancer cells [59].

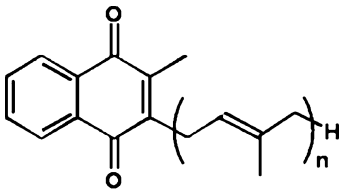

Vitamin K_2 derivatives

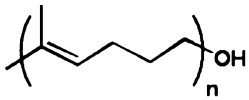

Prenylalcohols

Fig. 9 Structure of vitamin K_2 derivatives and prenylalcohols

Prenylalcohols are components of the side-chain of vitamin K_2. All-*trans* geranylgeraniol (GG), one of such prenylalcohols with four isoprenyl units, induced apoptotic cell death in human leukemic cell lines [60, 61]. We have recently reported that the cytotoxic activity and radical intensity of vitamin K was increased in the order $K_1 < K_2 < K_3$ [62–64]. Vitamin K_3 induced the cell death in a synergistic fashion with vitamin C [65, 66], possibly inducing the autoschizis characterized by exaggerated membrane damage and progressive loss of organelle-free cytoplasm through a series of self-excisions.

Among the 14 vitamin K_2 derivatives (MK-*n*, $n = 1\sim14$) (Fig. 9), MK-2 (with two isoprenyl groups) showed the greatest cytotoxicity, followed by MK-1 (with one isoprenyl group), MK-3 (with three isoprenyl groups). MK-1, MK-2, and MK-3 showed the highest tumor-specific cytotoxicity (*TS* = >2.0, 2.0 and >1.7, respectively) (Table 6). Among the ten isoprenyl alcohols ($n = 1\sim10$) (Fig. 9), geranylgeraniol (GG) (with four units of isoprenyl groups) showed the highest cytotoxicity, followed by farnesol (with three units of isoprenyl groups) and geranylfarnesol (GF) (with five isoprenyl groups).

Table 6 Cytotoxic activity of vitamin K_2 derivatives against human tumor and normal cells

Compound	MW	50% Cytotoxic concentration (CC_{50}, μM)								TS
		Tumor cell lines					Normal cells			
		HSC-2	HSC-3	HSC-4	$HepG_2$	HL-60	HGF	HPC	HPLF	
MK-1 ($n = 1$)	240	130 ±27	104 ±13	129 ±55	55 ±15	46 ±18	>200	>200	159 ±40	>2.0
MK-2 ($n = 2$)	308	114 ±24	76 ±3	79 ±38	104 ±36	30 ±5	169 ±21	166 ±23	142 ±13	2.0
MK-3 ($n = 3$)	377	159 ±40	137 ±26	93 ±76	193 ±8	13 ±6	>200	>200	>200	>1.7
MK-4 ($n = 4$)	445	>200	>200	>200	>200	>200	>200	>200	>200	><1.0
MK-5 ($n = 5$)	513	>200	>200	>200	>200	>200	>200	>200	>200	><1.0
MK-6 ($n = 6$)	581	>200	>200	>200	>200	>200	>200	>200	>200	><1.0
MK-7 ($n = 7$)	649	>200	>200	>200	>200	>200	>200	>200	>200	><1.0
MK-8 ($n = 8$)	717	>200	>200	>200	>200	>200	>200	>200	>200	><1.0
MK-9 ($n = 9$)	785	>200	>200	>200	>200	>200	>200	>200	>200	><1.0
MK-10 ($n = 10$)	853	>200	>200	>200	>200	>200	>200	>200	>200	><1.0
MK-11 ($n = 11$)	922	>200	>200	>200	>200	>200	>200	>200	>200	><1.0
MK-12 ($n = 12$)	990	>200	>200	>200	>200	>200	>200	>200	>200	><1.0
MK-13 ($n = 13$)	1058	>200	>200	>200	>200	>200	>200	>200	>200	><1.0
MK-14 ($n = 14$)	1126	>200	>200	>200	>200	>200	>200	>200	>200	><1.0

Each value represents the mean ± S.D. from four independent experiments
n number of isoprenyl units

GG showed the highest tumor specificity (*TS* = 1.8), followed by farnesol (*TS* = >1.4), GF (*TS* = >1.3) (Table 7).

Considerable difference in drug sensitivity was found between the cell lines. The sensitivity to MK-2 was in the order: HL-60 (CC_{50} = 30 μM) (most sensitive) > KG-1 (52 μM) > HSC-3 (76 μM) > K-562, HSC-4 (79 μM) > ML-1 (80 μM) > $HepG_2$ (104 μM) > HSC-2 (114 μM) > U87MG (115 μM) > HPLF (142 μM) > HPC (166 μM) > HGF (169 μM) > T98G (>200 μM) (most resistant) (Tables 6, 8). Similarly, the sensitivity to GG was in the order: HL-60 (CC_{50} = 9 μM) (most sensitive) > KG-1 (61 μM) > ML-1 (62 μM) > K-562, HSC-2 (CC_{50} = 67 μM) > HSC-4 (72 μM) > HSC-3 (94 μM) > U87MG (95 μM) > HPLF (137 μM) > HGF (143 μM) > $HepG_2$ (148 μM) > HPC (150 μM) > T98G (152 μM) (most resistant) (Tables 7, 8).

MK-2 did not induce internucleosomal DNA fragmentation in the human promyelocytic leukemia HL-60 and squamous cell carcinoma HSC-4 cell lines. GG induced internucleosomal DNA fragmentation marginally in the HL-60 cells, but to a lower extent than actinomycin D (positive control). However, GG did not induce DNA fragmentation in the HSC-4 cells (Fig. 10).

Table 7 Cytotoxic activity of prenylalcohols against human tumor and normal cells

Compound	MW	50% Cytotoxic concentration (CC_{50}, μM)								TS
		Tumor cell lines					Normal cells			
		HSC-2	HSC-3	HSC-4	$HepG_2$	HL-60	HGF	HPC	HPLF	
Prenol ($n = 1$)	86	>200	>200	>200	>200	>200	>200	>200	>200	><1.0
Geraniol ($n = 2$)	154	>200	>200	>200	>200	>200	>200	>200	>200	><1.0
Farnesol ($n = 3$)	222	131 ±11	166 ±34	139 ±11	173 ±28	61 ±10	209 ±63	221 ±59	179 ±27	>1.4
GG ($n = 4$)	290	67 ±12	94 ±20	72 ±12	148 ±7	9 ±2	143 ±9	150 ±8	137 ±9	1.8
GF ($n = 5$)	359	167 ±24	190 ±19	171 ±31	>200	19 ±7	>200	>200	>200	><1.3
FF ($n = 6$)	427	>200	>200	>200	>200	>200	>200	>200	>200	><1.0
GGF ($n = 7$)	495	>200	>200	>200	>200	>200	>200	>200	>200	><1.0
GFF ($n = 8$)	563	>200	>200	>200	>200	>200	>200	>200	>200	><1.0
Solanesol ($n = 9$)	631	>200	>200	>200	>200	>200	>200	>200	>200	><1.0
Decapr. ($n = 10$)	699	>200	>200	>200	>200	>200	>200	>200	>200	><1.0

Each value represents the mean ± S.D. from four independent experiments
n number of isoprenyl units, *GG* geranylgeraniol, *GF* geranylfarnesol, *FF* farnesylfarnesol, *GGF* geranylgeranylfarnesol, *GFF* geranylfarnesylfarnesol, *Decapr.* decaprenol

Table 8 Cytotoxic activity of vitamin K_2 derivatives against human leukemia and glioblastoma cell lines

Compound	50% Cytotoxic concentration (CC_{50}, μM)					
	Human leukemia				Human glioblastoma	
	HL-60	ML-1	KG-1	K-562	T98G	U87MG
Vitamin K_2 derivatives						
MK-1 ($n = 1$)	46	111	98	172	177	91
MK-2 ($n = 2$)	30	80	52	79	>200	115
MK-3 ($n = 3$)	13	36	36	29	>200	>200
MK-4 ($n = 4$)	>200	>200	>200	>200	>200	>200
Prenylalcohols						
Farnesol ($n = 3$)	61	62	41	72	148	122
GG ($n = 4$)	9	62	61	67	152	95

Each values represents the mean from duplicate determinations
n number of isoprenyl units

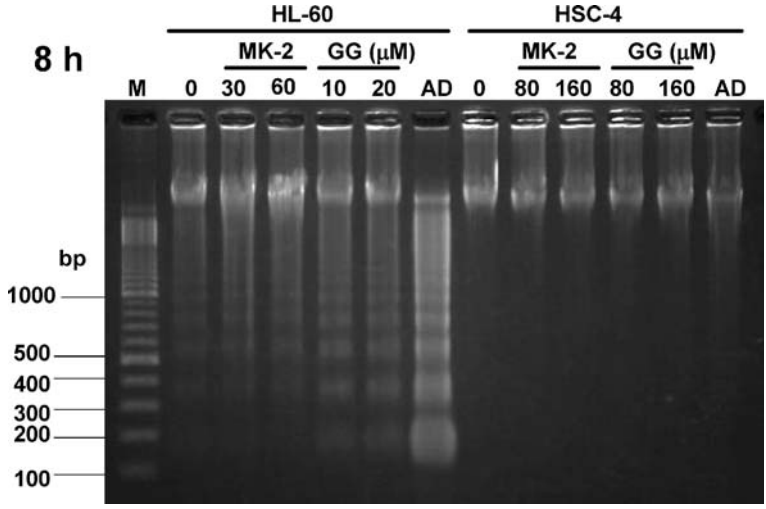

Fig. 10 Effect of MK-2 and GG on DNA fragmentation in HL-60 and HSC-2 cells (assayed by agarose gel electrophoresis). *AD* 1 μg/mL actinomycin D, *M* marker DNA

Actinomycin D induced the formation of autophagosomes, as judged by the granular distribution of acridine orange in the HSC-4 cells, whereas MK-2 and GG did not induce such morphological changes [27].

Since the intracellular concentration of putrescine, but not that of spermidine and spermine, declined during the apoptotic cell death of HL-60 cells [67, 68], we also investigated whether MK-2 and GG induce similar changes in polyamine levels. Neither MK-2 (7.5–200 μM; up to 7 × CC_{50}) nor GG (2.5–40 μM; 4 × CC_{50}) affected the intracellular concentration of putrescine, spermidine and spermine in the HL-60 cells [27]. Similarly, MK-2 (2.5–200 μM; 1.6 × CC_{50}) and GG (2.5–100 μM; 1.6 × CC_{50}) did not show any apparent effect on the polyamine levels in the HSC-2 cells [27].

Since there are some relationships between cytotoxic activity and radical generation/scavenging activity in several antioxidants [69], we investigated the radical intensity of MK-2 and prenylalcohol derivatives in relation to their cytotoxicity, using electron spin resonance (ESR) spectroscopy. Only MK-1 ($n = 1$), geranylgeranylfarnesol ($n = 7$) and geranylfarnesylfarnesol ($n = 8$), which had lower cytotoxicity, produced strong quintuplet signals under alkaline conditions, whereas the other compounds did not produce detectable ESR signals [27].

Both vitamin K_2 derivatives and prenylalcohols with various lengths of isoprenyl units attached showed surprisingly low tumor-specific cytotoxicity. Among them, MK-2 (with two isoprenyl groups) and GG (with four isoprenyl groups) showed the highest tumor specificity and cytotoxicity against various tumor cell lines, with TS values of as little as 2.0, possibly due to their optimal

hydrophobicity. With increasing length of the isoprenyl units, the solubility of the compounds declined below the level needed to express biological activity.

Considerable difference in the sensitivity to MK-2 and GG was found among the tumor cell lines used, with human leukemic cell lines (HL-60, ML-1, KG-1, K-562) the most sensitive and the human glioblastoma cell lines (T98G, U87MG) the most resistant. The sensitivity of the human oral squamous cell carcinoma cell lines (HSC-2, HSC-3, HSC-4) was intermediate. Consistent with previous reports [60, 61], GG induced apoptosis in the most sensitive HL-60 cells, but not in the less sensitive HSC-4 cells. This suggested that the type of cell death induced (either apoptosis or non-apoptosis) may depend on the target cells.

MK-2 induced apoptosis to a much lesser extent than GG. The major difference between MK-2 and GG is the α,β-unsaturated ketone structure present in MK-2 but not in GG. The induction of cell death by MK-2 or GG was not coupled with radical generation. It has recently been reported that the induction of apoptosis by MK-4 in human ovary cancer cells is mediated by oxidative stress in mitochondria [70]. Since autophagy plays an important role in reducing mitochondrial damage and reactive oxygen species, there is a possibility that the apoptosis-inducing activity of MK-4 may be derived from the inhibition of autophagy.

MK-2 and GG did not apparently affect the putrescine levels. This further supports the suggestion that these compounds induce non-apoptotic cell death, although the type of cell death has not yet been conclusively determined.

5 Conclusion

Heterocycles such as 4-trifluoromethylimidazole, phenoxazine, 3-formylchromone, coumarin derivatives, and vitamin K_2 derivatives were investigated for their cytotoxicity against human normal and tumor cells. These compounds induced moderate tumor-specific cytotoxicity. VitaminK_2 derivatives and prenylalcohols displayed disappointingly low tumor-specific cytotoxicity, although they have been reported to induce apoptosis-inducing activity. Human oral squamous cell carcinoma cell lines showed considerable variation in drug sensitivity. The type of cell death induced depended both on which types of cells and which inducers were used.

References

1. Wilfried R, Reed JC (2002) Nat Med 8:216
2. Yu L, Alva A, Su H, Dutt P, Freundt E, Welsh S, Baehrecke EH, Lenardo M (2004) Science 304:1500

3. Shintani T, Klionsky DJ (2004) Science 306:990
4. Daido S, Yamamoto A, Fujiwara K, Sawaya R, Kondo S, Kondo Y (2005) Cancer Res 65:4368
5. Paglin S, Hollister T, Delohery T, Hackett N, McMahill M, Sphicas E, Domingo D, Yahalom J (2001) Cancer Res 61:439
6. Kanzawa T, Zhang L, Xiao L, Germano IM, Kondo Y, Kondo S (2005) Oncogene 24:980
7. Kanzawa T, Kondo Y, Ito H, Kondo S, Germano I (2003) Cancer Res 63:2103
8. Daido S, Kanzawa T, Yamamoto A, Takeuchi H, Kondo Y, Kondo S (2004) Cancer Res 64:4286
9. Kanzawa T, Germano IM, Komata T, Ito H, Kondo Y, Kondo S (2004) Cell Death Differ 11:448
10. Yanagisawa-Shiota F, Sakagami H, Kuribayashi N, Iida M, Sakagami T, Takeda M (1995) Anticancer Res 15:259
11. Iida M, Doi H, Asamoto S, Sugiyama H, Kuribayashi N, Sakagami H, Matsumoto K (1999) Anticancer Res 19:1235
12. Kuribayashi N, Sakagami H, Iida M, Takeda M (1996) Anticancer Res 16:1225
13. Broker LE, Kruyt FAE, Giaccone G (2005) Clin Cancer Res 11:3155
14. Sakagami H, Kawase M, Wakabayashi H, Kurihara T (2007) Autophagy 3:493
15. Nakayachi T, Yasumoto E, Nakano K, Morshed SRM, Hashimoto K, Kikuchi H, Nishikawa H, Kawase M, Sakagami H (2004) Anticancer Res 24:737
16. Takeuchi R, Hoshijima H, Onuki N, Nagasaka H, Chowdhury SA, Kawase M, Sakagami H (2005) Anticancer Res 25:4037
17. Takeuchi R, Hoshijima H, Nagasaka H, Chowdhury SA, Kikuchi H, Kanda Y, Kunii S, Kawase M, Sakagami H (2006) Anticancer Res 26:3343
18. Ideo A, Sasaki M, Nakamura C, Mori K, Shimada J, Kanda Y, Kunii S, Kawase M, Sakagami H (2006) Anticancer Res 26:4335
19. Nam S, Smith DM, Dou QP (2001) Cancer Epidemiol Biomarkers Prev 10:1083
20. Stewart JR, Ward NE, Ioannides CG, O'Brian CA (1999) Biochemistry 38:13244
21. Sakagami H, Kobayashi M, Chien C-H, Kanegae H, Kawase M (2007) In Vivo 21:311
22. Takekawa F, Nagumo T, Shintani S, Hashimoto K, Kikuchi H, Katayama T, Ishihara M, Amano O, Kawase M, Sakagami H (2007) Anticancer Res 27(6): (in press)
23. Suzuki F, Hashimoto K, Ishihara M, Westman G, Samuelsson K, Kawase M, Motohashi N, Sakagami H (2007) Anticancer Res 27(6): (in press)
24. Kawase M, Tanaka T, Kan H, Tani S, Nakashima H, Sakagami H (2007) In Vivo 21:829
25. Kawase M, Sakagami H, Hashimoto K, Tani S, Hauer H, Chatterjee SS (2003) Anticancer Res 23:3243
26. Kawase M, Sakagami H, Motohashi N, Hauer H, Chatterjee SS, Spengler G, Vigyikanne AV, Molnar A, Molnar J (2005) In Vivo 19:705
27. Sakagami H, Hashimoto K, Suzuki F, Ishihara M, Kikuchi H, Katayama T, Satoh K (2007) Anticancer Res 27(6): (in press)
28. Grimmett MR (1984) In: Potts KT (ed) Comprehesive heterocyclic chemistry, vol. 5. Pergamon, Oxford, pp 345–498
29. Bellina F, Cauteruccio S, Rossi R (2007) Tetrahedron 63:4571
30. Anil KC, Jayarama SB, Salimath BP, Rangappa KS (2007) Invest New Drugs 25:343
31. Tron GC, Pirali T, Sorba G, Pagliai F, Busacca S, Genazzani AA (2006) J Med Chem 49:3033
32. Bellina F, Cauteruccio S, Monti S, Rossi R (2006) Bioorg Med Chem Lett 16:5757
33. Motohashi N, Mitscher LA, Meyer R (1991) Med Res Rev 11:239
34. Wesolowska O, Molnar J, Westman G, Samuelsson K, Kawase M, Ocsovszki I, Motohashi N, Michalak K (2006) In Vivo 20:109

35. Thimmaiah KN, Easton JB, Germain GS, Morton CL, Kamath S, Buolamwini JK, Houghton PJ (2005) J Biol Chem 280:31924
36. Kucukkikinc T, Ozer I (2007) Arch Biochem Biophys 461:294
37. Cincotta L, Foley JW, Cincotta AH (1993) Cancer Res 53:2571
38. Shirado K, Imaizumi K, Abe A, Tomoda A (2007) Biol Pharm Bull 30:331
39. Motohashi N (1993) Yakugaku Zasshi 103:364
40. Cui Q, Tashiro S, Onodera S, Ikejima T (2006) J Pharmacol Sci 101:230
41. Nawrot-Modranka J, Nawrot E, Graczyk J (2006) Eur J Med Chem 41:1301
42. Horton DA, Bourne GT, Smythe ML (2003) Chem Rev 103:893
43. Sabitha G (1996) Aldrichimica Acta 29:15
44. Wang B, Yang Z-Y, Li T (2006) Bioorg Med Chem 14:6012
45. Havsteen BH (2002) Pharmacol Therap 96:67
46. Nakano K, Nakayachi T, Yasumoto E, Morshed SRMD, Hashimoto K, Kikuchi H, Nishikawa H, Sugiyama K, Amano O, Kawase M, Sakagami H (2004) Anticancer Res 24:711
47. Foltinova P, Lacova M, Loos D (2000) Farmaco 55:21
48. Pisco L, Kordian M, Peseke K, Feist H, Michalik D, Estrada E, Carvalho J, Hamilton G, Rando D, Quincoces J (2006) Eur J Med Chem 41:401
49. Miller D, Wang S, Reid J, Xie W, Gauvin B, Kelley M, Sarup J, Sawutz DG, Miski M, Dolle RE, Faltynek CR (1995) Drug Develop Res 34:344
50. Barath Z, Radics R, Spengler G, Ocsovszki I, Kawase M, Motohashi N, Shirataki Y, Shah A, Molnar J (2006) In Vivo 20:645
51. Nohara A, Umetani T, Sanno YA (1974) Tetrahedron 30:3553
52. Murray RDH, Mendez J, Brown SA (1982) The natural coumarins: occurrence, chemisty and biochemistry. Wiley, New York, p 282
53. Finn GJ, Creaven BS, Egan DA (2004) Biochem Pharmacol 67:1779
54. Chuu C-Y, Tsai Y-Y, Wang C-J, Lin W-L, Tseng T-H (2001) Eur J Pharmacol 416:25
55. Kolodziej H, Kayser O, Woerdenbag HJ, van Uden W, Pras N (1997) Z Naturforsch 52c:240
56. Paya M, Goodwin PA, de las Heras B, Hoult RS (1994) Biochem Pharmacol 48:445
57. Sakai I, Hashimoto S, Yoda M, Hida T, Ohsawa S, Nakajo S, Nakaya K (1994) Biochem Biophys Res Commun 205:1305
58. Kameda T, Miyazawa K, Mori Y, Yuasa T, Shiokawa M, Nakamura Y, Mano H, Hakeda Y, Kameda A, Kumegawa M (1996) Biochem Biophys Res Commun 220:515
59. Shibayama-Imazu T, Sakairi S, Watanabe A, Aiuchi T, Nakajo S, Nakaya K (2003) J Cancer Res Clin Oncol 129:1
60. Masuda Y, Yoda M, Ohizumi H, Aiuchi T, Watabe M, Nakajo S, Nakaya K (1997) J Cancer 71:691
61. Masuda Y, Nakaya M, Aiuchi T, Hashimoto S, Nakajo S, Nakaya K (2000) Leukemia Res 24:937
62. Sakagami H, Satoh K, Hakeda Y, Kumegawa M (2000) Cell Mol Biol 46:129
63. Ishihara M, Takayama F, Toguchi M, Nakano K, Yasumoto E, Nakayachi T, Satoh K, Sakagami H (2000) Anticancer Res 20:4307
64. Okayasu H, Ishihara M, Satoh K, Sakagami H (2001) Anticancer Res 21:2387
65. Zhang W, Negoro T, Satoh K, Jiang Y, Hashimoto K, Kikuchi H, Nishikawa H, Miyata T, Yamamoto Y, Nakano K, Yasumoto E, Nakayachi T, Mineno K, Satoh T, Sakagami H (2001) Anticancer Res 21:3439
66. Jamison JM, Gilloteaux J, Nmassiri MR, Venugopal M, Nea DR, Summers JL (2004) Biochem Pharm 67:337
67. Sakagami H, Fujiwara E, Yokote Y, Akahane K, Asano K, Kochi M, Hara E, Shirahata A (2000) Anticancer Res 20:265

68. Nakamura C, Yasumoto E, Nakano K, Nakayachi T, Hashimoto K, Kusama K, Fukuda M, Sakashita H, Shirahata A, Sakagami H (2003) Anticancer Res 23:4797
69. Sakagami H, Satoh K, Ohata H, Takahashi H, Yoshida H, Iida M, Kuribayashi N, Sakagami T, Momose K, Takeda M (1996) Anticancer Res 16:2635
70. Shibayama-Imazu T, Sonoda I, Sakairi S, Aiuchi T, An W-W, Nakajo S, Itabe H, Nakaya K (2006) Apoptosis 11:1535

Top Heterocycl Chem (2008) 15: 201–252
DOI 10.1007/7081_2007_095

Published online: 22 December 2007

Advanced Dihydropyridines as Novel Multidrug Resistance Modifiers and Reversing Agents

Anamik Shah[1] (✉) · Jitender Bariwal[1] · Joseph Molnár[2] · Masami Kawase[3] · Noboru Motohashi[4]

[1]Department of Chemistry, Saurashtra University, University Road, 360005 Rajkot, India
anamik_shah@hotmail.com

[2]Institute of Medical Microbiology, University of Szeged, Dóm tér-10, 6720 Szeged, Hungary

[3]Faculty of Pharmaceutical Sciences, Matsuyama University, 4-2 Bunkyo-cho, Matsuyama-shi, 750-8578 Ehime, Japan

[4]Meiji Pharmaceutical University, 2-522-1 Noshio, Kiyose-shi, 204-8588 Tokyo, Japan

Abstract Dihydropyridines (DHPs) are recognized as one of the Ca^{+2} channel-blockers as a number of clinically used drugs are derivatives of various DHPs. Despite this, these DHPs are significantly potent in cancer chemotherapy along with clinically used drugs. This family of compounds is potent inhibitors of P-glycoprotein (Pgp), which are the main cause of the efflux of toxins the cells. This review mainly focuses on the Pgp inhibitory property of DHPs. The literature collection includes the latest developments in this area. This comprehensive review could also encompass their synthetic methodology for the preparation of the most active Pgp inhibitor DHPs. This article specifically covers the MDR reversal activity. However, this article does not cover their cardiovascular or rest of the pharmacological activities shown of DHPs.

Keywords Dihydropyridines (DHPs) · Multidrug resistance (MDR) · P-glycoprotein (Pgp)

1 Cancer and the Current Status in World

With more than 10 million new cases every year, cancer is one of the most devastating diseases worldwide. The disease burden is immense, not only for affected individuals but also for their relatives and friends. At the community level, cancer has posed considerable challenges for the health care systems in both poor and rich countries. The World Cancer Report (WCR) of 2007 provides a unique global view of cancer. It documents the frequency of cancer in different countries and trends in cancer incidence and mortality as well as describing the known causes of human cancer [1] (Table 1).

Table 1 The estimated numbers of new cases and deaths for each common cancer type [2, 3]

Cancer type	Estimated new cases	Estimated deaths
Bladder	67 160	13 750
Breast (Female – Male)	178 480–2030	40 460–450
Colon and Rectal (Combined)	153 760	52 180
Endometrial	39 080	7400
Kidney (Renal Cell) Cancer	43 512	10 957
Leukemia (All)	44 240	21 790
Lung (Including Bronchus)	213 380	160 390
Melanoma	59 940	8110
Non-Hodgkin's Lymphoma	63 190	18 660
Pancreatic	37 170	33 370
Prostate	218 890	27 050
Skin (Non-melanoma)	>1 000 000	<2000
Thyroid	33 550	1530

2 Role of ABC Transporters

Cancer chemotherapy is the treatment of choice in many malignant diseases. A major form of resistance against a variety of the antineoplastic agents currently used involves the function of a group of membrane proteins that extrude cytotoxic molecules, thus keeping intracellular drug concentration below a cell-killing threshold. Multidrug transporters belong to the super-

family of ATP-binding cassette (ABC) proteins, present in organisms from bacteria to humans. The medical significance of ABC proteins exceeds their role in cancer chemotherapy resistance; the transport function of several members was found to hinder the effective therapy of anticancer agents for many other widespread diseases (e.g., malaria and AIDS), and inherited diseases were also linked to mutations in these genes. The transport activity of ABC proteins has an important effect in general pharmacology, that is, in modulating the absorption, distribution, and excretion of numerous pharmacological cancer agents.

These substrate molecules exhibit a wide variety of chemical structures. Some ABC proteins facilitate the transport of inorganic ions, whereas others pump various organic compounds, including lipids, bile acids, glutathione and glucuronide conjugates, or even short peptides. Most ABC family proteins utilize the energy of ATP hydrolysis for this transport activity (active transporters), but some ABC transporters form specific membrane channels.

2.1
Structure of ABC Proteins

The typical structure of an ABC protein consists of membrane-embedded transmembrane domains (TMD) and ATP-binding domains. Typically, the transmembrane regions anchor the protein to the membrane and form a pore through which the transport of a surprisingly large variety of substrates occurs. The cytoplasmic nucleotide-binding domains provide the molecular compartment, where the energy of ATP is released. It is not known how the energy is conveyed from the ABC domains to the site of the transport and the precise mechanism of transport also remains elusive [4].

2.2
Role of Resistance in Cancer-The Players

Numerous clinical data revealed that the multidrug resistance (MDR) phenotype in tumors is associated with the overexpression of certain ABC transporters, called MDR proteins. The P-glycoprotein (Pgp, MDR1, ABCB1)-mediated MDR was the first discovered [5–7] and probably still is the most widely observed mechanism in clinical MDR [8–11]. Soon after the cloning and characterization of MDR1 it became evident that other efflux-pumps may also play a significant role in transport-associated drug resistance. There are two other ABC transporters that have been definitively demonstrated to participate in the MDR of tumors: the MDR protein 1 (MRP1, ABCC1), and the mitoxantrone resistance protein (MXR/BCRP, ABCG2) [11–15]. Furthermore, other human ABC proteins capable of actively transporting various compounds out of cells may also be their players in selected cases of MDR. These include ABCB4 (MDR3) and ABCB11 (sister Pgp or BSEP), two proteins re-

siding predominantly in the liver with a function involved in the secretion of phosphatidyl choline and bile acids, respectively, [16–18]. MDR3 has already been shown to transport certain drugs as well [19]. In addition to MRP1, five homologues (MRP2-MRP6) have been cloned. Overexpression of MRP2 (an organic anion transporter which can also extrude hydrophobic compounds) was definitively shown to confer cancer MDR [13, 20]. MRP3, an organic conjugate transporter, and MRP5, a nucleoside transporter, are also candidate proteins for causing certain forms of drug resistance [13].

2.3 Basic Mechanism of MDR in Cancer

The generally accepted mechanism of MDR is that the MDR proteins actively expel the cytotoxic drugs from tumor cells, maintaining the anticancer drug level below a cell-killing concentration. Drug extrusion mediated by these primary active transporters is driven by the energy of ATP hydrolysis. The most intriguing characteristic distinguishing the MDR proteins from other mammalian transporters is their wide substrate specificity. Unlike other selective (classical) transport proteins, multidrug transporters have been recognized and handled as a wide range of substrates. This wide substrate specificity explains the cross-resistance to several chemically unrelated compounds, the characteristic feature found in the MDR phenotype [8–11].

Different tumors with MDR protein overexpression (e.g., hepatomas, lung or colon carcinomas) often show primary (or intrinsic) resistance to cancer chemotherapy. In addition, cancer chemotherapy itself might induce the overexpression of these proteins, so that the MDR clones become less sensitive to chemotherapy (secondary drug resistance). Treatment failure due to MDR is also found in connection with conditions other than cancer, including some autoimmune disorders and infectious diseases [21–23].

2.4 Nomenclature, Basic Structure, and Membrane Topology of MDR Proteins

The ABC superfamily is one of the largest families in proteins. The most recent annotation of the human genome sequence revealed 48 genes for ABC proteins. The ABC proteins were grouped into seven sub-classes, ranging from ABCA to ABCG [24–28] based on genomic organization, order of domains and sequence homology. The phylogenetic tree of the ABC transporters involved in cancer MDR is presented in Fig. 1. A thick line and a circle label the three definite players, while the close relatives, which may have a role in drug resistance, are also indicated on this evolutionary diagram.

All ABC proteins contain at least three characteristic peptide sequences: the Walker A and B motifs, and the so-called ABC-signature sequence. Whereas the Walker motifs are present in several classes of ATP-binding pro-

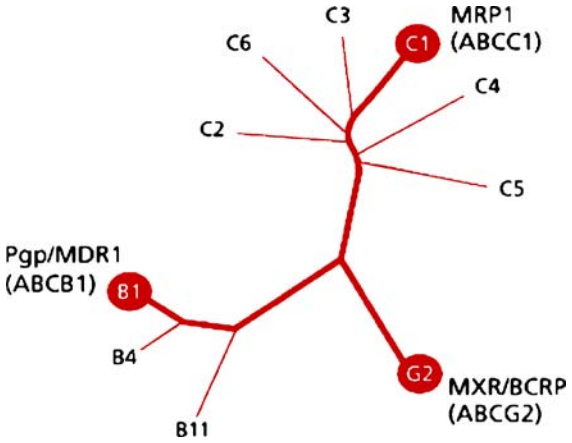

Fig. 1 Phylogenic tree of the MDR-related ABC transporters. The thick lines represent the proteins definitively involved in multi-drug resistance. (Reproduced from [4])

teins, the presence of the signature region is diagnostic for the ABC proteins. It is generally accepted that the minimum functional unit requirement for an ABC transporter is the presence of two transmembrane domains (TMDs) and two ATP-binding cassette (ABC) units. These may be present within one polypeptide chain ("full transporters"), or within a membrane-bound homo- or heterodimer of "half transporters" [8–11, 27, 28]. There are no high-resolution structural data presently available for any mammalian ABC transporter; therefore computer modelling and laborious biochemical experiments are necessary to elucidate the position and orientation of membrane spanning segments and other domains within the polypeptide chain. Figure 2 presents the most plausible membrane topology models for the key MDR-ABC transporters. As shown in Fig. 2, Pgp-MDR1 (ABCB1) is a "full transporter" with six TM helices in both TMDs of the protein, each followed by an ABC domain. A similar membrane topology has been predicted for ABCB4 (MDR3), and ABCB11 (sister Pgp) as well [24–28].

MRPs belong to the ABCC-subfamily, comprising 11 members in the human genome. Most of these proteins (ABCC1-6) have been identified as active, ATP-dependent membrane transporters for various anticancer agents and organic anions [12–14, 17]. In contrast to these active transporters, the cystic fibrosis transmembrane conductance regulator, ABCC7 (CFTR) is a regulated chloride channel, while ABCC8 (SUR1) and ABCC9 (SUR2) are called sulfonylurea receptors and are best described as intracellular ATP sensors, regulating the permeability of specific K^+ channels. Nothing is currently known about the function of ABCC10 and ABCC11 [11, 13, 27, 28].

The predicted membrane topology of MRP1 is shown in Fig. 2. According to the current notion, in addition to an MDR1-like core, MRP1 contains an additional *N*-terminal segment of about 280 amino acids. A major part of this

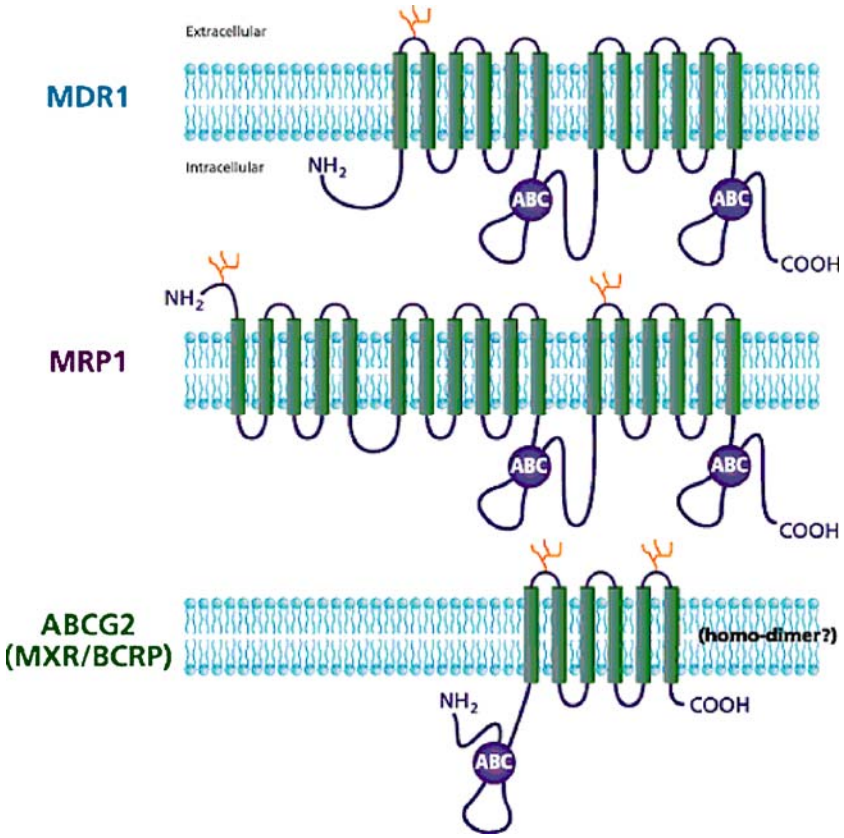

Fig. 2 Membrane topology models for the MDR-related ABC transporters. *Bars* represents predicted transmembrane helices, the *circles* represents the ABC domains, the *tree* are glycosylation sites at the extra cellular surface. (Reproduced from [4])

region is membrane-embedded with five transmembrane helices (TMD0), while a small cytoplasmic loop of about 80 amino acids (L0) connects this area to the core region [29–32]. Recent studies revealed that the TMD0 domain of ABCC1 does not play a crucial role in either the transport activity or the proper routing of the protein. However, the presence of the membrane-associated cytoplasmic L0 region (together with the core region) is necessary for both the transport activity and the proper intracellular routing of the protein. These studies indicate that the L0 region forms a distinct structural and functional domain, which interacts with the membrane and the core region of the MRP1 transporter [33].

The third ABC protein believed to play a role in clinical MDR, ABCG2 (MXR/BCRP) is a half transporter [15, 34], with a unique domain arrangement, where the ABC is located at the *N*-terminus (Fig. 2). This protein performs an active extrusion of hydrophobic, positively charged molecules

from the cells in an *N*-glycosylated mature form, and in contrast to many other ABC half-transporters is probably localized in the plasma membrane. Recently it has been shown that the human ABCG2 MDR protein forms an active homodimer for its transport function [35, 36].

There is no high-resolution three-dimensional structure available for any of the mammalian ABC transporters, thus the structural background of the MDR molecular mechanism is currently unresolved. A low-resolution structure of the MDR1 [37] indicates that the protein is embedded into the membrane as a cylinder with a large central pore, which is closed at the inner (cytoplasmic) face of the membrane. This structure also included an opening of this cylinder to the lipid phase.

The structure of a bacterial ABC transporter, MsbA of *E. coli*, has recently been determined by X-ray crystallography [38]. MsbA is a half-transporter with a TMD-ABC domain arrangement, organized as a homodimer. The structure reveals that each MsbA subunit contains a transmembrane domain with six transmembrane helices, an ABC-domain, and an "intracellular domain" which is composed of the three intracellular loops connecting the transmembrane segments to the ABC-domain. One of the most important conclusions of the MsbA structure is that the membrane-spanning segments of the polypeptide are indeed α-helices. The organization and interactions of these peptide domains will probably be a valuable foundation towards elucidating the structures of mammalian multidrug transporter ABC proteins.

3
Substrate Specificity of MDR-ABC Transporter

The three major MDR proteins are highly promiscuous transporters; they share the ability of recognizing and translocating a large number of structurally diverse, mainly hydrophobic compounds. In addition to their overlapping substrate specificity, each transporter can handle unique compounds.

Pgp is a transporter for large hydrophobic, either uncharged or slightly positively charged compounds, while the MRP family primarily transports hydrophobic anionic conjugates and extrudes hydrophobic uncharged anticancer drugs. The MRP1-related uncharged drug transport is quite an enigma, and is somehow linked to the transport or allosteric effect of cellular free reduced glutathione [13]. The exact spectrum of the MXR (ABCG2) transported substrates has not yet been explored in detail, and these studies are complicated by the variable substrate-mutants of MXR observed in the most recent studies [39].

In order to put the MDR substrates in their medical and pharmacological context, we present some of the key molecules in separate figures. Figure 3 shows anticancer drugs, which are, unfortunately for the patients, also MDR substrates. Figure 4 shows the chemical MDR modulators used experimen-

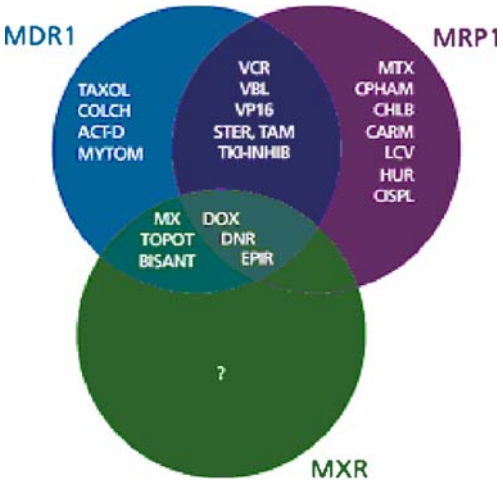

Fig. 3 Venn-diagram for selected compounds interacting with the key MDR-related ABC transporters. MDR-substrate anticancer agents. Abbreviations: VCR: vincristine, VP-16: etoposide, STER: steroids, TAM: tamoxiphen, TKI-INHIB: tyrosin kinase inhibitors e.g. STI-571, DOX: doxorubicine or adriamycin, DNR: daunorubicin, EPIR: epirubicin, MX: mitoxantrone, TOPOT: topotecan, iridotecan, BISANT: bisanthrone, COLCH: colchicin, ACT-D: actinomycin D, MYTOM: mytomycin, TX: methotrexate, CPHAM: cyclophosphamide, CHLB: chlorambucil, CARM: carmustine, LCV: leucovorin, HUR: hydroxy urea, CISPL: cisplatin, TAXOL: paclitaxel. (Reproduced from [4])

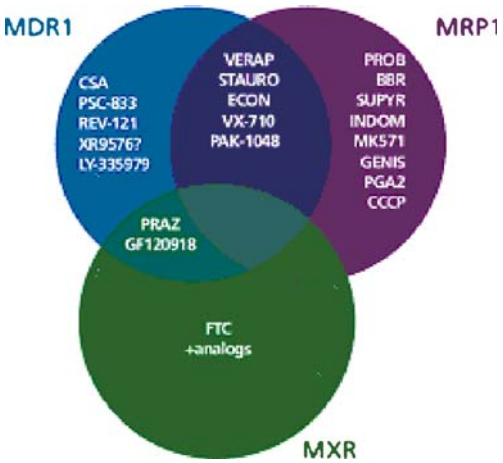

Fig. 4 Venn-diagram for selected compounds interacting with the key MDR-related ABC transporters. MDR-Modulating agents. Abbreviations: CSA: cyclosporin A, VERAP: verapamil STAURO: staurosporine, ECON: econazole, PRAZ: prazosine, FTC: fumitremorgin C, PROB: probenecide, BBR: benzbromarone, SUPYR: sulfinpyrazone, INDOM: indomethacin, GENIS: genistein, PGA2: prostaglandin A2, CCCP: chlorocarbonyl cyanide phenylhydrazine. (Reproduced from [4])

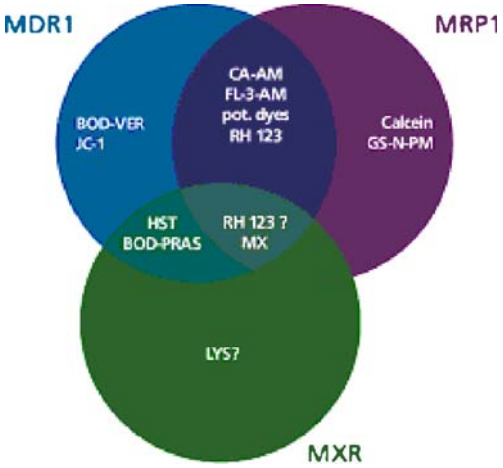

Fig. 5 Venn-diagram for selected compounds interacting with the key MDR-related ABC transporters. Fluorescent Compounds for the functional detection of multi drug resistance. Abbreviations: CA-AM: calcein AM, FL-3-AM: fluo-3AM, Pot. Dyes: potentiomeric dyes, RH123: rhodamine123, HST: Hoechst dye No. 33342, GS-N-PM: N-Pyrenemaleimide glutathione conjugate, BOD-VER: BODIPY verapamil, BOD-PRAS: BODIPY prazosin, MX: mitoxantrone, LYS: LysoTracker dye. (Reproduced from [4])

tally or in clinical trials, while Fig. 5 compiles the best-known MDR substrates used for functional diagnosis of the proteins [8–11, 40–43].

4 Cellular and Tissue Distribution of MDR-ABC Transporter

The tissue distribution of the MDR-ABC proteins is as varied as their substrate specificity. MRP1 is almost ubiquitously expressed, while the expression of Pgp is more restricted to tissues involved in absorption and secretion [8–11]. High-level MDR1 expression has also been shown in certain pharmacological barriers of the body, such as the blood–brain barrier (BBB) and the choroid plexus [44, 45]. It has been reported that MXR is highly expressed in the placenta, liver, and most interestingly, in various stem cells [34–46]. All multidrug transporters are localized predominantly in the plasma membrane. In polarized cells, Pgp-MDR1 is localized in the apical (luminal) membrane surface (e.g., in the epithelial cells of the intestine and the proximal tubules of kidney, or in the biliary canalicular membrane of hepatocytes) [47–49]. In contrast, MRP1 expression in polarized cells is restricted to the basolateral membrane. The expression of MRP2, MDR3, and of Sister Pgp (BSEP) is predominant in the canalicular membrane of hepatocytes, while MRP3 and MRP5 are expressed in the basolateral membranes of these

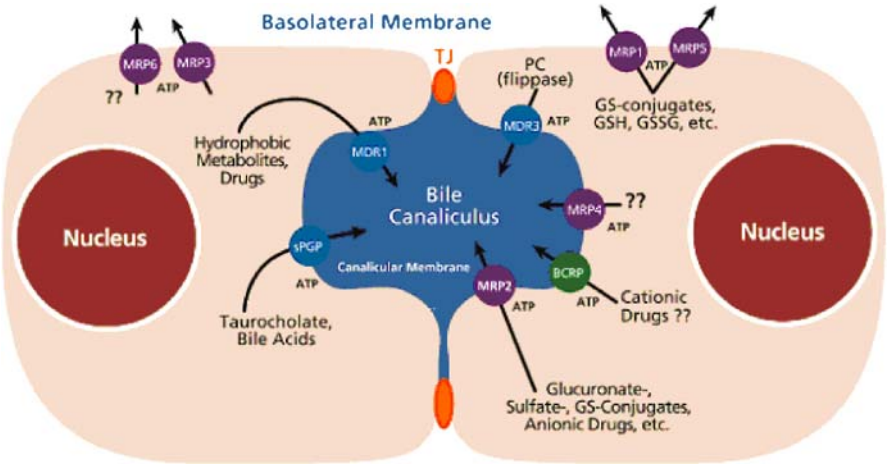

Fig. 6 Multi-drug transporters in the human liver hepatocytes. Abbreviations: *TJ* Tight junction. (Reproduced from [4])

cells (Fig. 6). MRP2 is also highly expressed in the apical membranes of kidney proximal tubules. In polarized cells, the MXR expression was reported to be mostly apical [50].

5 Molecular Mechanism of the Multidrug Pumps

Drug transport by MDR proteins requires the energy of ATP-hydrolysis, controlled by drug interaction, and closely coupled to the actual drug translocation. Interaction with the drug-substrate significantly enhances the basal ATPase activity of the multidrug transporters, that is, the transported drug-substrates increase the rate of ATP cleavage [51–53]. The schematic pictures of the proposed molecular mechanisms of the MDR1 and MRP1 proteins are depicted in Figs. 7 and 8.

The site(s) in multidrug transporters interacting with the drug-substrates are probably encoded in the transmembrane domains. Detailed mutagenesis studies of MDR1 and photochemical labeling with the reactive drug-derivatives revealed that transmembrane helices 5 and 6 (in the *N*-proximal transmembrane domain), helices 11 and 12 (in the C-proximal transmembrane domain), as well as the short cytoplasmic loops connecting these helices, are involved in the formation of an extended drug-binding site(s) [54]. There are strong indications that the hydrophobic substrates of MDR1 are recognized within the membrane bilayer or in its vicinity, and this type of recognition makes the MDR1 protein a highly effective pump, preventing the cellular entry of toxic compounds [55]. In the case of MRP1, a similar picture

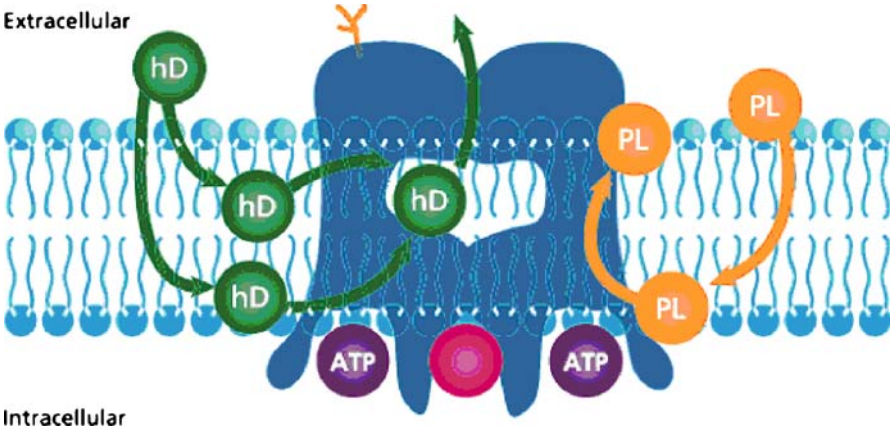

Fig. 7 Possible model for the molecular mechanism of multidrug transporters. MDR1-P-glycoprotein (substrates are recognized in, or near to the membrane lipid phase). Abbreviations: hD: hydrophobic drugs, PL: Phospholipids. (Reproduced from [4])

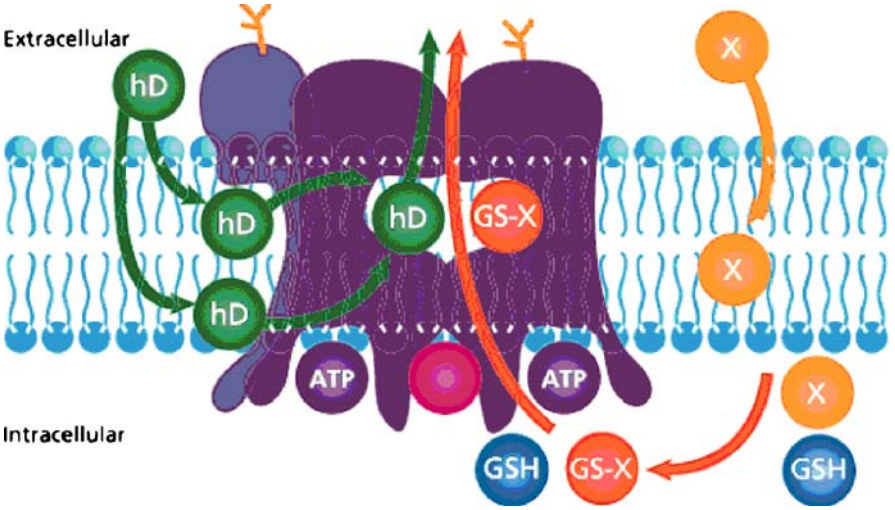

Fig. 8 Hydrophobic drugs and anionic conjugates, such as glutathione, are transported. The transport of some hydrophobic drugs may be coupled to reduced gluthatione (GSH) as GS-X molecules.. (Reproduced from [4])

has emerged. Recent studies have explored some parts of the transmembrane domains involved in drug interactions [56].

Based on the three-dimensional structures of bacterial ABC-units, the nucleotide-binding sites appear as shallow, more or less open grooves, forming atypical active sites. The close interaction of the two ABC units' likely results in the formation of a fully competent catalytic site. The regions connecting the ABC units to the transmembrane domains have an active key role

in the transfer of conformational information within the protein, and the ABC signature region may have a special function in this regard [57].

The transport and ATPase cycle of the MDR proteins is blocked by vanadate, a phosphate-mimicking inhibitory anion, which stabilizes a transition state intermediate of the ATPase cycle. An occluded nucleotide in the catalytic sites is locked within the ABC proteins in this interaction. Similar to their ATPase activity, the rate of the vanadate-dependent nucleotide occlusion in MDR-ABC proteins is greatly accelerated by the transported drug-substrates [58]. It has recently been shown that in the case of MDR1 the MDR1*MgADP*Vi complex exhibits a dramatically reduced binding affinity for the transported drug substrate, as compared to the MDR1*MgATP complex [59]. This observation suggests that the hydrolytic step triggers conformational changes, which reduces drug binding to the binding site (and presumably makes drug binding to another site favorable, from which the drug can be released to the extracellular space).

6 MDR Modulators

Considerable interest exists in circumventing MDR by a variety of strategies. The pharmacological approach began with the report by Tsuruo that the calcium channel blocker verapamil and a phenothiazine derivative trifluperazine potentiate the activity of vincristine [60]. MDR modulators (MDR reversal agents, MDR inhibitors, chemosensitizers) can be defined as compounds that permit the anticancer drug to reenter the cell by occupying the protein active or allosteric site(s), or by altering the physicochemical properties of the biomembranes.

The very heterogeneous chemical structure of the compounds with MDR reversal activity has prevented structure-activity studies, although most MDR-inhibiting molecules share a basic structural pattern comprising a cationic protonable site linked to an aromatic lipophilic part by a spacer of variable length [61]. Structure-activity relationship (SAR) studies yielded only qualitative indications [62–64] unless very homogeneous series of molecules are studied [65].

Most modulators identified interfere with Pgp by competitive or noncompetitive inhibition [66] of its drug effluxing activity. The modulators are normally Pgp substrates, but some of them can only bind to the protein but are not effluxed from the cells, and can thus be considered as pure antagonists. At least two other types of binding sites have been identified in the Pgp in addition to the ATP site, one for transport and other for modulation. It is therefore unknown whether one or more pharmacophores exist in the Pgp. The problem is further complicated by the possible existence of mutant forms of the Pgp in different tumors with modified responses to modulators.

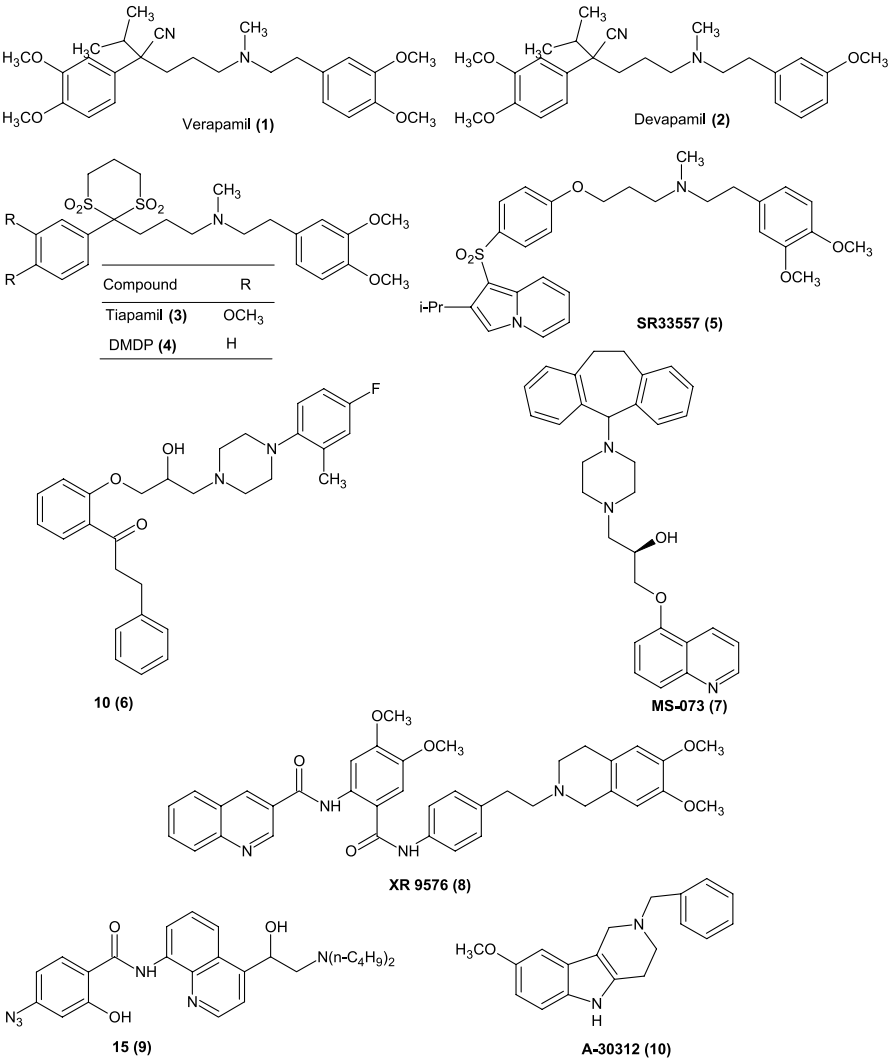

Fig. 9 Structures of various classes of drugs used as MDR reversal agents

Furthermore, the expression and function of the Pgp can be modulated by indirect mechanisms, such as interactions with membrane lipids [67] or inhibition of protein kinase C. The reversal of MDR is established using tumor cells lines that are made resistant by the exposure to an anticancer agent or by transfection of the *mdr1* or *mrp1* genes. The parameter most widely used to show the activity of MDR reversal agents is reversal factor (RF). This type of assay assumes that the reversal agent does not show inherent cytotoxicity at the concentrations tested.

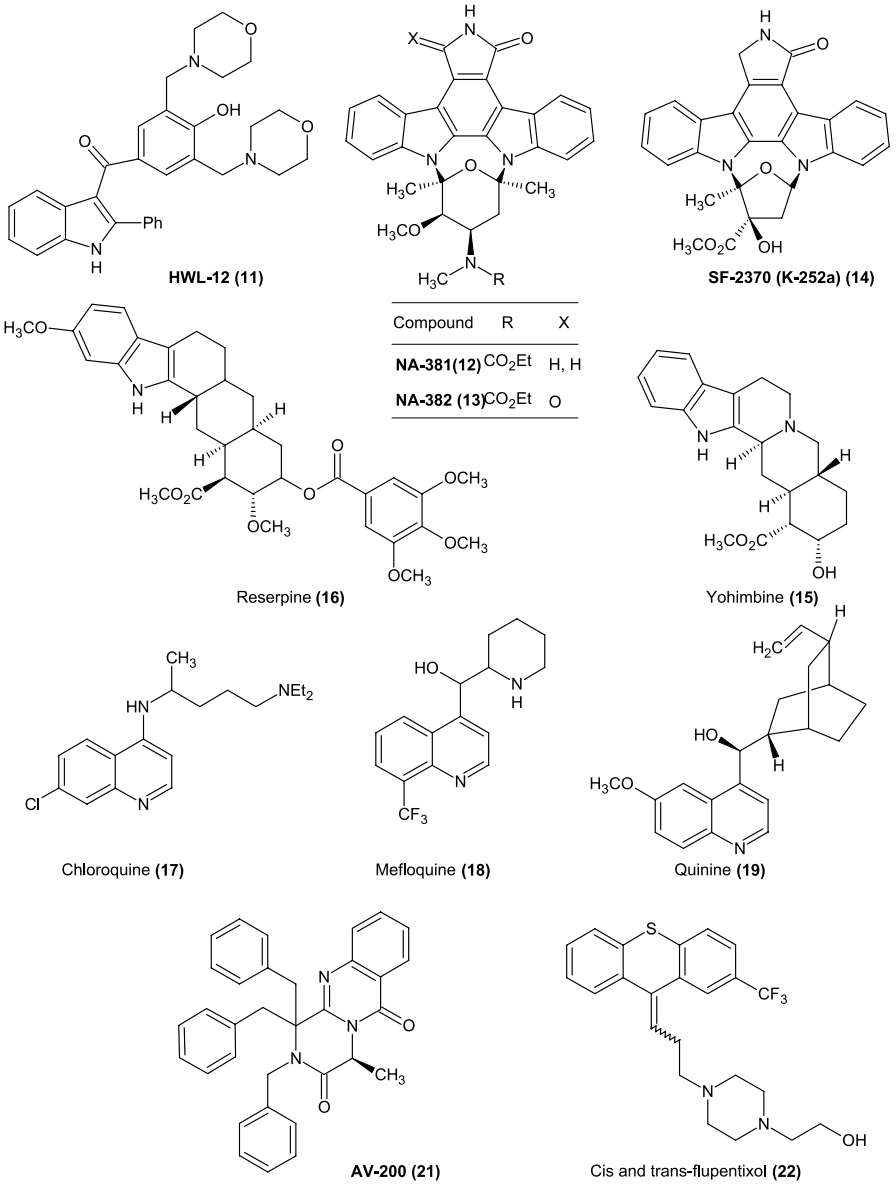

Fig. 10 Structures of various classes of drugs used as MDR reversal agents

The function and structure of ABC transporters along with their role and also in acquired immunodeficiency syndrome (AIDS) related lymphoma has been reviewed recently [68–72].

The MDR modulators according to their chemical structures includes the arylalkylamines including verapamil and its analogs (verapamil (**1**), de-

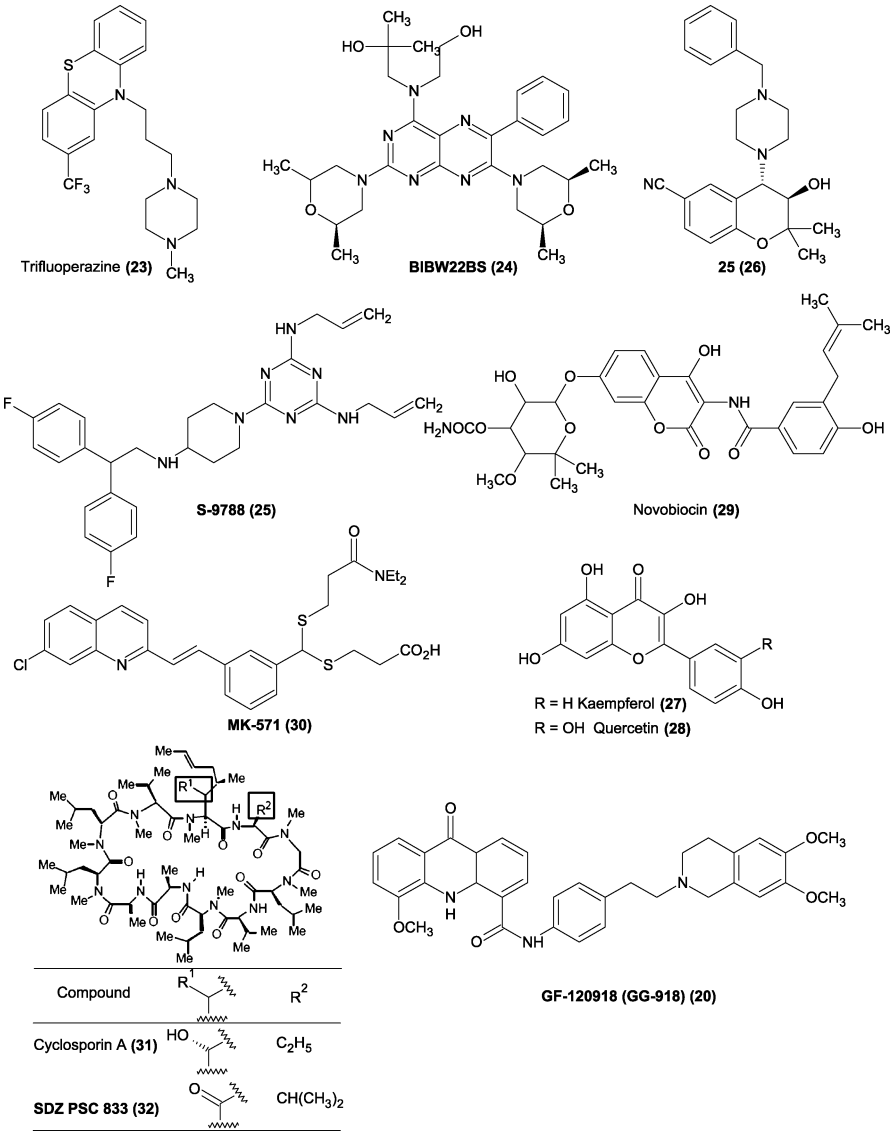

Fig. 11 Structures of various classes of drugs used as MDR reversal agents

vapamil (**2**) etc.), tiapamil and its analogs (tiapamil (**3**) and DMDP (**4**)) and miscellaneous arylalkylamines (**SR33557**) (**5**), aryloxypropanolamines (propafenone-related compound **10** (**6**)), quinolyloxypropanolamine derivatives (**MS-073**) (**7**), anthranylamides (**XR9576**) (**8**), salicylamides (**15**) (**9**) and related derivatives, nitrogen heterocycles including pyrrole derivatives (**A-30312 (10)**, **HWL-12** (**11**)), staurosporine and analogs (**NA-381** (**12**), **NA-382**

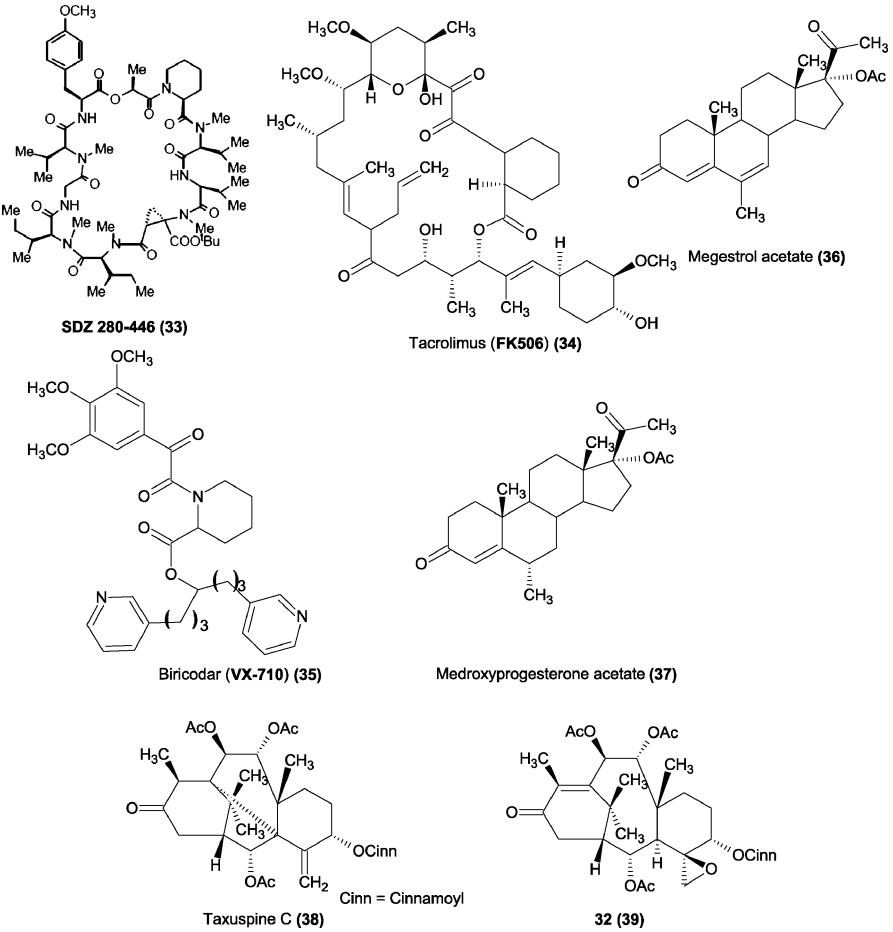

Fig. 12 Structures of various classes of drugs used as MDR reversal agents

(**13**) and **SF-2370** (**14**)), indole derivatives (yohimbine (**15**) and reserpine (**16**)), quinoline and isoquinoline derivatives (chloroquine (**17**), mefloquine (**18**) and quinine (**19**)), acridin-9-ones and related compounds (**GF-120918** (**GG-918**)) (**20**), quinazolines (**AV-200**) (**21**), phenothiazines and related heterocycles [73] (flupentixol (**22**) and trifluoperazine (**23**)), pteridines and related condensed heterocycles (**BIBW22BS**) (**24**), 1,3,5-triazines and related compounds (**S-9788**) (**25**), oxygen heterocycles includes pyran derivatives (**25**) (**26**), flavonoids (kaempferol (**27**) and quercetin (**28**)) and coumarin derivatives (novobiocin (**29**)), glutathione-related compounds as MRP reverters (**MK-571**) (**30**), cyclic peptides (cyclosporin A (**31**), **SDZ PSC 833** (**32**)), depsipeptides (**SDZ 280-446**) (**33**) and *macrolactones* and *macrolactams* (**FK506** (**34**) and **VX-710** (**35**)), steroids and related derivatives (mege-

strol acetate (**36**), medroxyprogesterone acetate (**37**)), terpenes and miscellaneous lipophilic compounds (taxuspine (**38**) and taxinine derivatives **32** (**39**)) and most importantly, dihydropyridines [74]. Structures of representing molecules from each class are given in Figs. 9, 10, 11, and 12.

7
DHPs as Potential MDR Reversal Agents

7.1
Historical Background

Some members of calcium channel blockers, such as nicardipine (**40**) and nimodipine (**41**), were identified as potent MDR antagonists. This early work stressed the lack of correlation between the calcium channel blocking and anti-MDR potencies [75]. It has been reported that DHPs bind to a site that is allosterically coupled to the receptor site which binds anticancer agents and other MDR reversal agents [76, 77]. DHPs are well recognized as "privileged structure" for their multi-receptor affinity [78, 79].

In the derivatives bearing a stereogenic center at C-4, such as nicardipine, nimodipine, nitrendipine (**42**), felodipine (**43**), isradipine (**44**) and niguldipine (**45**), both stereoisomers differ markedly in their potencies as calcium channel blockers but they are about equally effective as MDR reversal modulatores [80, 81]. This has led to use of the *R* isomers as MDR modulators, as in the case of dexniguldipine (**45**).

The ability to overcome MDR in many 1,4-DHPs varies considerably with the nature of the 3,5-substituents. The pyridylalkyl esters are specially suitable, as in the case of **NIK-250** (**46**) [82, 83] related derivatives bearing dihydro-1,4-dioxene, dihydro-1,4-dithiane or dihydropyran substituents at C-4 [84]. Other representatives of this group that contain an alkyl group at C-4 (**19** (**47**)) have also shown potent and selective anti-MDR activity [85]. Compounds **PAK-200** (**48**) [86, 87] and **PAK 104P** (**49**) [88] exemplify the absence of correlation between calcium channel and MDR antagonism, since neither *N*-alkyl-1,4-DHPs nor pyridines have significant calcium channel-blocking activity.

A systematic study of *N*-alkylated DHPs as MDR modulators has shown that the derivatives with an arylalkyl substituent on the nitrogen atom were more active than verapamil in potentiating the anticancer activity of vincristine in in vitro, but not in in vivo. However, the additional introduction of basic substituents in the C-3 ester group led to DHPs with in vivo activity [89] (e.g. **20** (**50**)).

The most widely studied anti-MDR DHPs is dexniguldipine hydrochloride (**45**) (DNIG) [90, 91]. In preclinical studies, it was particularly effective in taxane resistances of ovarian carcinoma MDR cell lines, where other chemosen-

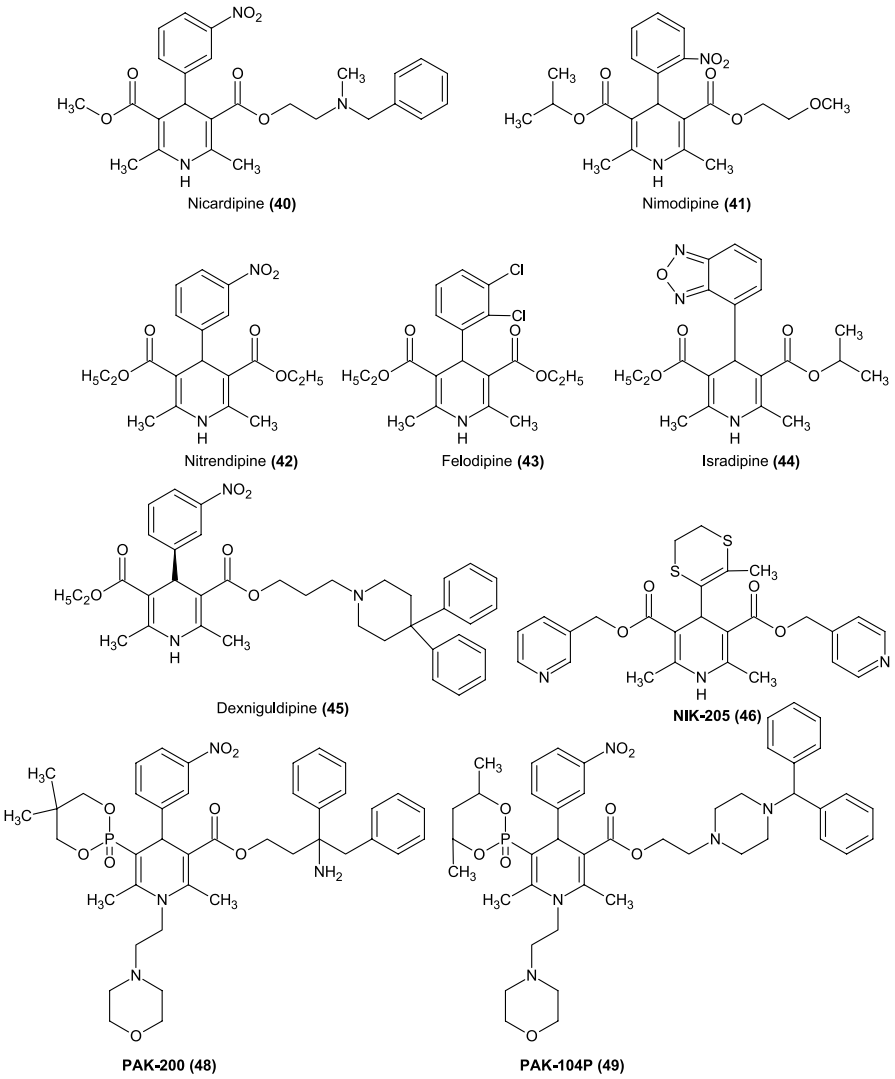

Fig. 13 Structures of various DHPs known as MDR reversal agents

sitizers were rather ineffective [92]. Besides its ability to reverse the MDR, dexniguldipine is a potent anticancer agent with well-documented anti-protein kinase C activity [93, 94] and it inhibits cleavage and relegation reactions of eukaryotic DNA topoisomerase I in a similar fashion to campothecin [95].

Over and above these clinically established molecules, some other DHPs are also noted for their potent MDR reversal property.

[3*H*]azidopine (**51**), a radioactive photoactive DHPs calcium channel blocker, photolabels Pgp in membrane vesicles from KBCl cells. This pho-

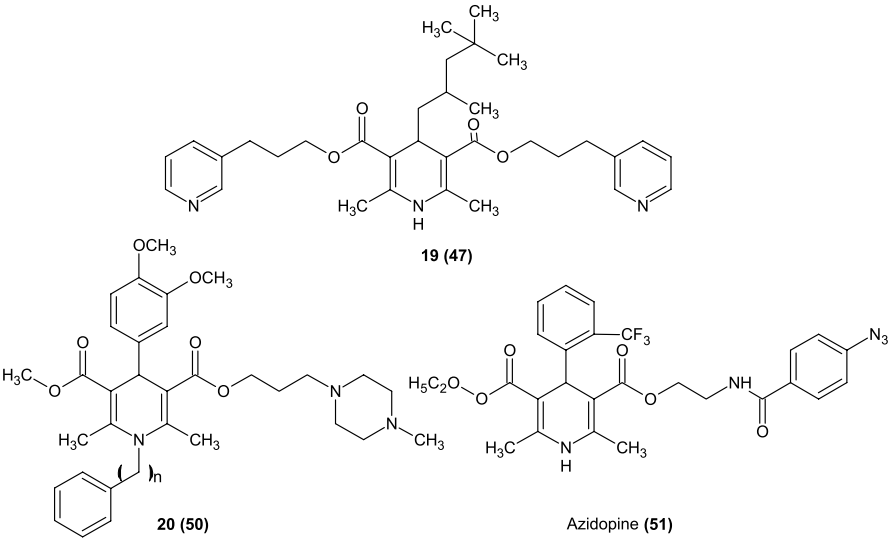

Fig. 14 Structures of various DHPs known as MDR reversal agents

tolabeling was almost completely inhibited by the excess DHPs analogues that reversed or lowered drug resistance. In contrast, the labeling was not significantly inhibited by analogues that do not reverse resistance. Inferencing from this M. Kamiwatari et al. screened a series of DHPs analogues for their MDR reverting ability in human KB cells. **PAK-1** (**52**) was found to be a weaker calcium channel-blocking activity when compared with other members of the series including the standard nifedipine but completely reverses the drug resistance. Nifedipine (**53**) and other analogs are better at blocking calcium channels than **PAK-1**, however, but they only partially reverse the resistance [96].

Two isomers of teludipine (**54**), *R*-enantiomer (**GR66234A**) and *L*-enantiomer (**GR66235 A**) which were originally developed as a new lipophilic calcium channel blocker by Glaxo were evaluated for daunorubicin resistance reversal activity and found to be more effective than verapamil. Additionally, the difference in activity was also found on different cells. Verapamil and the enantiomers of teludipine are more active in ARNII cells than in MCF 7/R cells. There were no apparent differences in cellular daunorubicin accumulation between ARNII and MCF 7/R following exposure to teludipine and no differences in intracellular daunorubicin distribution in the presence of either MDR reversing agent were observed [97].

In an attempt to characterize chemosensitizer domains on Pgp, Boer et al. found that DHPs label multiple chemosensitizer domains on Pgp, distinct from the vinblastine interaction site. **(–)-[3*H*]BZDC-DHPs** (**55**) represents a valuable tool to characterize the molecular organization of

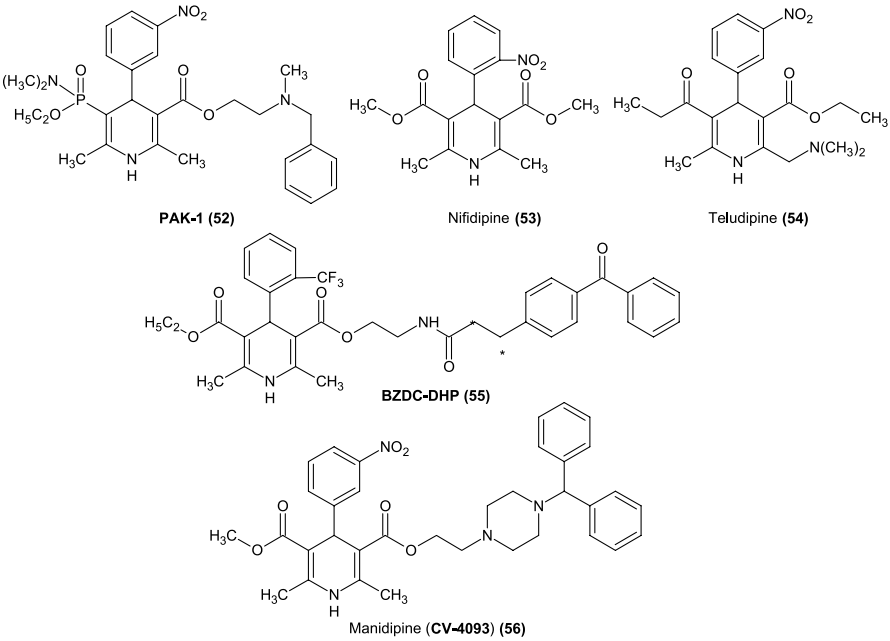

Fig. 15 Structures of new DHPs

chemosensitizer-binding domains on Pgp by both reversible binding and photo-induced covalent modification. It provides a novel simple screening assay for Pgp active drugs. Photoreactive DHPs, **BZDC-DHPs** (2,6-dimethyl-4-(2-(trifluoromethyl)-phenyl)-1,4-dihydropyridine-3,5-dicarboxylic acid {2-[3-(4-benzoylphenyl) propionylamino]ethyl} ester ethyl ester), and its tritiated derivative were synthesized as novel probes for human Pgp. (–)-**[3H]BZDC-DHPs** specifically photolabeled Pgp in membranes of multidrug-resistant CCRF-ADR5000 cells. In reversible labeling experiments, a saturable, vinblastine-sensitive and high-affinity binding component was present in CCRF-ADR5000 membranes but absent in the sensitive parent cell line. Binding was inhibited by cytotoxics and known chemosensitizers with a Pgp. The DHPs such as niguldipine and a structurally related pyrimidine stereoselectively stimulated reversible (–)-[3*H*]**BZDC-DHPs** binding, suggesting that more than one DHPs molecule can bind to Pgp at the same time [98, 99].

B859-35, a DHP, which was previously shown in vitro to be highly effective in reversing MDR of Pgp positive tumor cell lines, such as the adriamycin (ADR) resistant erythroleukemia F4-6RADR cells. In in vivo studies, **B859-35** was highly active in reducing the number of viable cells in the resistant tumor nodule by $67 \pm 9\%$. This model provides evidence that even in vivo, MDR modulators can be effective in reversing drug resistance. In addition, it presents a potentially useful and rapid preclinical system for in vivo studies on the modification of drug resistance [100].

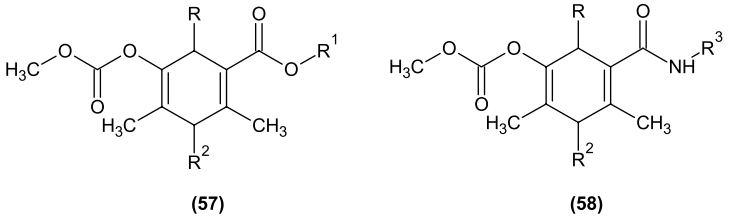

Fig. 16 Structures of (**57**) and (**58**) DHPs

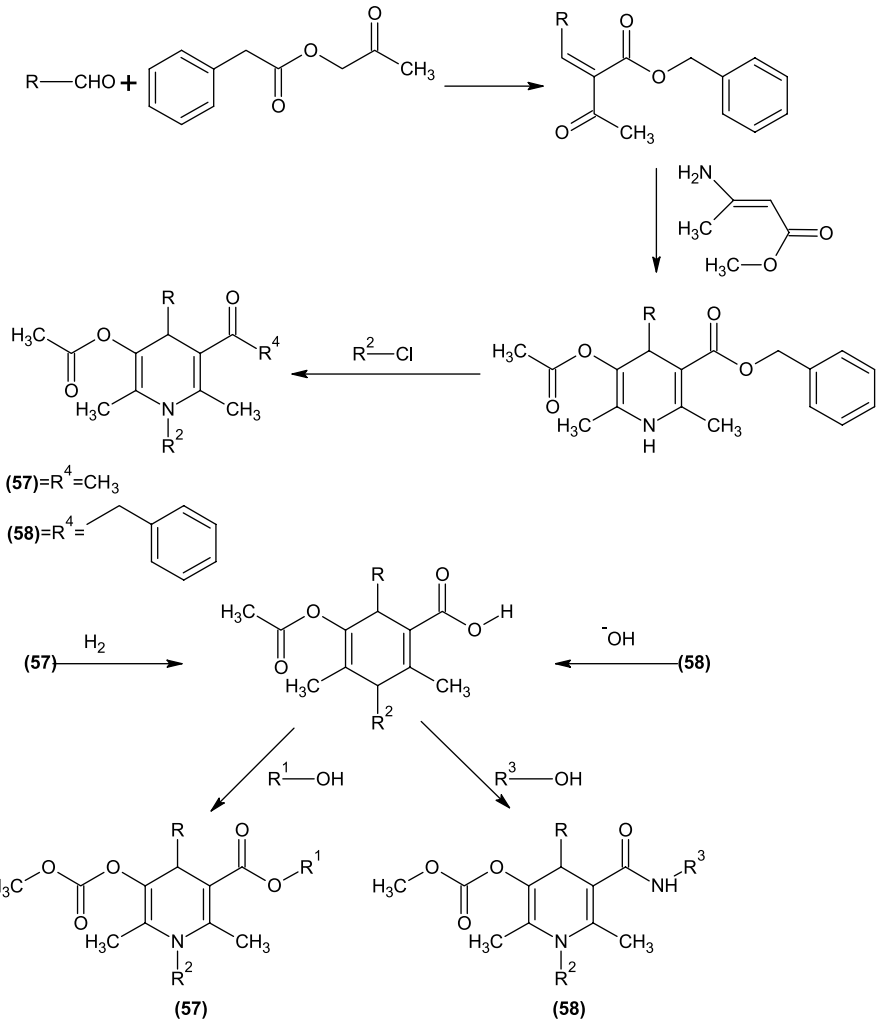

Scheme 1 Synthetic scheme for (**57**) and (**58**) series

The modulatory activity of the novel pyridine analogue **PAK-104P** on MRP-mediated resistance to doxorubicin and paclitaxel was investigated in two doxorubicin-selected human tumor cells [HT1080/DR4 (sarcoma) and HL60/ADR (leukemia)]. The experiment demonstrated that **PAK-104P** was effective in restoring cellular doxorubicin concentrations in resistant cells to levels comparable to those obtained in parental cells. In addition to reversing Pgp-mediated MDR, the pyridine analogue provides an example of an effective in vivo modulator of MRP-mediated MDR [101].

From QSAR studies of several hundreds of DHPs, seven DHPs were found to be very active. From these predictions, manidipine (**CV-4093**) (**56**), a newly synthesized DHPs calcium channel blocker, was predicted to be an extremely active MDRR agent. The probability for the DHP to show MDRR activity is very high (99%), owing to the presence of several biophores [102].

Earlier, *N*-alkylated 1,4-DHPs of general formula (**57**) & (**58**) were synthesized that were found to possess a remarkable activity for overcoming resistance to anticancer agents. The DHPs were used in combination with anticancer agents. The DHPs were also found very potent in enhancing the therapeutic activity of anticancer agents [103].

In continuation of this, new *N*-alkylated 1,4-DHPs derivatives were synthesized and their ability to overcome MDR was examined in vincristine-resistant P388 cells (P388/VCR cells). DHPs that possessed an arylalkyl substituent on the DHPs ring nitrogen (**3e** (**59**), **3f** (**60**), **4d** (**61**)) were more potent than verapamil in potentiating the cytotoxicity of vincristine against P388/VCR cells. However, neither drug effectively enhanced the antitumor activity of vincristine in tumor-bearing mice. Introduction of basic nitrogen-containing substituents on the side chain of 1,4-DHPs gave improved activity in vitro and in vivo. The piperazine derivative **12c** (**62**) and **12o** (**63**) were more than ten times as potent as verapamil in vitro. Four compounds (**12a**

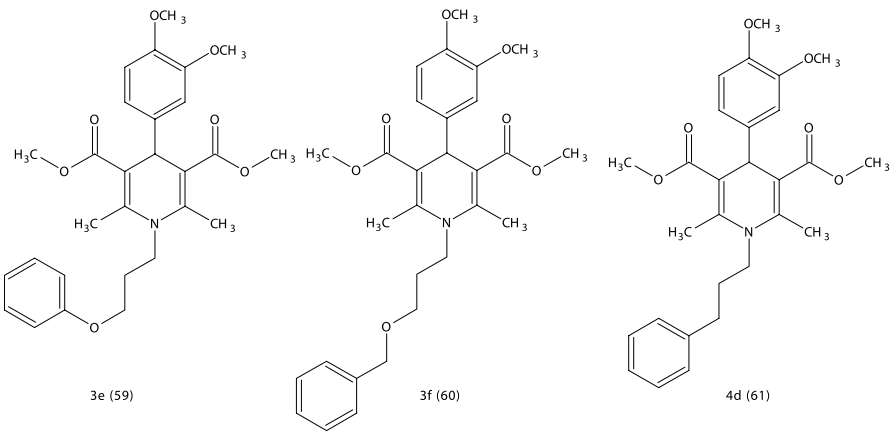

Fig. 17 Structures of various *N*-substituted DHPs

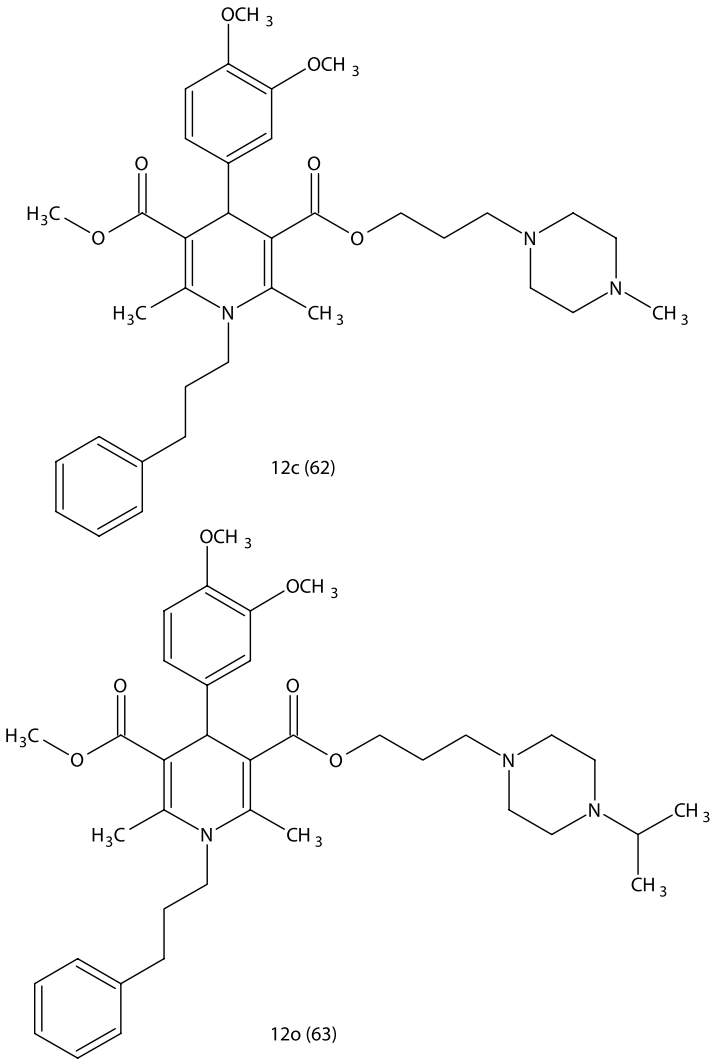

Fig. 18 Structures of various *N*-substituted DHPs

(**64**), **12h** (**65**), **12p** (**66**) and **13a** (**67**)) selected for in vivo testing showed superior antitumor activity in P388/VCR-bearing mice in combination with vincristine. The SARs of the compounds are discussed [89].

Further, eleven 4-phenyl-3,5-diacetyl-1,4-DHPs substituted at the C-4 phenyl ring were synthesized and compared for their cytotoxic activity and MDR reversing activity in in vitro assay systems. Among them, compound **G7** (**68**) showed the highest cytotoxic activity against human promyelocytic leukemia HL-60 and human squamous cell carcinoma HSC-2 cells. However, no compounds tested produced radicals at pH 7.4–12.5. The activity of Pgp

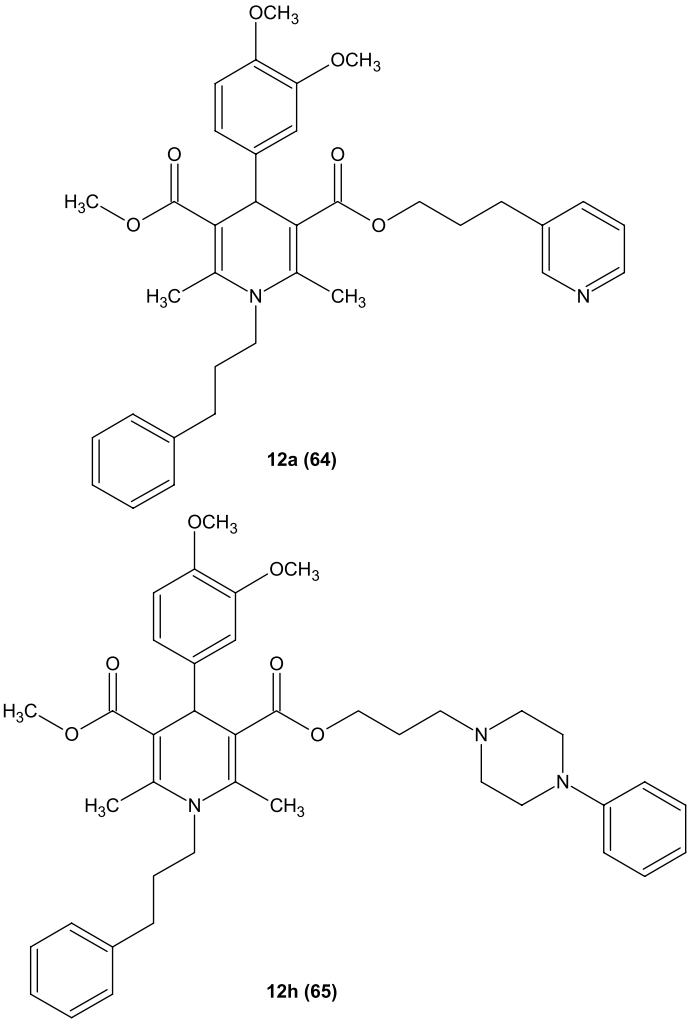

Fig. 19 Structures of various *N*-substituted DHPs

responsible for MDR in tumor cells was reduced by compounds **G2** (**69**), **G3** (**70**), **G6** (**71**), **G5** (**72**), **G8** (**73**), **G1** (**74**) and **G11** (**75**). However, compounds **G4** (**76**), **G7** (**68**) and **G10** (**77**) were hardly active, while **G9** (**78**) did not show a MDR reversing effect at 2.0–20 μg/mL [104]. These DHPs also showed synergistic interaction with ampicillin and erythromycin on *E. coli* K12LE140/F'lac. The antibacterial effect of ampicillin was enhanced by most analogues, but none of the DHPs had any effect on a MDR clinical isolate of *E. coli* Gy-1/$A_{res}Er_{res}$ [105].

When the acetyl group of G series was replaced with the benzoyl group (3, 5-dibenzoyl-1,4-DHPs) for GB series and test for their antibacterial effect

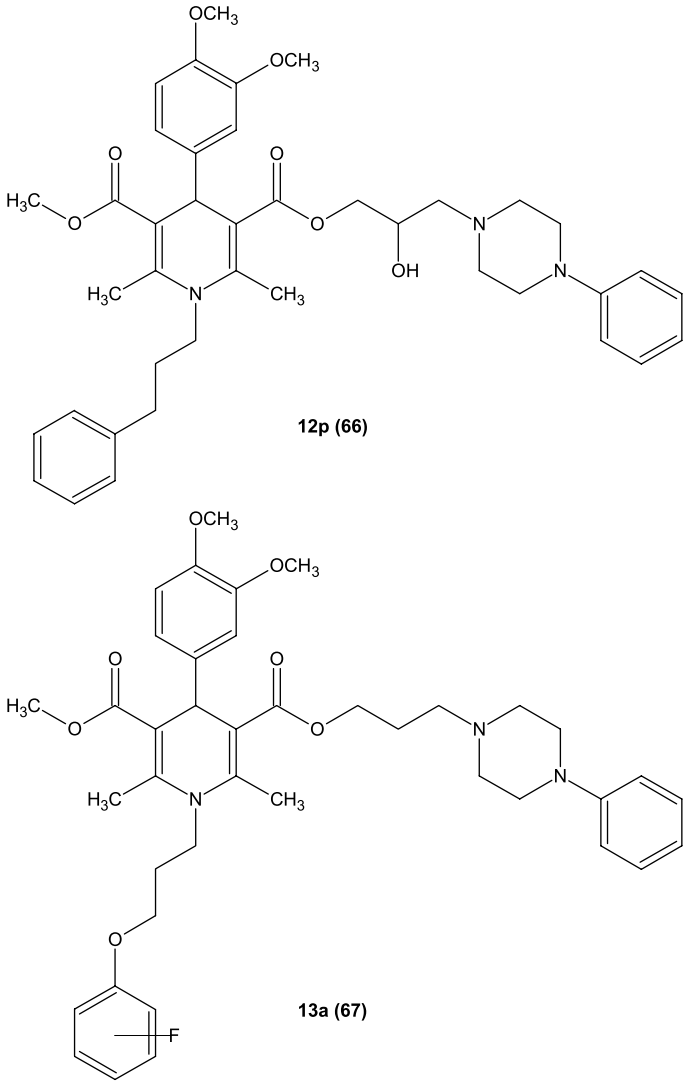

Fig. 20 Structures of various *N*-substituted DHPs

along with Erythromycin, the MIC values are reduced against clinical isolates of *E.coli* Gy-1/$A_{res}Er_{res}$. Compound **GB12** (**79**) was the most effective in enhancing the activity of erythromycin [106]. Fifteen 4-phenyl-3,5-dibenzoyl-1,4-dihydropyridines substituted at the 4-phenyl ring were synthesized and compared for their cytotoxic activity and MDR reversing activity in in vitro assay systems. Among them, 2-CF_3, 2-Cl and 3-Cl derivatives showed the highest cytotoxic activity against human oral squamous carcinoma (HSC-2) cells. The activity of Pgp response for MDR in tumor cells was reduced

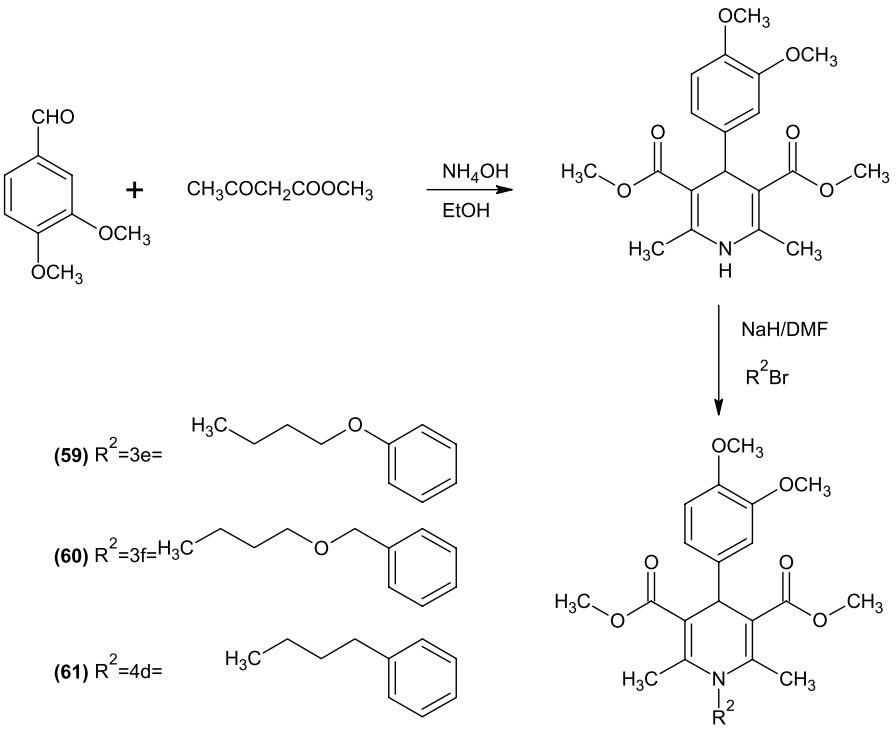

Scheme 2 Synthetic scheme for DHP (**59**), (**60**) and (**61**)

by some of new derivatives, verapamil and nifedipine. These data suggest that 3,5-dibenzoyl-4-(3-chlorophenyl)-1,4-dihydro-2,6-dimethylpyridine (**GB12**) can be recommended as a new drug candidate for MDR cancer treatment [107].

Further, it was found that 4-(2′trifluoromethylphenyl)- (**GB5**) (**80**) and 4-(3′chlorophenyl)-3,5-dibenzoyl-2,6-dimethyl-1,4-dihydropyridine (**GB12**) showed not only MDR reversal activity, but also markedly higher cytotoxicity against two human oral tumor cell lines than one normal cell (human gingival fibroblast). In this report, tumor-specificity of **GB5** and **GB12** was first confirmed using a total of seven human cells, including four tumor cell lines (squamous cell carcinoma HSC-2, HSC-3, submandibular carcinoma HSG, promyelocytic leukemia HL-60) and three normal cells (gingival fibroblast HGF, pulp cells HPC, periodontal ligament fibroblast HPLF). **GB5** and **GB12** were also capable of inducing apoptotic cell death in HL-60 and HSC-2 cells, monitored by using several apoptosis associated markers, such as internucleosomal DNA fragmentation, activation of caspases-3, -8 and -9 and expression of pro-apoptotic proteins and an anti-apoptotic protein (Bcl-2). It was proposed that cell death was induced by **GB5** and **GB12** via radical-mediated reaction [108].

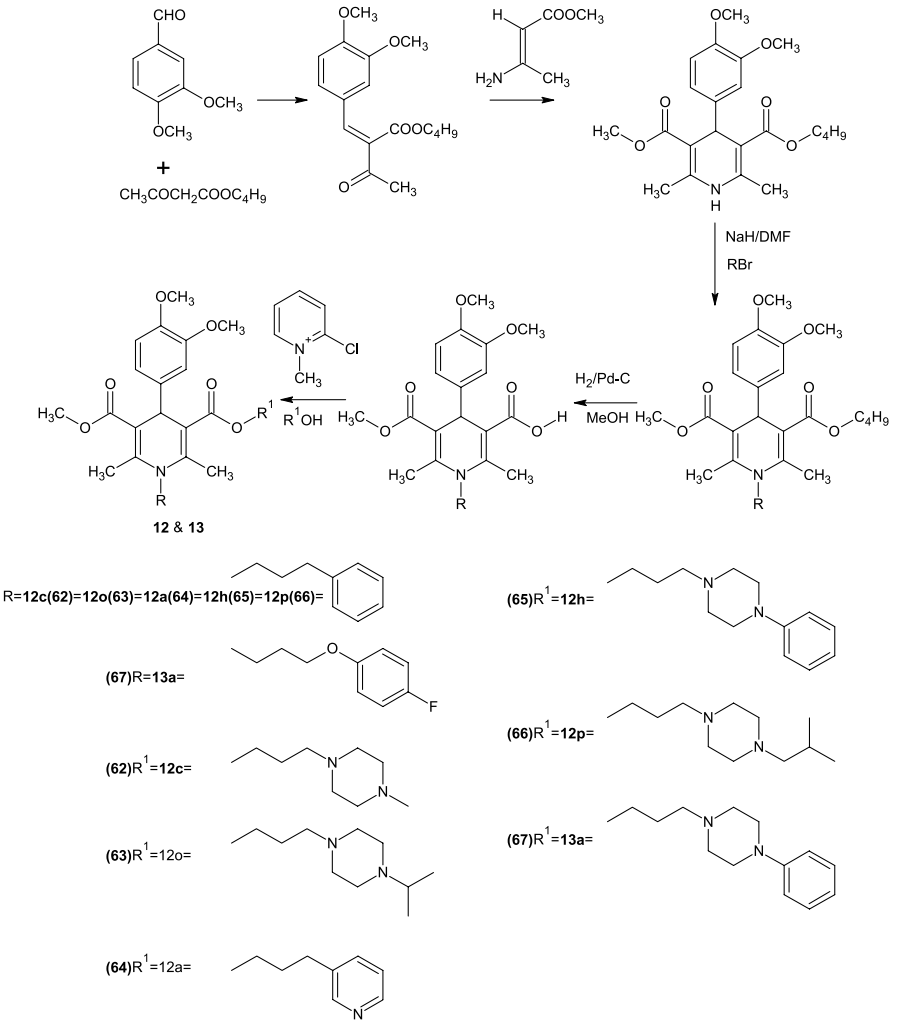

Scheme 3 Synthetic scheme for DHPs (**62**) to (**67**)

When the effects of DP series (selective molecules from G and GB series) namely 3,5-diacetyl and 3,5-dibenzoyl-1,4-DHPs were investigated on vascular functions in vitro by comparing their mechanical and electrophysiological actions in rat aorta rings and single rat tail artery myocytes, respectively, along with their MDR reversing activity in L5178 Y mouse T-lymphoma cells transfected with MDR1 gene, **DP7** (**GB4**) (**81**) was found to inhibit L-type Ca^{2+} current recorded in artery myocytes in a concentration-dependent manner, with IC_{50} (M) values ranging between 1.12×10^{-6} and 6.90×10^{-5}. Other derivatives that are tested for MDR reverting activity tested in L5178 MDR cell line, **DP1** (**G11**) (**75**), **DP2** (**G2**) (**69**) and **DP7**, exhibited an MDR rever-

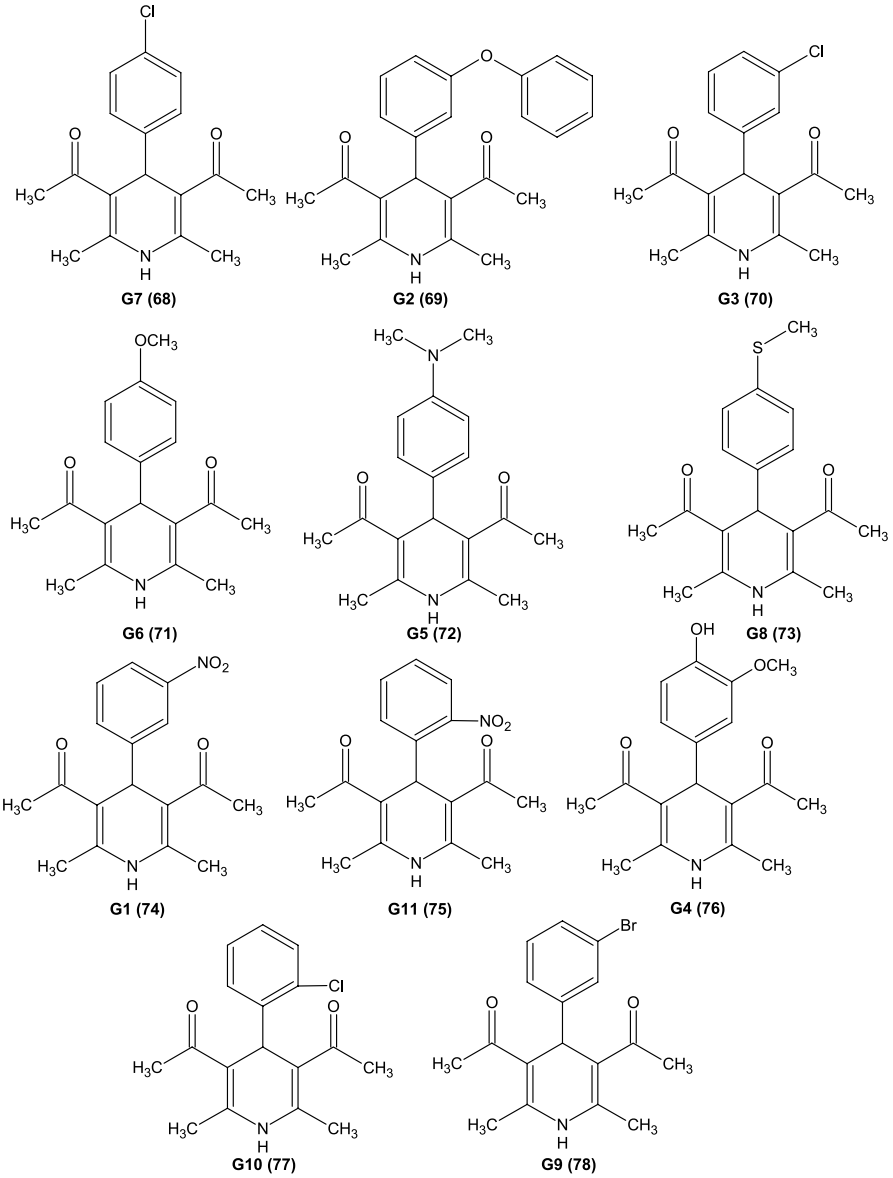

Fig. 21 Structure of G series DHPs

sal activity, with IC_{50} values ranging between 3.02×10^{-7} and 4.27×10^{-5}, **DP7** being the most potent. From this study, **DP7** represents a lead compound for the development of potent DHPs MDR chemosensitizers devoid of vascular effects [109]. **DP7** has been shown to be a powerful Pgp inhibitor, almost devoid of cardiovascular effects, but capable of inhibiting liver

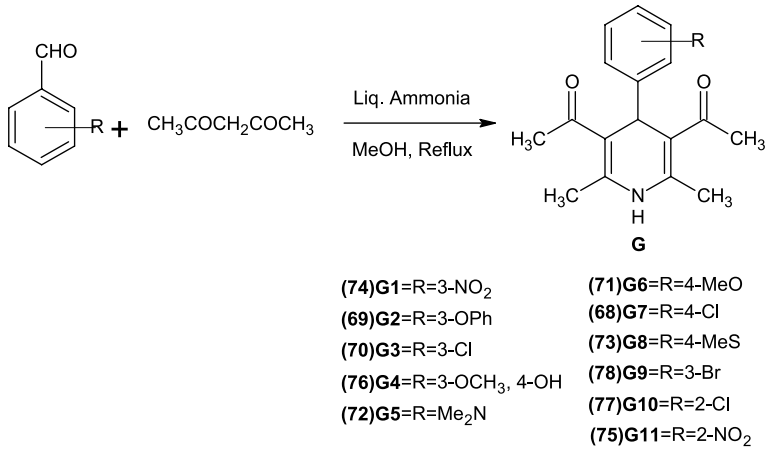

Scheme 4 Synthetic scheme for G series DHPs

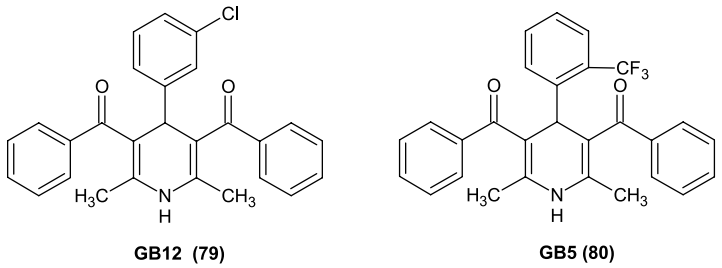

Fig. 22 Structures of active GB DHPs

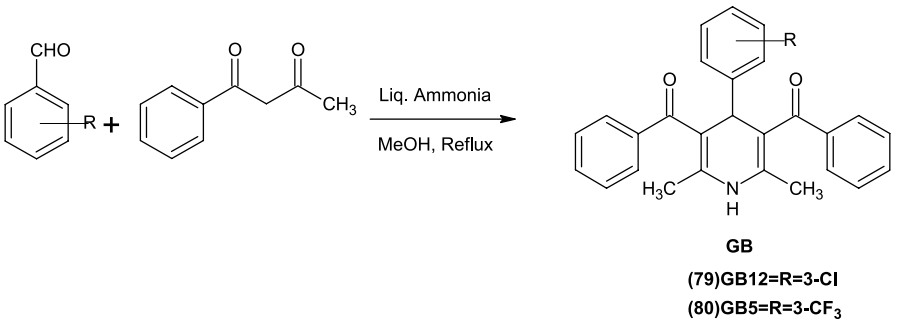

Scheme 5 Synthetic scheme for GB series DHPs

CYP3A. **DP7** is now considered a lead compound for the development of novel DHPs which do not affect CYP enzyme system but still retain the activity towards ABC-efflux transporters [110, 111]. Cardiac effects of **DP7** using

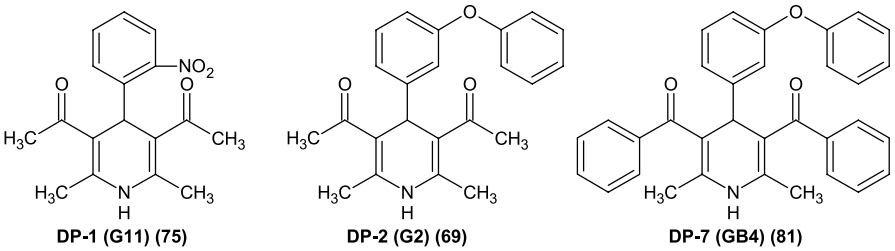

Fig. 23 Structures of active DP DHPs

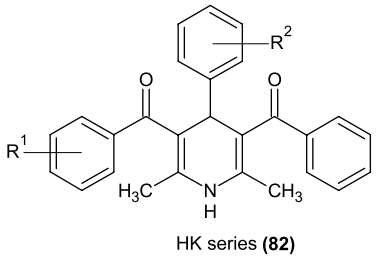

Fig. 24 Common structure of HK series DHPs

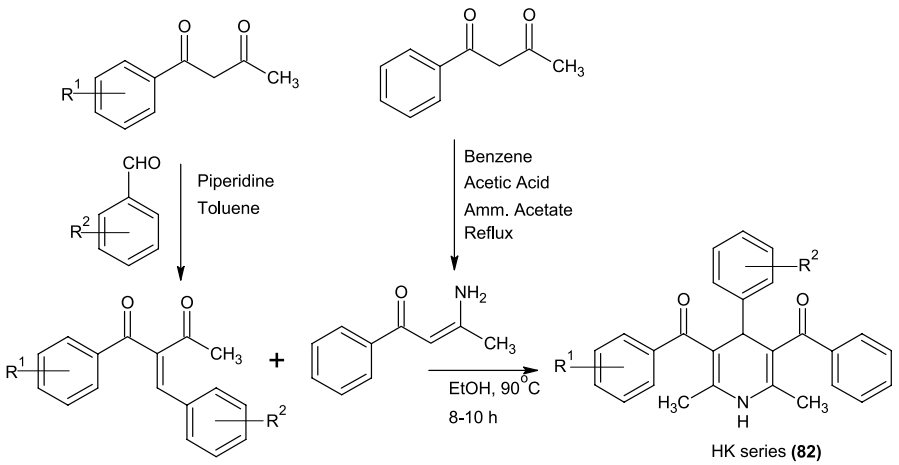

Scheme 6 Synthetic scheme for HK series DHPs

Langendorff-perfused rat heart have been investigated and compared to that of nifedipine. Nifedipine decreased concentration-dependent ($IC_{50} = 8.89 \pm 1.09 \times 10^{-8}$ M) left ventricular pressure leaving unaltered coronary perfusion pressure, whereas **DP7** did not affect these parameters. Nifedipine did not modify QRS and QT intervals of ECG [112]. It has also been investigated that neither pyruvate kinase nor lactate dehydrogenase was inhibited by **DP7**

which, however, inhibited concentration-dependently both Pgp ATPase activities, with IC50 value of 1 μM [113].

In an attempt to further modify the **DP7**, various modifications were done, particularly on C-5 benzoyl group and C-4 phenyl ring as in HK series (**82**) [114].

In a recent study by E. Azizi et al., the work apparently initiated on basis of results from DP series, new series of DHPs modified at C-4 position carrying 1,3-thiazole substituted at C-2 has been investigated for inhibitory effects on cell proliferation of parental and moderately resistant T47D breast cancer cells. New DHPs were also studied for their effects on MDR1 reversal agent in these breast cancer cells and compared to verapamil as standard. Two DHPs of **7a** (**83**) and **7d** (**84**) showed noticeable potentiation of doxorubicin cytotoxicity compared to doxorubicin alone, particularly in resistant cells. This effect was similar to that of verapamil. Compound **7d** showed the highest effect on resistant cells. Two newly synthesized DHPs derivatives, **7a** and **7d**, are showing promise as potential new MDR1 reversal agents [115].

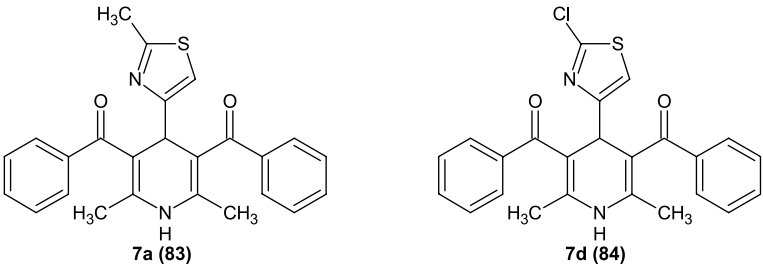

Fig. 25 Structure of **7a** (**83**) and **7d** (**84**)

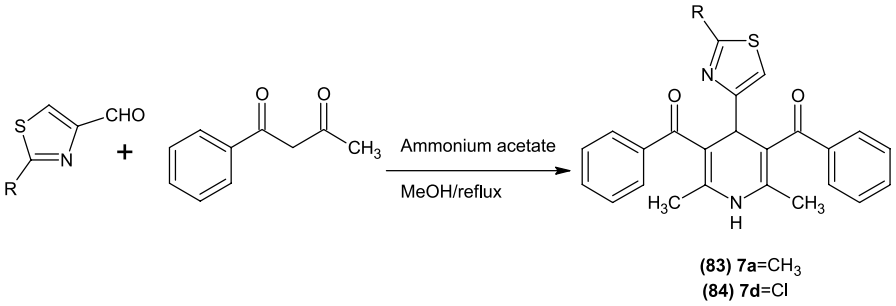

Scheme 7 Synthetic scheme for DHPs (**7a** (**83**) and **7d** (**84**))

Some new hybridized derivatives of 1,4-DHPs having *m*-nitrophenyl group at C-4 and changing variable substitutions at C-3 and C-4 were investigated for their inhibitory activity for Pgp by flow cytometry in the MDR human colon

cancer cell lines (COLO320) and in human MDR1 gene-transfected mouse lymphoma cells (L 5178 Y). The cytotoxicities of the DHPs were also examined against human normal and cancer cell lines. The majority of the tested DHPs proved to be effective inhibitors of rhodamine 123 outward transports. Some DHPs displayed higher cytotoxic activity against four human oral tumor cell lines against three normal human oral cell lines. New ring substituents could prevent the oxidation of the ring of the aromatic compound. Some DHPs at the higher concentration were found to be toxic as indicated by deformation in the cell size and the intracellular structures of the cells were changed during the short-term experiments. The majority of the DHPs tested were shown to enhance the drug retention in the cells by inhibiting the efflux-pump activity. Among the DHPs, **DL8-10** (**85**, **86**, **87**), **DL12** (**88**), **DL13** (**89**) and **DL15** (**90**) were found to be the most effective MDR modulators. These DHPs caused a dose-dependent inhibition of the MDR Pgp [116].

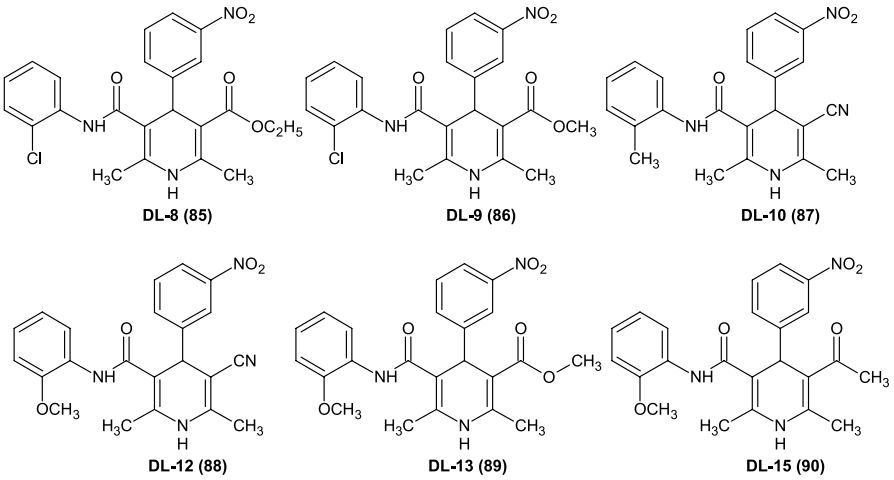

Fig. 26 Structure of active DL DHPs

Further, symmetrical di-carbamoyl and di-carboxamide derivatives (CDU (**91**), CDS (**92**) & DA (**93**) series) were synthesized and studied for their anti-Pgp activity, most of the studied compounds were moderately active against L-5178 cells [117].

The structures of the DHPs reported from the author's research group were proved by X-ray crystallographic studies [118–120]. Some similar DHPs were also found to be very potent against *M. tuberculosis* [121, 122].

New C-4 fused heterocyclic systems in DHPs, **AHC-52** (**94**) (methyl 2-(*N*-benzyl-*N*-methylamino) ethyl-2,6-dimethyl-4-(2-isopropyl-pyrazolo[1,5-*a*]-pyridine-3-yl)-1,4-dihydropyridine-3,5-dicarboxylate) and its pyridine analog **AHC-93** (**95**) has also been reported to reverse MDR by inhibiting Pgp [123–125].

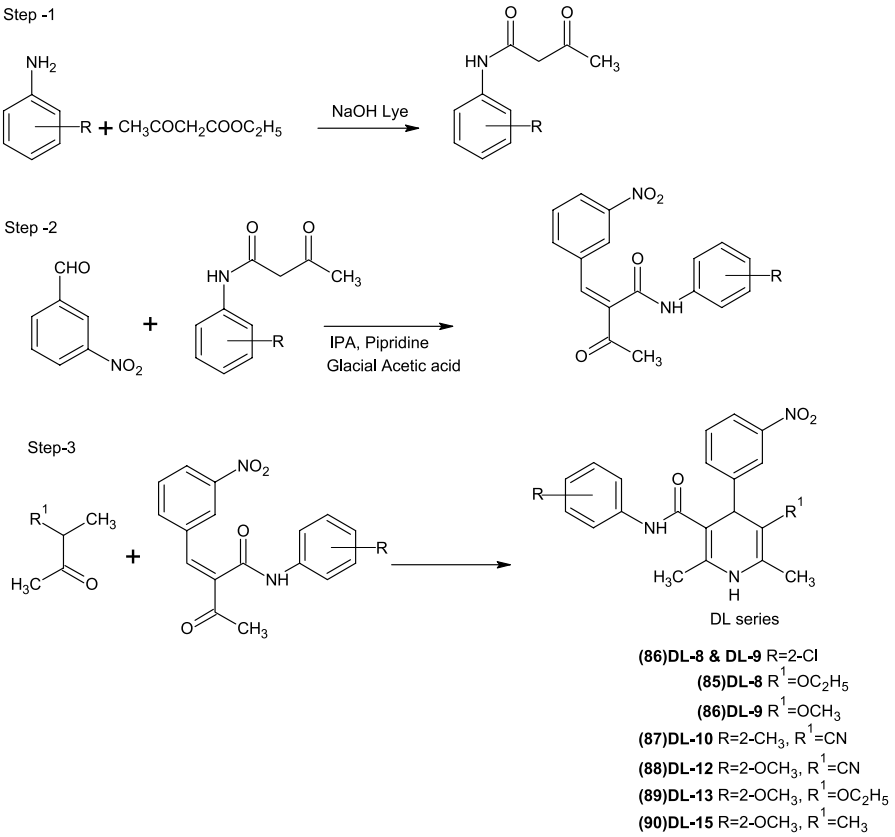

Scheme 8 Synthetic scheme for DL series DHPs (**85** to **90**)

A series of 4-aryl-1,4-DHPs and corresponding aromatized 4-arylpyridines has been synthesized aimed to enhance MDR activity, while minimizing Ca^{2+} channel binding. Synthesized DHPs were evaluated for [^{3}H]vinblastine accumulation studies. 4-Aryl-1,4-DHPs and all 4-arylpyridines can successfully restore intracellular accumulation of vinblastine in a resistant human breast adenocarcinoma cell line, MCF-7/adr, which overexpresses Pgp. The most potent DHPs (**Ip** (**96**), **Iq** (**97**) and **IIf** (**98**)) led to an approximately 15-fold increase of vinblastine accumulation. All of the DHPs tested were also able to substantially reduce IC50 values of daunomycin and increase its cytotoxicity in MCF-7/adr-resistant cells, confirming the results of the vinblastine accumulation studies. Out of these DHPs, eight have a negligible effect on calcium channel binding over the concentration range from 15 to 2500 nM [126].

(±)3-(3-(4,4-diphenylpiperidin-1-yl)propyl) 5-methyl 4-(3,4-dimethoxyphenyl)-2,6-Dimethyl-1,4-dihydropyridine-3,5-dicarboxylate ((±)-**DHPs-014**) (**99**), is a new 4-aryl-1,4-DHPs that can reverse MDR mediated by the ATP-

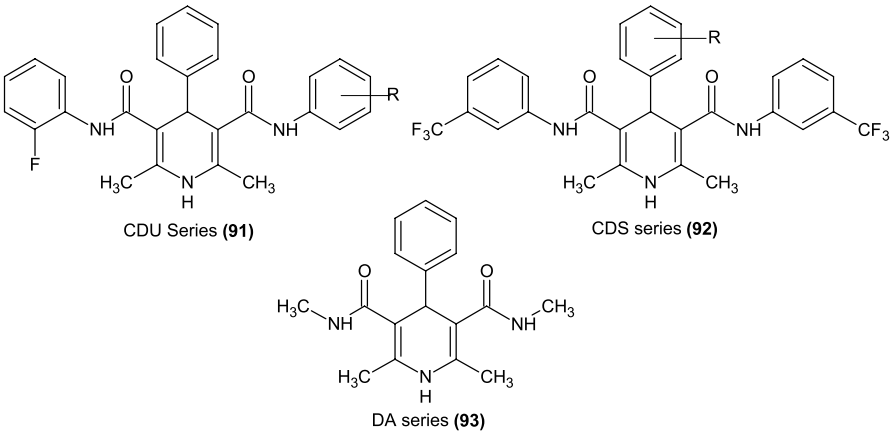

Fig. 27 Structure of CDU (**91**), CDS (**92**) and DA (**93**) series DHPs

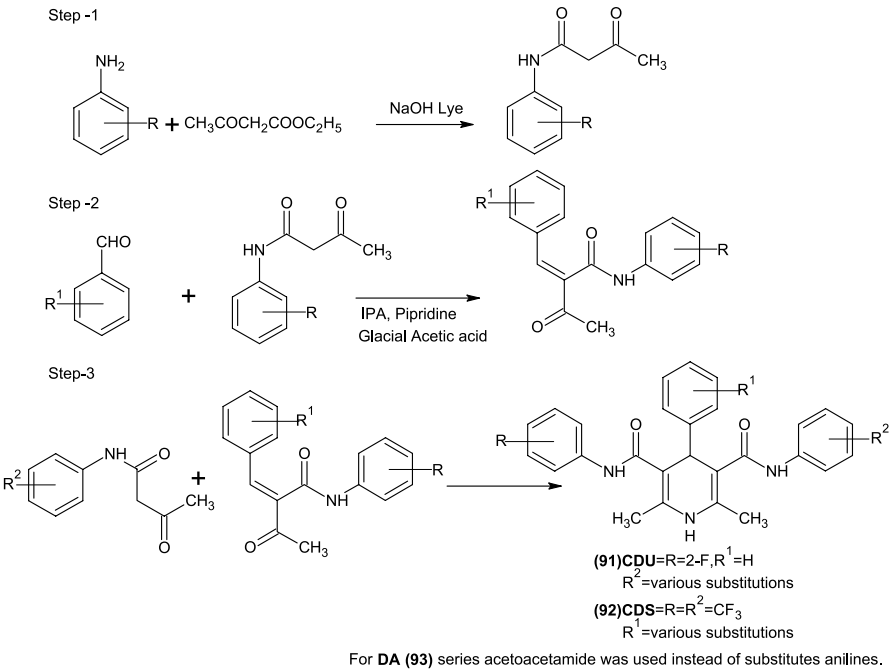

Scheme 9 Synthetic scheme for CDU (**91**), CDS (**92**) and DA (**93**) series DHPs

binding cassette (ABC) transport proteins, Pgp, MDR1 and breast cancer resistance protein; this DHP exhibits negligible Ca^{2+} channel-blocking activity. Three intravenous (1, 2 and 5 mg/kg) and two oral (25 and 50 mg/kg) doses were administered to female Sprague-Dawley rats. A two-compartment model with nonlinear elimination best characterized the pharmacokinetic

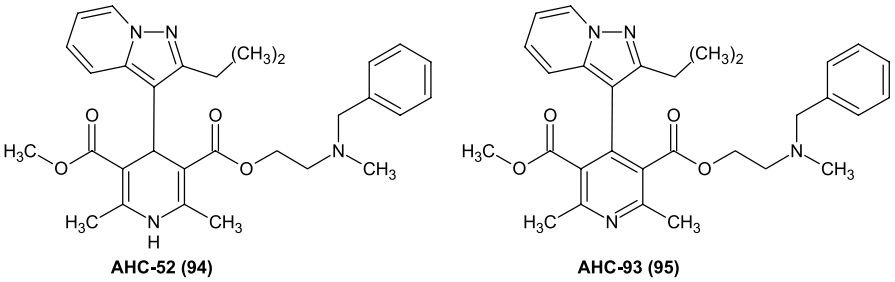

Fig. 28 Structure of AHC-52 and AHC-93

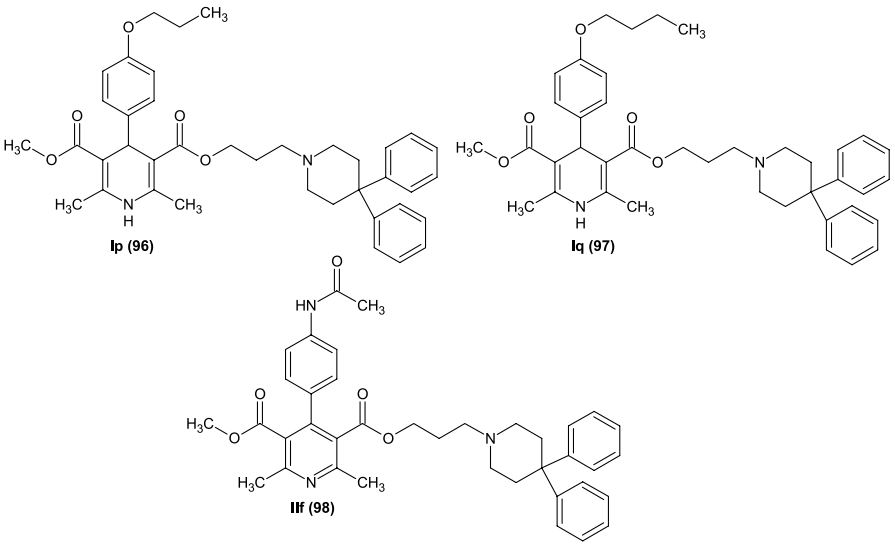

Fig. 29 Structures of active DHPs from I (**96**, **97**) and II (**98**) series

profiles after intravenous and oral administration in rats. The terminal half-life of (±)-**DHPs-014** (**99**) increased and the systemic clearance significantly decreased at higher doses, indicating nonlinear elimination. The dose-dependent clearance is likely due to the saturation of metabolism. The apparent volume of distribution of this DHP was 2.0 L/kg in rats and was unchanged with increasing intravenous doses. The estimated oral bioavailability was 8.2%. The poor bioavailability is likely due to the poor solubility of the compound, as well as to substantial first-pass elimination [127].

While comparing **DHPs-014** (**99**) with niguldipine, nicardipine, nifedipine, and nitrendipine for their effects on breast cancer resistance protein (BCRP) mediated efflux and on the cytotoxicity of the BCRP substrate and chemotherapeutic agent mitoxantrone, **DHPs-014** (**99**) was found to be a potent BCRP and Pgp inhibitor in vitro. This DHP may be promising agents for

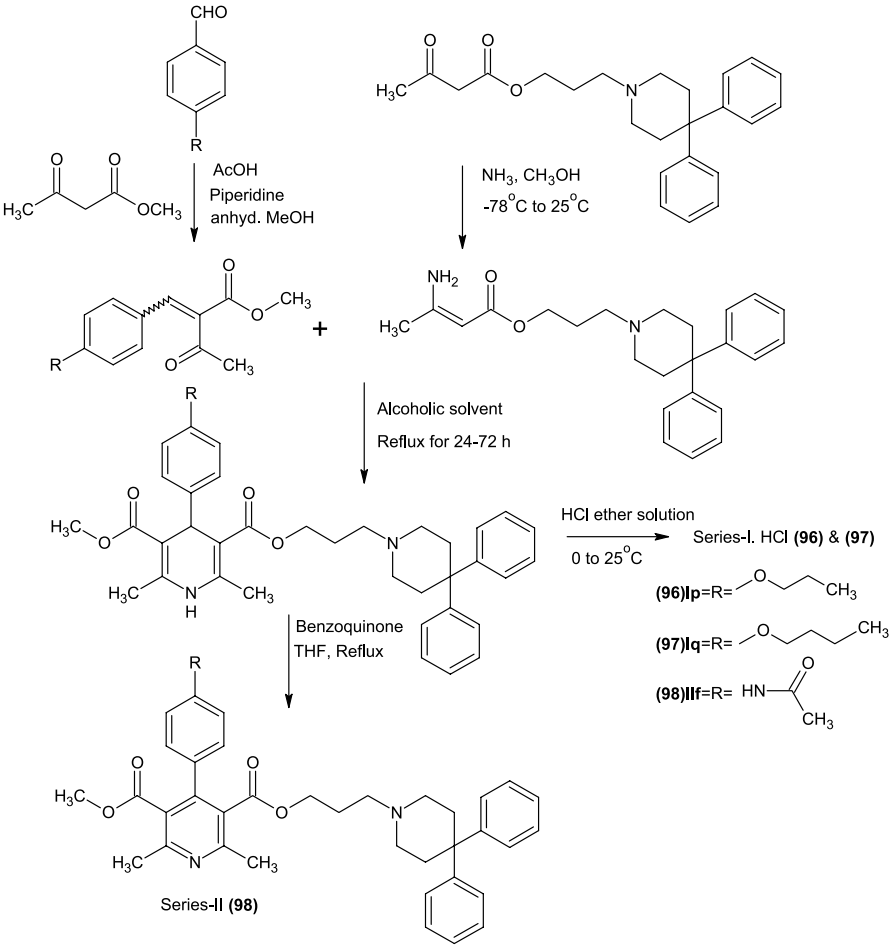

Scheme 10 Synthetic scheme for series I (**96, 97**) & II (**98**) DHPs

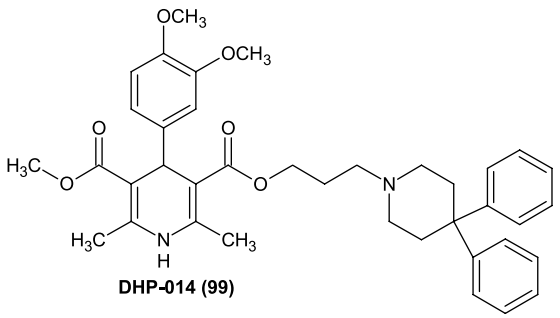

Fig. 30 Structure of DHPs-014

clinical application due to their potent inhibition of both BCRP and Pgp. This study represents the first report that DHPs and pyridines as potent inhibitors of BCRP [128].

Quantitative structure-activity/pharmacokinetic relationships (QSAR/QSPKR) for a series of synthesized DHPs and pyridines as Pgp (type **I** (**100**) & **II** (**101**)) inhibitors was generated by 3D molecular modelling using SYBYL and KowWin programs. A multivariate statistical technique, partial least square (PLS) regression, was applied to derive a QSAR model for Pgp inhibition and QSPKR models. Cross-validation using the "leave-one-out" method was performed to evaluate the predictive performance of models. For Pgp reversal, the model obtained by PLS could account for most of the variation in Pgp inhibition ($R^2 = 0.76$) with fair predictive performance ($Q^2 = 0.62$). Nine structurally related 1,4-DHPs drugs were used for QSPKR analysis. The models could explain the majority of the variation in clearance ($R^2 = 0.90$), and cross-validation confirmed the prediction ability ($Q^2 = 0.69$) [129].

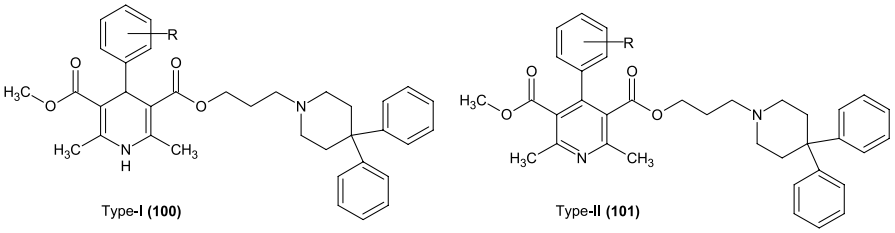

Fig. 31 Structure of Type-I (**100**) and Type-II (**101**) DHPs

Optically pure DHPs substituted at C-4 with 3-nitro phenyl as shown in structure **1** (**102**) are capable of potentiating the activity of anticancer agents in tumor cells (synergism). This overcoming of resistance is not only limited to resistance to cytostatics but also to other therapeutics such as for the treatment of malaria [130].

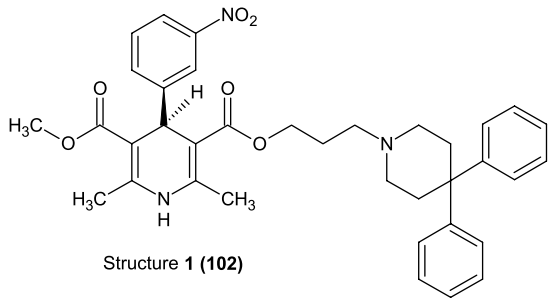

Fig. 32 Structure of 1 (**102**)

In a similar vein, several newly synthesized 4-aryl-1,4-DHPs and respective aromatized pyridines on drug efflux mediated by MDR associated protein 1 (MRP1, ABCC1) in human small cell lung cancer H69AR (overexpressing MRP1) and wild type H69 cells, five out of sixteen DHPs and six out of nine pyridines were found to significantly increase the intracellular accumulation of vinblastine in resistant H69AR cells ($p < 0.01$) at a concentration of 2.5 μM. Four DHPs, which significantly increased vinblastine accumulation, were tested for their effect on daunomycin cytotoxicity in H69AR cells and found to significantly decrease the IC_{50} of daunomycin, confirming the accumulation study results. The DHPs were also tested for their effect on intracellular glutathione (GSH) concentrations, a co-substrate for MRP1-mediated efflux in H69AR and Panc-1 cells. After 2-h and 24-h incubation with a DHP compound, $\mathbf{I}_m$ (**103**) and its pyridine derivative $\mathbf{II}_m$ (**104**) there was a small (~20%) but statistically significant decrease in intracellular GSH in Panc-1 cells [131].

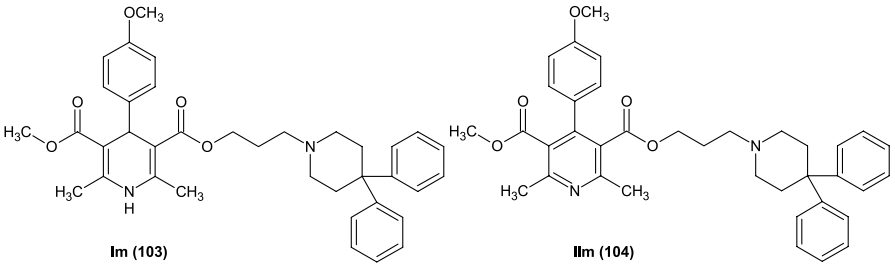

Fig. 33 Structures of Im (**103**) and IIm (**103**) DHPs

A series of *N*-substituted cage dimeric 1,4-DHPs was also evaluated as inhibitors of membrane efflux pump Pgp in MDR cancer cells. Some of the reported 1,4-DHPs have MDR modulating effect on Pgp, significantly superior to that of verapamil. The most active 1,4-DHPs are lipophilic substituted *N*-benzyl and -phenyloxycarbonyl derivatives **3b** (**105**) and **3e** (**106**). Some P-gp

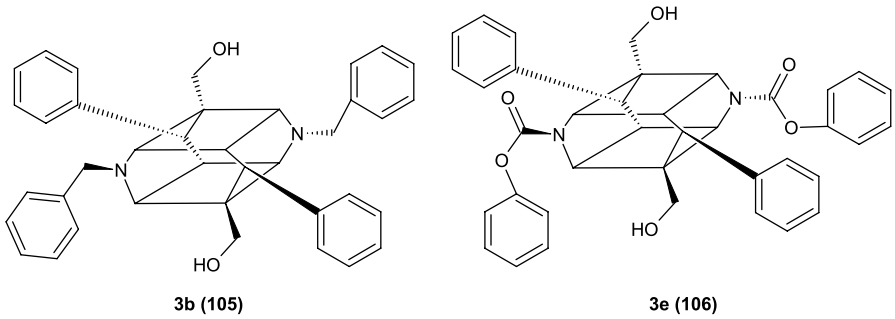

Fig. 34 Structure of **3b** (**105**) and **3e** (**106**) DHPs

substrate properties have been suggested only for the *N*-phenyloxycarbonyl compound **3e**. Competitive studies with cytotoxic Pgp substrate epirubicin indicated the overcoming of MDR in comparison of the cell line at concentrations below cytotoxic ranges of the most effective MDR-modulating concentrations of the compounds themselves. The *N*-benzyl DHPs exhibited the highest activity and practically no Pgp substrate properties. It could be a promising lead candidate for further clinical studies and structural improvement for the overcoming of MDR [132].

Additional study on quantitative structure-activity relationships (QSAR) of newly synthesized 1,4-DHPs possessing a 1-pentyl group at the 4-position was carried out. 3-Pyridylpropylester was found to be one of the effective fragments for overcoming Pgp-mediated MDR in cultured human cancer cells, in vitro. It was found to increase the life span of mice having Pgp over expressing MDR P388 leukemia. All 1,4-DHPs had weak calcium antagonistic activities, but there appeared no relationship between MDR reversing effect and calcium antagonistic activity. Some 1,4-DHPs such as **N276-13** (**107**) and **N276-16** (**108**) with weak calcium antagonistic activities showed effective MDR-reducing activities both in vitro and in vivo. In particular, **N276-16** (**108**) was expected to be the most suitable compound to overcome MDR [133].

Two other DHPs, **N276-15** (**109**) and **N276-27** (**110**) were also found to be potent antagonist against cancer cells with potentiation of anticancer agents [134, 135].

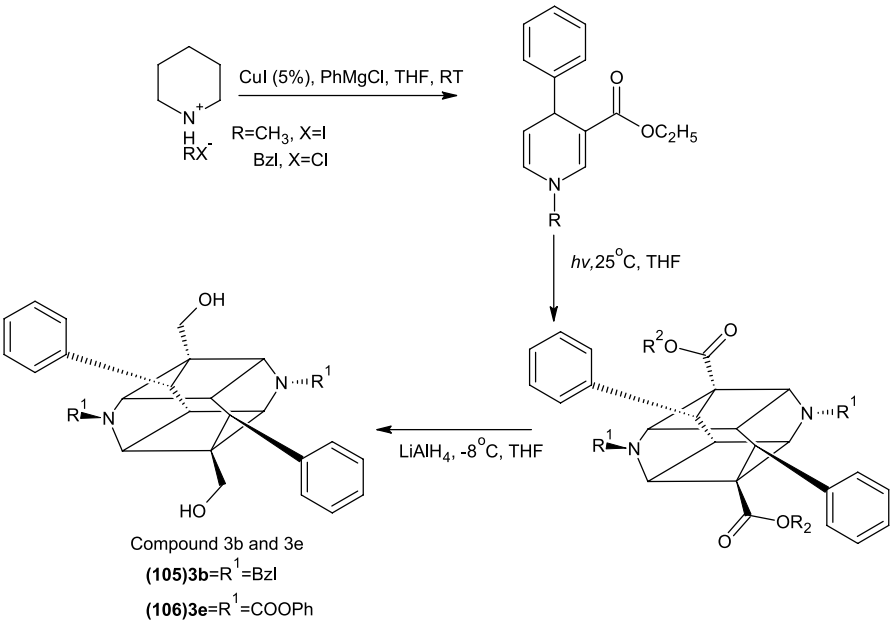

Scheme 11 Synthetic scheme for DHPs **3b** (**105**) and **3e** (**106**)

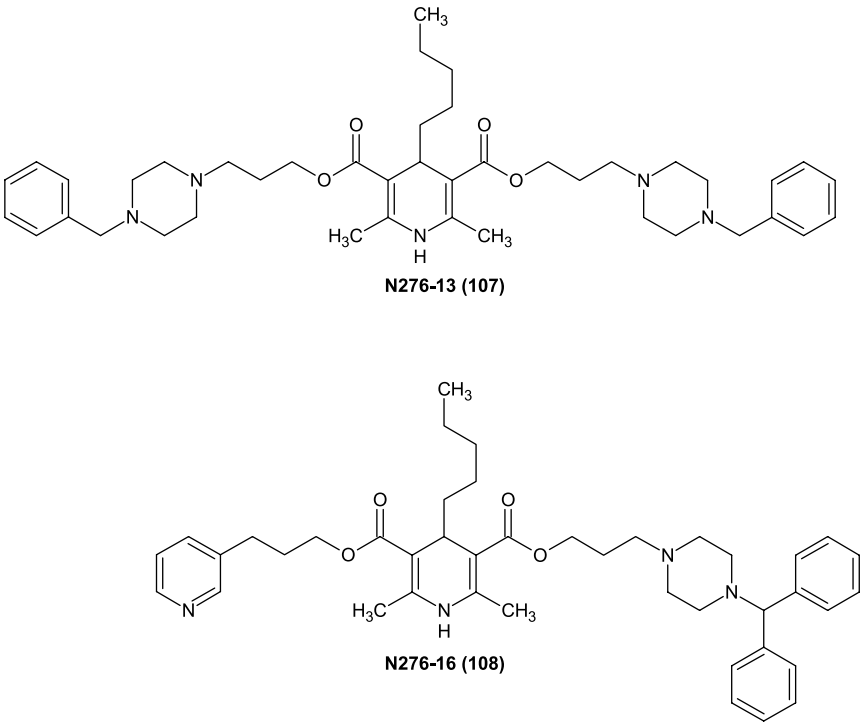

Fig. 35 Structures of N276-13 (**107**) and N276-16 (**108**)

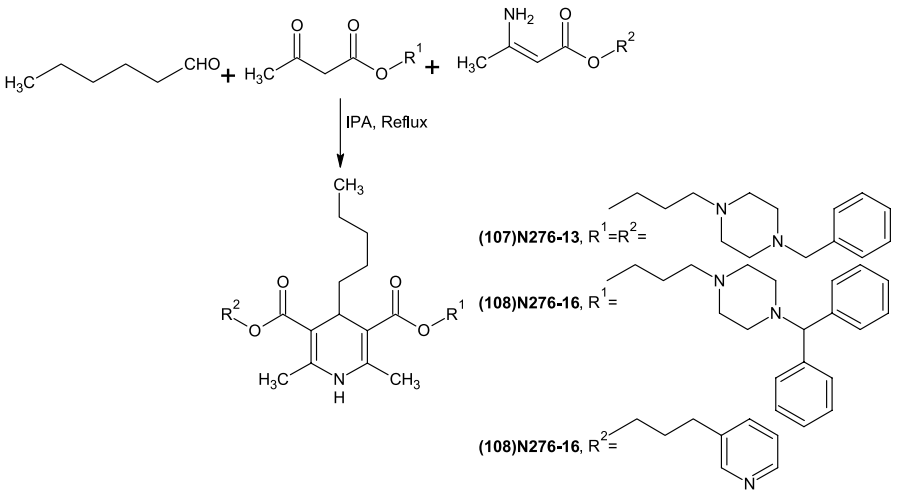

Scheme 12 Synthetic scheme for N276-13 (**107**) and N276-16 (**108**)

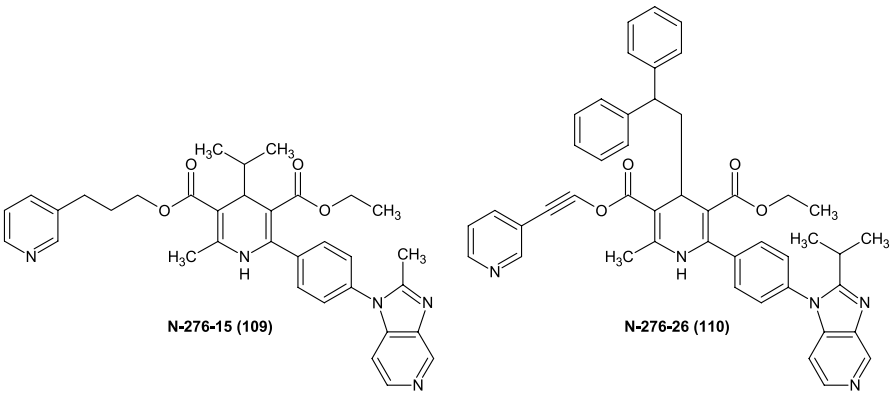

Fig. 36 Structures of N-276-15 (**109**) and N-276-26 (**110**)

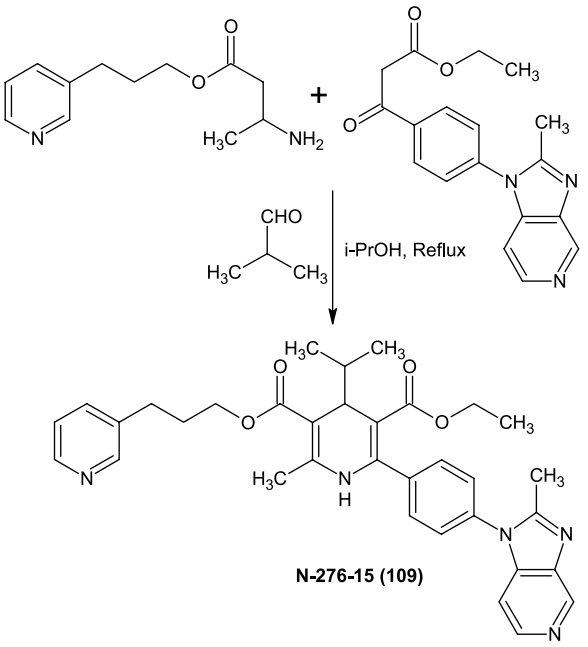

Scheme 13 Synthetic scheme for N-276-15 (**109**)

A series of novel *N*-acyloxy-1,4-DHPs (**D**) (**110**) have been synthesized and evaluated as Pgp inhibitors in vitro. QSAR were also established to identify significance and regiospecific influence of certain functional groups [136].

Modification at position 2 of 1,4-DHP such as in DHPs of formula **I** (**112**), **II** (**113**) and **III** (**114**) increases very significantly the sensitivity of cancer cells to anticancer agents as well as the sensitivity of cancer cell that have

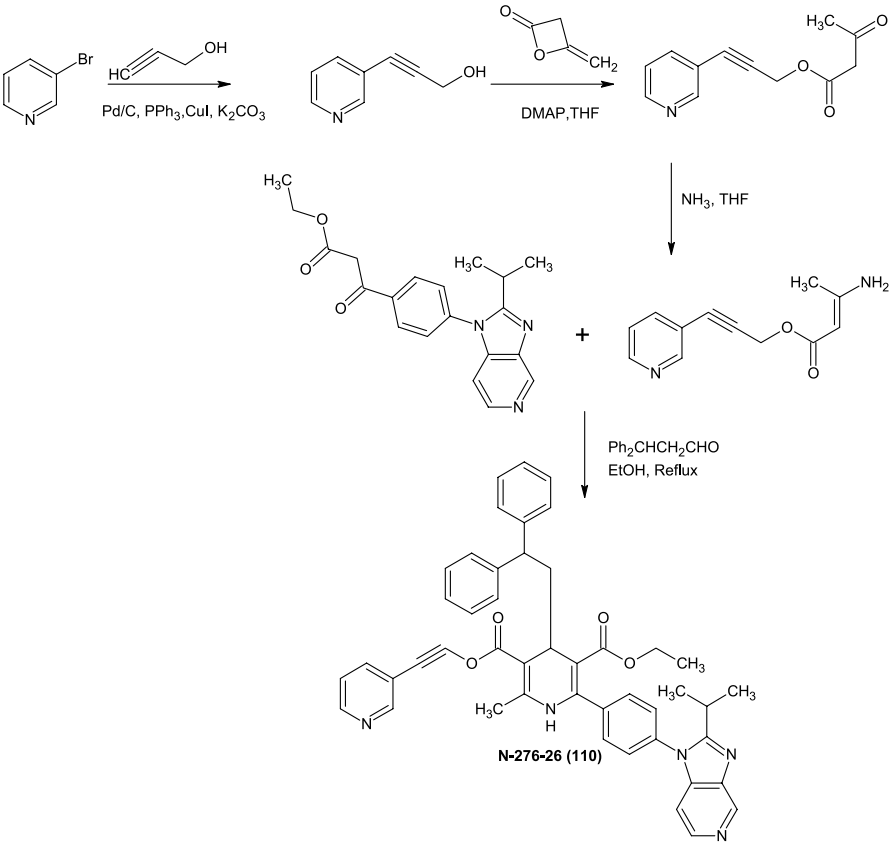

Scheme 14 Synthetic scheme for N-276-26 (**110**)

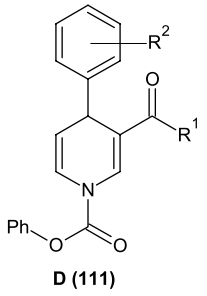

Fig. 37 Structure of compound D (**111**)

acquired a resistance to different anticancer agents, but at the same time exhibits only weak calcium channel-blocking properties, which suppress their pharmacological hypotensive effect and make it possible for them to be used in anticancer therapy without causing undesirable side effects [137].

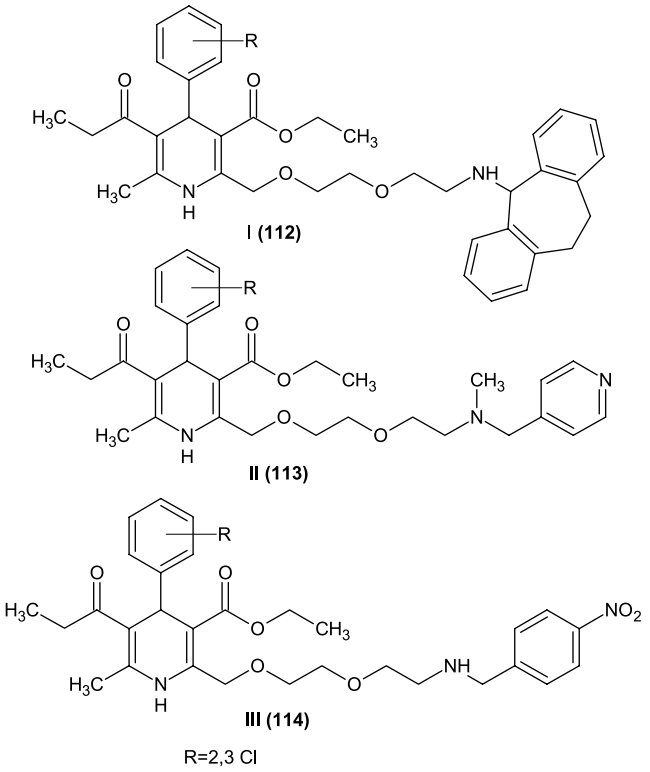

Fig. 38 Structures of I (**112**), II (**113**) and III (**114**) DHPs

8 Conclusions

DHPs are the molecules of diverse pharmacological interest mainly in cardiovascular diseases but they are now also established as potent inhibitors of Pgp which is the main cause of chemotherapy failure in cancer. There is lot of scopes in the DHPs molecules as at least five main positions are available for modification. Moreover, the particular position can be modified according to structural need. For Pgp inhibitory activity, replacement of C-3 and C-5 ester groups was explored in most of the cases as these positions are responsible for cardiovascular selectivity. Even the C-2 position was studied. Thus, this "privileged structural" class studied extensively and identified in recent years for their very promising other therapeutic activity spectrum such as Pgp inhibitors, MDR modifier and immunomodulators. Many other targets like aromatase and adenosine receptor inhibitor are also attributed to this class of compounds. The current review article, covering the literature up to 2007, suggests the scope of reducing calcium channel activity of 1,4-DHPs

to a level so that these DHPs can be used as MDR reverting agents. Though the chemistry is simple, diverse molecule generation is possible, which culminates into systematic transformation and careful structural manipulation that may help to arrive at some new drug for MDR reversal in cancer therapy in the near future.

Acknowledgements The authors thank Prof. D.J Triggle, University of Buffalo, USA and Prof. H. Timmermann, Vrije Universiteit Amsterdam, The Netherlands, for their constant support and encouragement. We would also like to thank the past research scholars, namely Gaveriya H, Kothari HM, Parecha A, Manvar D, Kothari H, Adlakha P, Dholakia CS, Joshi M, Thaker DA, Naliapara Y, Sureja D, Desai B (India), International colleagues, namely Saito S, Sakagami H, Satoh K, Tada Y, Solymosi A, Walfard K, Morshed Sufi Reza, Hashimoto K, Murotani Y, Kikuchi H, Nishikawa H, Maki J, Kurihara T (Japan), Fusi F, Sgaragli G, Saponara S, Valoti M, Dragoni S, D'Elia P, Sgaragli T, Alderighi D, Ferrara A, Gorelli B, Alderighi D, Dragoni S, Valoti M, Frosini M (Italy), Gunics G, Farkas S, Ugocsai K, Ocsovszki I, Engi H, (Hungary) and Varga A (Germany) for their contribution in a large number of biological experiments and conclusions.

References

1. Stewart BW, Kleihues P (2003) IARC Non serial Publication (World Cancer Report), http://www.who.int
2. Atlanta GA (2007) Cancer Facts and Figures 2007. American Cancer Society http://www.cancer.org
3. Lipworth L, Tarone RE, McLaughlin JK (2006) The epidemiology of renal cell carcinoma. J Urol 176:2353–2358
4. Sarkadi B, Szakas G, Varadi A (2007) http://www.sigmaaldrich.com
5. Juliano RL, Ling V (1976) A surface glycoprotein modulating drug permeability in Chinese hamster ovary cell mutants. Biochim Biophys Acta 455:152–162
6. Chen CJ, Chin JE, Ueda K, Clark DP, Pastan I, Gottesman MM, Roninson IB (1986) Internal duplication and homology with bacterial transport proteins in the mdr1 (P-glycoprotein) gene from multidrug-resistant human cells. Cell 47:381–389
7. Ueda K, Cardarelli C, Gottesman MM, Pastan I (1987) Expression of a full-length cDNA for the human MDR1 gene confers resistance to colchicine, doxorubicin, and vinblastine. Proc Natl Acad Sci USA 84:3004–3008
8. Endicott JA, Ling V (1989) The biochemistry of P-glycoprotein-mediated multidrug resistance. Annu Rev Biochem 58:137–171
9. Higgins CE (1992) ABC transporters: from microorganisms to man. Ann Rev Cell Biol 8:67–113
10. Gottesman MM, Pastan I (1993) Biochemistry of multidrug resistance mediated by the multidrug transporter. Annu Rev Biochem 62:385–427
11. Gottesman MM, Fojo T, Bates SE (2002) Multidrug resistance in cancer: role of ATP-dependent transporters. Nat Rev Cancer 2:48–58
12. Cole SP, Bhardwaj G, Gerlach JH, Mackie JE, Grant CE, Almquist KC, Stewart AJ, Kurz EU, Duncan AM, Deeley RG (1992) Overexpression of a transporter gene in a multidrug-resistant human lung cancer cell line. Science 258:1650–1654
13. Borst P, Evers R, Kool M, Wijnholds J (2000) A family of drug transporters: the multidrug resistance-associated proteins. J Natl Cancer Inst 92:1295–1302

14. Deeley RG, Cole SP (1997) Function, evolution and structure of multidrug resistance protein (MRP). Sem Cancer Biol 8:193–204
15. Litman T, Druley TE, Stein WD, Bates SE (2001) From MDR to MXR: new understanding of multidrug resistance systems, their properties and clinical significance. Cell Mol Life Sci 58:931–959
16. Lecureur V, Courtois A, Payen L, Verhnet L, Guillouzo A, Fardel O (2000) Expression and regulation of hepatic drug and bile acid transporters. Toxicology 153:203–219
17. Paulusma CC, Bosma PJ, Zaman GJR, Bakker CTM, Otter M, Scheffer GL, Scheper RJ, Borst P, Elferink RPJO (1996) Congenital jaundice in rats with a mutation in a multidrug resistance-associated protein. Gene Sci 271:1126–1128
18. Paulusma CC, Kool M, Bosma PJ, Scheffer GL, terBorg F, Scheper RJ, Tytgat GNJ, Borst P, Baas F, Oude Elferink RPJ (1997) A mutation in the human canalicular multispecific organic anion transporter gene causes the Dubin-Johnson syndrome. Hepatology 25:1539–1542
19. Alexander JS, van Ardy H, van Gerrit M, Katalin S, Ervin W, Gergely S, Andras V, Balazs S, Piet B (2000) MDR3 P-glycoprotein, a phosphatidylcholine translocase, transports several cytotoxic drugs and directly interacts with drugs as judged by interference with nucleotide trapping. J Biol Chem 275:23530–23539
20. Kool M, de Haas M, Scheffer GL, Scheper RJ, van Eijk MJ, Juijn JA, Baas F, Borst P (1997) Analysis of expression of cMOAT (MRP2), MRP3, MRP4, and MRP5, homologues of the multidrug resistance-associated protein gene (MRP1), in human cancer cell lines. Cancer Res 57:3537–3547
21. Alan FL, Kenneth JK, Cheryl LW, David RH, Diane LP, Marilyn LS, Robert D, Chatchada K, Harry EH, James HD, Muhammad S, Frederick RA (2001) Benefit of cyclosporine modulation of drug resistance in patients with poor-risk acute myeloid leukemia: a Southwest Oncology Group study. Blood 98:3212–3220
22. Ambudkar SV, Dey S, Hrycyna CA, Ramachandra M, Pastan I, Gottesman MM (1999) Biochemical, cellular, and pharmacological aspects of the multidrug transporter. Annu Rev Pharmacol Toxicol 39:361–398
23. Sarkadi B, Muller M (1997) Search for specific inhibitors of multidrug resistance in cancer. Semin Cancer Biol 8:171–182
24. Kast C, Gros P (1997) Topology mapping of the amino-terminal half of multidrug resistance-associated protein by epitope insertion and immunofluorescence. J Biol Chem 272:26479–26487
25. Kast C, Gros P (1998) Epitope Insertion Favors a Six Transmembrane Domain Model for the Carboxy-Terminal Portion of the Multidrug Resistance-Associated Protein. Biochemistry 37:2305
26. Dean M, Rzhetsky A, Allikmets R (2001) The human ATP-binding cassette (ABC) transporter superfamily. Genome Res 11:1156–1166
27. Klein I, Sarkadi B, Varadi A (1999) An inventory of the human ABC proteins. Biochim Biophys Acta 1461:237–262
28. Ueda K, Taguchi Y, Morishima M (1997) How does P-glycoprotein recognize its substrates? Sem Cancer Biol 8:151–159
29. Gao M, Loe DW, Grant CE, Cole SP, Deeley RG (1996) Reconstitution of ATP-dependent leukotriene C4 transport by Co-expression of both half-molecules of human multidrug resistance protein in insect cells. J Biol Chem 271:27782–27787
30. Bakos E, Hegedus T, Hollo Z, Welker E, Tusnady GE, Zaman GJR, Marcel JF, Varadi A, Sarkadi B (1996) Membrane topology and glycosylation of the human multidrug resistance-associated protein. J Biol Chem 271:12322–12326

31. Gao M, Yamazaki M, Loe DW, Westlake CJ, Grant CE, Cole SPC, Deeley RG (1998) Multidrug resistance protein. Identification of regions required for active transport of leukotriene C4. J Biol Chem 273:10733–10740
32. Bakos E, Evers R, Szakacs G, Gabor ET, Welker E, Szabo K, de Haas M, van Liesbeth D, Borst P, Varadi A, Sarkadi B (1998) Functional multidrug resistance protein (MRP1) lacking the N-terminal transmembrane domain. J Biol Chem 273:32167–32175
33. Bakos E, Evers R, Calenda G, Tusnady GE, Szakacs G, Varadi A, Sarkadi B (2000) Characterization of the amino-terminal regions in the human multidrug resistance protein (MRP1). J Cell Sci 113:4451–4461
34. Bates SE, Robey R, Miyake K, Rao K, Ross DD, Litman T (2001) The role of half-transporters in multidrug resistance. J Bioenerg Biomembr 33:503–511
35. Ozvegy C, Litman T, Szakacs G, Nagy Z, Bates S, Varadi A, Sarkadi B (2001) Functional characterization of the human multidrug transporter, ABCG2, expressed in insect cells. Biochem Biophys Res Commun 285:111–117
36. Kage K, Tsukahara S, Sugiyama T, Asada S, Ishikawa E, Tsuruo T, Sugimoto Y (2002) Dominant-negative inhibition of breast cancer resistance protein as drug efflux pump through the inhibition of S – S dependent homodimerization. Int J Cancer 97:626–630
37. Rosenberg MF, Callaghan R, Ford RC, Higgins CF (1997) Structure of the multidrug resistance P-glycoprotein to 2.5 nm resolution determined by electron microscopy and image analysis. J Biol Chem 272:10685–10694
38. Chang G, Roth CB (2001) Structure of MsbA from *E. coli*: a homolog of the multidrug resistance ATP-binding cassette (ABC) transporters. Science 293:1793–1800
39. Honjo Y, Hrycyna CA, Yan QW, Medina-Perez WY, Robey RW, van de Laar A, Litman T, Dean M, Bates SE (2001) Acquired mutations in the MXR/BCRP/ABCP gene alter substrate specificity in MXR/BCRP/ABCP-overexpressing cells. Cancer Res 61:6635–6639
40. Krishna R, Mayer LD (2000) Multidrug resistance (MDR) in cancer. Mechanisms, reversal using modulators of MDR and the role of MDR modulators in influencing the pharmacokinetics of anticancer drugs. Eur J Pharm Sci 11:265–283
41. Leslie EM, Deeley RG, Cole SP (2001) Toxicological relevance of the multidrug resistance protein 1, MRP1 (ABCC1) and related transporters. Toxicology 167:3–23
42. Ambudkar SV, Dey S, Hrycyna CA, Ramachandra M, Pastan I, Gottesman MM (1999) Biochemical, cellular, and pharmacological aspects of the multidrug transporter. Annu Rev Pharmacol Toxicol 39:361–398
43. Lehne G (2000) P-glycoprotein as a drug target in the treatment of multidrug resistant cancer. Curr Drug Targets 1:85–99
44. Rao VV, Dahlheimer JL, Bardgett ME, Snyder AZ, Finch RA, Sartorelli AC, Piwnica-Worms D (1999) Choroid plexus epithelial expression of MDR1 P glycoprotein and multidrug resistance-associated protein contribute to the blood-cerebrospinal-fluid drug-permeability barrier. Proc Natl Acad Sci USA 96:3900–3905
45. Bart J, Groen HJ, Hendrikse NH, van der Graaf WT, Vaalburg W, de Vries EG (2000) The blood-brain barrier and oncology: new insights into function and modulation. Cancer Treat Rev 26:449–462
46. Zhou S, Schuetz JD, Bunting KD, Colapietro AM, Sampath J, Morris JJ, Lagutina I, Grosveld GC, Osawa M, Nakauchi H, Sorrentino BP (2001) The ABC transporter Bcrp1/ABCG2 is expressed in a wide variety of stem cells and is a molecular determinant of the side-population phenotype. Nat Med 9:1028–1034

47. Thiebaut F, Tsuruo T, Hamada H, Gottesman MM, Pastan I, Willingham MC (1987) Cellular localization of the multidrug-resistance gene product P-glycoprotein in normal human tissues. Proc Natl Acad Sci USA 84:7735–7738
48. van Helvoort A, Smith AJ, Sprong H, Fritzsche I, Schinkel AH, Borst P, van Meer G (1996) MDR1 P-glycoprotein is a lipid translocase of broad specificity, while MDR3 P-glycoprotein specifically translocates phosphatidylcholine. Cell 87:507–517
49. Kipp H, Arias IM (2000) Intracellular trafficking and regulation of canalicular ATP-binding cassette transporters. Semin Liver Dis 20:339–351
50. Jonker JW, Smit JW, Brinkhuis RF, Maliepaard M, Beijnen JH, Schellens JH, Schinkel AH (2000) Role of breast cancer resistance protein in the bioavailability and fetal penetration of topotecan. J Natl Cancer Inst 92:1651–1656
51. Sarkadi B, Price EM, Boucher RC, Germann UA, Scarborough GA (1992) Expression of the human multidrug resistance cDNA in insect cells generates a high activity drug-stimulated membrane ATPase. J Biol Chem 267:4854–4858
52. Ambudkar SV, Lelong IH, Zhang J, Cardarelli CO, Gottesman MM, Pastan I (1992) Partial purification and reconstitution of the human multidrug-resistance pump: characterization of the drug-stimulatable ATP hydrolysis. Proc Natl Acad Sci USA 89:8472–8476
53. Scarborough GA (1995) Drug-stimulated ATPase activity of the human P-glycoprotein. J Bioenerg Biomembr 27:37–41
54. Loo TW, Clarke DM (2001) Determining the dimensions of the drug-binding domain of human P-glycoprotein using thiol cross-linking compounds as molecular rulers. Biol Chem 276:36877–36880
55. Higgins CF, Gottesman MM (1992) Is the multidrug transporter a flippase? Trends Biochem Sci 17:18–21
56. Qian Y-M, Qiu W, Gao M, Westlake CJ, Cole SPC, Deeley RG (2001) Characterization of binding of leukotriene C4 by human multidrug resistance protein 1: evidence of differential interactions with NH2- and COOH-proximal halves of the protein. J Biol Chem 276:38636–38644
57. Szakacs G, Ozvegy C, Bakos E, Sarkadi B, Varadi A (2001) Role of glycine-534 and glycine-1179 of human multidrug resistance protein (MDR1) in drug-mediated control of ATP hydrolysis. Biochem J 356:71–75
58. Szabo K, Welker E, Bakos E, Muller M, Roninson I, Varadi A, Sarkadi B (1998) Drug-stimulated nucleotide trapping in the human multidrug transporter MDR1. Cooperation of the nucleotide binding domains. J Biol Chem 273:10132–10138
59. Sauna ZE, Smith MM, Muller M, Kerr KM, Ambudkar SV (2001) The mechanism of action of multidrug-resistance-linked P-glycoprotein. J Bioenerg Biomembr 33:481–491
60. Tsuruo T, Iida H, Tsukagoshi S, Sakurai Y (1981) Overcoming of vincristine resistance in P388 leukemia in vivo and in vitro through enhanced cytotoxicity of vincristine and vinblastine by verapamil. Cancer Res 41:1967–1972
61. Zamora JM, Pearce HL, Beck WT (1998) Physical-chemical properties shared by compounds that modulate multidrug resistance in human leukemic cells. Mol Pharmacol 33:454–462
62. Pommerenke EW, Osswald H, Hahn EW, Volm M (1990) Activity of various amphiphilic agents in reversing multidrug resistance of L 1210 cells. Cancer Lett 55:17–23
63. Klopman G, Srivastava S, Kolossvary I, Eppant RF, Ahmed N, Eppant RM (1992) Structure-activity study and design of multidrug-resistant reversal compounds by a computer automated structure evaluation methodology. Cancer Res 52:4121–4129

64. Ramu A, Ramu N (1994) Reversal of multidrug resistance by bis(phenylalkyl)amines and structurally related compounds. Cancer Chemother Pharmacol 34:423–430
65. Chiba P, Tell B, Jager W, Richter E, Hitzler M, Ecker G (1997) Studies on Propafenone-type Modulators of Multidrug-resistance IV: Synthesis and Pharmacological Activity of 5-Hydroxy and 5-Benzyloxy. Arch Pharm 330:343–347
66. Wigler PW, Patterson FK (1993) Inhibition of the multidrug resistance efflux pump. Biochim Biophys Acta 1154:173–181
67. Wadkins RM, Houghton PJ (1993) The role of drug-lipid interactions in the biological activity of modulators of multi-drug resistance. Biochim Biophys Acta 1153:225–236
68. Choi CH (2005) ABC transporters as multidrug resistance mechanisms and the development of chemosensitizers for their reversal. Cancer Cell Int 5:30–43
69. Borowski E, Bontemps-Gracz MM, Piwkowska A (2005) Strategies for overcoming ABC-transporters-mediated multidrug resistance (MDR) of tumor cells. Acta Biochemic Polonica 52:609–627
70. Teodori E, Dei S, Martelli C, Scapecchi S, Gualtieri F (2006) The functions and structure of ABC transporters: implications for the design of new inhibitors of Pgp and MRP1 to control multidrug resistance (MDR). Curr Drug Targets 7:893–909
71. Taub ME, Podila I, Ely D, Almeida I (2005) Functional assessment of multiple *p*-glycoproteins (P-gp) probe substrates: influence of cell line and modulator concentration on P-gp activity. Drug Metab Dispos 33:1679–1687
72. Tulpule A (2005) Multidrug resistance in AIDS-related lymphoma. Curr Opin Oncol 17:466–468
73. Shah A, Naliapara Y, Sureja D, Motohashi N, Kurihara T, Kawase M, Satoh K, Sakagami H, Molnar J (1998) Biological activity of 6,12-dihydro-1-benzopyrano[3,4-*b*][1,4]benzothiazin-6-ones. Anticancer Res 18:61–64
74. Avendano C, Carlos MJ (2002), Inhibitors of multidrug resistance to antitumor agents (MDR). Curr Med Chem 9:159–193
75. Tsuruo T, Iida H, Tsukagoshi S, Sakurai Y (1983) Potentiation of Vincristine and Adriamycin Effects in Human Hemopoietic Tumor Cell Lines by Calcium Antagonists and Calmodulin Inhibitors. Cancer Res 43:2267–2276
76. Malkandi PJ, Ferry DR, Boer R, Gekeler V, Ise W, Kerr DJ (1994) Dexniguldipine-HCl is a potent allosteric inhibitor of [^{3}H]vinblastine binding to P-glycoprotein of CCRF ADR 5000 cells. Eur J Pharmacol Mol Pharmacol 288:105–114
77. Ferry DR, Malkandi PJ, Russell MA, Kerr DJ (1995) Allosteric regulation of [3*H*]vinblastine binding to *P*-glycoprotein of MCF-7 ADR cells by dexniguldipine. Biochem Pharmacol 49:1851–1861
78. Rampe D, Triggle DJ (1993) New synthetic ligands for L-type voltage-gated calcium channels. Prog Drug Res 40:191–238
79. Triggle DJ (2003) Drug targets in the voltage-gated calcium channel family: why some are and some are not. Assay Drug Dev Technol 1:719–733
80. Hollt V, Kouba M, Dietel M, Vogt G (1992) Stereoisomers of calcium antagonists which differ markedly in their potencies as calcium blockers are equally effective in modulating drug transport by *P*-glycoprotein. Biochem Pharmacol 43:2601–2608
81. Hofmann J, Wolf A, Spitaler M, Bock G, Drach J, Ludescher C, Grunicke HH (1992) Reversal of multidrug resistance by B859–35, a metabolite of B859–35, niguldipine, verapamil and nitrendipine. J Cancer Res Clin Oncol 118:361–366
82. Tasaki Y, Nakagawa M, Hogata J, Kiue A, Tanimura H, Kuwano M, Nomura YJ (1995) Reversal by a digydropyridine derivative of non-P-glycoprotien-mediated multidrug

resistance in Etoposide-resistance human prostrate cancer cell line. J Urol 154:1210–1216
83. Abe T, Koike K, Ohga T, Kubo T, Wada M, Kohno K, Mori T, Hiraka K, Kuwano M (1995) Chemosensitisation of spontaneous multidrug resistance by a 1,4-dihydropyridine analogue and verapamil in human glioma cell lines overexpressing MRP or MDR1. Br J Cancer 72:418–423
84. Kiue A, Sano T, Suzuki KI, Inada H, Okumura M, Kikuchi J, Sato SI, Kohno K, Kuwano M (1990) Activities of newly synthesized dihydropyridines in overcoming of vincristine resistance, calcium antagonism, and inhibition of photoaffinity labeling of P-glycoprotein in rodents. Cancer Res 50:310–317
85. Tanabe H, Tasaka SH, Ohmori H, Gomi N, Sasaki Y, Machida T, Iino M, Kiue A, Naito S, Kuwano M (1998) Newly synthesized dihydropyridine derivatives as modulators of P-glycoprotein-mediated multidrug resistance. Bioorg Med Chem 6:2219–2227
86. Niwa K, Yamada K, Shudo N, Seto K, Matsumoto T, Takao S, Akiyama SI, Shimadzu H (1992) Effect of a dihydropyridine analogue, 2-[benzyl(phenyl)amino]ethyl 1,4-dihydro-2,6-dimethyl-5-(5,5-dimethyl-2-oxo-1,3,2-dioxaphosphorinan-2-yl)-1-(2-morpholinoethyl)-4-(3-nitrophenyl)-3-pyridinecarboxylate on reversing in vivo resistance of tumor cells to adriamycin. Cancer Res 52:3655–3660
87. Vanhoefer U, Muller MR, Hilger RA, Lindtner B, Klaassen U, Schleucher N, Rustum YM, Seeber S, Hastrick A (1999) Reversal of MDR1-associated resistance to topotecan by PAK-200S, a new dihydropyridine analogue, in human cancer cell lines. Br J Cancer 81:1304–1310
88. Shudo N, Mizoguchi T, Kiyosue T, Arita M, Yoshimura A, Seto K, Sakoda R, Akiyama S (1990) Two pyridine analogues with more effective ability to reverse multidrug resistance and with lower calcium channel-blocking activity than their dihydropyridine counterparts. Cancer Res 50:3055–3061
89. Ohsumi K, Ohishi K, Morinaga Y, Nakagawa R, Suga Y, Sekiyama T, Akiyama Y, Tsuji T, Tsuruo T (1995) *N*-alkylated 1,4-dihydropyridines: new agents to overcome multidrug resistance. Chem Pharm Bull 43:818–828
90. Hofmann J, Gekeler V, Ise W, Noller A, Miterdorfer J, Hofer S, Utz I, Goiwald M, Boer R, Glossmann H, Grunicke HH (1995) Mechanism of action of dexniguldipine-HCl (B8509–035), a new potent modulator of multidrug resistance. Biochem Pharmacol 49:603–609
91. Reyman A, Loofp G, Woermann C, Dietel M, Erttmann R (1993) Reversal of multidrug resistance in Friend leukemia cells by dexniguldipine-HCl. Cancer Chemother Pharmacol 32:25–30
92. Ise W, Heuser M, Sanders K, Beck J, Gekeler V (1996) *P*-glycoprotein-associated resistance to taxol and taxotere and its reversal by dexniguldipine-HCl, dexverapamil-HCl, or cyclosporin A. Int J Oncol 8:951
93. Qin Y, Tang Y, Schally AV, Beckman BS (1995) Dexniguldipine hydrochloride inhibits growth of human HT-29 colon carcinoma cells and expression of protein kinase C. DELTA. and. zeta. Int J Oncol 7:1073
94. Patterson KK, Beckman BS, Kolz DM, Mallia CM, Jeter JR (1996) Dexniguldipine hydrochloride, a protein-kinase-C-specific inhibitor, affects the cell cycle, differentiation, P-glycoprotein levels, and nuclear protein phosphorylation in Friend erythroleukemia cells. J Cancer Res Clin Oncol 122:465–475
95. Straub T, Boesenberg C, Gekeler V, Boege F (1997) The dihydropyridine dexniguldipine hydrochloride inhibits cleavage and religation reactions of eukaryotic DNA topoisomerase I. Biochemistry 36:10777–10783

96. Kamiwatari M, Nagata Y, Kikuchi H, Yoshimura A, Sumizawa T, Shudo N, Sakoda R, Seto K, Akiyama S (1989) Correlation between reversing of multidrug resistance and inhibiting of [3*H*]azidopine photolabeling of P-glycoprotein by newly synthesized dihydropyridine analogues in a human cell line. Cancer Res 49:3190–3195
97. Tolomeo M, Gancitano RA, Musso M, Porretto F, Perricone R, Abbadessa V, Cajozzo A (1994) Effects of R-enantiomer (GR66234A) and L-enantiomer (GR66235A) of telupidine, a new dihydropyridine derivative, on cell lines displaying the multidrug resistant phenotype. Haematologica 79:328–333
98. Boer R, Dichtl M, Borchers C, Ulrich WR, Marecek JF, Prestwich GD, Glossmann H, Striessnig J (1996) Global folds of highly deuterated, methyl-protonated proteins by multidimensional NMR. Biochemistry 35:1389–1401
99. Ferry DR, Russell MA, Cullen MH (1992) *P*-glycoprotein possesses a 1,4-dihydropyridine-selective drug acceptor site which is alloserically coupled to a vinca-alkaloid-selective binding site. Biochem Biophys Res Commun 188:440–445
100. Dietel M, Boss H, Reymann A, Pest S, Seidel A (1996) In vivo reversibility of multidrug resistance by the MDR-modulator dexniguldipine (niguldipine derivative B859–35) and by verapamil. J Exp Ther Oncol 1:23–29
101. Vanhoefer U, Cao S, Minderman H, Toth K, Scheper RJ, Slovak ML, Rustum YM (1996) PAK-104P, a pyridine analogue, reverses paclitaxel and doxorubicin resistance in cell lines and nude mice bearing xenografts that overexpress the multidrug resistance protein. Clin Cancer Res 2:369–377
102. Klopman G, Shi LM, Ramu A (1997) Quantitative structure-activity relationship of multidrug resistance reversal agents. Mol Pharmacol 52:323–334
103. Ohsumi K, Sekiyama T, Nakagawa R, Tsuji T, Morinaga Y, Ohishi K (1994) 1,4-dihydropyridine compounds useful as reverse resistance agents. US Patent 5 292 757
104. Shah A, Gaveriya H, Motohashi N, Kawase M, Saito S, Sakagami H, Satoh K, Tada Y, Solymosi A, Walfard K, Molnar J (2000) 3,5-diacetyl-1,4-dihydropyridines: synthesis and MDR reversal in tumor cells. Anticancer Res 20:373–377
105. Gunics G, Farkas S, Motohashi N, Shah A, Harsukh G, Kawase M, Molnar J (2002) Interaction between 3,5-diacetyl-1,4-dihydropyridines and ampicillin, and erythromycin on different E. coli strains. Int J Antimicrob Agents 20:227–229
106. Gunics G, Motohashi N, Molnar J, Farkas S, Kawase M, Saito S, Shah A (2001) Enhanced antibacterial effect of erythromycin in the presence of 3,5-dibenzoyl-1,4-dihydropyridines. Anticancer Res 21:269–273
107. Kawase M, Shah A, Gaveriya H, Motohashi N, Sakagami H, Varga A, Molnar J (2002) 3,5-dibenzoyl-1,4-dihydropyridines: synthesis and MDR reversal in tumor cells. Bioorg Med Chem 10:1051–1055
108. Morshed Sufi Reza MD, Hashimot K, Murotani Y, Kawase M, Shah A, Satoh K, Kikuch H, Nishikawa H, Mak J, Sakagami H (2005) Tumor-specific cytotoxicity of 3,5-dibenzoyl-1,4-dihydropyridines. Anticancer Res 25:2033–2038 (Synthline data base (2006) entry no.318546)
109. Saponara S, Kawase M, Shah A, Motohashi N, Molnar J, Ugocsai K, Sgaragli G, Fusi F (2004) 3,5-Dibenzoyl-4-(3-phenoxyphenyl)-1,4-dihydro-2,6-dimethylpyridine (DP7) as a new multidrug resistance reverting agent devoid of effects on vascular smooth muscle contractility. Br J Pharmacol 141:415–422
110. Fusi F, Saponara S, Valoti M, Dragoni S, D'Elia P, Sgaragli T, Alderighi D, Kawase M, Shah A, Motohashi N, Sgaragli G (2006) Cancer cell permeability-glycoprotein as a target of MDR reverters: possible role of novel dihydropyridine derivatives. Curr Drug Targets 7:949–959

111. Fusi F, Saponara S, Valoti M, Dragoni S, D'Elia P, Sgaragli T, Alderighi D, Kawase M, Shah A, Motohashi N, Sgaragli G (2006) Cancer cell permeability-glycoprotein as a target of MDR reverters: possible role of novel dihydropyridine derivatives. Curr Drug Targets 7:1729
112. Saponara S, Ferrara A, Gorelli B, Shah A, Kawase M, Motohashi N, Molnar J, Sgaragli G, Fusi F (2007) 3,5-Dibenzoyl-4-(3-phenoxyphenyl)-1,4-dihydro-2,6-dimethylpyridine (DP7): a new multidrug resistance inhibitor devoid of effects on Langendorff-perfused rat heart. Eur J Pharmacol 563:160–163
113. Alderighi D, Sgaragli T, Dragoni S, Frosini M, Valoti M, Saponara S, Fusi F, Shah A, Kawasae M, Motohashi N, Molnar J, Sgaragli G (2007) 33° National Conference of the Italian Society of Pharmacology, Cagliari, 6–9 June 2007
114. Unpublished data (PhD thesis by Kothari HM, Department of Chemistry Saurashtra University, Rajkot-360005, India (2005))
115. Bazargan L, Fouladdel S, Shafiee A, Amini M, Ghaffari SM, Azizi E (2007) Evaluation of anticancer effects of newly synthesized dihydropyridine derivatives in comparison to verapamil and doxorubicin on T47D parental and resistant cell lines in vitro. Cell Biol Toxicol Article (in press) (DOI 10.1007/s10565–007-9026-x)
116. Engi H, Sakagami H, Kawase M, Parecha A, Manvar D, Kothari H, Adlakha P, Shah A, Motohashi N, Ocsovszki I, Molnar J (2006) Tumour-specific cytotoxicity and MDR-reversal activity of dihydropyridine. In Vivo 20:637–644
117. Unpublished data (PhD thesis by Dholakia CS, Department of Chemistry Saurashtra University, Rajkot-360005, India (2005))
118. Loknath NK, Shridher MS, Prasad JS, Joshi M, Thaker DA, Shah A (1997) Crystal structure of 4-(4′-chlorophenyl)-2,6-dimethoxy carbonyl-1,4-dihydropyridine, $C_{17}H_{18}ClNO_4$. Z Kristallogr 212:13–14
119. Deverajegowda HC, Prasad JAS, Sridhar MA, Gevariya HC, Shah A (2000) Crystal and molecular structure of 1,4-dihydropyridine with different substituents. Mol Cryst Liq Cryst 348:301–316
120. Mahendra M, Doreswamy BH, Sridhar MA, Prasad JS, Patel GR, Patel JA, Shah A (2004) Crystal and molecular structure of 2,6-dimethyl-3-acetyl-5-carbomethoxy-4-(4′-methoxyphenyl)-1,4-dihydropyridine. J Chem Crystallogr 34:441–445
121. Desai B, Sureja D, Naliapara Y, Shah A, Saxena AK (2001) Synthesis and QSAR studies of 4-substituted phenyl-2,6-dimethyl-3, 5-bis-*N*-(substituted phenyl)carbamoyl-1,4-dihydropyridines as potential antitubercular agents. Bioorg Med Chem 9:1993–1998
122. Kharkar PS, Desai B, Gaveria H, Varu B, Loriya R, Naliapara Y, Shah A, Kulkarni VM (2002) Three-dimensional quantitative structure-activity relationship of 1,4-dihydropyridines as antitubercular agents. J Med Chem 45:4858–4867
123. Tanaka H, Shigenobu K (2000) AHC-52, a dihydropyridine compound with chloride current-blocking and cardioprotective activities. Cardiovasc Drug Rev 18:93–102
124. Kobayashi Y, Yamashiro T, Nagatake H, Yamamoto T, Watanabe N, Tanaka H, Shigenobu K, Tsuruo T (1994) Expression and function of multidrug resistance P-glycoprotein in a cultured natural killer cell-rich population revealed by MRK16 monoclonal antibody and AHC-52. Biochem Pharmacol 48:1641–1646
125. Shinoda H, Inaba M, Tsuruo T (1989) In vivo circumvention of vincristine resistance in mice with P388 leukemia using a novel compound, AHC-52. Cancer Res 49:1722–1726
126. Zhou X, Zhang L, Tseng E, Scott-Ramsay E, Schentag JJ, Coburn RA, Morris ME (2005) New 4-aryl-1,4-dihydropyridines and 4-arylpyridines as *P*-glycoprotein inhibitors. Drug Metab Dispos 33:321–328

127. Zhou X, MacDiarmid J, Coburn RA, Morris ME (2005) Pharmacokinetics and bioavailability of a newly synthesized dihydropyridine compound with multidrug resistance reversal activity. Biopharm Drug Dispos 26:279–285
128. Zhou XF, Yang X, Wang Q, Coburn RA, Morris ME (2005) Effects of dihydropyridines and pyridines on multidrug resistance mediated by breast cancer resistance protein: in vitro and in vivo studies. Drug Metab Dispos 33:1220–1228
129. Zhou XF, Shao Q, Coburn RA, Morris ME (2005) Quantitative structure-activity relationship and quantitative structure-pharmacokinetics relationship of 1,4-dihydropyridines and pyridines as multidrug resistance modulators. Pharm Res 22:1989–1996
130. Ulrich W-R (1996) 1,4-Dihydropyridines for application in combatting resistance to drugs. US Patent 5 514 664 and WO91/18599
131. Zhou X, Coburn RA, Morris ME (2005) Effects of new 4-aryl-1,4-dihydropyridines and 4-arylpyridines on drug efflux mediated by multidrug resistance-associated protein 1. J Pharm Sci 94:2256–2265
132. Richter M, Molnar J, Andreas H (2006) Biological evaluation of bishydroxymethyl-substituted cage dimeric 1,4-dihydropyridines as a novel class of *p*-glycoprotein modulating agents in cancer cells. J Med Chem 49:2838–2840
133. Tasaka S, Ohmori H, Gomi N, Iino M, Machida T, Kiue A, Naitob S, Kuwano M (2001) Synthesis and structure–activity analysis of novel dihydropyridine derivatives to overcome multidrug resistance. Biorg Med Chem Lett 11:275–277
134. Tasaka S, Tanabe H, Omori H, Kiue A (1998) 1,4-Dihydropyridine derivatives. EP Patent 0943615, JP Patent 1998204061, WO Patent 1998023607. (Synthline data base entry no.266982)
135. Tasaka S, Omori H, Tanabe H, Gomi N, Kiue A (2001) 1,4-Dihydropyridine derivatives. EP Patent 1 055 672, JP Patent 2 000 044 559, US Patent 6 306 853, WO Patent 1 999 041 250. (Synthline data base entry no. 282013)
136. Voigt B, Coburger C, Monar J, Andreas H (2007) Structure-activity relationships of novel *N*-acyloxy-1,4-dihydropyridines as *P*-glycoprotein inhibitors. Biorg Med Chem 15:5110–5120
137. Peglion JL, Aasssi G, Pierre A, Kraus-Berthier L, Guilbaud N, Vilaine JP (1995) 1,4-Dihydropyridine compounds. US Patent 5 389 644

Top Heterocycl Chem (2008) 15: 253–279
DOI 10.1007/7081_2007_090

Published online: 29 February 2008

Theoretical Studies on Phenothiazines, Benzo[*a*]phenothiazines, and Benz[*c*]acridines

Teruo Kurihara[1] (✉) · Kazumi Shinohara[1] · Makoto Inabe[1] · Hidetsugu Wakabayashi[1] · Noboru Motohashi[2] · Hiroshi Sakagami[3] · Joseph Molnar[4]

[1]Faculty of Science, Josai University, Sakado, Saitama, Japan
tkuri@josai.ac.jp

[2]Meiji Pharmaceutical University, Tanashi, Tokyo, Japan

[3]Division of Pharmacology, Department of Diagnostic and Therapeutic Sciences, Meikai University School of Dentistry, Sakado, Saitama, Japan

[4]University of Szeged, Institute of Microbiology and Immunobiology, Albert Szent-Gyorgyi Medical Center, Dom ter 10, H-6720 Szeged, Hungary

Abstract Quantitative structure–activity relationship (QSAR) analysis for minimum inhibitory concentration (MIC) of phenothiazines and benzo[*a*]phenothiazines was investigated based on the theoretical calculations. Four different dipole moments (μ_G, $\mu_{ESP\text{-}G}$, μ_W, and $\mu_{ESP\text{-}W}$) and heats of formation (ΔH_f) of the phenothiazines [**1–20**], benzo[*a*]phenothiazines [**21–29**], and benz[*c*]acridines [**30–41**] were separately calculated in the gas-phase and the water-solution by the conductor-like screening model/parametric method 3 (COSMO/PM3) technique. The MIC values of phenothiazines [**1–20**] were well correlated to $\Delta\Delta H_f$, HOMO energy and μ_G. QSAR may be applicable to predict the MIC of phenothiazines.

Keywords Benz[*c*]acridines · Benzo[*a*]phenothiazines · Biological activity · Phenothiazines · QSAR · Theoretical calculations

1 Introduction

Phenothiazines, benzo[*a*]phenothiazines, and benz[*c*]acridines show biological activity including antitumor [1] or carcinogenic activity [2]. The molecular configuration of a phenothiazine molecule is nearly planar or folded along the nitrogen-sulfur axis. The skeleton of phenothiazine is proposed to be non-planar—using crystallographic [3] and dipole moment measurements [4]—because phenothiazine has a dihedral angle of 145±5° between the plane of benzene rings of phenothiazine [3, 4]. On the basis of these facts, we have obtained the following evidences: Regarding the calculated π-spin densities (Q_π) between the radical producing benzo[*a*]phenothiazines and non-radical producing benzo[*a*]phenothiazines, the radical producing benzo[*a*]phenothiazines at the N-12 position had positive π-spin density (Q_π), whereas non-radical producing benzo[*a*]phenothiazines had the opposite π-spin density [5]. All the carcinogenic benz[*c*]acridines were shown to have elevated π-spin density at their 12th nitrogen atom as compared with non-carcinogenic benz[*c*]acridines. The interaction between chlorpromazine (CPZ) and 2′-deoxyguanosine-5′-mono- phosphate (dGMP) was examined using the PM3 method. First, the optimized geometrical structure of a CPZ, dGMP, and CPZ-dGMP system in both the aqueous- and gaseous-phase was investigated; this was followed by their geometric and electric changes and force calculations. From the force calculations, three vibrations at 835, 800, and 737 cm^{-1} have been identified as the antisymmetric and symmetric P – O stretching vibrations of the PO_3^{2-} group in Z-dGMP, respectively. The vibrations at 889, 803, and 799 cm^{-1} represent the C5′ – O – PO_3^{2-} stretching vibrations, which show correspondingly higher wave numbers when compared to those of CPZ-dGMP alone [6]. The special affinity of phenothiazine to the G-C-rich region of DNA can explain the suppression of the MDR-gene promoter in the presence of promethazine and trifluoropromazine; consequently phenothiazine can prevent the induction of MDR at the gene level because the promoter contains a large number of G-C-rich regions [7]. In tests carried out on 54 cancer cell lines, colon-cancer cells were the most sensitive to six "half-mustard-type" phenothiazines. Our quantitative molecular calculations showed the distribution of electrostatic potential (ESP) on the surface of the urea site could play a role in the interaction of half-mustard-type phenothiazines—showing variability in the energy of the lone pair orbital and net atomic charges of N1, O, and N3 atoms—with the DNA base sequence of target cancer cell structures [8]. Among 12 phenothiazine-related compounds, the cytotoxic activity of six half-mustard-type phenothiazines was significantly higher than that of six phthalimido compounds with the highest cytotoxic activity in parallel with high $\Delta\mu$ (the difference between two dipole moments, μ_g and μ_e). A positive rela-

tionship between cytotoxic activity and molecular orbital energy including π-LUMO, π-HOMO, and lone pair orbitals originating from O, N1, and N3 atoms was apparently observed. This means that cytotoxic activity of half-mustard-type phenothiazines could be predicted by their dipole moments and molecular orbital energies [8, 9]. On the basis of a molecular orbital calculation concerning the physicochemical parameters and the minimum inhibitory concentration (MIC) of phenothiazines, antitumor activity of benzo[*a*]phenothiazines and carcinogen activity of benz[*c*]acridines, the purpose of this paper is to present the QSAR of phenothiazines, benzo[*a*]phenothiazines, and benz[*c*]acridines.

1.1 Materials and Methods

Chemicals. Twenty phenothiazines [**1**–**20**], nine benzo[*a*]phenothiazines [**21**–**29**], and 12 benz[*c*]acridines [**30**–**41**] were synthesized, as described previously [1, 10] (Figs. 1 and 2).

Theoretical calculations. Molecular orbital calculations using parametric method 3 (PM3) were performed with application of the winMOPAC

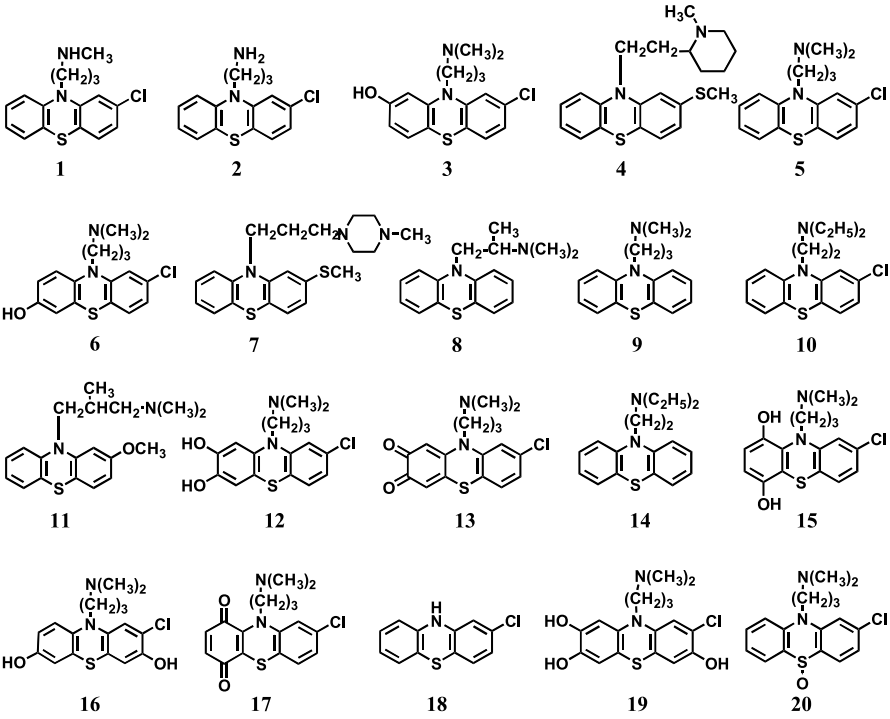

Fig. 1 Structures of phenothiazines [**1**–**20**]

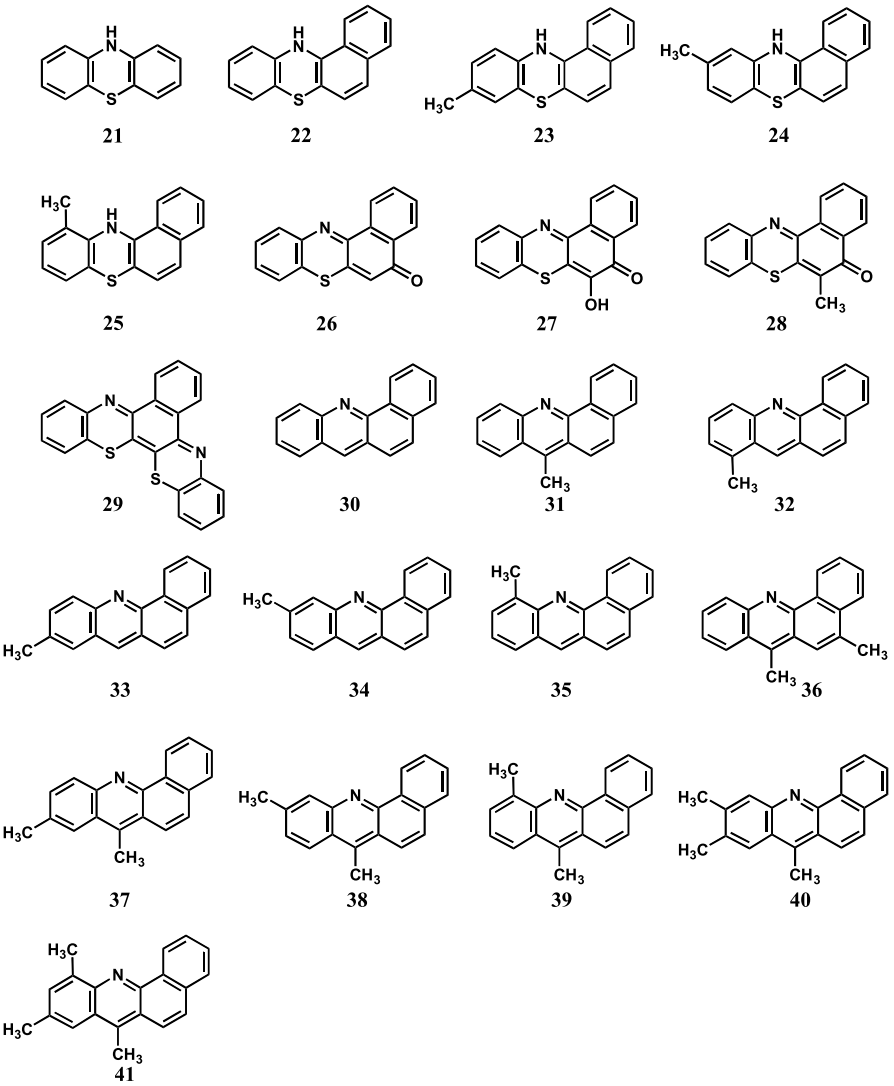

Fig. 2 Structure of benzo[*a*]phenothiazines [**21**–**29**] and benz[*c*]acridines [**31**–**41**]

program[1]. The geometries of the phenothiazines [**1**–**20**], benzo[*a*]phenothiazines [**21**–**29**], and benz[*c*]acridines [**30**–**41**] were optimized with respect to all geometrical parameters using the Broyden–Fletcher–Goldfarb–Shanno algorithm incorporated into the program. The geometries of the phenothiazines [**1**–**20**], benzo[*a*]phenothiazines [**21**–**29**], and benz[*c*]acridines [**30**–

[1] PM3 semi-empirical MO calculations were performed by MOPAC version 3.5 (Fujitsu Limited) on a DELL XPS DXG061 personal computer.

41] in water-solution were compared to those in the gas-phase using the conductor-like screening model orbital (COSMO) and electrostatic potential (ESP) calculations. The COSMO procedure generates a conducting polygonal surface around the system at van der Waal's distance. The standard value of the number of geometrical segments per atom (NSPA) was 60, and that of the dielectric constant was 78.4 at 25 °C (water). The values of the dipole moment (μ_G and μ_W) in the gas-phase and in the water-solution of these compounds [**1–41**] were calculated using the ESP/PM3 and COSMO/PM3 methods. For these calculations, a DELL XPS DXG061 personal computer was used.

2
QSAR of Phenothiazine and Phenothiazine Derivatives

2.1
Electronic Structures and Optimized Geometries of Phenothiazines

PM3 is a reasonably reliable method for the prediction of heats of formation and molecular geometries of many organic molecules. The geometry optimization of phenothiazines [**1–20**] in the gas-phase and in water-solution was carried out with optimization of all geometrical parameters with no assumptions. In all cases, the PM3-optimized geometries were slightly non-planar, and the structures are shown in Figs. 3 to 4 in the gas-phase and Figs. 5 to 6 in the water-solution.

The dihedral angles between the plane of two benzene rings along the N10–S5 axis were about 165±5 degrees. Thus, in the case of the gas-phase, the C5a-S5-C4a-C4 dihedral angles were 161–173 degrees and the C9a-N10-C10a-C1 dihedral angles were 161–170 degrees except for compounds [**7**, **11**, and **20**]. In the case of compound [**20**], the C5a-S5-C4a-C4 dihedral angle was 145.04 degrees and the C9a-N10-C10a-C1 dihedral angle was 136.2 degrees. In the water-solution, the dihedral angles were similar to those in the gas-phase.

In the gas-phase, the C – C bond lengths of phenothiazines were 1.39–1.407 Å and the formal double bond lengths were 1.386–1.398 Å except for the central bond lengths such as C4a-C10a and C5a-C9a which were 1.400–1.409 and 1.446–1.449 Å, respectively. The C – S bond lengths of C4a-S5 and S5-C5a were 1.750–1.760 Å. The C – Cl bond lengths were 1.685–1.686 Å and the C – S bond lengths were 1.762 Å. The C – O bond lengths were 1.364–1.369 Å. In the water-solution, the bond lengths of phenothiazines were similar to those in the gas-phase. In the gas-phase, the distance between N10 and the propylene nitrogen atom were about 5.071 Å. In compounds [**4**] and [**7**], the distance between N10 and the propylene nitrogen atom were 4.434 Å and 4.390 Å, respectively. The distances between N10 and two methylene nitrogen atoms were about 3.859 Å. In the water-solution, the distance between N10 and alkylated nitrogen atoms were similar to those in the gas-phase. Some correlation seems

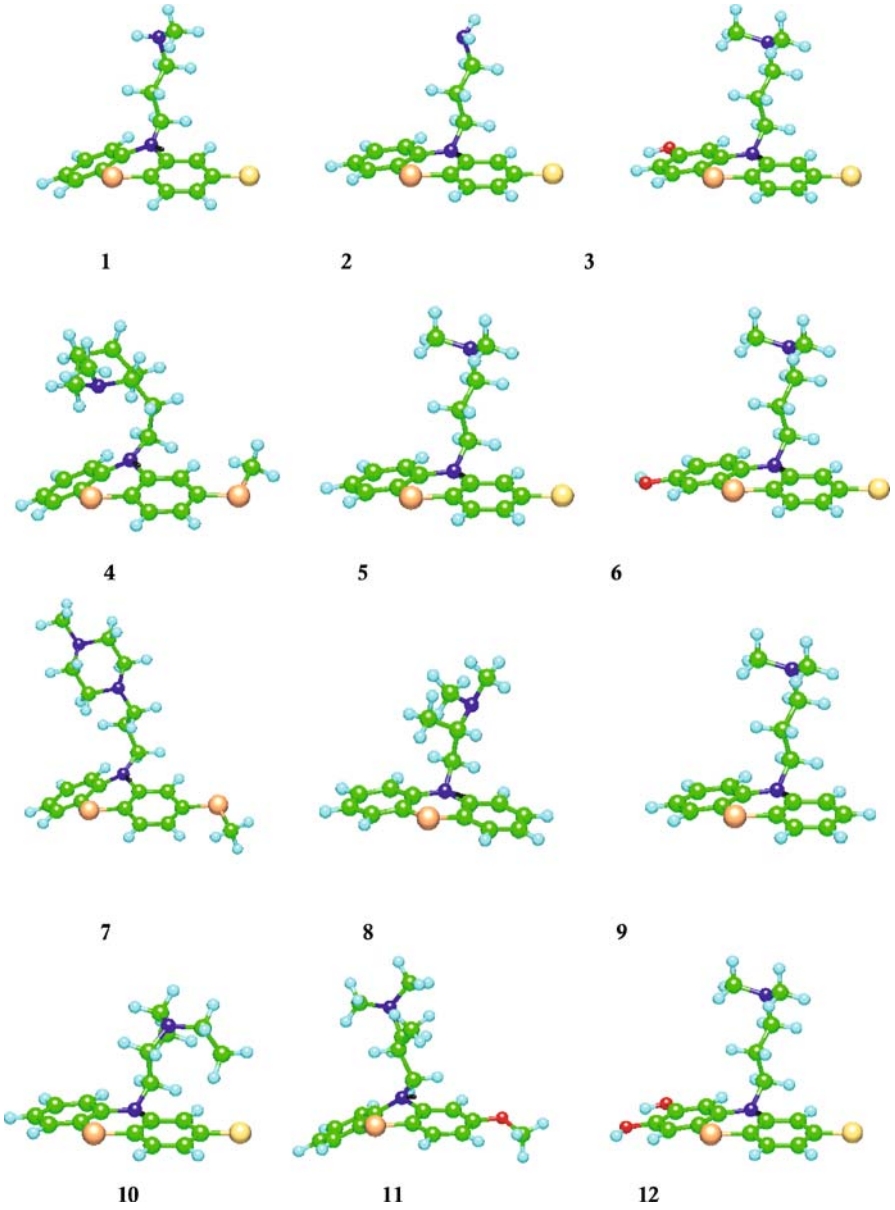

Fig. 3 PM3-optimized geometries of phenothiazines [**1–12**] in the gas-phase

to exist between the pharmacological activity and the length of the carbon chain joining the phenothiazine and the phenothiazine nitrogen atom.

Electrophilic and nucleophilic attacks on phenothiazines should be favored at the atom with the largest π-HOMO and π-LUMO coefficients, respectively.

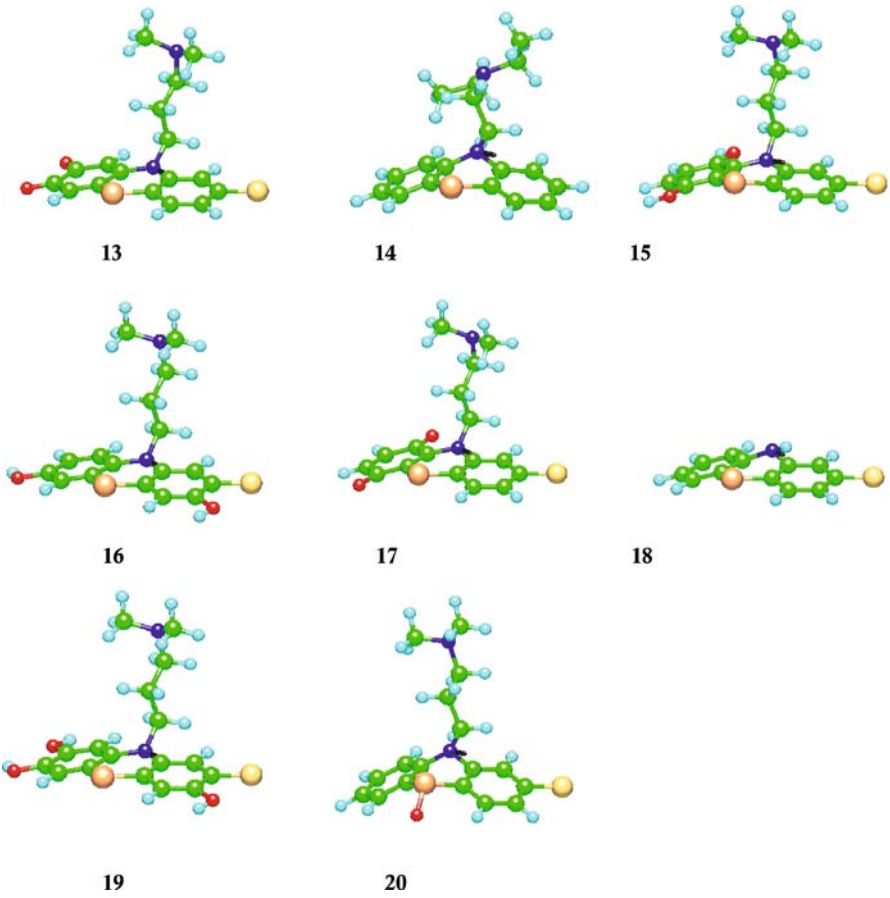

Fig. 4 PM3-optimized geometries of phenothiazines [**13–20**] in the gas-phase

Tables 1 and 2 show the π-HOMO coefficients of phenothiazines [**1–20**] in the gas-phase and water-solution, respectively.

The π-HOMO coefficients are in the order S5 > N10 and thus an electrophilic attack may occur at position S5 (Tables 1 and 2) except for compound [**20**]. Tables 3 and 4 show the π-LUMO coefficients of [**1–20**] in the gas-phase and water-solution, respectively. In all cases, the π-LUMO coefficients are in the order C4a > C10a, and thus a nucleophilic attack may occur at the position C4a except for compounds [**8**, **11**, **13**, and **17**].

2.2 Classical QSAR of Phenothiazines

Antibacterial activity of 20 phenothiazines against *E. coli* K12 was compared with their electronic properties. A partition coefficient log P was used as an

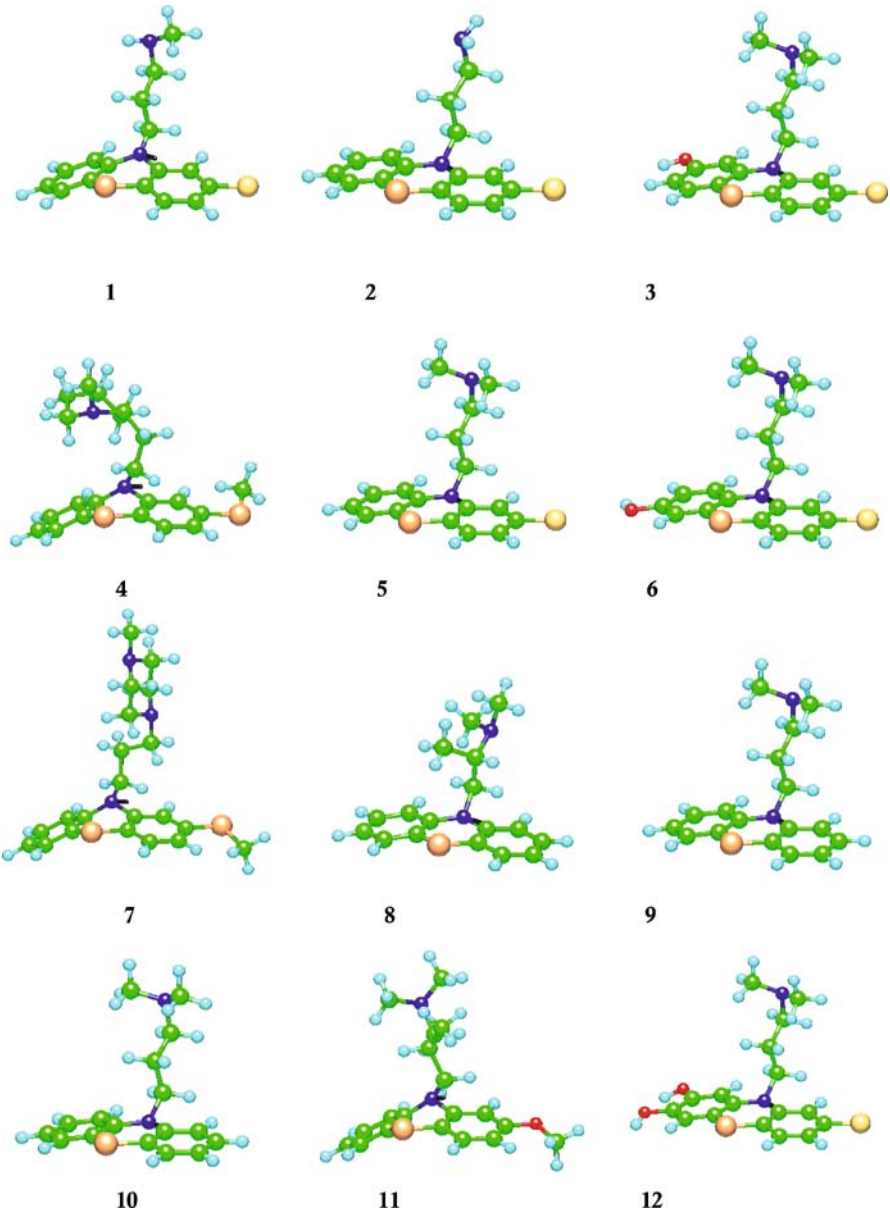

Fig. 5 PM3-optimized geometries of phenothiazines [**1–12**] in the water-solution

index of the QSAR analysis for new drug designing. A stereo hydrophobic parameter dGW was obtained by the PM3 method. The dGWs were defined as their free-energy changes for the association in the aqueous solution and in the gas-phase [11]. From the calculations, the structure–activity re-

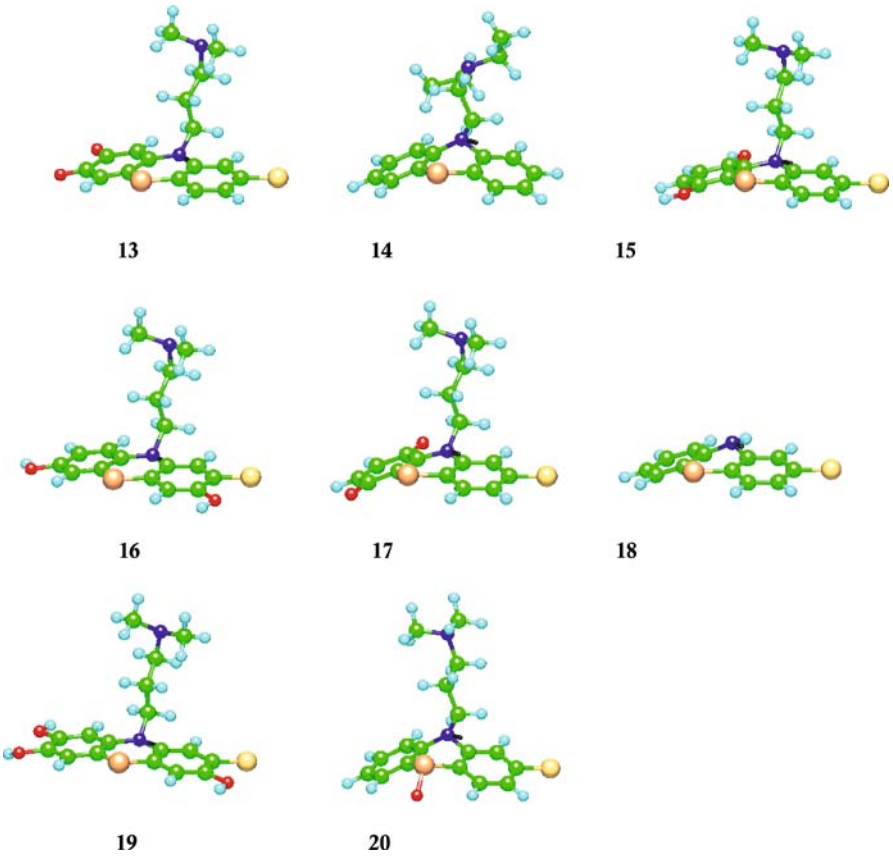

Fig. 6 PM3-optimized geometries of phenothiazines [**13–20**] in the water-solution

lationship analysis revealed that the hydrophobicity of the whole molecule ($\Delta\Delta H_f$) and the dipole moment (μ) might control the antibacterial activities of the phenothiazine and related compounds. Recently, we reported the QSAR between cytotoxic activity and the three QSAR parameters of $\Delta\Delta H_f$, I_{OH} and $\mu_{ESP\text{-}G}$ on 3-benzazepine derivatives [12] and the relationship between electronic structure and cytotoxic activity of azulenes [13], tropolones [14], azulenequinones, and trihaloacetylazulenes [15]. On the basis of our previous results, the relationship between the MIC values and the individual QSAR parameters was investigated.

The $\Delta\Delta H_f$, the highest occupied molecular orbital (HOMO), the lowest unoccupied molecular orbital (LUMO) energy and the dipole moment (μ) of phenothiazines [**1–20**] calculated by the PM3 method are provided in Table 5. Four types of dipole moment were calculated by the PM3 method. Among the phenothiazines [**1–20**], the value of $\Delta\Delta H_f$ increased in the following order: [**18**] ($\Delta\Delta H_f$ = 42.33 kJ/mol) < [**10**] (48.33 kJ/mol) < [**8**] (50.38 kJ/mol) < [**5**]

Table 1 HOMO coefficients of phenothiazines [**1**–**20**] in the gas-phase

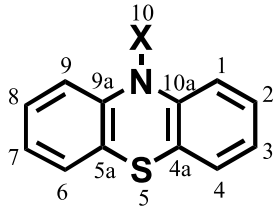

Compound No.	C-1	C-2	C-3	C-4	C-4a	S-5	C-5a	C-6	C-7	C-8	C-9	C-9a	N-10	C-10a
1	0.080	−0.190	−0.193	0.112	0.274	−0.563	0.259	0.096	−0.176	−0.179	0.087	0.217	−0.387	0.219
2	−0.082	0.190	0.191	−0.114	−0.273	0.566	−0.261	−0.097	0.177	0.181	−0.087	−0.219	0.387	−0.218
3	0.070	−0.189	−0.178	0.119	0.260	−0.573	0.294	0.116	−0.204	−0.184	0.035	0.195	−0.361	0.214
4	−0.054	0.202	0.227	−0.100	−0.295	0.500	−0.227	−0.066	0.149	0.136	−0.081	−0.191	0.385	−0.202
5	−0.081	0.190	0.193	−0.112	−0.275	0.563	−0.259	−0.096	0.176	0.179	−0.088	−0.216	0.388	−0.219
6	−0.092	0.177	0.195	−0.098	−0.270	0.526	−0.239	−0.040	0.187	0.208	−0.114	−0.253	0.401	−0.208
7	0.030	−0.206	−0.223	0.119	0.296	−0.511	0.219	0.070	−0.134	−0.141	0.058	0.193	−0.350	0.198
8	0.110	−0.178	−0.193	0.094	0.268	−0.547	0.263	0.086	−0.185	−0.170	0.105	0.210	−0.414	0.227
9	0.101	−0.184	−0.187	0.102	0.266	−0.561	0.263	0.094	−0.181	−0.179	0.094	0.217	−0.398	0.230
10	−0.095	0.184	0.197	−0.108	−0.275	0.552	−0.261	−0.096	0.183	0.176	−0.101	−0.216	0.417	−0.212
11	0.054	−0.190	−0.219	0.118	0.299	−0.529	0.230	0.074	−0.142	−0.148	0.063	0.204	−0.372	0.202
12	0.082	−0.172	−0.178	0.104	0.252	−0.533	0.291	0.052	−0.232	−0.214	0.042	0.233	−0.373	0.199
13	0.061	−0.227	−0.245	0.093	0.341	−0.527	0.088	0.210	0.011	0.011	0.222	0.052	−0.393	0.264
14	0.106	−0.182	−0.190	0.099	0.262	−0.519	0.239	0.069	−0.155	−0.150	0.074	0.213	−0.399	0.218
15	0.083	−0.191	−0.200	0.106	0.279	−0.544	0.236	0.083	−0.133	−0.129	0.083	0.188	−0.383	0.223
16	0.102	−0.212	−0.220	0.031	0.262	−0.481	0.230	0.026	−0.186	−0.190	0.121	0.235	−0.407	0.249
17	−0.075	0.196	0.197	−0.113	−0.278	0.572	−0.270	−0.019	0.019	0.018	−0.015	−0.208	0.396	−0.224
18	0.087	−0.195	−0.202	0.115	0.279	−0.564	0.256	0.094	−0.175	−0.175	0.090	0.230	−0.395	0.220
19	−0.088	0.207	0.200	−0.047	−0.244	0.497	−0.268	−0.032	0.214	0.215	−0.062	−0.232	0.376	−0.240
20	−0.158	0.136	0.270	0.020	−0.280	0.215	−0.260	0.045	0.185	0.084	−0.123	−0.202	0.456	−0.198

Table 2 HOMO coefficients of phenothiazines [**1**–**20**] in the water-solution

Compound No.	C-1	C-2	C-3	C-4	C-4a	S-5	C-5a	C-6	C-7	C-8	C-9	C-9a	N-10	C-10a
1	0.093	−0.182	−0.222	0.069	0.296	−0.496	0.281	0.050	−0.209	−0.171	0.105	0.225	−0.419	0.223
2	0.095	−0.181	−0.224	0.067	0.297	−0.495	0.282	0.049	−0.211	−0.170	0.108	0.226	−0.425	0.223
3	0.077	−0.180	−0.201	0.080	0.279	−0.510	0.331	0.072	−0.241	−0.191	0.030	0.202	−0.380	0.214
4	0.084	−0.186	−0.251	0.046	0.306	−0.408	0.243	0.010	−0.178	−0.117	0.091	0.210	−0.420	0.205
5	0.093	−0.182	−0.222	0.068	0.296	−0.496	0.281	0.050	−0.210	−0.171	0.105	0.225	−0.418	0.223
6	0.105	−0.158	−0.213	0.053	0.276	−0.445	0.262	−0.035	−0.236	−0.210	0.125	0.282	−0.425	0.202
7	0.096	−0.178	−0.251	0.047	0.303	−0.406	0.243	0.006	−0.178	−0.113	0.090	0.209	−0.417	0.203
8	0.122	−0.166	−0.220	0.046	0.283	−0.478	0.284	0.038	−0.219	−0.163	0.120	0.222	−0.436	0.232
9	−0.118	0.172	0.221	−0.048	−0.286	0.486	−0.285	−0.044	0.217	0.168	−0.114	−0.226	0.432	−0.237
10	−0.105	0.174	0.223	−0.064	−0.294	0.484	−0.279	−0.048	0.213	0.165	−0.115	−0.224	0.445	−0.215
11	−0.083	0.174	0.261	−0.048	−0.322	0.413	−0.244	−0.010	0.174	0.119	−0.084	−0.213	0.418	−0.203
12	−0.086	0.159	0.190	−0.068	−0.259	0.468	−0.315	0.008	0.269	0.235	−0.047	−0.261	0.383	−0.194
13	0.112	−0.199	−0.276	0.037	0.346	−0.436	0.076	0.163	0.022	0.047	0.294	0.053	−0.455	0.262
14	−0.138	0.157	0.235	−0.020	−0.277	0.396	−0.248	−0.005	0.186	0.121	−0.094	−0.223	0.443	−0.226
15	−0.111	0.168	0.237	−0.040	−0.292	0.416	−0.212	0.027	0.209	0.087	−0.158	−0.236	0.432	−0.220
16	0.118	−0.206	−0.234	−0.020	0.260	−0.407	0.246	−0.038	−0.222	−0.189	0.126	0.256	−0.421	0.257
17	−0.105	0.176	0.229	−0.058	−0.289	0.471	−0.334	−0.034	0.025	0.032	0.002	−0.147	0.439	−0.222
18	0.122	−0.172	−0.246	0.048	0.304	−0.456	0.275	0.023	−0.216	−0.145	0.119	0.240	−0.444	0.222
19	−0.102	0.202	0.213	−0.001	−0.247	0.434	−0.302	0.014	0.258	0.209	−0.055	−0.237	0.390	−0.246
20	0.199	−0.102	−0.284	−0.063	0.268	−0.151	0.240	−0.073	−0.211	−0.061	0.146	0.210	−0.497	0.190

Table 3 LUMO coefficients of phenothiazines [**1**–**20**] in the gas-phase

Compound No.	C-1	C-2	C-3	C-4	C-4a	S-5	C-5a	C-6	C-7	C-8	C-9	C-9a	N-10	C-10a
1	−0.089	0.437	−0.314	−0.147	0.462	−0.033	−0.282	0.077	0.213	−0.254	−0.006	0.289	0.022	−0.379
2	0.097	−0.447	0.318	0.151	−0.470	0.039	0.271	−0.075	−0.205	0.243	0.007	−0.280	−0.025	0.381
3	0.068	−0.423	0.322	0.126	−0.453	0.038	0.254	−0.027	−0.227	0.253	0.058	−0.324	−0.014	0.386
4	0.138	−0.460	0.297	0.186	−0.467	0.010	0.186	−0.044	−0.179	0.201	0.003	−0.212	−0.017	0.337
5	−0.088	0.436	−0.313	−0.146	0.460	−0.032	−0.284	0.077	0.215	−0.256	−0.005	0.291	0.021	−0.379
6	−0.095	0.416	−0.286	−0.153	0.436	−0.011	−0.340	0.144	0.221	−0.292	0.059	0.269	0.023	−0.353
7	0.113	−0.460	0.313	0.160	−0.459	0.007	0.182	−0.041	−0.176	0.194	0.008	−0.204	−0.023	0.358
8	−0.004	−0.328	0.278	0.086	−0.371	−0.016	0.375	−0.092	−0.285	0.343	−0.008	−0.372	0.003	0.363
9	0.008	−0.344	0.284	0.096	−0.387	−0.008	0.368	−0.094	−0.277	0.335	−0.008	−0.362	−0.003	0.369
10	−0.071	0.425	−0.320	−0.130	0.452	−0.035	−0.300	0.070	0.231	−0.261	−0.019	0.309	0.023	−0.385
11	−0.070	−0.324	0.301	0.024	−0.335	−0.036	0.281	−0.051	−0.251	0.276	0.010	−0.285	0.002	0.401
12	0.088	−0.434	0.312	0.146	−0.458	0.032	0.276	−0.080	−0.199	0.256	0.014	−0.291	−0.022	0.378
13	0.078	−0.033	−0.055	0.068	0.023	−0.142	0.377	−0.401	−0.279	−0.257	−0.338	0.334	−0.116	−0.025
14	−0.003	−0.346	0.295	0.089	−0.385	−0.030	0.272	−0.061	−0.241	0.276	−0.001	−0.279	0.005	0.374
15	0.033	−0.303	0.234	0.096	−0.326	−0.029	0.372	−0.071	−0.319	0.367	−0.020	−0.380	0.016	0.297
16	0.188	−0.426	0.217	0.253	−0.472	0.024	0.322	−0.154	−0.195	0.286	−0.078	−0.245	−0.009	0.281
17	0.040	0.064	−0.071	−0.027	0.089	0.100	−0.331	−0.275	−0.313	0.285	0.329	0.354	−0.106	−0.097
18	−0.039	0.406	−0.329	−0.108	0.436	−0.018	−0.272	0.045	0.237	−0.245	−0.037	0.289	0.016	−0.389
19	−0.201	0.445	−0.226	−0.264	0.493	−0.041	−0.276	0.131	0.170	−0.262	0.046	0.237	0.010	−0.286
20	−0.141	0.496	−0.306	−0.217	0.477	0.089	−0.050	−0.012	0.132	−0.106	−0.024	0.132	0.045	−0.378

Table 4 LUMO coefficients of phenothiazines [**1**–**20**] in the water-solution

Compound No.	C-1	C-2	C-3	C-4	C-4a	S-5	C-5a	C-6	C-7	C-8	C-9	C-9a	N-10	C-10a
1	−0.091	0.446	−0.310	−0.171	0.472	−0.035	−0.265	0.082	0.194	−0.236	0.105	0.281	0.024	−0.391
2	−0.088	0.444	−0.310	−0.168	0.470	−0.035	−0.271	0.083	0.198	−0.239	0.108	0.286	0.024	−0.392
3	−0.091	0.454	−0.319	−0.170	0.481	−0.045	−0.220	0.048	0.178	−0.211	0.030	0.282	0.023	−0.399
4	0.185	−0.497	0.294	0.233	−0.490	0.007	0.103	−0.026	−0.127	0.136	0.091	−0.147	−0.041	0.343
5	0.092	−0.447	0.309	0.172	−0.472	0.035	0.265	−0.082	−0.194	0.235	0.105	−0.281	−0.024	0.391
6	0.105	−0.450	0.300	0.182	−0.470	0.029	0.285	−0.126	−0.177	0.237	0.125	−0.251	−0.031	0.382
7	0.177	−0.496	0.297	0.227	−0.486	0.009	0.109	−0.029	−0.129	0.140	0.090	−0.149	−0.041	0.346
8	0.002	0.355	−0.280	−0.119	0.403	0.006	−0.343	0.099	0.253	−0.312	0.120	0.357	0.005	−0.391
9	−0.003	−0.343	0.270	0.117	−0.390	−0.007	0.369	−0.113	−0.262	0.332	−0.114	−0.370	−0.002	0.379
10	−0.077	0.437	−0.314	−0.159	0.465	−0.039	−0.283	0.080	0.207	−0.243	−0.115	0.296	0.028	−0.395
11	0.023	0.346	−0.256	−0.100	0.355	0.043	−0.268	0.092	0.215	−0.280	−0.084	0.265	−0.006	−0.376
12	−0.100	0.453	−0.309	−0.177	0.478	−0.040	−0.258	0.096	0.171	−0.229	−0.047	0.263	0.026	−0.390
13	0.074	−0.018	−0.062	0.053	0.046	−0.136	0.350	−0.354	−0.341	−0.331	0.294	0.349	−0.136	−0.034
14	−0.009	0.347	−0.258	−0.132	0.381	0.045	−0.259	0.092	0.213	−0.279	−0.094	0.266	−0.007	−0.363
15	0.093	−0.424	0.285	0.173	−0.440	0.000	0.241	−0.089	−0.215	0.253	−0.158	−0.281	−0.021	0.367
16	−0.188	0.453	−0.255	−0.270	0.503	−0.040	−0.263	0.130	0.153	−0.227	0.126	0.227	0.017	−0.312
17	0.061	0.063	−0.091	−0.016	0.103	0.067	−0.286	−0.305	−0.251	0.242	0.002	0.388	−0.142	−0.109
18	0.093	−0.444	0.303	0.173	−0.459	0.013	0.228	−0.059	−0.194	0.222	0.119	−0.249	−0.028	0.383
19	−0.186	0.459	−0.265	−0.268	0.512	−0.053	−0.230	0.094	0.148	−0.214	−0.055	0.240	0.013	−0.319
20	0.166	−0.504	0.275	0.258	−0.475	−0.125	0.014	0.016	−0.108	0.082	0.146	−0.102	−0.061	0.376

Table 5 QSAR parameters of phenothiazines [1–20]

Compound No.	MIC	*M.W.*	ΔH_f (in kJ/mol) in gas	in water	$\Delta\Delta H_f$	$\Delta\Delta H_f/M.W.E_{H(G)}$	$E_{H(W)}$	$E_{L(G)}$	$E_{L(W)}$	μ_G	$\mu_{ESP\text{-}G}$	μ_W	$\mu_{ESP\text{-}W}$
1	0.47	304.84	203.12	148.23	54.89	0.18	−8.06	−8.58	−0.46	−0.75	0.73	0.48	1.11	0.66
2	0.73	290.81	217.61	159.27	58.34	0.20	−8.00	−8.57	−0.41	−0.75	1.99	1.04	3.12	2.38
3	0.90	334.86	4.75	−70.99	75.75	0.23	−7.99	−8.53	−0.44	−0.74	1.60	1.11	2.21	1.75
4	1.90	370.57	210.27	136.91	73.35	0.20	−7.78	−8.62	−0.29	−0.84	4.54	2.49	7.26	5.74
5	2.00	318.86	194.31	140.46	53.85	0.17	−8.05	−8.58	−0.45	−0.75	1.07	0.82	1.45	1.05
6	2.42	334.86	8.51	−67.23	75.75	0.23	−8.03	−8.52	−0.46	−0.75	1.88	0.89	3.10	2.16
7	2.50	385.58	237.68	147.3	90.38	0.23	−7.99	−8.62	−0.41	−0.82	1.40	0.88	2.61	2.25
8	3.00	284.42	229.85	179.46	50.38	0.18	−7.89	−8.55	−0.22	−0.62	2.05	1.32	2.96	2.26
9	3.09	284.42	221.85	167.69	54.16	0.19	−7.97	−8.58	−0.26	−0.62	0.85	0.41	1.62	1.02
10	3.10	332.89	164.19	115.86	48.33	0.15	−7.94	−8.52	−0.42	−0.77	2.20	1.19	3.26	2.39
11	3.50	328.47	55.07	−12.85	67.92	0.21	−7.94	−8.65	−0.23	−0.62	1.76	1.13	2.98	2.47
12	3.60	350.86	−174.74	−263.1	88.36	0.25	−7.96	−8.46	−0.45	−0.74	1.73	1.17	2.40	1.86
13	3.87	348.85	−26.60	−128	101.40	0.29	−8.83	−8.79	−1.81	−1.92	5.19	5.10	8.25	8.30
14	4.30	298.45	203.94	147.63	56.31	0.19	−8.00	−8.70	−0.25	−0.63	2.93	1.70	5.18	4.34
15	5.60	350.86	−139.16	−233.5	94.34	0.27	−8.01	−8.67	−0.48	−0.78	3.19	1.64	4.94	3.62
16	5.70	350.86	−172.06	−270.89	98.83	0.28	−7.98	−8.45	−0.46	−0.74	1.78	0.92	2.67	1.89
17	6.40	348.85	−5.04	−99.86	94.82	0.27	−8.32	−8.60	−1.91	−1.91	0.65	0.41	2.73	2.48
18	16.00	233.72	222.70	180.37	42.33	0.18	−8.06	−8.60	−0.48	−0.74	1.98	1.24	3.47	2.82
19	22.50	366.86	−353.70	−467.7	114.00	0.31	−7.95	−8.40	−0.46	−0.74	1.54	0.62	2.57	1.71
20	24.30	334.86	86.37	−26.5	112.88	0.34	−8.74	−8.84	−0.57	−0.72	3.60	2.92	6.26	5.75

(53.85 kJ/mol) < [**9**] (54.16 kJ/mol) < [**1**] (54.89 kJ/mol). The value of HOMO energy in the gas-phase increased in the following order: [**4**] (–7.78 eV) < [**8**] (–7.89 eV) < [**10**] = [**11**] (–7.94 eV) < [**19**] (–7.95 eV) < [**12**] (–7.96 eV). The value of the dipole moment (μ_G) in the gas-phase calculated by the ESP/PM3 method increased as follows: [**17**] (0.65 D) < [**1**] (0.73 D) < [**9**] (0.85 D) < [**5**] (1.07 D) < [**7**] (1.40 D) < [**19**] (1.54 D).

On the other hand, the MIC value of [**1**] against the *E. coli* K12 was the lowest (MIC = 0.47×10^{-4} M), followed by [**2**] (0.73×10^{-4} M), [**3**] (0.90×10^{-4} M), and [**4**] (1.90×10^{-4} M) [15]. Their antibacterial activity could not be related to the individual QSAR parameters, such as $\Delta\Delta H_f$, HOMO energy and μ_G in the gas-phase. The correlation coefficient (r^2) and the Fisher statistic (F) are important in assessing the "goodness" of a regression fit. In order to obtain a more quantitative characteristic of the goodness of a model, the well-known Fisher statistic value was used. Of the 20 phenothiazines, desmethylchlorpromazine [**1**] showed the highest MIC value against *E. coli* K12 (17). In order to obtain a quantitative correlation between the MIC and electronic properties, the coefficient of the multiple determinations and the F value were calculated. The structure–activity relationship analysis revealed that the hydrophobicity of the molecule ($\Delta\Delta H_f$), the HOMO energy ($E_{H(G)}$) and the dipole moment (μ_G) in the gas-phase might greatly con-

Table 6 Observed and estimated MIC of phenothiazines [**1**–**20**]

Compound No.	MIC obs.	estim.	$\Delta\Delta H_f$	$E_{H(G)}$	$\mu_{ESP\text{-}G}$
1	0.47	0.39	54.89	–8.06	0.48
2	0.73	2.01	58.34	–8.00	1.04
3	0.90	2.98	75.75	–7.99	1.11
4	1.90	5.29	73.35	–7.78	2.49
5	2.00	1.54	53.85	–8.05	0.82
6	2.42	2.64	75.75	–8.00	0.89
7	2.50	2.85	90.38	–7.99	0.88
8	3.00	0.96	50.38	–7.89	1.32
9	3.09	–1.41	54.16	–7.97	0.41
10	3.10	1.12	48.33	–7.94	1.19
11	3.50	1.88	67.92	–7.94	1.13
12	3.60	3.48	88.36	–7.96	1.17
13	3.87	34.12	101.40	–8.83	5.10
14	4.30	4.52	56.31	–8.00	1.70
15	5.60	6.49	94.34	–8.01	1.64
16	5.70	3.28	98.83	–7.98	0.92
17	6.40	6.39	94.82	–8.32	0.41
18	16.00	2.82	42.33	–8.06	1.24
19	22.50	2.37	114.00	–7.95	0.62
20	24.30	24.3	112.88	–8.74	2.92

tribute to antibacterial activity. Consequently, the following correlation Eq. 1 was obtained for the *E. coli* K12.

$$\mathrm{MIC} = -153.53 + 0.03 \times \Delta\Delta H_\mathrm{f} - 18.63 \times E_{H(G)} + 3.30 \times \mu_\mathrm{G} \quad (1)$$
$$n = 5(\mathbf{1}, \mathbf{9}, \mathbf{10}, \mathbf{17}, \mathbf{20}), \quad r^2 = 0.999, \quad F = 7118.53$$

The MIC values estimated from Eq. 1 are shown in Table 6.

The expected MIC values of most of the phenothiazines [**1–20**] against *E. coli* K12 were almost superimposed with those for the MIC values for the corresponding compounds except [**9**, **13**, **18**, and **19**]. However, the theoretical calculations such as frontier molecular orbital, dipole moments and $\Delta\Delta H_\mathrm{f}$ may be applicable to predict the MIC values of phenothiazines.

3
Classical QSAR of Benzo[*a*]phenothiazines

3.1
Electronic Structures and Optimized Geometries of Benzo[*a*]phenothiazines

The geometry optimization of phenothiazine [**21**] and benzo[*a*]phenothiazines [**22–29**] and benz[*c*]acridines [**30–41**] in the gas-phase and in the water-solution was carried out with optimization of all geometrical parameters with no assumptions. In the cases of compounds [**26–29**], the PM3 optimized geometries were planar. In the cases of compounds [**21**] and [**22–25**], the PM3 optimized geometries were slightly non-planar, and the structures are shown in Figs. 7, 8, 9, 10, 11, and 12. The dihedral angles between the benzene ring and naphthalene ring to the S7-N12 axis were about 170 degrees. In the gas-phase, the C – C bond lengths of benzo[*a*]phenothiazines were 1.402–1.445 Å and the double bond lengths were 1.380–1.394 Å, except for the central bond lengths such as C4a-C12b, C6a-C12a, and C7a-C11a which were 1.414–1.418 Å. The bond lengths of C11a-N12 and N12-C12a were 1.402–1.404 and 1.385–1.386 Å, respectively. The bond lengths of C6a-S7 and S7-C7a were 1.730–1.737 Å. In the water-solution, the bond lengths of benzo[*a*]phenothiazines were similar to those in the gas-phase.

3.2
Classical QSAR of Benzo[*a*]phenothiazines

Some of the benzo[*a*]phenothiazines exhibit antitumor activity against a solid type of *Ehrlich carcinoma* [17]. The differentiation-inducing activity of 12*H*-benzo[*a*]phenothiazine [**22**] against human myelogenous lekemic cell lines (ML-1) ($17.4\,A_{590}/10^7$ cells at 25 μg/mL) and 5-oxo-5*H*-benzo[*a*]phenothiazine [**26**] ($17.2\,A_{590}$) are the greatest, followed by 10-

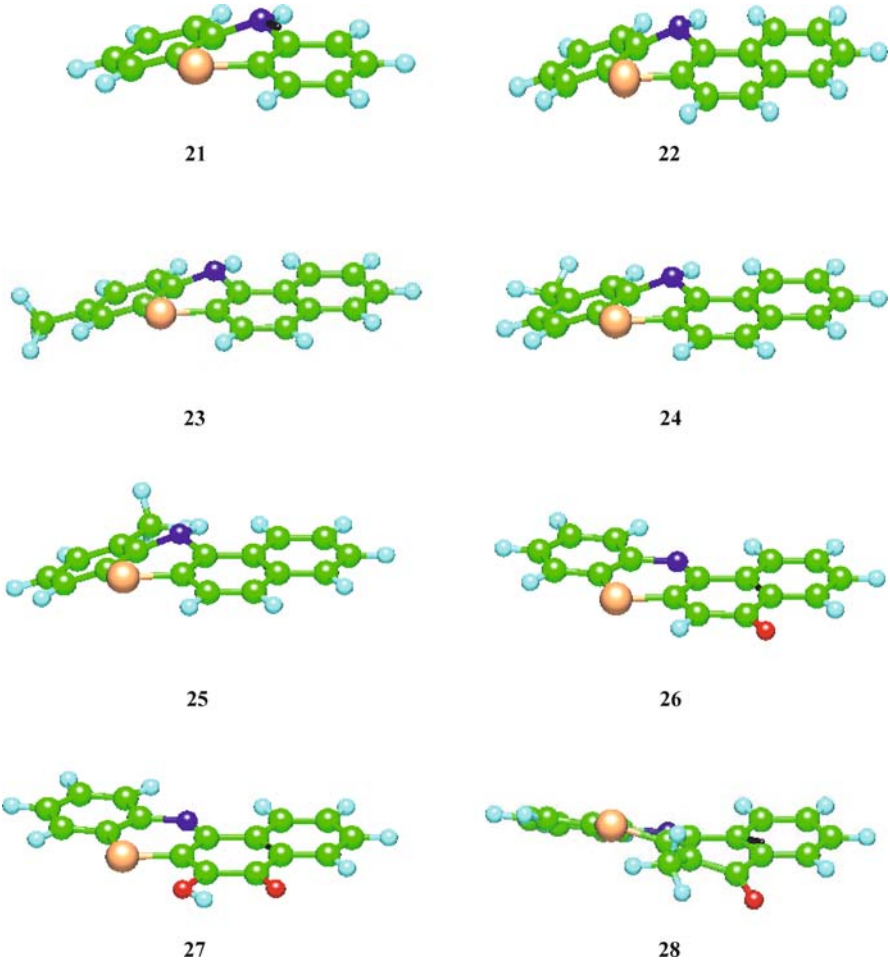

Fig. 7 PM3 optimized geometries of benzo[*a*]phenothiazines [**21–28**] in the gas-phase

methyl-12*H*-benzo[*a*]phenothiazine [**24**] ($7.4A_{590}$), 9-methyl-12*H*-benzo[*a*]-phenothiazine [**23**] ($6.3A_{590}$) and 11-methyl-12*H*-benzo[*a*]phenothiazine [**25**] ($2.5A_{590}$). Among eight benzo[*a*]phenothiazines, 12*H*-benzo[*a*]phenothiazine [**22**], 9-methyl-12*H*-benzo[*a*]phenothiazine [**23**] and 11-methyl-12*H*-benzo[*a*]phenothiazine [**25**] produce small cell bodies, which are stained strongly with NBT-reducing agents. The differentiation-inducing activity of 12*H*-benzo[*a*]phenothiazine [**22**] ($17.4A_{590}$) is 11-times higher than of phenothiazine [**21**] ($1.6A_{590}$).

The $\Delta\Delta H_f$, π-HOMO and π-LUMO energy and μ of phenothiazine [**21**] and benzo[*a*]phenothiazines [**22–29**] are summarized in Table 7.

Among the phenothiazine [**21**] and benzo[*a*]phenothiazines [**22–29**], the value of $\Delta\Delta H_f/M.W.$ was increased in the following order: [**29**]

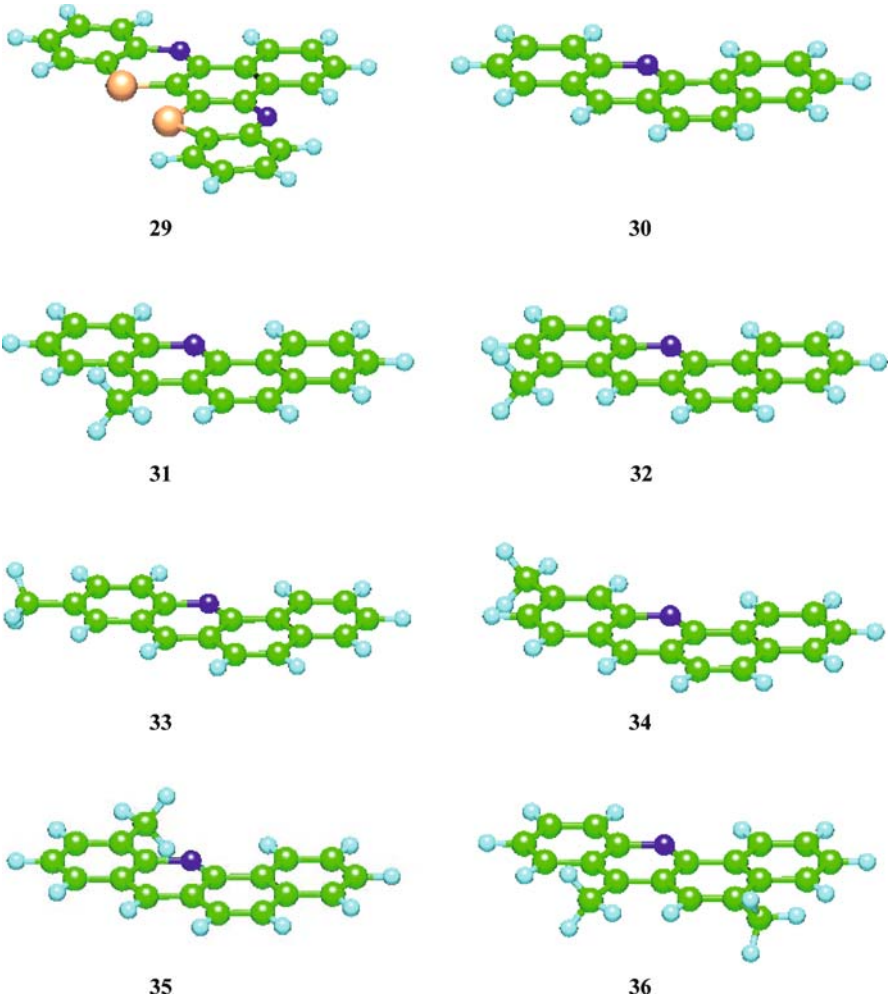

Fig. 8 PM3 optimized geometries of benzo[*a*]phenothiazine [**29**] and benz[*c*]acridines [**30**–**36**] in the gas-phase

($\Delta\Delta H_f/M.W.$ = 0.14 kJ/mol/g) < [**23**] = [**25**] (0.18 kJ/mol/g) < [**22**] = [**24**] = [**28**] (0.19 kJ/mol/g) < [**26**] (0.22 kJ/mol/g) < [**27**] (0.25 kJ/mol/g). The value of LUMO energy ($E_{L(W)}$) in the water-solution was increased in the following order: [**29**] (– 2.15 eV) < [**26**] (– 1.95 eV) < [**28**] (– 1.94 eV) < [**27**] (– 1.89 eV) < [**25**] (– 1.06 eV) < [**22**] = [**23**] = [**24**] (– 1.05 eV). The value of the dipole moment (μ_W) in the water-solution calculated by ESP/PM3 method also was in the following order: [**26**] (5.48 D) > [**24**] (4.86 D) > [**25**] (4.83 D) > [**28**] (4.62 D) > [**22**] (4.61 D) > [**23**] (4.52 D). Their NBT-reducing activity could not be related to the individual QSAR parameters, such as $\Delta\Delta H_f/M.W.$, LUMO energy and μ_W in the water-solution. The structure–activity relation-

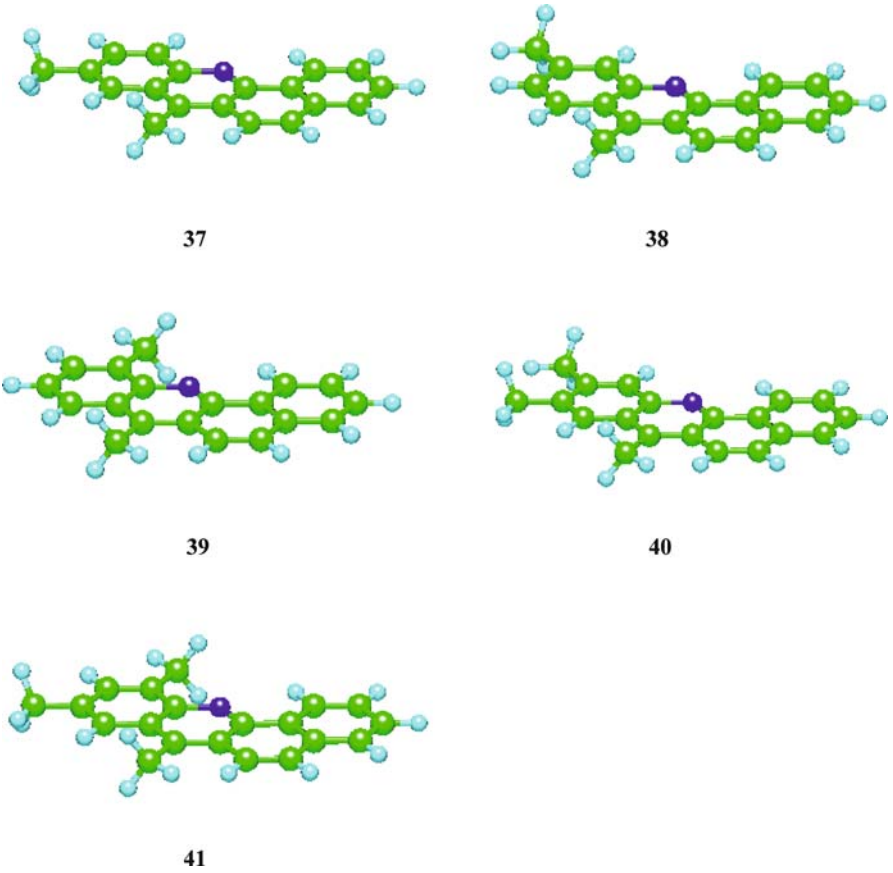

Fig. 9 PM3 optimized geometries of benz[*c*]acridines [**37–41**] in the gas-phase

ship analysis revealed that the hydrophobicity of the molecule ($\Delta\Delta H_f$), the LUMO energy ($E_{L(W)}$) and the dipole moment (μ_W) in the water-solution might greatly contribute to NBT-reducing activity (NBT-RA). Consequently, the following correlation equation **2** was obtained for the *ML-1* cells.

$$\begin{aligned} \text{NBT-RA} =& -74.19 + 819.38 \times \Delta\Delta H_f/M.W. \\ &+ 15.06 \times E_{L(W)} - 11.16 \times \mu_W \qquad (2) \\ n = 5(\mathbf{24, 25, 26, 28, 29}) &, \quad r^2 = 0.999 , \quad F = 2512.11 \end{aligned}$$

The values of NBT-reducing activity estimated from the equation 2 are shown in Table 8. The expected values of the NBT-reducing activity of most of benzo[*a*]phenothiazines [**22–29**] against *ML-1* cells were almost superimposed with those for the experimentally obtained NBT values for the corres-

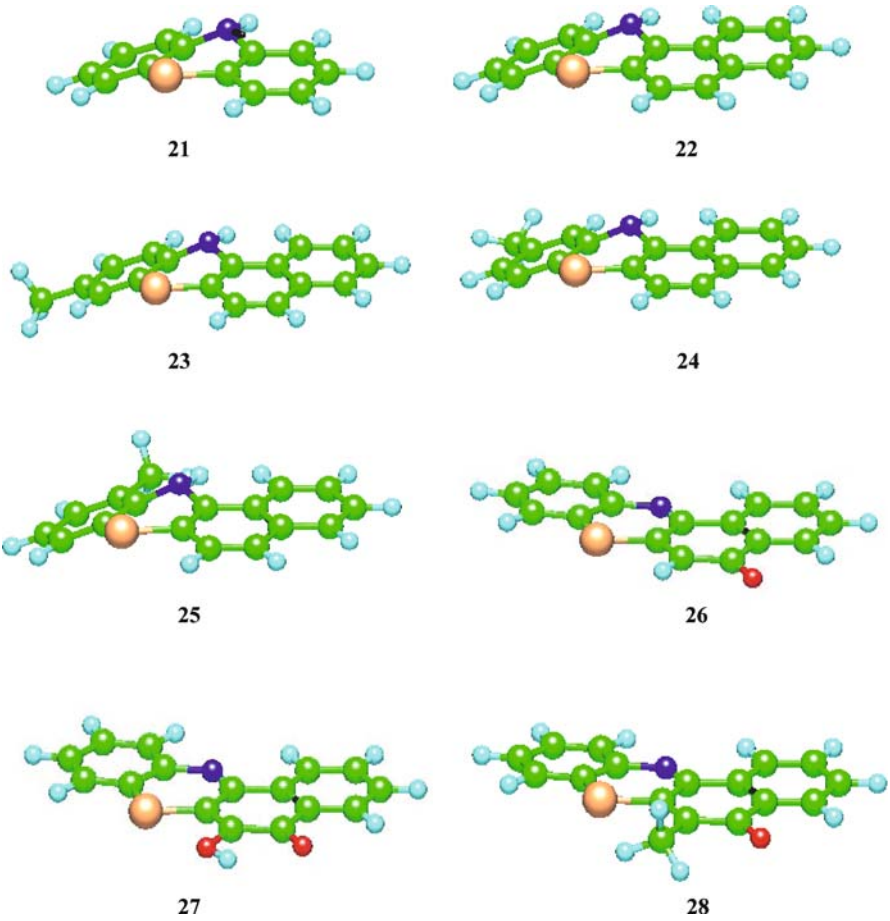

Fig. 10 Optimized geometries of benzo[*a*]phenothiazines [**21**–**28**] in the water-phase

ponding compounds except [**27**]. However, the theoretical calculations such as frontier molecular orbital, dipole moments and $\Delta\Delta H_f$ may be applicable to predict the NBT activity of benzo[*a*]phenothiazines.

4
Classical QSAR of Benz[*c*]acridines

4.1
Electronic Structures and Optimized Geometries of Benz[*c*]acridines

The geometry optimization of benz[*c*]acridines [**30**–**41**] in the gas-phase and in the water-solution was carried out with the optimization of all geometrical

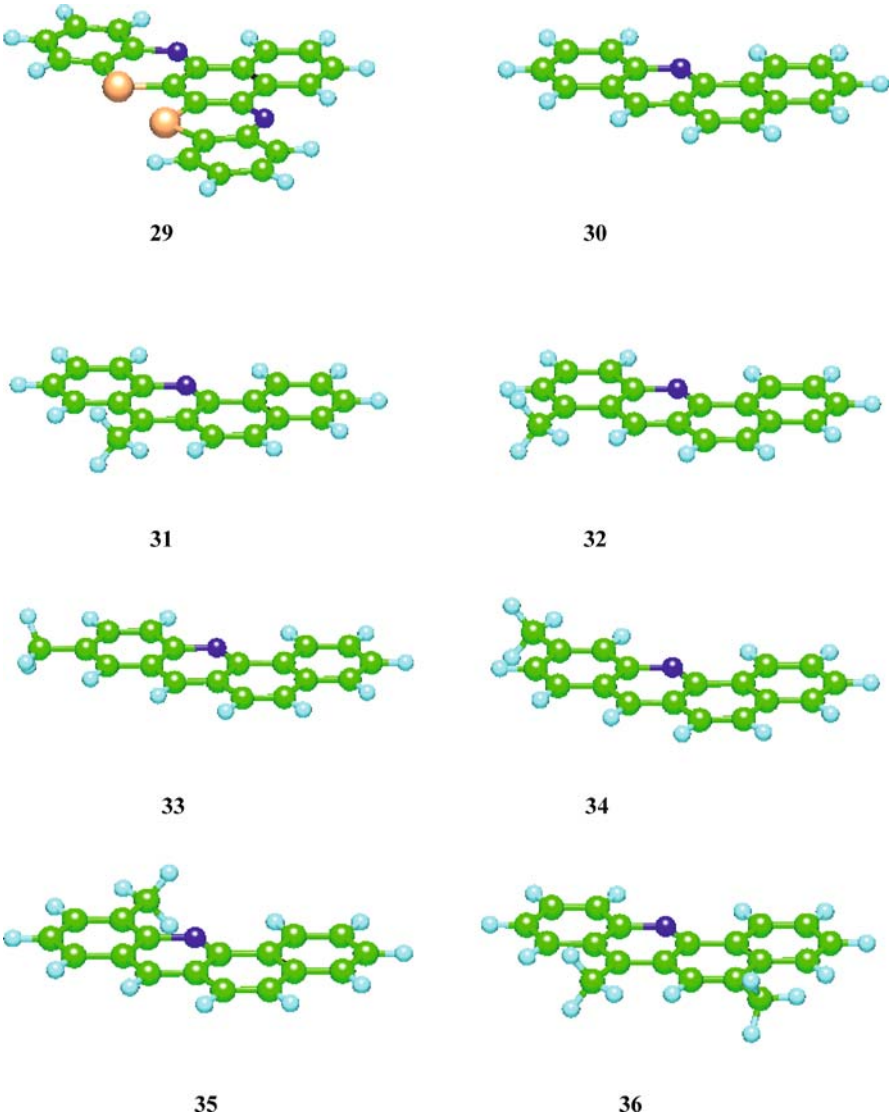

Fig. 11 Optimized geometries of a benzo[*a*]phenothiazine [**29**] and benz[*c*]acridines [**30**–**36**] in the water-phase

parameters with no assumptions. In all cases, the PM3-optimized geometries were planar, and the structures are shown in Figs. 2, 7, 8, 9, 10, 11, and Fig. 12. In the gas-phase, the C – C bond lengths of benz[*c*]acridines were 1.402–1.445 Å and the double bond lengths were 1.380–1.394 Å, except for the central bond lengths such as C4a-C12b, C6a-C12a, and C7a-C11a which were 1.414–1.418 Å. The bond lengths of C11a-N12 and N12-C12a

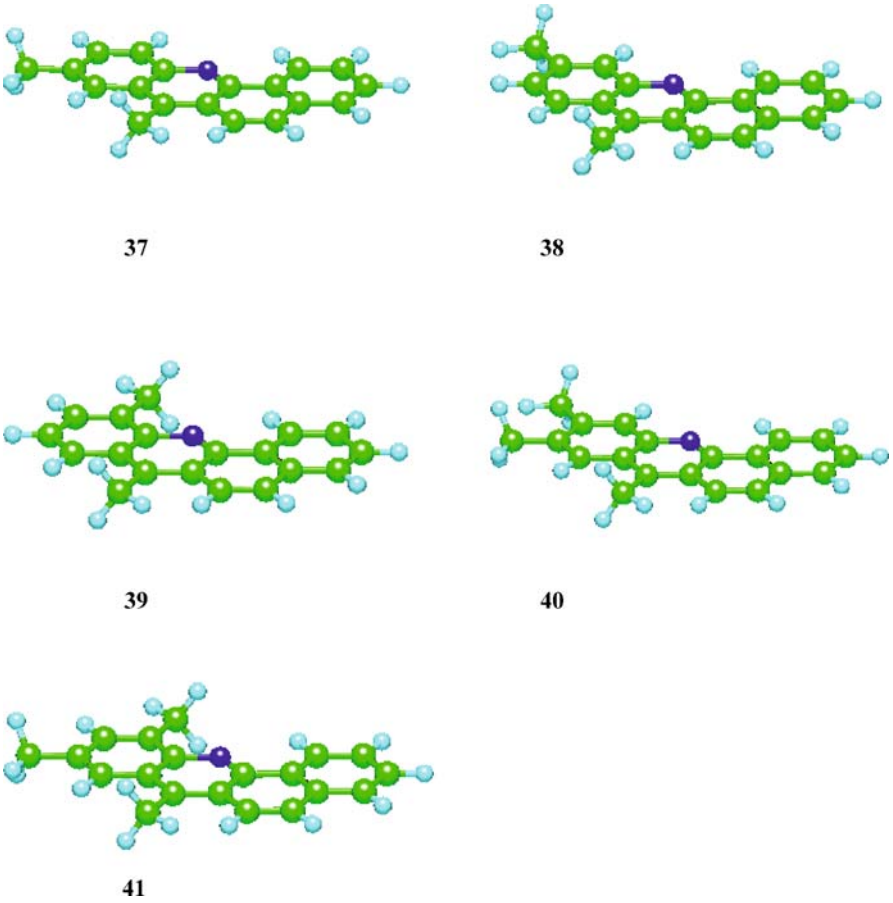

Fig. 12 Optimized geometries of benz[*c*]acridines [**37**–**41**] in the water-phase

were 1.402–1.404 and 1.385–1.386 Å, respectively. In the water-solution, the bond lengths of benz[*c*]acridines were similar to those in the gas-phase.

4.2 Classical QSAR of Benz[*a*]acridines

Some methylbenz[*c*]acridines are strongly carcinogenic, whereas their derivatives are inactive [18–22]. Previously, we reported on the relationship between the carcinogenic activity of benz[*a*]acridines [**30**–**40**] and the π-spin density [25] and the relationship between the carcinogenic activity of benz[*a*]acridines [**30**–**41**] and the values of the resonance energy per π-electron (REPE) [26, 27]. Consequently, by clockwise rotation on an angular ring or naphthalene moiety, the distribution of the π-spin dens-

Table 7 QSAR parameters of benzo[a]phenothizines [**21**–**29**]

Compound No.	NBT	*M.W.*	ΔH_f (in kJ/mol) in gas	in water	$\Delta\Delta H_f$	$\Delta\Delta H_f/M.W.$	$E_{H(G)}$	$E_{H(W)}$	$E_{L(G)}$	$E_{L(W)}$	Dipole moments (in Debye units) μ_G	$\mu_{ESP\text{-}G}$	μ_W	$\mu_{ESP\text{-}W}$
21	1.60	199.27	250.24	207.28	42.96	0.22	−7.97	−8.60	−0.30	−0.62	2.25	1.28	4.05	3.23
22	17.40	249.33	326.80	278.72	48.08	0.19	−7.85	−8.46	−0.75	−1.05	2.46	1.42	4.61	3.72
23	6.30	263.36	287.71	239.37	48.34	0.18	−7.81	−8.44	−0.73	−1.05	2.37	1.33	4.52	3.66
24	7.40	263.36	287.38	238.57	48.80	0.19	−7.81	−8.45	−0.73	−1.05	2.65	1.50	4.86	3.88
25	2.50	263.36	292.01	244.93	47.08	0.18	−7.85	−8.51	−0.73	−1.06	2.71	1.47	4.83	3.77
26	17.20	263.31	265.81	207.35	58.46	0.22	−8.72	−8.92	−1.71	−1.95	3.68	2.99	5.48	4.91
27	0.90	279.31	92.66	21.62	71.04	0.25	−8.33	−8.71	−1.70	−1.89	2.56	1.90	3.04	2.28
28	0.80	277.34	237.64	184.92	52.72	0.19	−8.64	−8.88	−1.57	−1.94	2.72	2.29	4.62	4.14
29	3.20	368.47	636.09	585.52	50.57	0.14	−8.01	−8.46	−1.76	−2.15	0.38	1.62	0.24	1.43

Table 8 Observed and estimated NBT of benzo[*a*]phenothiazines [**22–29**]

Compound No.	NBT obs.	estim.	$\Delta\Delta H_f$/M.W.	$E_{L(W)}$	μ_W
22	17.40	16.55	0.19	−1.05	4.61
23	6.30	9.91	0.18	−1.05	4.52
24	7.40	7.50	0.19	−1.05	4.86
25	2.50	2.40	0.18	−1.06	4.83
26	17.20	17.17	0.22	−1.95	5.48
27	0.90	71.72	0.25	−1.89	3.04
28	0.80	0.84	0.19	−1.94	4.62
29	3.20	3.19	0.14	−2.15	0.24

ity at the C-1, C-2, C-3, C-4, C-4a, C-5, C-6, C-6a, C-12a, and C-12b position on carcinogenic benz[*c*]acridines [**31**, **37–41**] changed alternately from negative π-spin density to positive π-spin density. However, non-carcinogenic benz[*c*]acridines [**30**, **32–36**] did not obey this rule. Carcinogenic benz[*c*]acridines must involve large negative values of the π-spin density at both C-1 and C-3 positions, and the large positive values of the π-spin density at both C-2 and C-4 positions. Therefore, active singlet oxygen might attack the M-region at the C-3 and C-4 positions or the bay-region at the C-1 and C-2 positions of benz[*c*]acridines.

The ΔPB, $\Delta\Delta H_f$, π-HOMO and π-LUMO energy and μ of benz[*c*]acridines [**30–41**] are summarized in Table 9. The difference of *t* REPE value (ΔPB) between the parent compound's REPE value and the REPE value of carbocation species derived from the ring-opening of the bay-region was calculated by Aihara's topological resonance energy (TRE) method [26, 27]. Consequently, the REPE difference values ($\Delta PB = 0.0084\beta$ to 0.0092β) of the five non-carcinogenic benz[*c*]acridines [**30**, **32–36**] were higher than the REPE difference values ($\Delta PB = 0.0073\beta$ to 0.0083β) of the six carcinogenic benz[*c*]acridines [**31**, **37–41**] except for non-carcinogenic 5,7-dimethylbenz[*c*]acridines [**36**, $\Delta PB = 0.0078\beta$] (Table 9).

Of the benz[c]acridines [**30–41**], the value of $\Delta\Delta H_f$ increased in the following order: [**31**] ($\Delta\Delta H_f = 40.13$ kJ/mol) < [**34**] (40.38 kJ/mol) < [**36**] (40.56 kJ/mol) < [**38**] (40.95 kJ/mol) < [**40**] (41.59 kJ/mol). The value of HOMO energy in the gas-phase increased in the following order: [**31**] (−8.51 eV) < [**32**] (−8.53 eV) < [**34**] = [**35**] (−8.55 eV) < [**33**] (−8.57 eV) < [**30**] (−8.61 eV). The value of the dipole moment (μ_W) in the water-solution calculated by the ESP/PM3 method increased as follows: [**32**] (3.56 D) < [**34**] (3.73 D) < [**31**] (3.75 D) < [**38**] (3.76 D) < [**36**] (3.78 D) < [**40**] (3.81 D). Their carcinogenic activity could not be related to the individual QSAR parameters, such as $\Delta\Delta H_f$, HOMO energy, and μ_W. Since there were no numerical data for carcinogenicity index, we have not discussed QSAR an-

Table 9 QSAR parameters of benz[*c*]acridines [**30–41**]

Compound No.	ΔPB[1]	Carcino-genicity index[2]	M.W.	ΔH_f (in kJ/mol) in gas	in water	$\Delta\Delta H_f$	$\Delta\Delta H_f$/ M.W.	$E_{H(G)}$	$E_{H(W)}$	$E_{L(G)}$	$E_{L(W)}$	Dipole moments (in Debye units) μ_G	$\mu_{ESP\text{-}G}$	μ_W	$\mu_{ESP\text{-}W}$
30	0.0092	–	229.28	344.28	305.86	38.42	0.17	−8.61	−8.94	−1.13	−1.51	1.47	1.20	3.18	3.12
31	0.0083	+	243.31	312.52	272.92	39.60	0.16	−8.51	−8.89	−1.12	−1.54	1.87	1.43	3.67	3.44
32	0.0084	–	243.31	307.95	268.77	39.18	0.16	−8.53	−8.89	−1.12	−1.53	1.79	1.35	3.56	3.32
33	0.0084	–	243.31	304.36	265.74	38.62	0.16	−8.57	−8.94	−1.10	−1.51	1.58	1.25	3.16	3.03
34	0.0084	–	243.31	304.29	265.08	39.20	0.16	−8.55	−8.92	−1.10	−1.51	1.45	1.22	3.20	3.20
35	0.0085	–	243.31	310.31	279.11	31.20	0.13	−8.55	−8.88	−1.11	−1.47	1.16	1.01	2.50	2.56
36	0.0078	–	257.33	277.95	237.84	40.12	0.16	−8.42	−8.81	−1.10	−1.56	1.99	1.46	3.71	3.38
37	0.0078	+	257.33	272.75	232.87	39.87	0.15	−8.47	−8.88	−1.09	−1.54	1.97	1.47	3.66	3.35
38	0.0077	+	257.33	273.58	233.14	40.43	0.16	−8.45	−8.86	−1.10	−1.55	1.79	1.41	3.60	3.43
39	0.0078	+	257.33	279.00	246.74	32.26	0.13	−8.45	−8.82	−1.10	−1.50	1.56	1.25	2.99	2.88
40	0.0073	+	271.36	241.12	200.20	40.92	0.15	−8.41	−8.85	−1.07	−1.56	1.97	1.50	3.67	3.39
41	0.0074	+	271.36	239.35	206.76	32.60	0.12	−8.41	−8.80	−1.07	−1.50	1.66	1.28	2.99	2.79

[1] $\Delta PB = REPE(P) - REPE(B)$ [26]
[2] Carcinogenicity index [17–20]
+: carcinogenic
–: non-carcinogenic

alysis. However, the results of the present study suggest the applicability of theoretical calculations, such as π-spin density, resonance energy per π-electron and HOMO energy, for the prediction of the carcinogenic activity of benz[*c*]acridines.

5 Conclusions

The results of the present study suggest the applicability of theoretical calculations such as frontier molecular orbital, dipole moments and $\Delta\Delta H_f$ in the prediction of biological activity of phenothiazines, benzo[*a*]phenothiazines, and benz[*c*]acridines.

References

1. Motohashi N (1988) Antitumor activities of phenothiazines. In: Gupta RR (ed) Phenothiazines and 1,4-benzothiazines. Elsevier, Amsterdam, pp 705–774
2. Motohashi N, Kurihara T, Sakagami H, Molnar J (1992) Relationship between resonance energy and carcinogenic activity of benz[*c*]acridines. Anticancer Res 12:2105–2108
3. Wood RC, McCale CH, Williams G (1941) Phenothiazine, phenoxathiin, phenoxaselenia and phenoxatellurin. Phil Mag 31:71–80
4. Leonard NJ, Sutton LE (1948) The Use of Fluoro Compounds in the Determination of Valency Angles by Electric Dipole Moment Measurements. J Am Chem Soc 70:1564–1571
5. Kurihara T, Watanabe T, Yoshikawa K, Motohashi N (1998) Radical productions and pi-spin density by UHF/PM3 method on benz[*c*]acridines and benzo[*a*]phenothiazines. Anticancer Res 18:429–432
6. Kurihara T, Motohashi N, Kobayashi H, Yamanaka W, Dohyashiki S, Molnar J (1998) Interaction of chlorpromazine with 2′-deoxyguanosine-5′-monophosphate by PM3 calculation. Anticancer Res 18:3493–3497
7. Molnar J, Szabo D, Mandi Y, Mucsi L, Fischer J, Varga A, Koenig S, Motohashi N (1998) Multidrug resistance reversal in mouse lymphoma cells by heterocycloc compounds. Anticancer Res 18:3033–3038
8. Kurihara T, Nojima K, Sakagami H, Motohashi N, Molnar J (1999) Electronic structure and cytotoxic activity of half-mustard type phenothiazines by MM3 and PM3 methods. Anticancer Res 19:3895–3899
9. Kurihara T, Motohashi N, Sakagami H, Molnar J (1999) Relationship between cytotoxic activity and dipole moment for phthalimido- and chloroethyl-phenothiazines. Anticancer Res 19:4081–4083
10. Molnar J, Sakagami H, Motohashi N (1993) Diverse biological activities displayed by phenothiazines, benzo[*a*]phenothiazines and benz[c]acridines. Anticancer Res 13:1019–1026
11. Ohkura K, Hori H (1998) Analysis of structure-permeability correlation of nitrophenol analogs in newborn rat abdominal skin using semiempirical molecular orbital calculation. Bioorg Med Chem 7:309–314

12. Kurihara T, Yamada A, Kawase M, Motohashi N, Sakagami H, Molnar J (2004) Relationship between electronic structure and cytotoxic activity of dopamine and 3-benzazepine derivatives. In Vivo 18:443–448
13. Kurihara T, Noguchi M, Noguchi T, Wakabayashi H, Motohashi N, Sakagami H (2006) Relationship between electronic structure and cytotoxic activity of azulenes. In Vivo 20:358–390
14. Kurihara T, Mine H, Satoh Y, Wakabayashi H, Motohashi N, Sakagami H (2006) Relationship between electronic structure and cytotoxic activity of tropolones. In Vivo 20:391–396
15. Kurihara T, Satoh R, Miyagawa T, Wakabayashi H, Motohashi N, Sakagami H (2007) Relationship between electronic structure and cytotoxic activity of azulenequinones and trihaloacetylazulenes. In Vivo 21:715–720
16. Chakrabarty AN, Molnar J, Dastidar SG, Motohashi N (eds) (1998) Non Antibiotics. NISCOM, New Delhi, India, pp 100–113
17. Motohashi N, Kurihara T, Satoh K, Sakagami H, Mucsi L, Pusztai R, Szabo M, Molnar J (1999) Antitumor activity of benzo[*a*]phenothiazines. Anticancer Res 19:1837–1842
18. Lacassagne A, Buu-Hoi NP, Daudel R, Zajdela F (1956) The relation between carcinogenic activity and the physical and chemical properties of angular benzacridines. Adv Cancer Res 4:315–369
19. Chang RJ, Levin W, Wood AW, Kumar S, Yagi H, Jerina DM, Lehr RE, Conney AH (1984) Tumorigenicity of dihydrodiols and diol-epoxides of benz[*c*]acridines in newborn mice. Cancer Res 44:5161–5164
20. Chang RJ, Levin W, Wood AW, Shirai N, Ryan AJ, Duke CC, Jerina DM, Holder GM, Conney AH (1986) High tumorigenicity of the 3,4-dihydrodiol of 7-methylbenz[*c*]acridines on mouse skin and in newborn mice. Cancer Res 46:4552–4555
21. Levin W, Wood AW, Chang RL, Kumar S, Yagi H, Jerina DM, Lehr RE, Conney AH (1983) Tumor-initiating activity of benz[*c*]acridines and twelve of its derivatives on mouse skin. Cancer Res 43:4625–4628
22. Walker BA, Rogan EG, Cromwell NH (1984) Mutagenicity of selected functinalized benz[*c*]acridines and a benz[a]phenazine in the salmonella typhimurium/microsome assay. Anticancer Res 4:399–402
23. Motohashi N, Kurihara T, Sakagami H, Molnar J (1992) Relationship between resonance energy and carcinogenic activity of benz[c]acridines. Anticancer Res 12:2105–2108
24. Kurihara T, Sakagami H, Molnar J, Motohashi N (1994) Quantumchemical structure of carcinogenic benz[*c*]acridines. Anticancer Res 14:1811–1822
25. Kurihara T, Watanabe T, Yoshikawa K, Motohashi N (1998) Radical Productions and π-Spin Density by UHF/PM3 Method on benz[*c*]acridines and benzo[*a*]phenothiazines. Anticancer Res 18:429–432
26. Aihara J (1976) A new definition of Dewar-type resonance energies. J Am Chem Soc 98:2750–2758
27. Kurihara T, Motohashi N, Gui-Lin Pang, Higano M, Kiguchi K, Molnar J (1996) Correlation between topological resonance energy of methyl-substituted Benz[*c*]acridines, Benzo[*a*]phenothiazines and Chrysenes, and their carcinogenic or antitumor activites. Anticancer Res 16:2757–2766

Subject Index